U. PORTO

DOUTORAMENTO

BIOTECNOLOGIA MOLECULAR E CELULAR APLICADA ÁS CIÊNCIAS DA SAÚDE

Immunomodulatory functionalized nanoparticles to improve the chemotherapeutic treatment in metastatic colorectal cancer

Maria José Silveira

D
2024



U. PORTO

Maria José Silveira.

Immunomodulatory functionalized nanoparticles to improve the chemotherapeutic treatment in metastatic colorectal cancer



D.ICBAS **2024**

Immunomodulatory functionalized nanoparticles to improve the chemotherapeutic treatment in metastatic colorectal cancer

Maria José da Costa Pinho Silveira

INSTITUTO DE CIÊNCIAS BIOMÉDICAS ABEL SALAZAR



Maria José da Costa Pinho Silveira

Immunomodulatory functionalized nanoparticles to improve the chemotherapeutic treatment in metastatic colorectal cancer

Tese de Candidatura ao grau de Doutor em Biotecnologia Molecular e Celular Aplicada às Ciências da Saúde submetida ao Instituto de Ciências Biomédicas Abel Salazar da Universidade do Porto e Faculdade de Farmácia da Universidade do Porto

Orientador:

Doutor Bruno Filipe Carmelino Cardoso Sarmento

Categoria – Investigador Principal/ Professor Associado Convidado

Afiliação – i3S – Instituto de Investigação e Inovação em Saúde, INEB – Instituto de Engenharia Biomédica, Universidade do Porto & IUCS - Instituto Universitário de Ciências da Saúde

Co-orientador:

Doutora Maria José Cardoso Oliveira

Categoria – Investigadora Principal/ Professora Associada Convidada

Afiliação – i3S – Instituto de Investigação e Inovação em Saúde, INEB – Instituto de Engenharia Biomédica, Universidade do Porto & ICBAS - Instituto de Ciências Biomédicas Abel Salazar da Universidade do Porto

To those who filled me with love and
encouraged me to pursue my dreams

The work presented in this thesis was developed at:

Nanomedicines & Translational Drug Delivery
i3S - Instituto de Investigação e Inovação em Saúde
INEB - Instituto Nacional de Engenharia Biomédica
Universidade do Porto
Rua Alfredo Allen 208, 4200-135 Porto, Portugal
www.i3s.up.pt | www.ineb.up.pt





And

Tumour and Microenvironment Interactions
i3S - Instituto de Investigação e Inovação em Saúde
INEB - Instituto Nacional de Engenharia Biomédica
Universidade do Porto
Rua Alfredo Allen 208, 4200-135 Porto, Portugal
www.i3s.up.pt | www.ineb.up.pt





And

Advanced Organ Bioengineering and Therapeutics
Technical Medical Centre
Faculty of Science and Technology
University of Twente

Drienerlolaan 5, 7522 NB Enschede, The Netherlands

https://www.utwente.nl/en/tnw/aot/

UNIVERSITY OF TWENTE. | TECHMED CENTRE

Eu, Maria José da Costa Pinho Silveira, declaro que a presente tese é de minha autoria e não foi utilizada previamente noutro curso ou unidade curricular, desta ou de outra instituição. As referências a outros autores (afirmações, ideias, pensamentos) respeitam escrupulosamente as regras da atribuição, e encontram-se devidamente indicadas no texto e nas referências bibliográficas, de acordo com as normas de referenciação. Tenho consciência de que a prática de plágio e auto-plágio constitui um ilícito académico.

Porto, 8 de Maio de 2024



FINANCIAL SUPPORT

This work was funded by national funds through Foundation for Science and Technology (FCT), under the projects: PTDC/NAN-MAT/1431/2021 – *"Multifunctional cell membrane-camouflaged polymeric micelles for combination therapy of colorectal cancer" and the project Norte-01-0145-FEDER-000051 - "Cancer Research on Therapy Resistance: From Basic Mechanisms to Novel Targets". This support was facilitated by the Norte Portugal Regional Operational Programme (NORTE 2020) under the PORTUGAL 2020 Partnership Agreement, which is backed by the European Regional Development Fund as well as by FCT as part of Maria José Silveira's national PhD scholarship (SFRH/BD/151015/2021). Additionally, the research benefited from financial contributions from the COST Actions CA 17140 "Cancer Nanomedicine from the Bench to the Bedside" initiative, sponsored by COST (European Cooperation in Science and Technology), and the FCT PhD BiotechHealth Programme (Doctoral Programme on Cellular and Molecular Biotechnology Applied to Health Sciences).*



SCIENTIFIC ACHIEVEMENTS

Publications

The research conducted in this doctoral thesis has been published in peer-reviewed scientific journals, in accordance with the conditions outlined in Article 31, paragraph 2, subparagraph of Decree-Law No. 115/2013 dated August 7. Furthermore, additional research work is currently in preparation for publication, as detailed in the forthcoming sections. The author of this doctoral thesis holds exclusive first authorship responsibility for each subsequent publication, ensuring that they do not constitute an integral part of any other academic theses or dissertations.

Research articles in peer-reviewed journals:

- **MJ Silveira,** C Martins, T Cruz, F Castro, A Amorim-Costa, K Chester, MJ Oliveira, B Sarmento. "*scFv biofunctionalized nanoparticles to effective and safe targeting of CEA-expressing colorectal cancer cells*". Journal of Nanobiotechnology, 21, 357 (2023).

  In this original research article, I was responsible for the conceptualization, methodology, and writing - original draft. The supervisors were responsible for reviewing, editing, and submitting the manuscript. This article was not previously included in another PhD thesis, and it is reproduced in this thesis. The authorization from the journal to reuse the manuscript in this thesis were included in Appendix.

- **MJ Silveira,** C Martins, AP Cardoso, MJK Ankone, MJ Oliveira, J Prakash, B Sarmento. "*Precision Therapy in Colorectal Cancer: Harnessing IL-12 pH-Responsive Nanoparticles to Modulate the Tumor Microenvironment*". (Manuscript under revision).

  In this original research article, my roles included the conceptualization, methodology development, and the writing of the initial draft. The supervisory team was tasked with the review, editing, and submission of the manuscript. This article has not been previously included in any other PhD thesis and is reproduced in full in this thesis.

Review articles in peer-reviewed journals:

- **MJ Silveira**, F Castro, MJ Oliveira, B Sarmento. "*Immunomodulatory Nanoparticles for Colorectal Cancer Treatment, a landscape to be explored?*" Biomaterials Science, 9, 3228-3243 (2021).

  In this review article, I was responsible for the conceptualization, bibliographic research, and writing. The supervisors were responsible for reviewing, editing, and submitting the manuscript. This review was not previously included in another PhD thesis, and it is partially reproduced in this thesis. The full review paper and the authorization from the journal to reuse the manuscript in this thesis were included in Appendix.

Publications outside the scope of this doctoral thesis, co-authored during its development, and relevant to its context include:

Research articles in peer-reviewed journals:

- S Carvalho, **MJ Silveira**, M Domingues, B Ferreira, CL Pereira, MP Gremião, B Sarmento. "*Multicellular Quadruple Colorectal Cancer Spheroids as an In Vitro Tool for Antiangiogenic Potential Evaluation of Nanoparticles"*. Advanced Therapeutics, 6, 2200282 (2023).

Review articles in peer-reviewed journals:

- F Castro, C Martins, **MJ Silveira**, R Moura, CL Pereira, B Sarmento. "Advances on erythrocyte-mimicking nanovehicles to overcome barriers in biological microenvironments". Advanced Drug Delivery Reviews,170, 312-339 (2021).
- F Castro, CL Pereira, M Macedo, A Almeida, **MJ Silveira**, S Dias, AP Cardoso, MJ Oliveira, B Sarmento. "*Advances on Colorectal Cancer 3D models: The needed translational technology for nanomedicine screening*". Advanced Drug Delivery Reviews, 175, 113824 (2021).

Communications

The research conducted in this doctoral thesis led to the following presentations:

Oral communications:

- **MJ Silveira**, MJ Oliveira, J Prakash, B Sarmento. "*Two fronts of attack: modeling the tumor microenvironment and targeting CEA- expressing colorectal cancer cells using a combinatory nano-strategy*" at the Nanomedicine and Nanobiotechnology International Conference, Barcelona, Spain (2024).
- **MJ Silveira**, MJ Oliveira, B Sarmento. "*Combinatory nano strategy to target CEA-expressing colorectal cancer cells and the weakly acidic tumor microenvironment*" in the i3S Young scientist seminars, Porto, Portugal (2023).
- **MJ Silveira**, MJ Oliveira, B Sarmento. "*Polymeric nanoparticles as novel immunomodulatory chemotherapy to selectively target CEA-expressing colorectal cancer cells*" on the III Biotech Day, Porto, Portugal (2022).
- **MJ Silveira**, T Cruz, MJ Oliveira, B Sarmento. **"***Polymeric nanoparticles as novel immunomodulatory chemotherapy to selectively target CEA-expressing colorectal cancer cells*" at the 4th Symposium on Immunomodulation in Cancer & Regeneration, Porto, Portugal (2022).
- **MJ Silveira**, M de La Fuente, MJ Oliveira, B Sarmento. "*Development of novel targeted immunomodulatory nanoparticles for colorectal cancer treatment*" in the 1st CA17140 STSM VIRTUAL CONFERENCE, Virtual (2022).
- **MJ Silveira**, MJ Oliveira, B Sarmento. "*Development and characterization of CEA-targeted nanoparticles as novel chemotherapy for metastatic colorectal cancer treatment*" in the CRS annual meeting, virtual (2021).
- **MJ Silveira**, MJ Oliveira, B Sarmento. "*Towards the synthesis of targeting polymeric conjugate to manufacture 5-FU loaded nanoparticles for colorectal cancer chemotherapy*" in the Biotech Day: The Future is now. Virtual (2021).
- **MJ Silveira**, MJ Oliveira, B Sarmento. "*CEA-targeted Nanoparticles as novel Chemotherapy for metastatic Colorectal Cancer treatment*", WG2 ONLINE CA17140 COST CONFERENCE, Virtual (2021).
- **MJ Silveira**, MJ Oliveira, B Sarmento. "*Development of functionalized nanoparticles for colorectal cancer treatment*" in the 2º Encontro Nacional de Jovens Investigadores em Oncologia - Liga Portuguesa contra o cancro, Porto, Portugal (2020)
- **MJ Silveira**, MJ Oliveira, B Sarmento. "Chemotherapeutic strategy to metastatic colorectal cancer treatment using functionalized CEA-targeted nanoparticles" in the

BiotecHDay, virtual (2020).

- **MJ Silveira**, MJ Oliveira, B Sarmento. "*Immunomodulatory functionalized nanoparticles to improve chemotherapeutic treatment in metastatic colorectal cancer*" in the VI Biotech Health Annual Symposium, Porto, Portugal (2019).

Poster communications:

- **MJ Silveira**, MJ Oliveira, J Prakash, B Sarmento. *"Dual-pronged strategy: modelling the tumor microenvironment and targeting CEA-expressing colorectal cancer cells using a combinatory nano-strategy*" in the XV Spanish-Portuguese Conference on Controlled Drug Delivery, Lisbon, Portugal (2024).
- **MJ Silveira**, MJ Oliveira, J Prakash, B Sarmento. "*Smart combinatory strategy targeting CEA-expressing colorectal cancer cells and weakly acidic tumor microenvironment*" at the CRS Annual meeting, Las Vegas, USA (2023).
- **MJ Silveira**, T Cruz, MJ Oliveira, B Sarmento. "*Unraveling the therapeutic potential of CEA-targeted nanoparticles in colorectal cancer cells and to modulate its tumor microenvironment*", in the EACR 2022 Congress - Innovative Cancer Science: Translating Biology to Medicine, Seville, Spain (2022).
- **MJ Silveira**, MJ Oliveira, B Sarmento. "*CEA-targeted Nanoparticles as a novel chemotherapy for metastatic Colorectal cancer treatment*" in the 4th PhDAY: Break borders and build opportunities, Porto, Portugal (2021).
- **MJ Silveira**, MJ Oliveira, B Sarmento. "*Establishment of CEA-targeted Nanoparticles to novel Chemotherapy towards metastatic Colorectal Cancer*", in the 3rd SPLC-CRS Young Scientists Meeting, Virtual (2021).
- **MJ Silveira**, MJ Oliveira, B Sarmento. "*Combinatory therapeutic strategy to metastatic colorectal cancer treatment using functionalized nanoparticles*", at UKCRIS Symposium, virtual (2020).
- **MJ Silveira**, MJ Oliveira, B Sarmento. "*Functionalized nanoparticles to delivery chemotherapeutic drugs in metastatic Colorectal Cancer*", PhDay, virtual (2020).
- **MJ Silveira**, MJ Oliveira, B Sarmento. "*Functionalized nanoparticles to delivery chemotherapeutic drugs in metastatic Colorectal Cancer*" in the Cancer biology: from basic to translational research Webinar - Liga Portuguesa contra o cancro, virtual (2020).
- **MJ Silveira**, MJ Oliveira, B Sarmento. "*Chemotherapeutic strategy to metastatic colorectal cancer treatment using functionalized CEA-targeted nanoparticles*", in the BiotechDay, virtual (2020).
- **MJ Silveira**, MJ Oliveira, B Sarmento. "*CEA-targeted nanoparticles to metastatic*

Colorectal Cancer treatment" in the 47th Controlled Release Society Annual Meeting, virtual (2020).

- **MJ Silveira**, S Velho, MJ Oliveira, B Sarmento. "*Targeting tumor microenvironment to improve the chemotherapeutic treatment in metastatic Colorectal Cancer*" in the EACR-AACR Basic & Translational Research Conference on Tumor Microenvironment, Lisbon, Portugal (2020).
- **MJ Silveira**, F Sousa, MJ Oliveira, B Sarmento. "*Combinatory therapeutic strategy to metastatic colorectal cancer treatment using functionalized CEA-targeted nanoparticles*" in the XIII Spanish-Portuguese Conference on Controlled Drug Delivery, Santiago de Compostela, Spain (2020).
- **MJ Silveira**, F Sousa, S Velho, MJ Oliveira, B Sarmento. "*Novel Immunomodulatory approach to improve chemotherapeutic treatment in metastatic colorectal cancer*" at 8th i3S Annual Meeting, Axis Vermar Conference & Beach Hotel, Póvoa do Varzim, Portugal (2019).
- **MJ Silveira**, F Sousa, S Velho, MJ Oliveira, B Sarmento. "*Immunomodulatory functionalized nanoparticles to improve chemotherapeutic treatment in metastatic colorectal cancer*" at PhDay – PhD countdown: a time for Science, Porto, Portugal (2019).

Prizes and awards

The research undertaken in this doctoral thesis garnered the following prizes and awards:

- Short-term Scientific Mission Grants from Nano2Clinic COST Action CA17140 (2021).
- Young Scientist Travel Grant Award in the CRS 2023 Annual Meeting & Expo– Paris Hotel, Las Vegas, NV, USA (2023)

ACKNOWLEDGEMENTS

O caminho faz-se caminhando, e é através dos variados e enigmáticos caminhos da vida que aprendemos a andar, movidos pela curiosidade e coragem que aperfeiçoam o sonho que nos motivou a embarcar nessa jornada. O PhD, tal como a vida é um trajeto em forma de montanha-russa, cheio de altos e baixos, mas surpreendente pelos lugares mais bonitos que nos permite ver, e pelas emoções fortes que dele advém. No espaço da superação encontramos a felicidade, agradecemos o amor que cultivamos, as pessoas que connosco estiveram e os momentos bonitos que passamos. Por todo o apoio e confiança daqueles que choraram comigo, sorriram e vibraram com as pequenas conquistas não posso deixar de agradecer a forma como impactaram a minha vida e os quais levarei sempre num lugar bonito do meu coração.

Neste sentido, gostaria de começar por agradecer aos meus pais por sempre me terem incentivado a não me ficar pelo verbo sonhar, de modo a provar o doce sabor da concretização. Para nós, os últimos anos não foram fáceis, mas sei que no meio de qualquer adversidade que a vida nos possa colocar, juntos e unidos pelo amor ultrapassaremos qualquer obstáculo. Obrigada por sempre me apoiarem, limparem as minhas lágrimas e transformarem as minhas dores em lugares bonitos de aprendizagem. Ao meu irmão que, por ser tão diferente de mim, me torna uma pessoa melhor e ensina em todos os sentidos que a vida possa ter. Aos 3, obrigada por fazerem de mim a pessoa que sou hoje e, por estarem sempre ao meu lado desejando que eu possa usufruir da paisagem que o final da escalada nos permite contemplar.

Ao meu amor, Diogo, por todo o equilíbrio que traz à minha vida, por ser o meu ombro amigo, o melhor colo e o melhor lugar onde posso encontrar amor. Por toda a calma que o teu mundo traz ao meu, por confiares e veres em mim tanto de bom. Por sofreres comigo quando choro sem parar, quando transmito as minhas angústias e os meus receios, mas por trazeres a confiança que necessito e a visão que muitas vezes parece estar embaciada pelos meus medos. Entraste na minha vida sem querer e sei que para nunca mais saíres. Obrigada por tudo, mas principalmente por me devolveres a cor que eu própria desvaneço na minha vida.

Profunda gratidão ao meu orientador, Professor Bruno Sarmento, pela oportunidade de trilhar este caminho, ainda que cheio de obstáculos, permanecendo sempre no espaço da mentoria, ajudando-me a encarar as dificuldades com mais leveza, foco e determinação. Por ter sido a primeira pessoa a acreditar nas minhas capacidades, permitindo-me perseguir os meus sonhos e a experimentar a doce sensação de realização. Por ser um exemplo para mim, capaz de transformar as preocupações em sorrisos e tranquilidade.

Obrigada por me ter dado a mão sem a largar, mesmo nos momentos mais difíceis desta jornada.

Gostaria também de estender os meus agradecimentos à minha co-orientadora, Professora Maria José Oliveira, por me ter acolhido com tanto carinho no seu grupo de investigação. Por ter sido a minha casa durante estes últimos anos, onde chorei, sorri e vibrei de muita alegria. Por todas as palavras encorajadoras e todos os abraços que me souberam tão bem.

Gostaria ainda de expressar a minha gratidão ao Professor Jai Prakash, não apenas pela valiosa contribuição científica, mas por me acolher no seu grupo de investigação e me tratar como um membro do seu grupo. Agradeço todas as conversas motivadoras, palavras de encorajamento e amizade que transformaram os meus medos em sorrisos. Muito obrigado por tudo!

Gostaria ainda de manifestar a minha gratidão a todos os membros do grupo Nanomedicines & Translational Drug Delivery cujo ambiente e pessoas contribuíram para o desenvolvimento bem-sucedido do meu trabalho de doutoramento. Neste sentido gostaria de agradecer de forma especial à Sofia Barros por todo o carinho e prestabilidade ao longo destes anos, à Rute Nunes pelos conselhos tão prudentes e pelas discussões científicas no início do meu PhD que me fizeram pensar e redirecionar o desenvolvimento do mesmo sempre num bom sentido e por fim à Cláudia Martins por todas as discussões científicas, apoio incondicional e amizade. Por todos os momentos juntas que jamais esquecerei, lágrimas, dúvidas e tantos sorrisos. Obrigada por tudo e por tanto.

Gostaria também de expressar a minha mais profunda gratidão aos membros do grupo Tumour and Microenvironment Interactions cujo ambiente ao longo destes anos foi excecional e os quais apesar de serem de uma área tão distinta se esforçaram por ouvir as minhas dúvidas científicas de forma a encontrarmos juntos, respostas para as mesmas, com os quais ri muito e passei momentos muito felizes. A todos sem exceção o meu sincero obrigada. Ângela Costa pela sua forma tão direta e tão melhor de estar na vida. Patrícia Cardoso que apesar de ser tão reservada, se demonstrar sempre disponível para ajudar. Tânia Cruz, a pessoa com a qual dividi as minhas dúvidas e as minhas ansiedades e que sempre esteve disponível para me ajudar e aconselhar em todos os momentos. À banda dos 4, Ana Borges, pela pessoa bonita que é por dentro e por fora, pela amizade incondicional e por todo o carinho que sempre partilhamos; Diogo Estevão por me fazer rir até chorar com as suas cantorias, escolhas musicais e porque “entre nós não há lágrimas, só se forem de tanto rir!” E por fim, mas não menos importante, à Ângela Magalhães, por ser a minha alma gémea dentro do i3S, a pessoa com a qual desde o primeiro minuto partilhei os meus medos, as minhas angústias, com quem ri até chorar e partilhei muitas dúvidas científicas. Obrigada por seres a pessoa mais divertida que conheci na minha vida

e por teres de forma inesperada aparecido neste caminho do PhD, para em conjunto o tornarmos mais leve e mais feliz. Obrigada aos 3 por serem os amiguinhos que a minha alma jamais esquecerá e porque os 4 juntos, pintamos de prateado as paredes cinzentas do i3S! Muito obrigada por tudo!

Uma breve nota de agradecimento a todos os membros do grupo AOT da universidade de Twente principalmente ao Kunal, Chen, Lena e Marcel por me fazerem sentir parte integrante do vosso grupo e por me ajudarem e ensinarem. Muito obrigada.

À Francisca Diniz, por ser a minha parceira do lab ao lado, a melhor amiga dos i3S PhD representatives e por estar sempre ao meu lado durante os últimos 4 anos.

Aos meus colegas do Centro Hospitalar do Baixo Vouga, por sempre acreditarem nas minhas capacidades e me incentivarem a ir mais além. Especialmente, à Corina Lopes, que sempre me encorajou e confiou nas minhas capacidades, mesmo quando eu não imaginava o que seria o meu futuro, e com quem trabalhar era muito melhor e mais divertido. As minhas palavras nunca serão suficientes para expressar a minha gratidão. À Vanda Simões, a melhor orientadora de estágio e mais tarde colega de referência. A pessoa que sempre me incentivou a explorar as minhas capacidades e a não me deixar acomodar no conforto que a minha vida tinha na altura e com quem partilho ainda hoje tanto. Obrigada pelas tuas palavras de encorajamento, pelas conversas sempre leves e felizes e porque só tu entendes verdadeiramente as dúvidas da minha alma. Guardo-te e guardar-te-ei sempre num dos lugares mais bonitos do meu coração. Ao Dr Elmano, Dra Manuela, Manel, Olga, Nani, Luísa, Dina, Elsa, Hugo e Elva por me terem considerado uma referência como profissional e porque ainda que, sem compreenderem as minhas escolhas, me apoiaram nas minhas decisões. Obrigada a todos sem exceção por tanto que me deram e ensinaram nos anos que partilhamos juntos. Muito obrigada do fundo do coração.

Finalmente gostaria de agradecer aos meus amigos de sempre e para sempre: Sara, Joana, Victor, Teresa, Diana, Andreia, Cátia, Joana, Catarina e prós do ski, porque ainda que, não entendam as dificuldades encontradas ao longo deste meu caminho, sempre caminharam comigo, incentivando-me e trazendo tanta felicidade e cor aos meus dias. Obrigada por todos os momentos que partilhamos juntos durante estes anos todos, por tantas histórias e tanta felicidade.

Por último, à Maria e ao Paulo, por serem os meus anjos guias na terra e para os quais é tão difícil ter palavras suficientes de gratidão profunda. Às pessoas que trazem luz no meio da minha escuridão, que me ensinam a pintar com a cores mais bonitas e brilhantes a minha história e por me fazerem ver com sensatez que as adversidades mais não são do que aprendizagens e que por isso, só há sucesso. Umas vezes aprendemos outras atingimos os nossos objetivos! Gratidão sem fim!

“Caminante, no hay camino, se hace camino al andar.”

Antonio Machado

TABLE OF CONTENTS

ABSTRACT xxv

RESUMO xxvii

ACRONYMS AND ABBREVIATIONS LIST xxxi

CHAPTER I – LITERATURE REVIEW 1

Abstract 3

Keywords 3

Background 5

CRC physiopathology and CEA 7

Understanding TME and immune system in CRC 8

Colorectal cancer therapy 13

Radiotherapy 13

Chemotherapy 13

Targeted therapies and immunotherapy 15

Immunomodulatory therapeutic strategies for CRC 17

Tumor Necrosis Factor-α (TNF-α) 18

Interferon-gamma (IFN-γ) 18

Interleukins (ILs) 19

Extracellular matrix-mediated CRC immunomodulation 21

Nanomedicines for enhanced therapy and diagnosis 22

Immunomodulatory nanomedicine to improve CRC therapy 24

Nanomedicine for antigen and adjuvant delivery in CRC 30

Nanomedicine for immunomodulatory strategies in CRC 34

Combinatory nanotherapies 36

Challenges and future perspectives 37

References 39

CHAPTER II – OVERVIEW, MOTIVATIONS, OBJECTIVES AND TASKS.....55

Overview and Motivation 57

Aims and Objectives 59

Main aim 59

Collaboration of supervision and institutions 61

References 63

CHAPTER III –TARGETED NANOPARTICLES TO EFFECTIVE TARGETING OF CEA-EXPRESSING COLORECTAL CANCER CELLS 67

Abstract 69

Keywords 69

Background 71

Methods 72

Anti-CEA scFv chemical conjugation to the PLGA-PEG-mal polymer.....73

Characterization of targeted polymer PLGA-PEG-scFv 74

Manufacture of 5-FU loaded CEA-targeted nanoparticles.....74

Characterization of nanoparticles 75

Average particle size, polydispersity index, surface charge and morphology of nanoparticles 75

5-FU association efficiency and drug loading 75

Colloidal stability of nanoparticles.....76

5-FU in vitro cumulative release 76

Cell lines and cell culture 76

Ethics statement 76

Human monocytes isolation.....77

CEA expression evaluation.....77

Cell-nanoparticle interaction evaluations 77

Imaging flow cytometry 78

Confocal Laser-Scanning Microscopy 78

Cell metabolic activity 79

Impact of NPs on macrophage polarization 79
Statistical analysis 80
Results 80
Chemical synthesis of Anti-CEA scFv with PLGA-PEG-mal polymer 80
Manufacture and characterization of 5-FU-loaded CEA-targeted NPs 81
CEA expression analysis in colorectal cancer cell lines 83
Targeting capacity of anti-CEA scFv functionalized NPs towards CEA^{high} and CEA^{low} CRC cells 84
Effect of 5-FU-loaded CEA-targeted NPs in the metabolic activity of CRC cells 87
Impact of 5-FU-loaded F NPs on the polarization of macrophages 89
Conclusions 92
Supporting Information 93
References 97

CHAPTER IV – IL-12 PH-RESPONSIVE NANOPARTICLES TO MODULATE THE TUMOR MICROENVIRONMENT 103

Abstract 105
Keywords 105
Background 107
Materials and Methods 108
Chemical conjugation and characterization of the DMMA and PLGA polymer composite 109
Manufacture of IL-12 loaded pH responsive nanoparticles 110
Characterization of nanoparticles 110
Average particle size, polydispersity index, surface charge and morphology of nanoparticles 110
Evaluation of nanoparticles pH responsiveness 111
IL-12 association efficiency and drug loading 111
IL-12 in vitro cumulative release 111
Cell lines and cell culture reagents 112

Ethics statement 112
Human monocytes isolation 112
2D Macrophages differentiation 112
Assessment of the metabolic activity in 2D macrophages cells 113
Nitric oxide (NO) release bioassay in 2D macrophages 113
In vitro efficacy studies in 2D macrophages by IFN-γ production 114
3D colorectal cancer spheroid establishment 114
Characterization of the average diameter, metabolic activity, and circularity of 3D colorectal spheroids 115
Histological analysis of the 3D colorectal spheroids 115
3D colorectal spheroids immunofluorescence analysis 116
Characterization 3D colorectal spheroids through flow cytometry analysis 116
Uptake of NPs into 3D colorectal cancer spheroids 117
Effect of NPs on macrophages polarization and anti-proliferative effect of 3D colorectal cancer spheroids 117
Effect of NPs on NO, IFN-Γ and IL-10 levels of 3D colorectal cancer spheroids 118
Statistical analysis 118
Results 118
Production and characterization of the pH-responsive NPs 118
Therapeutic effect of the IL-12-loaded pH-responsive NPs in 2D *in vitro* models of macrophages 121
Refinement and characterization of heterotypic CRC 3D spheroids 124
Establishment and optimization of the CRC monospheroid 3D model 124
Establishment of heterotypic immunospheroid as a screening therapeutic platform 126
Effect of NPs on cellular interactions and metabolic activity of 3D CRC spheroids 129
Impact of the NPs in the polarization of macrophages 129
Effect of pH-responsive NPs containing IL-12 on the production of IFN-γ and IL-10 131
Conclusions 135
Supporting Information 137
References 141

CHAPTER V – COMBINATORY STRATEGY TO IMPROVE COLORECTAL CANCER THERAPY 145

Abstract 147

Keywords 147

Background 149

Methods 151

Cell lines and culture supplies 152

Ethical Considerations 152

Isolation of human monocytes 152

CEA^{high} and CEA^{low} 3D CRC spheroids development 152

Characterization of the average diameter, metabolic activity, and circularity of 3D colorectal spheroids 153

Histological and immunofluorescence analysis of the 3D colorectal spheroids 153

Characterization 3D colorectal spheroids through flow cytometry analysis 154

Uptake of 5-FU-CEA-NPs by 3D CRC spheroids 154

Effect of 5-FU-CEA-NPs and IL-12 pH-responsive on the metabolic activity of 3D colorectal cancer spheroids 155

Effect of the IL-12 pH-responsive NPs monotherapy or combinatory NPs strategy on the polarization of macrophages 155

Effect of the combinatory NPs on NO, IFN-γ and IL-10 levels of 3D colorectal cancer spheroids 155

Statistical analysis 156

Results 156

Development and characterization of the CEA^{low} mono spheroids 156

Establishment and characterization of the heterotypic 3D CRC immunospheroids 157

..... 161

Assessing the effects of 5-FU-CEA-NPs and IL-12 pH-Responsive NPs as Monotherapies on CEA^{high} and CEA^{low} 3D CRC spheroids 161

Impact of Combinatorial Strategy on Metabolic Activity, IFN-γ, and IL-10 Production in 3D CRC Spheroids, and Subsequent Stimulus for M1-like Polarization Profile 165

Conclusions 169

Supporting Information 171

References 173

CHAPTER VI – GENERAL DISCUSSION AND FUTURE PERSPECTIVES 177

General Discussion 179

Future Perspectives 182

References 185

APPENDIX – DOCTORAL THESIS SUPPLEMENTARY DOCUMENTS 187

ABSTRACT

Colorectal cancer (CRC) stands as the second deadliest cancer worldwide, primarily driven by its high tendency to metastasize. Despite some progress in treatment options, the prognosis for metastatic CRC continues to be bleak, with a five-year survival rate of only 14%. Additionally, the CRC tumor microenvironment (TME), characterized by its immunosuppressive nature and weakly acidic pH (approximately 6.5), plays a significant role in promoting tumorigenesis by enabling cancer cells to evade immune detection and furthering disease progression, thereby influencing treatment outcomes.

5-fluorouracil (5-FU), the standard treatment for CRC, is plagued by severe side effects, low local bioavailability, and poor tumor specificity. Furthermore, IL-12, which has shown potential in solid tumor immunotherapy by stimulating IFN-γ production, is limited in clinical use due to the undesirable severe systemic effects. These challenges underscore the urgent need for more targeted and effective therapeutic strategies in CRC treatment.

To address these issues, there is an increasing interest in exploring combinatorial strategies that may enhance disease prognosis and circumvent the limitations of current monotherapies. The CEA, a glycoprotein often overexpressed in colorectal tumors, presents a promising target for developing novel CRC treatment strategies. In this PhD research work, an innovative combinatorial approach was developed using nanoparticles (NPs) engineered to target not only CRC cells that express carcinoembryonic antigen (CEA) but also to modulate the surrounding immunosuppressive TME. This strategy aims to improve treatment precision and effectiveness, offering hope for better management of CRC.

Addressing a significant clinical need, this PhD work involved creating a smart nanoplatform based on chemical conjugation of an anti-CEA single-chain variable fragment (scFv), MFE-23, with matrix PLGA-PEG to deliver the standard 5-FU chemotherapy to CRC cells. Consequently, we successfully demonstrated the specificity of the developed CEA-targeted NPs on the internalization by CEA-expressing CRC cells, with an enhance of 3-fold in cell uptake. Additionally, CEA-targeted NPs loaded with 5-FU significantly increased cytotoxicity in target cells at 24- and 48-hours post-treatment, underlining their therapeutic specificity. Safety assessments in donor-isolated macrophages confirmed that the developed CEA-targeted NPs loaded with 5-FU did not adversely affect cellular metabolic activity or polarization, affirming their potential as a safe and effective targeted treatment approach for CRC.

Furthermore, to target and modulate the immunosuppressive CRC TME, we developed pH-responsive NPs that encapsulate IL-12, designed to enhance efficacy while minimizing

unwanted immune responses. Therefore, the IL-12 pH-responsive NPs exhibited activity at pH ~6.5, typical of tumor environments, promoting antitumoral inflammation through increased release of IFN-γ and nitric oxide (NO), without adversely affecting macrophage metabolic activity.

To assess and validate the primary objective of this PhD work, i.e., the specificity of our NPs, both as monotherapies and within a combinatorial approach, we established CRC CEA-expressing (CEA^{high}) and non-expressing (CEA^{low}) MSI 3D spheroids that closely replicate the spatial organization and extracellular matrix of tumors. The interaction of the IL-12 pH-responsive NPs with these spheroids demonstrated their pH responsiveness and minimal impact on metabolic activities for both CEA^{high} and CEA^{low} 3D spheroids. Moreover, the developed responsive NPs, effectively induced macrophage polarization, shifting from tumor-promoting M2-like markers to pro-inflammatory M1-like markers, which support tumor suppression. Furthermore, treatment with IL-12 pH-responsive NPs increased IFN-γ levels and decreased IL-10 secretion, emphasizing their potential in targeted cancer therapy by modifying the tumor microenvironment to enhance antitumor immunity.

Conversely, consistent with observations from 2D assays, CEA-targeted NPs delivering 5-FU specifically targeted CEA^{high} 3D spheroids, significantly affecting their metabolic activity. Additionally, the combinatorial strategy not only replicated the aforementioned effects but also induced favorable macrophage polarization, reducing the anti-inflammatory M2-like markers while increasing the pro-inflammatory M1-like counterparts, and modulated cytokine levels, elevating IFN-γ levels and reduced IL-10 secretion, underlining the efficacy of combining these therapies.

Overall, the internalization of targeted NPs mediated by CEA offers promising new directions for chemotherapy strategies in cancers associated with CEA and their metastatic sites, meriting expanded research into other solid tumors. Moreover, altogether, our findings highlight the effectiveness of combinatorial strategies in accurately targeting specific cells, while simultaneously triggering anti-tumoral and pro-inflammatory immune responses, improving macrophage-mediated detection and destruction of cancer cells, paving the way for further research on similar strategies across various solid tumors.

RESUMO

O cancro colorretal (CCR) é o segundo cancro mais mortal em todo o mundo, maioritariamente devido à sua alta tendência para metastizar. Apesar dos progressos efetuados na terapêutica, o prognóstico do CCR metastático continua a ser sombrio, com uma taxa de sobrevivência em cinco anos de apenas 14%. Além disso, o microambiente tumoral do CCR, caracterizado pela sua natureza imunossupressora e pH fracamente ácido (aproximadamente 6,5), desempenha um papel significativo na promoção da tumorigénese, permitindo que as células cancerígenas escapem à deteção imunológica e promovam a progressão da doença, influenciando assim os resultados do tratamento.

O 5-fluorouracil (5-FU), tratamento padrão para o CCR, é associado a efeitos adversos graves, baixa biodisponibilidade e baixa especificidade tumoral. Além disso, a IL-12, uma citoquina com potencial imunomodelador em tumores sólidos por estimular a produção de IFN-γ, é limitada no uso clínico devido aos efeitos sistémicos graves inaceitáveis. Estes desafios sublinham a necessidade urgente do desenvolvimento de estratégias terapêuticas alternativas, mais direcionadas e eficazes no tratamento do CCR.

Na tentativa de ultrapassar as questões mencionadas acima, a investigação de estratégias combinatórias que melhorarem o prognóstico da doença e contornem as limitações das monoterapias atuais, tem vindo a ser discutida. O CEA, uma glicoproteína frequentemente sobre-expressa em tumores colorretais, apresenta-se como alvo promissor para o desenvolvimento de novas estratégias para o tratamento desta doença. Deste modo, neste trabalho de doutoramento, desenvolvemos uma abordagem combinatória inovadora usando nanopartículas (NPs) projetadas para atingir não apenas as células do CCR que expressam o CEA, mas também para modular o microambiente imunossupressivo do CCR. Esta estratégia visa melhorar a precisão e eficácia do tratamento, oferecendo esperança para uma melhor gestão do CCR.

Atendendo a uma necessidade clínica significativa, este trabalho de doutoramento envolveu a criação de uma nanoplataforma inteligente com base na conjugação química de um fragmento variável da cadeia simples, anti-CEA (scFv), MFE-23, com os polímeros PLGA-PEG para promover a entrega direcionada da quimioterapia padrão 5-FU às células do CCR. Consequentemente, demonstramos com sucesso a especificidade das NPs desenvolvidas pela afinidade com o CEA, demonstrando um aumento de 3 vezes mais na internalização das mesmas por células que expressam CEA. Além disso, as NPs direcionadas para o CEA e carregadas com 5-FU aumentaram significativamente a citotoxicidade nas células alvo às 24 e 48 horas pós-tratamento, sublinhando uma vez mais a especificidade terapêutica das NPs desenvolvidas. Além disso as NPs foram avaliadas

em relação à segurança da sua administração em macrófagos isolados de doadores saudáveis, confirmando que as NPs desenvolvidas direcionados ao CEA e carregadas com 5-FU não afetavam negativamente a atividade metabólica celular ou a polarização dos macrófagos. Estes resultados realçam, uma vez mais, o seu potencial como uma abordagem de tratamento direcionado seguro e eficaz para o CCR.

Para modular o microambiente tumoral imunossupressor do CCR, desenvolvemos ainda neste trabalho, NPs responsivas ao pH carregadas com IL-12, projetadas para aumentar a eficácia da IL-12 e, ao mesmo tempo, minimizar respostas imunes indesejadas. Neste sentido, no trabalho apresentado é demonstrado que as NPs responsivas ao pH da IL-12 exibiram atividade em pH ~ 6,5, típica de ambientes tumorais, promovendo inflamação anti tumoral através do aumento da libertação de IFN-γ e óxido nítrico (NO), sem afetar adversamente a atividade metabólica dos macrófagos.

Para avaliar e validar o objetivo principal deste trabalho de doutoramento - a especificidade das NPs desenvolvidas, quer como monoterapias quer numa abordagem combinatória – estabelecemos modelos 3D de esferoides MSI com expressão e sem expressão de CEA, que foram capazes de replicar a organização espacial e matriz extracelular de tumores colorretais. Neste sentido, a interação das NPs responsivas ao pH que encapsulavam a IL-12 com os esferóides descritos acima, demonstraram a sua capacidade de resposta ao pH e impacto mínimo nas atividades metabólicas de ambos os esferoides. Além disso, as NPs responsivas induziram efetivamente a polarização de macrófagos, reduzindo os marcadores M2 promotores de tumor e aumentando os marcadores pró-inflamatórios M1, que apoiam a supressão do tumor. Além disso, o tratamento com as NPs responsivas ao pH carregadas com IL-12 aumentaram os níveis de secreção do IFN-γ e diminuíram a secreção da IL-10, enfatizando seu potencial na terapia direcionada ao cancro, devido à indução na modificação do microambiente tumoral no aumento e sustentação da imunidade anti tumoral.

Por outro lado, consistente com observações dos ensaios 2D, as NPs direcionadas para o CEA carregadas com 5-FU demonstraram afinidade especifica em esferoides 3D com expressão do CEA, afetando significativamente a sua atividade metabólica. Além disso, a estratégia combinatória não apenas replicou os efeitos acima mencionados, nas monoterapias, mas também induziu uma polarização vantajosa dos macrófagos, reduzindo os marcadores M2 enquanto aumentava os marcadores pró-inflamatórios M1 e modulando os níveis de citocinas, elevando os níveis de IFN-γ e reduzindo a secreção de IL-10. sublinhando a eficácia da combinação destas terapias.

No geral, a internalização de nanopartículas-alvo mediadas pelo antigénio CEA permite a sua pesquisa em novas direções promissoras para o desenvolvimento de estratégias de quimioterapia em cancros associados ao CEA assim como para os seus locais

metastáticos. Além disso, no conjunto, este trabalho de doutoramento destaca a eficácia das estratégias combinatórias no direcionamento de fármacos para células específicas, enquanto desencadeiam respostas imunes anti tumorais e pró-inflamatórias de modo a melhorar a deteção e a destruição de células cancerígenas mediadas por macrófagos. Deste modo, os resultados apresentados sustentam a abertura de futuras investigações sobre estratégias semelhantes em vários tumores sólidos.

ACRONYMS AND ABBREVIATIONS LIST

1H NMR: Proton nuclear magnetic

5-FU:5-fluorouracil

5FU-CEA-NPs: 5-FU loaded CEA-targeted nanoparticles

Ab: Antibodies

AE: Association efficiency

AJCC: American Joint Committee on Cancer

ANOVA: Analysis of variance

AOM: Azoxymethane

APC: Antigen-presenting cells

ATC: Adoptive T cell therapy

ATCC: American Type Culture Collection

ATP: Adenosine triphosphate

BCA: Bicinchoninic acid assay

BSA: Bovine serum albumin

CAF: Cancer-associated fibroblasts

CAPOX/XELOX: Oral capecitabine plus oxaliplatin

CC: Colon cancer

CD: Cluster Differentiation

CE: Conjugation efficiency

CEA: Carcinoembryonic antigen

CEACAM: Carcinoembryonic antigen-related cell adhesion molecule

CHUSJ: Centro Hospitalar Universitário São João

CIMP: CpG island methylator phenotype

CLM: Colorectal liver metastasis

CMSs: consensus molecular subtypes

COL-I: Collagen Type I

CRC: Colorectal cancer

CTLA-4: Cytotoxic T lymphocyte antigen 4

CTLs: Cytotoxic T lymphocytes

Da: Dalton

DAPI: 4′,6-diamidino-2-phenylindole

DC: Dendritic cell

DCM: Dichloromethane

DL: Drug Loading

DLS: Dynamic light scattering

DMEM: Dulbecco's modified Eagle's medium

DMMA: 2,3-dimethylmaleic anhydride

dMMR: Mismatch repair deficiency

DMSO: Sulfanilamide, dimethyl sulfoxide

DNA: Deoxyribonucleic acid

DOX: Doxorubicin

DSS: Dextran sulfate sodium

ECM: Extracellular matrix

EGFR: Epidermal growth factor receptor

EGFRi: Epidermal Growth Factor Receptor inhibitor

ELISA: Enzyme-linked immunosorbent assay

EMA: European Medicines Agency

EPR: Enhanced permeability and retention

F NPs: Functionalized nanoparticles

FACS: Fluorescence-Activated Cell Sorting

FasL: Fas ligand

FBS: Fetal bovine serum

FDA: U.S. Food and Drug Administration

FOLFIRI: Irinotecan plus infusion 5-FU/leucovorin

FOLFOX: Oxaliplatin plus infusion 5-FU/leucovorin,

FOLFOXIRI: 5-FU/leucovorin infusion plus oxaliplatin and irinotecan

FTIR: Fourier-transform infrared spectroscopy

H&E: hematoxylin and eosin

HEPES: N-2-hydroxyethylpiperazine-N-2-ethane sulfonic acid

ICD: Immunogenic cell death

ICIs: immune checkpoint inhibitors

INFGR: Interferon-gamma receptor

IL-10: Interleukin-10

IL-12 pH-responsive NPs: IL-12 loaded pH-responsive nanoparticles

IL-12: Interleukin-12

ILs: interleukins

IFN-γ: Interferon-gamma

JAK: Janus kinase

KDa: Kilodaltons

KRAS: Kirsten rat sarcoma virus

LDA: Laser Doppler anemometry

LPS: Lipopolysaccharide

Mal: Maleimide

mCRC: metastatic CRC

MDSCs: Myeloid-derived suppressor cells

MEK: Mitogen-activated protein Kinase

MFI: Mean fluorescence intensity

MHC: Complex of histocompatibility

mRNA: Messenger RNA

MSI: Microsatellite instability

MSS: Microsatellite stability

MT: Masson's Trichrome

MW: Molecular weight

NF NPs: Non-functionalized nanoparticles

NF- kB: Nuclear Factor- kB

NH2: aminyl

NK: Natural Killers

NPs: Nanoparticles

OS: Overall survival

PBMCs: Peripheral blood mononuclear cells

PBS: Phosphate buffered saline

PD-1: Programmed cell death 1

PDL-1: Programmed cell death ligand 1

PDXs: Patient-derived xenografts

PEG: Polyethylene Glycol

PFA: Paraformaldehyde

PLGA: Poly Lactic-co-Glycolic Acid

PTX: Paclitaxel

PVA: Polyvinyl alcohol

RC: Rectal cancer

RFU: Relative fluorescence units

RNA: Ribonucleic acid

ROS: Reactive oxygen species

RPMI: Roswell Park Memorial Institute

RT: Radiotherapy

RT: Room temperature

scFv: Single-chain variable fragment

SD: Standard deviations

SEM: Scanning electron microscopy

shRNA: Short hairpin RNA

SR: Sirius Red

SSC: Side scatter

STAT: Signal transducer and activator of transcription

STAT3: Signal Transducer and Activator of Transcription 3

TAAs: Tumor-associated antigens

TAMs: Tumor-associated macrophages

TCEP: Tris(2-carboxyethyl) phosphine

TCM: Tumor cell membranes

TCRs: T cells receptors

TEM: Transmission electron microscopy

TFA: Trifluoroacetic acid

TGF-β: Transforming growth factor-β

TLRs: Toll-Like Receptors

TME: Tumor microenvironment

TNF-α: Tumor necrosis factor-alpha

TNFR: Tumor necrosis factor receptor

Tregs: Regulatory T cells

TSAs: Tumor-specific antigens

TYK2: Tyrosine kinase 2

VEGF: Vascular endothelial growth factor

VEGFi: Vascular Endothelial Growth Factor inhibitor

WT:Wild-Type

CHAPTER I – LITERATURE REVIEW

This chapter was based on the following publications:

- **MJ Silveira**, F Castro, MJ Oliveira, B Sarmento. “Immunomodulatory Nanoparticles for Colorectal Cancer Treatment, a landscape to be explored?” Biomaterials Science, 9, 3228-3243 (2021).

For this review article, I handled the conceptualization, bibliographic research, and composition. The supervisory team took charge of reviewing, editing, and submitting the manuscript. This review has not been part of another PhD thesis previously and is partially reproduced in this thesis. The complete review paper and the journal's authorization for its reuse in this thesis are included in the Appendix.

- **MJ Silveira**, MJ Oliveira, B Sarmento. “Transformative Approaches for Modulating the Colorectal Tumor Microenvironment: An Overview of the Potential of IL-12” (Manuscript in preparation).

Abstract

Colorectal cancer (CRC) is one of the deadliest cancers in the world mainly due to metastasis events. Despite recent improvements, the available treatment modalities for metastatic cases are limited being generally associated with poor prognosis. As well-known the immunosuppressive tumor microenvironment (TME) plays a key role in tumorigenesis, promoting cancer cell immune escape and disease progression. In addition, accumulating evidence indicates that the immunosuppressive microenvironment is a critical barrier for antitumor immunity in CRC, being extremely important to modulate the immune microenvironment and inhibit the tumor-promoting immune response. Therefore, new, and effective cancer immunotherapeutic approaches demand a better control over the TME to reverse these immunosuppressive conditions. Nanoparticles to target immunosuppressive cells, to deliver antigens, immunomodulatory agents or recruit immune cells to the TME, provide a promising strategy to eliminate CRC. In this review, we summarize the importance of TME in the progression and treatment response of CRC, exploring the potential of the nanotechnology for the development of immunomodulatory therapeutic strategies.

Keywords: Tumor Microenvironment; Colorectal Cancer; Immunomodulation; Target Therapies, Nanoparticles.

Background

Colorectal cancer (CRC) is the second most significant cause of global cancer-related deaths [2]. This correlation may be attributed to the occurrence of metastasis, which impacts 15%-30% of patients, and 20%-50% of those initially diagnosed with localized disease [3]. Additionally, metastatic CRC displays a 5-year survival rate of approximately 14% [4].

The dynamic and heterogeneous nature of CRC tumor microenvironment (TME) is being recognized as a critical factor of tumor advancement and treatment response [5]. In fact, tumor cells have the capability to engage with both cellular and non-cellular elements, instigating significant molecular, cellular, and structural alterations within the TME [6]. Moreover, the TME can negatively impact the metabolic activities of tumor, immune, and stromal cells, leading the appearance of different metabolic phenotypes [7].

Besides, the complex interaction of TME and CRC cells, the multistep carcinogenic process and anatomical characteristics of colon and rectum, contributes to the high heterogeneity of the disease [8]. Therefore, to molecularly classify CRC and better predict the treatment, four consensus molecular subtypes (CMSs) have been established, each with distinctive features: CMS1 (microsatellite instability immune) characterized by hypermutation, microsatellite instability, and strong immune activation; CMS2 (canonical) marked by epithelial features and heightened WNT and MYC signaling activation; CMS3 (metabolic) exhibiting epithelial traits and evident metabolic dysregulation; and CMS4 (mesenchymal) displaying prominent transforming growth factor–β (TGF- β) activation, stromal invasion, and angiogenesis [9]. Furthermore, ongoing efforts have been made for a comprehensive characterization of CRC, summarizing histopathologic and RNA sequencing features, TME characteristics, multi-omics attributes, treatment strategies, and prognostic factors [6].

Carcinoembryonic Antigen (CEA) is a glycoprotein present in CRC cells of most patients. However, its production primarily occurs in gastrointestinal tissues during fetal development and ceases after birth [10]. Therefore, high CEA levels are directly associated with the CRC progression, leading to the recommendation of CEA as a prognostic marker for diagnostic and therapy monitoring [11]. Due to its importance in CRC, researchers have explored CEA as a potential target for cancer therapy and diagnostic methods [12].

Currently, a variety of methods, mainly including traditional approaches such as surgery, radiation, and chemotherapy, are employed in the treatment of CRC [5]. Nevertheless, none have been able to completely eliminate this life-threatening disease [13]. Chemotherapy is a commonly therapeutic approach used to treat localized and metastatic CRC (mCRC) and relies on three main drugs: 5-fluorouracil (5-FU), oxaliplatin,

and irinotecan [14]. These drugs are frequently combined in therapeutic regimens known as FOLFOX, FOLFIRI, and FOLFOXIRI, specifically applied to different stages of CRC [15-18]. However, personalized therapies are rising and being approved, involving the combination of chemotherapy with targeted monoclonal antibodies, such as anti-epidermal growth factor receptor (EGFR) or anti-vascular endothelial growth factor (VEGF) antibodies [19]. In addition, over the past decade, the approval of immunotherapy has presented a fresh option for either individual or combined therapeutic approaches in CRC [20]. However, its efficacy relies significantly on tumor's characteristics, including overall tumor mutational burden such as DNA mismatch repair deficiency (dMMR) or high microsatellite instability (MSI-H), as well as in the composition of the tumors, particularly in the infiltration of intratumoral immune cells [21]. Furthermore, the effectiveness of this strategy in CRC is limited, given that the majority of tumors exhibit proficient DNA mismatch repair (pMMR), low microsatellite instability (MSI-L), or stable microsatellites (MSS) [22, 23]. Consequently, ongoing efforts aim to uncover the molecular mechanisms of tumor immunomodulation, to enhance the efficacy of immunotherapies and improve treatment outcomes, particularly in patients who do not respond to conventional treatments [24].

In the TME, interactions such as cell-cell, cell-soluble factors and cell-matrix are considered crucial to understand disease response and overcome therapy outcomes [24]. Particularly soluble factors like chemokines and cytokines, including interleukins (ILs), are pivotal in regulating immune, tumor, and stromal cells [25]. Specifically, IL-12, has been studied in numerous clinical trials for CRC treatment [26]. It activates and induces the secretion of the pro-inflammatory cytokine, interferon-gamma (IFN-γ), promoting robust adaptive immunity and macrophages polarization toward a pro-inflammatory M1-like phenotype, both associated with favorable prognosis in CRC [27]. However, IL-12 is generally linked to high toxicity and severe side effects associated with autoimmunity and nonspecific inflammation [28].

Despite therapeutic advancements, CRC treatment faces challenges like drug resistance, non-specific targeting, low retention, pharmacokinetic shortages and normal cell adverse effects [29]. Novel strategies, particularly those based on nanomaterials, offer potential for safer and more effective anticancer treatments [30].

This literature review summarizes the importance of the TME in the CRC progression and treatment response, highlighting the potential of nanotechnology in developing immunomodulatory therapeutic approaches capable of regulating the TME. Therefore, an overview of CRC biological features, IL-12 based therapies and therapies based on nanotechnology with immunomodulatory effects are presented.

CRC physiopathology and CEA

CRC is a heterogeneous malignancy arising from a cascade of genetic and epigenetic changes that convert normal glandular epithelial cells in the rectum or colon into neoplastic cells [31]. Therefore, the disease begins by initially presenting in colon or rectum mucosa, benign polyps, that gradually advance in size over time [32]. Among these, adenomas, or adenomatous polyps, are the most common, originated from glandular cells that have the potential to become cancerous [17, 33]. On a molecular level, the emergence of these abnormalities correlates with the activation of oncogenes or the deactivation of tumor-suppressor genes [34-36]. Therefore, depending on the source of the mutation, colorectal carcinomas can be categorized as sporadic, inherited, or familial [37]. Consequently, these tumors display a varied background, aligning with one of three tumorigenesis mechanisms: chromosomal instability, microsatellite instability (MSI), or CpG island methylator phenotype (CIMP) [37]. Most colorectal cancer diagnoses stem from sporadic occurrences, commonly linked with the chromosomal instability pathway [38].

Moreover, approximately 10% of adenomas progress to invasive cancer [32]. Once established these malignant cells can spread into the wall of colon or rectum and potentially invade blood or lymph vessels, leading to metastases in distant organs and tissue [33, 39]. CRC is staged according to a system developed by the American Joint Committee on Cancer (AJCC) and the Union for International Cancer Control into five stages which define the prognosis and the treatment decision to be used [40, 41]. This system provides an extended description of anatomy and histological classification remaining the most important guideline [41, 42]. However, despite the variations in molecular genetics, this classification provides limited information about the prognosis and predict response to therapy [43].

The relevant molecular biomarkers for prognostic assessment and therapeutic predictive response constitute relevant factors for CRC pathophysiological understanding and in formulating personalized treatment strategies [44]. Therefore, the use of specific molecular biomarkers, in the clinic, facilitates the use and development of several novel chemotherapeutic drugs [15-18].

CEA is a glycoprotein primarily engaged in cell adhesion expressed in most CRC patients and stands out as a prominent marker to assess both prognosis and recurrence in CRC [45]. Typically, CEA is produced in gastrointestinal tissues during fetal development [45]. However, its production stops before birth and its levels remains undetectable or low in the blood of healthy adults (0–5 ng/mL) [46]. In inflammatory non-neoplastic conditions such as inflammatory bowel disease, hepatitis, pancreatitis and pulmonary infections, CEA presents intermediate levels around 10ng/mL and in gastrointestinal, lung and breast or

metastatic tumors its levels rise until serum titers bigger than 20 µg/L [46, 47]. These findings could be correlated with the secretion of CEA in CRC stages [47]. In healthy intestinal cells, CEA is secreted into the lumen from the apical surface of columnar cells [48]. However, in CRC cells, as polarity diminishes, CEA accumulates at the cell surface [49]. Subsequently, due to the obstruction of gland lumens and the proliferation of adjacent blood or lymphatic vessels, CEA is released into the bloodstream [49]. Therefore, as the tumor grows in size, the level of CEA also rises [48]. CEA, also referred to as CEACAM5 or CD66, is a member of the CEACAM protein family, implicated in tumor progression and metastasis [49]. Consequently, CEA may inhibit anoikis, potentially due to its endoluminal expression and adhesive properties, thereby contributing to tumor pathogenesis [50]. Additionally, as a glycophosphatidylinositol-(GPI-) linked membrane-anchored protein, CEA can be released, facilitating the formation of immune complexes with elicited antibodies [46]. Furthermore, CEA has been shown to modulate anticancer immunity, promoting cancer progression and metastasis [49] and its circulating half-life is approximately 7 days [51].

In CRC, CEA ratio between pre-therapy and post-therapy as demonstrated accuracy to monitor patient response along treatment [48]. Additionally, persistent enhancement of circulating CEA after colorectal surgical resection is associated with worse survival [50], since CEA levels are expected to normalize 4 to 6 weeks after tumor excision [51]. Hence, CEA is being explored for diagnosis applications, targeted chemo and immune- therapies [47, 52].

Understanding TME and immune system in CRC

In a small percentage of patients, CRC can be associated to hereditary mutations. However, most of them are developed due to errors during normal cell division, environmental exposure, or a chronic inflammation condition [53, 54]. Thus, in the last decade, CRC was started to be understood, not only due to the genetic alterations but also as its interactions with microenvironment which is composed for a multiple distinct cell types derived from the neighboring mesenchymal stroma [55-57].

The tumor microenvironment (TME), composed not only by cancer cells but also by resident and recruited inflammatory immune cells, fibroblasts, endothelial cells, inflammatory cytokines, growth factors, stromal cells, stellate cells and adipocytes, plays a key role in host immune system's fight against cancer cells [58]. Inflammatory cells, as well as their cytokines and chemokines, promote and regulate tumor growth, producing an attractive environment by the migration and differentiation of all cell types in the TME, facilitating genomic instability and promoting angiogenesis [59]. As known, inflammation

when controlled contributes for the maintenance of homeostasis [60]. However, chronic uncontrolled inflammation creates an environment with immunosuppressive activity, such as immature or dysfunctional dendritic cells (DCS), anti-inflammatory macrophages, myeloid-derived suppressor cells (MDSCs) and regulatory T cells (Tregs), which favors immune escape and tumor progression [61-64]. Moreover inflammatory signals, such as Nuclear Factor-κB (NF-κB) and Signal Transducer and Activator of Transcription 3 (STAT3) can promote angiogenesis and suppress immune-mediated tumor elimination [58]. Besides, tumor cells produce transforming growth factor-β (TGF-β), interleukin-10 (IL-10) and other immunosuppressive cytokines leading to a permissive TME [65]. Colorectal tumors are also able to recruit Tregs that can further produce immunosuppressive cytokines to suppress cytotoxic T cell response and maintain immune tolerance [65]. Tumor-associated macrophages (TAMs) play also an important role in CRC tumorigenesis, due to its ability to polarize into an anti-inflammatory and pro-invasive phenotype (M2-like) [66]. Furthermore, several immune checkpoint inhibitors are expressed on the surface of cancer cells but also of immune cells, binding to the programmed cell death 1 (PD-1), Fas type I transmembrane protein or cytotoxic T lymphocyte antigen 4 (CTLA-4), receptors expressed on the surface of T cells, suppressing their immune response [67]. Immune tolerance of T cells can also occur through anergy, deletion, suppression or death induced by host regulatory cells, or when T cells ignore antigen-positive cells due to inadequate affinity for host complex of histocompatibility (MHC) molecules (Figure 1) [68].

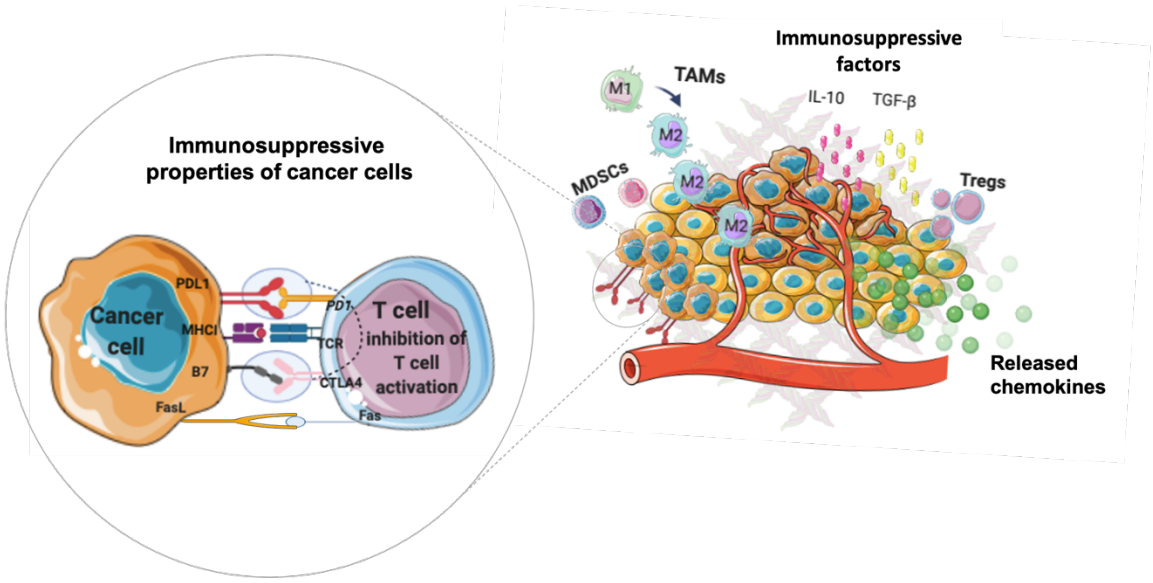


Figure 1- Summary of the immunosuppressive mechanisms in the CRC TME: (i) production and secretion of immunosuppressive factors into the microenvironment (such as TGF-β and IL-10); (ii) recruitment of immunosuppressive cells (Tregs, MDSCs and TAMs), (iii) release of chemokines by the tumor which triggers the accumulation of Tregs and of MDSCs at the tumor sites;(iv) expression of immunosuppressive molecules on the surface of the tumor cells (Co-inhibitory signals such PD-L1 and PD-L2) promoting T cell inhibition. The

ligands of the B7 co-stimulators family (CD80 or CD86) bound to CTLA-4, inactivating T cells. Similarly, membrane-bound programmed cell death ligand 1 (PD-L1) or Fas ligand (FasL) can engage PD-1 or Fas, respectively, of T cells leading to its inactivation or apoptosis.

Similarly, immune escape of tumor cells is connected with three main factors: secretion of immunosuppressive factors; recruitment of immunosuppressive cells, loss of the immunogenicity via down regulation of MCH-I or impairment of T cell activity through the expression of PD-1 or of PDL-1 immune checkpoints [69, 70]. Hence, tumor cells also regulate the immune response being important modulators of the immunosuppressive TME, and crucial orchestrators of the escape to immune surveillance [71].

At the CRC microenvironment, infiltrating B and T cells were found, in tissues and related lymph nodes, both *in vitro* and *in vivo* [72]. CD4+ Tregs are, generally, the most abundant lymphoid subpopulation, having the ability to suppress the activation and function of other immune cells [72]. Moreover, MHCI-loss-detecting Natural Killers (NK) cells were also found in CRC, leading to an ineffective tumor elimination [69]. Additionally, the immune infiltrated tumors with a high amount of CD8+ and CD4+ T cells infiltration within the tumor tissue and surrounding stroma has been associated with favorable outcomes in CRC, suggesting a possible role for immunoediting in the controlling of tumor growth [20, 73]. Thus, in order to predict treatment outcome, recurrence risk and prognosis, CRC tumors are classified in two main subtypes based on their immunoscore: immunogenic, inflamed or hot and non-immunogenic or cold tumors [74]

Currently, the terms ‘hot’ and ‘cold’ are routinely used to classify tumors according to the T cell-infiltration: immune activated with a huge amount of T-cell infiltrated (CMS1), inflamed but non-infiltrated (CMS4), and non-inflamed tumors (CMS2 and CMS3), reflecting well the higher and lower immunoscore category (Figure 2) [75]. Hence, T cells are currently recognized as the key population to fight against tumors, making the use of the immunoscore an attractive option to complement prognosis and to help in guiding treatment selection [75].

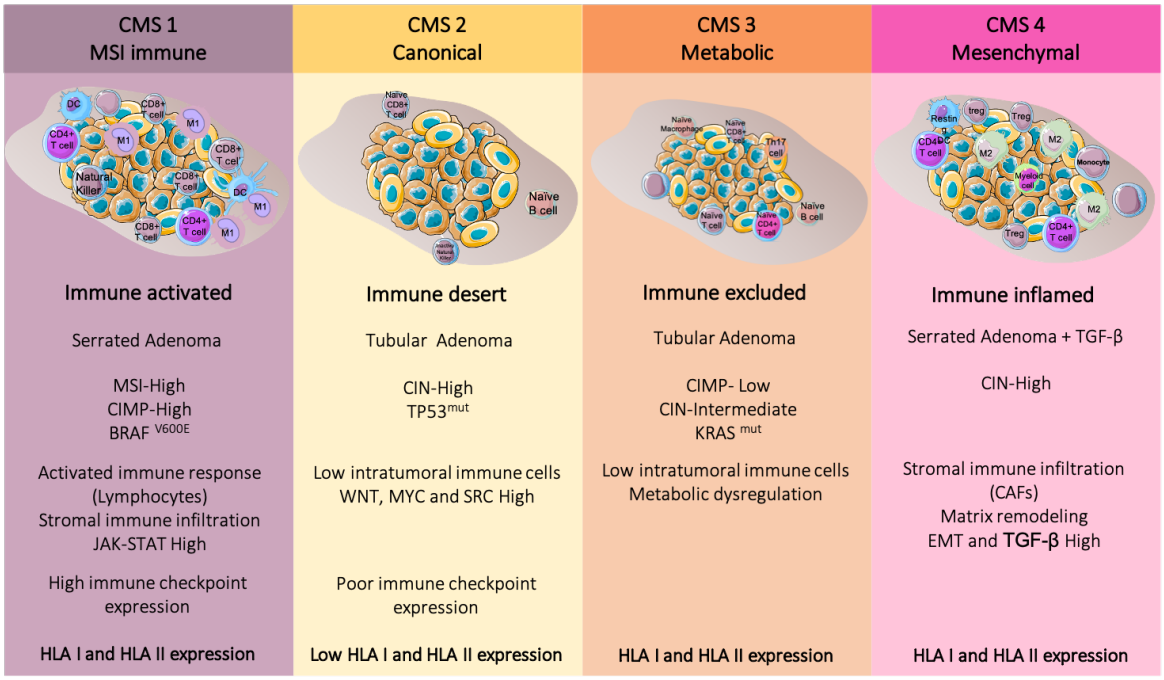


Figure 2 – Schematic illustration of the classification according to the Colorectal Cancer Consensus Molecular subtypes with the genetic modifications and intratumoral immune phenotypes. CMS1 and CMS4 are considered hot tumors due to the intense immune cells' infiltration conferring a specific functional immune landscape. CMS1 tumors are enriched with activated CD4 and CD8 T cells, express high levels of HLA and immune checkpoints and have a high neoantigen load, being highly immunogenic; CMS4 tumors display an unfavorable immunosuppressive inflamed immune environment characterized by the high expression of TGF-β, VEGF, complement components and infiltration by immunosuppressive cells (Tregs, M2 macrophages, MDSCs). However, CMS2 and CMS3 are termed cold tumors due to their similar immune phenotype with poor or low immune cells infiltration. However, CMS3 tumors maintain the HLA and IC expression which differs of the CMS2 [76-78]

Efforts to overcome and define strategies to convert non-immunogenic cold CRC tumors (CMS-2 and CMS-3) into immunogenic inflamed ones and to restore a "CMS-1 like" immune microenvironment in the immunosuppressive CMS-4 subtype tumors are being performed through many clinical trials exploiting new or combined therapies [79]. In that way, the use of the CMS classification model is very helpful to define potential therapeutic options for activating host immune responses taking in account the different strategies to treat hot tumors (CMS1 and CMS4) or to treat the ones with a lack of immune activation, termed cold tumors (CMS2 and CMS3) [80].

In a retrospective analysis, Dienstmann R. and co-workers, evaluated the ratios of CD8+ cytotoxic lymphocytes and cancer-associated fibroblasts (CAF) infiltration in the tumor tissue confirming the linkage of the therapy resistance and the poor outcome of the treatment with the CAF content existing at the tumor microenvironment between different CMS CRC subtypes [81].

Moreover, Li Liang group has studied the impact of the TME, in particularly the histologic and molecular features of different CRC subtypes for better understanding and prediction of the therapeutic efficacy and prognosis (Figure 3) [6]. The classification of CRC was performed into 4 subtypes, being C2 and C3 subtypes associated to the presence of high tumor stroma, while C1 and C4 were associated with active DNA repair and cell proliferation [6]. Additionally, C2 and C4 displayed abundant immune elements [6]. C1, C2, and C3 exhibited low immunogenicity, T cell dysfunction, and T cell exclusion, respectively [6]. In contrast, C4 had extensive anti-tumor immune infiltration, suggesting immune equilibrium and a favorable prognosis, indicating potential immunological control over the tumor [6].

Having this in consideration, understanding the immune mechanisms within the TME and their relationship with CRC evasion and defense launches the basis for enhancing the efficacy of CRC immunotherapies [5]. Specifically, interactions among cells, soluble factors, and the extracellular matrix play crucial roles in shaping immunomodulatory strategies [24].

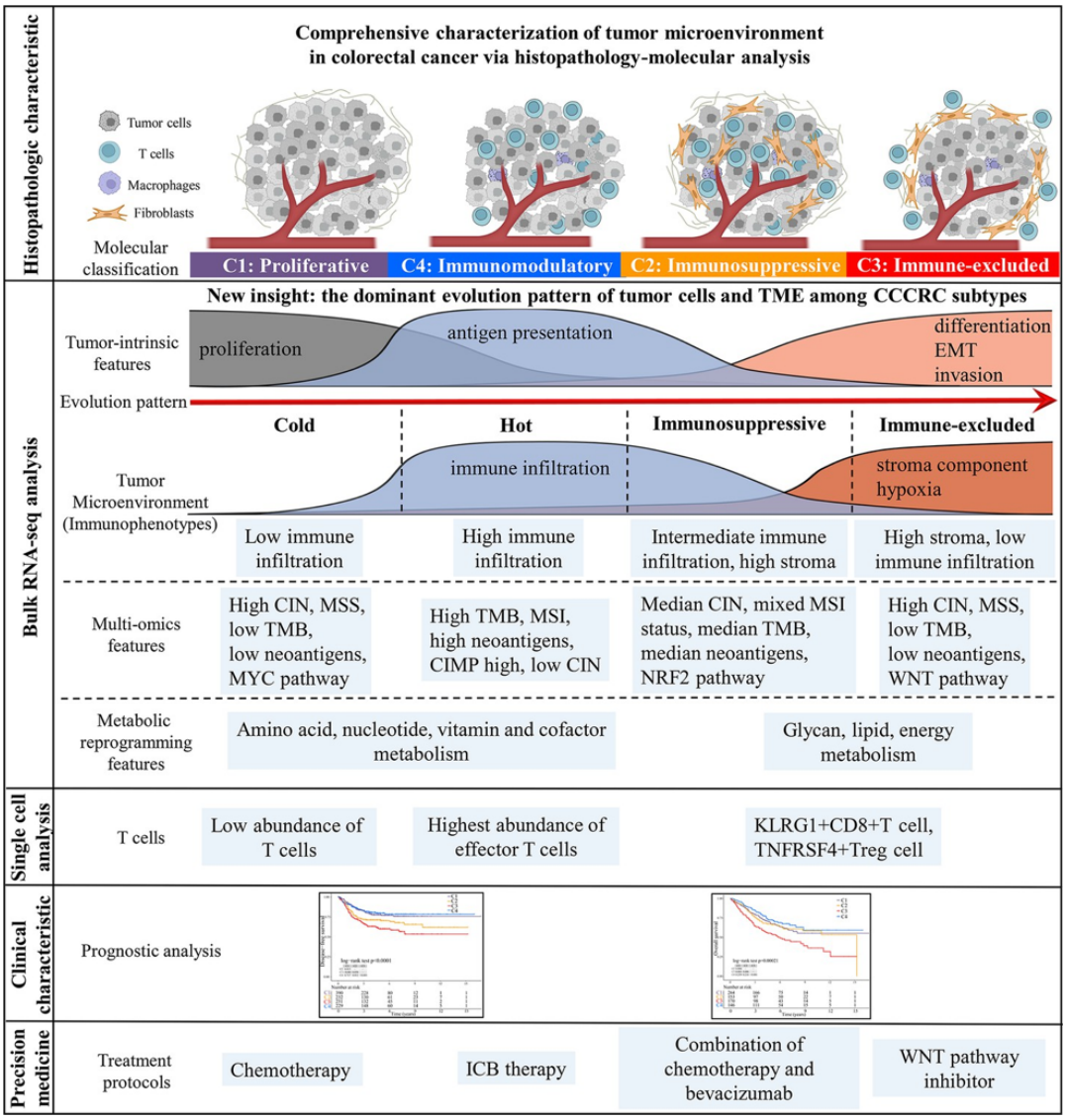


Figure 3 : Summary of the comprehensive characterization features of colorectal cancer subtypes [6]

In summary, the immunosuppressive tumor microenvironment significantly influences the therapeutic response, restricting the efficacy of both conventional and novel immunotherapeutic approaches. Therefore, targeting and modulating the immune TME could be pivotal to enhance current therapeutics and to develop more effective innovative strategies [82-85].

Colorectal cancer therapy

The treatment of CRC is largely based on the stage of the disease [86]. Therefore, the assessment of the tumor stage, presence of malignant lymph nodes and distant metastases as well as of specific molecular markers, help to direct the treatment and to predict the therapy response. In early stages, surgery is the first-line treatment mostly applied [86]. In colon cases, the use of adjuvant chemotherapy can dramatically improve the clinical outcome. However, in rectal cases the use of the neoadjuvant chemotherapy in non-metastatic cancers or stage III is an integral part of the successful treatment [86]. For mCRC, standard treatment mainly includes chemotherapy, surgery, targeted therapies and immunotherapy which can be managed alone or in combination with other therapeutic options [87]. Moreover, those therapies can be combined with radiotherapy in the treatment of rectal cancer [88]. Briefly, the current therapeutics for CRC are discussed below.

Radiotherapy

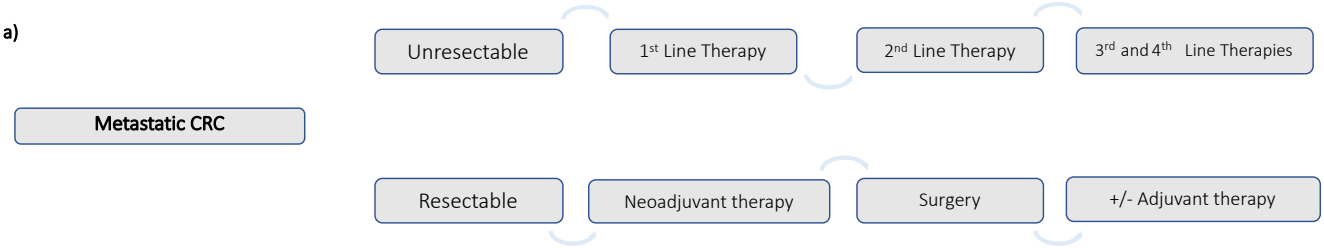
CRC is a complex disease which can be divided into two major subtypes: colon (CC) and rectal cancer (RC) [88]. In early stages, due to the close proximity of the rectum to the pelvic structures and organs, radiotherapy (RT) is indicated as neoadjuvant or adjuvant therapy option for RC, in order to improve the patient OS rates [88]. Chemoradiotherapy can also be associated in the treatment of RC stages II and III as a neoadjuvant therapy, providing a significant reduction of local recurrences [88]. Zhao *et al.,* suggested that neoadjuvant RT can be also adopted for T3/4N+M0 RC with lymph node infiltration but without distant metastasis [88]. In CC, Alexander *et al.,* studied the use of RT as a neoadjuvant treatment for T4 colon cancer patients and demonstrated its impact on improving patients OS, suggesting also that neoadjuvant RT in those patients should be assessed case-by-case, to clearly define its risks and benefits [89].

Chemotherapy

In CRC chemotherapeutic treatment, 5-fluorouracil (5-FU) can be used as a monotherapy or in combination with one or several drugs such, leucovorin (folinic acid),

irinotecan, oxaliplatin and capecitabine [90-92]. These drugs are administrated in adjuvant doublet or triplet chemotherapy regimens named FOLFOX (oxaliplatin plus infusion 5-FU/leucovorin), FOLFIRI (irinotecan plus infusion 5-FU/leucovorin) or FOLFOXIRI (5-FU/leucovorin infusion plus oxaliplatin and irinotecan) and CAPOX/XELOX (oral capecitabine plus oxaliplatin) to treat patients in stage III and IV [14]. In the first line therapy, the single agent-based therapy is given to the patients with poor performance or low risk of deterioration while the combined regimes remain the mainstream [69]. In metastatic cases the use of chemotherapy improved for 20 months patients OS, becoming the backbone of CRC treatment [69]. However, chemotherapy is associated with systemic toxicity, unsatisfying response rates, unpredictable innate and acquire resistance and low tumor-specific selectivity [93-95]. Consequently, in order to refine or even to replace the existing chemotherapy, new approaches were developed taking into account all prognostic markers and factors (genetic profiles, molecular biomarkers and anatomic variances) for a better treatment with minimal adverse effects (Figure 4) [96].

a)



b)

Conventional therapy of 1st and 2nd Line			
KRAS Mut CMS3	BRAF Mut CMS 1	KRAS WT /BRAF WT	
		Right colon CMS4	Left colon CMS2
FOLFOX response or CAPOX +/- VEGFi (bevacizumab)	FOLFOXIRI? + /- VEGFi (bevacizumab) 5-FU no response Immunotherapy response	FOLFIRI response +/- VEGFi (bevacizumab) FOLFOX and cetuximab no response	FOLFIRI response + EGFRi (cetuximab or panitumumab) Response FOLFOX no response

Figure 4 –Schematic illustration of the conventional treatment for mCRC: a) Summarized scheme of the therapeutic approaches, according to the resectability of the tumor; b) Summary of the response of the conventional options to treat mCRC according to the molecular stratification and CMS classification of CRC patients. Mutated [97]; Wild-Type (WT); With or Without (+/-); Vascular Endothelial Growth Factor inhibitor (VEGFi); Epidermal Growth Factor Receptor inhibitor (EGFRi).

In the sense of the CMS stratification, prospective trials are being performed to facilitate the employment of the novel designed treatment strategies, elucidating the need of specific treatments and detaching the one-size-fits-all treatment [78]. Isella and co-

workers, using CRC patient-derived xenografts (PDXs) assessed cancer-cell intrinsic transcriptional features of the different CMS subtypes evaluating the therapy response in those subtypes [98]. Moreover, Medema's team evaluated the therapy response using *in vitro* and *in vivo* models. Both of them, observed a decrease in 5-FU therapy response in CMS1 and CMS4 subtypes [99]. The same approach was performed for CMS2 and CMS3 subtypes showing a better response with FOLFOX therapy in both cases [98, 99]. Finally, in the CMS4 subtype no response for FOLFOX therapy was shown [98, 99]. However, in that case, FOLFIRI therapy was available with good rates of response [98, 99].

Targeted therapies and immunotherapy

Since 2004, targeted therapies have been developed and approved for CRC treatment [69]. Those therapies can directly inhibit cancer cells proliferation and migration or can indirectly act at the level of the TME, impairing the endothelial or immune cells function, hindering tumor growth, attacking or endorsing the immune surveillance [69]. Targeted agents can target specific receptors, inhibiting potential pathways involved on the promotion of cancer cell growth, migration, invasion and metastasis [100]. For instance, the anti-epidermal growth factor receptor (EGFR) inhibitor, Cetuximab, and the anti-angiogenesis inhibitor, Bevacizumab, were the first targeted therapies used to block pathways critical for CRC progression [101]. In fact, these targeted therapies led, when combined with chemotherapy, to an improvement of mCRC patients survival [69]. However, the successful of those therapies often depends on KRAS and BRAF tumor status, reveling the crucial understanding of the molecular pathogenesis of the tumor, to appropriate treatment selection [102].

To elucidate the impact of targeted therapies in CRC CMS subtypes, studies led by Medema's group and Isella correlated the use of different targeted therapies with the outcome in each CMS subtype [98, 99]. Therefore, for CMS1 group, bevacizumab treatment showed a favorable prognosis compared with cetuximab [99]. In contrast, in a clinical trial CALBG/SWOG80405, CMS2 patients with cetuximab treatment had favorable prognosis compared with those with bevacizumab treatment [103]. Both anti-EGFR antibody and anti-VEGF antibody treatments offered fewer benefits for CMS1/4 compared with CMS2/3 [103]. Moreover, in the FIRE3 clinical trial, prognostic difference between anti-EGFR or anti-VEGF agents were not found in accordance with CMS subtype [104]. In other clinical trial, AGITG MAX trial, patients with CMS2/3 showed benefits from the combination chemotherapy with bevacizumab compared with CMS1/4 in the first line chemotherapy [105].

Finally, in CMS4 subtype cetuximab therapy was shown with no response as well FOLFOX therapy [98, 99].

The discovery of immune checkpoints, like PD-1 and CTLA-4, that suppress the immune response against cancer, triggered the development and approval of blocking monoclonal antibodies with the purpose to impair their receptor binding and to enhance immune surveillance [69].

CRC have an extensive and complex signature in terms of mutational and TME immune cells infiltration burden [106]. Therefore, the immunogenic microenvironment differs in subgroups of CRC limiting the applicability of the immunotherapy in that different subgroups [76]. Patients with CRC, who have mismatch repair-deficient (dMMR) and/or microsatellite instability-high (MSI-H) tumors, are treated with immune checkpoint inhibitors (ICI) therapy with durable responses [107]. Nivolumab and pembrolizumab, as well as nivolumab in combination with low-dose ipilimumab (all ICIs), are currently approved by the U.S. Food and Drug Administration (FDA) for patients with MSI-H/dMMR mCRC which progressed following treatment with fluoropyrimidine, oxaliplatin, and irinotecan [108]. In regard of CMS subtypes, studies led by Medema's group exhibited a good response in MSI CMS1 cell lines and MSI PDX treated with immunotherapy [99].

Overman *et al.* examined the efficacy of nivolumab alone and in combination with ipilimumab in patients with dMMR-MSI-H CRC with high T cells infiltration burden, evidencing an increment of 73% and 85% twelve-month OS rate, respectively [109]. However, tumors with reduced inflammation and T cell infiltration, such in proficient MMR-MSI-Low (pMMR-MSI-L) or Microsatellite Stable (MSS) colorectal tumors, immunotherapy was not effective. Thus, to develop a combinatory targeted therapy, Eng *et al.* combined a Mitogen-activated protein Kinase (MEK) inhibitor with an anti-PD-L1, demonstrating an increase of infiltrated CD8+ T cells but without any improvement in the response or survival in mouse models [110]. Therefore, to apply the promising immunotherapy to tumors with a low mutational and immunogenic profile, unable to stimulate immune cells recruitment and activation, novel strategies, such vaccinations and adoptive T cell therapy (ATC), are currently being explored [106].

Vaccines comprise a promising strategy which can induce an immune response through a direct stimulation of the immune system by delivering antigens to dendritic cells (DC) – antigen-presenting cells (APC), which prime and activate CD4+ and CD8+ T cells to initiate tumor destruction [106]. Cancer vaccines can deliver tumor-associated antigens (TAAs) or tumor-specific antigens (TSAs) allowing T cell binding to these antigens and promoting tumor cell recognition and elimination by the immune system [111]. Also, approaches like ATC, which are specific for a particular mutated antigen, may prove favorable options in combination with ICI [106]. Gros *et al,* proved that circulating PD-1^{+}-expressing CD4+ and CD8+ lymphocytes can recognize human gastrointestinal cancer neoantigens, allowing the identification of circulating neoantigen-reactive lymphocytes or T

cells receptors (TCRs) constituting an attractive strategy for the development of personalized immunotherapies targeting neoantigens [112].

Furthermore, TGF-β signaling has been shown by Mariathasan *et al.* to cause resistance to ICI. They also proved, that the inhibition of TGF-β signaling in combination with ICI led to a greater tumor regression, in preclinical studies using EMT6 mouse mammary carcinoma model [113].

Additionally, new combinations of treatments should be developed to produce an improvement in the response to ICI in dMMR-MSI-H CRC, and thereby in the response that has not yet been achieved in pMMR-MSI-L CRC.

Immunomodulatory therapeutic strategies for CRC

The molecular interactions at the CRC TME are the key factors for tumor inflammation and modulation [20]. Interactions among cells, soluble factors, and the extracellular matrix play crucial roles in shaping immunomodulatory strategies [24].

At the TME, cell-cell interactions may regulate anti-tumor immune responses [114]. These interactions, facilitated by surface receptors and ligands, can trigger signaling in engaged cells, dictating their behavior [24]. Therefore, cancer cells carry genetic mutations, yielding neoantigens recognized by the immune system [115]. The over-express antigens, termed tumor-associated antigens (TAAs), such CEA can constitute a unique opportunity since they can be fragmented and presented on antigen-presenting cells (APCs) for recognition by T cells [115]. Additionally, immune cells, specially, T cells can induce tumor cell apoptosis via FasL or TRAIL binding, potentially limiting tumor growth [116] . However, CRC cells may resist T-cell-induced apoptosis and upregulate FasL, suppressing anti-tumor T cell responses [116]. Moreover, CRC cells can escape cytotoxic T lymphocytes recognition by downregulating MHC I expression or inhibit natural killer cells activity through binding of the MHC I present at tumor cells surface to iKIR (inhibitory killer cell immunoglobulin-like receptor) [117].

Phagocytosis, is a vital process for clearing dying cells triggered by pro-phagocytic signals like calreticulin, often upregulated in MSI-H CRC [117]. However, tumor cells can express anti-phagocytic receptors like CD47 (“don’t eat me signal”), inhibiting macrophage phagocytic activity [118]. Additionally, β2-microglobulin and CD24, also known as "do not eat me" signals, act by binding to LILRB1 (leukocyte immunoglobulin like receptor B1) and Siglec-10 on TAMs [118]. Moreover, existing cell-cell interactions may involve crucial receptors in different innate immune mechanisms like antibody-mediated interactions or immune clearance [24].

Soluble signals, particularly cytokines and chemokines, present a crucial role in immune response maturation and on all cell-cell interactions aforementioned [119]. In fact, soluble factors may be released into the TME through controlled secretion by immune, tumor, or stromal cells, or through uncontrolled release during cell death [119]. In CRC, chronic inflammation, associated to high range of cytokines, is a crucial hallmark [120]. Inflammatory cytokines, are associated with the immune regulation of tumor cells [119]. Moreover, interleukins, interferons, growth factors, and chemokines are the main representatives at the CRC TME [119] .

Tumor Necrosis Factor-α (TNF-α)

Tumor necrosis factor-alpha (TNF-α) is a cytokine, primarily released by activated macrophages and tumor cells that promotes inflammation, angiogenesis, and tumor dissemination [121]. Moreover, TNF-α is correlated with acute phase responses, mediated by the regulation of cytokine production, such as in inflammatory bowel disease [122]. Additionally, TNF-α enhances vascular permeability, leukocyte recruitment, oncogene activation, tumor invasion, and angiogenesis [123]. TNF-α, can also be described as tumor-promoting factor, when expressed by tumor cells since it can induce immune cell apoptosis and consequently, downregulation of the CRC immune response [124]. Moreover, TNF-α exhibits dual effects on tumorigenesis, mediated by two primary receptors: the ubiquitously expressed 55 kDa TNFR1 and the more selectively expressed 75 kDa TNFR2, found mainly in immune cells [125]. While TNFR1 orchestrates complex pro-apoptotic or pro-survival signals, TNFR2's role is less understood but involves moderating TNFR1-induced apoptosis, especially in immune cells [126]. Therefore, several authors have been studying the expression of TNF-α mRNA in CRC different stages and comparing with the normal tissue, finding high levels of TNF-α genes associated with advanced stages of the disease (Stage III and IV) comparing with early stages [126, 127]. Consequently, TNF-α can constitute a promising targeting for diagnosis of CRC stage and treatment prognosis [126]. Although, anti-TNFα monoclonal antibodies have been explored to act as inhibitors of tumor progression, in the TME of CRC orthotopic transplant mice models [128], targeting TNF-α immunotherapy did not enter yet in the clinical use [129].

Interferon-gamma (IFN-γ)

Interferon-gamma (IFN-γ), or type II interferon, is a crucial cytokine in innate and adaptive immunity, showcasing antiviral, immune regulatory, and antitumor functions by bolstering natural killer (NK) cell activity, antigen presentation and leukocyte migration [130]. Additionally, IFN-γ activates macrophages and augments Class II MHC expression,

primarily sourced from NK cells, CD4 Th1 cells, CD8 cytotoxic T lymphocytes (CTLs), and non-cytotoxic innate lymphoid cells (ILCs), when stimulated by other cytokines like IL-12 and type I INFs [131]. Therefore, IFN-γ interacts with the INFGR receptor, promoting Th1 immune responses while inhibiting Th2 and Th17 responses [130]. Additionally, IFN-γ promotes M1 polarized macrophages, MHC expression, and APCs, enhances cytotoxicity in T and NK cells, and hinders tumor proliferation, thus being explored in CRC immunotherapy trials [24]. IFN-γ initiates gene expression via the JAK–STAT pathway, activating JAK tyrosine kinases and phosphorylating STAT1, which translocate to the nucleus where they regulate the activity of promotors, inducing the transcription of sevral IFN-γ responsive genes [132]. It also prompts transcription factors like IRF1 and CIITA, facilitating the expression of genes encoding inducible nitric oxide synthase and class II MHC, favoring the expression of pro-inflammatory genes [133].

Genetic variants of IFN-γ and its receptor associate strongly with CRC risk and patient survival [1]. Deficiency in IFN-γ or on its receptor losses fosters colorectal cancer development, whereas its specific expression activates innate immunity and inhibits tumorigenesis [134]. However, IFN-γ signaling may impair antitumor immunity by inducing immune checkpoint molecules on T and tumor cells [135]. Additionally, it acts as a cytotoxic cytokine, prompting tumor cell apoptosis [119]. The IFN-γ/JAK2/STAT signaling pathway drives programmed death-ligand 1 (PD-L1) expression in various cancers, correlating with poor CRC prognosis [119]. PD-L1 expression on tumor-infiltrating immune cells also correlates with CRC patient survival [119].

IFN-γ exhibits survival benefits in bladder carcinoma and melanoma, especially in stage 2 and 3 ovarian carcinomas[97]. Although not approved for CRC, it is under investigation in some clinical trials, being crucial to elucidate the need of more exhaustive research on the IFN-γ pathway in CRC and on its interaction with intestinal flora to potentially enhance cancer treatment by leveraging the immune system [136]. Recently, a phase I trial combining IFN-γ and nivolumab in metastatic solid tumors reveals mostly low-grade, IFN-γ-related adverse events, with three dose-limiting toxicities at higher doses [137]. Moreover, correlative assessments indicate monocytes with increased PD-L1 expression correlating with IFN-γ dose and duration [137]. Notably, IFN-γ have being also associated with inducing enhanced levels of circulating chemokines [137].

Interleukins (ILs)

Interleukins (ILs) are a subgroup of cytokines crucial for modulating immune cell functions during inflammation [120]. From the past years, they are being categorized over 40 subfamily members according to their genomic organization, structure, or receptor-binding properties. Therefore, according to their structure, ILs interact with various cells,

impacting the immune system and influencing cancer development [119]. Particularly, in CRC, ILs have been described with significant roles promoting tumorigenesis, growth, angiogenesis, invasion, and metastasis [138]. Furthermore, ILs are produced by distinct cell types, regulating immune cell activation, differentiation, proliferation, migration, and adhesion, with both pro- and anti-inflammatory properties [138]. ILs are also, largely defined as acting through high-affinity receptors on cell surfaces, leading to different functions in paracrine and autocrine responses [139]. Moreover, according ILs impact during different stages of CRC and tumorigenesis, they are being explored as potential biomarkers [140]. Considering the ILs pivotal roles in orchestrating the TME and in regulating interactions between tumors and immune cells, ongoing clinical trials have been raised with promising prospects for CRC diagnosis and treatment [140]. However, there are insufficient research correlating cytokine profiles with clinical utility in cancer diagnosis, primarily due to a limited understanding of their interactions and regulatory mechanisms in healthy individuals [119].

Nevertheless, the generated knowledge correlating cytokines and cellular impact in CRC has facilitated the development of novel therapeutic strategies involving their neutralization and the use of recombinant and engineered forms [140].

Particularly in CRC, IL-12 has gained attention due to its predominant production by myeloid cells and its protective role by inducing IFN-γ expression [141]. IL-12 is a cytokine with two subunits encoded by separate genes, IL-12A (p35) and IL-12B (p40). Moreover, upon protein synthesis, these genes produce an active heterodimer known as p70 and a homodimer termed p40 [142]. Interestingly, the IL-12A consists in four alpha helices, while IL-12B comprises three beta sheet domains [142]. IL-12 mechanism of action involves binding to IL-12 receptor chains IL-12Rβ1 and IL-12Rβ2, initiating the Janus kinase (JAK)-signal transducer and, consequently, activating the transcription pathway [143]. Therefore, IL-12Rβ-1 starts to recruit the tyrosine kinase 2 (TYK2), while IL-12Rβ2 binds to JAK2, leading to their phosphorylation [143]. Afterwards, the activated transcription factors translocate to the nucleus, where they regulate gene transcription mainly through STAT4, although STAT1, STAT3, and STAT5 may also be involved with minor functions [143]. Phosphorylated STAT4 dimerizes and regulates gene transcription by binding to target DNA of IFN-γ [143]. This cascade ultimately leads to IFN-γ production and secretion [142]. Additionally, IL-12p70 heterodimer activates T and NK cells, stimulating IFN-γ secretion, while IL-12p40 monomer competitively binds IL-12R without inducing IFN-γ production [24]. Moreover, IL-12p70 promotes differentiation of naïve CD4+ T cells into Th1 cells, enhancing cytotoxic adaptive immunity and polarization of macrophages towards a pro-inflammatory M1 phenotype, associated with favorable CRC prognosis [24]. Despite IL-12's focus in CRC trials, its high toxicity limits clinical benefit [144]. Improved IL-12 administration or combined

immunomodulatory strategies or IL-12 delivery mediated-nanoparticles may enhance anti-tumor efficacy, warranting further investigation.

Extracellular matrix-mediated CRC immunomodulation

The CRC TME comprises the most abundant and important non-cellular component, the extracellular matrix (ECM), which tightly regulates cell behavior by providing adhesion sites, controlling the release of cell-secreted factors, presenting matrix-bound factors, and supplying bioactive ligands [145]. The ECM is produced mainly by fibroblasts and constantly remodeled by cells through the secretion of matrix metalloproteases (MMPs) and tissue inhibitors of matrix metalloproteases (TIMPs) [146]. Particularly, at the CRC the extracellular matrix is marked by increased fibrillar collagens, particularly type I collagen which leads to dense, fibrotic, and a stiffer microenvironment [147]. The CRC stiffness affects biomechanical sensors that regulate immune cell recruitment and function, impairing T cell activity and promoting macrophage infiltration [148]. Additionally, ECM glycoproteins, like fibronectin and tenascin, are overexpressed further modulating the biomechanical properties of the TME and providing additional cell-matrix adhesion sites [148].

Collagen is a classic key component of the ECM, which plays a significant role in promoting the advancement of CRC, suggesting novel avenues for clinical treatments and potential biomarkers [145]. Therefore, cancer cells alter collagen to drive neoplasia, invasion, and metastasis [145]. In the TME, collagen reduces chemokine production, hampering the anti-tumor immune response [149]. Additionally, researchers have reported, type I collagen as an element that may accelerate cancer growth by regulating immunosuppressive factors as TGF-β, IL-18 and CCL18 [150]. Moreover, upregulated expression of collagen-related genes as COL1A1-2, COL3A1, COL4A3, COL4A6, and MMP2 have been associated with worse CRC prognosis, serving as potential biomarkers for CRC prognosis [151].

Increased levels of collagen type I, III, and IV are being identified in CRC patients' sera, particularly in more advanced stages [24]. In this context, several efforts have been made to identify potential biomarkers for CRC, with type I collagen emerging as a promising candidate due to its elevated levels in tumor tissues compared to healthy tissues [152]. Furthermore, type I and IV collagen are upregulated in the urine and plasma of patients with colorectal liver metastasis (CLM), respectively, suggesting their clinical relevance in CRC [146]. Circulating type IV collagen levels notably rise in patients with liver metastases, indicating its potential as a potential prognostic marker [146]. Combining type IV collagen with CEA enhances CLM detection compared to using either marker alone, making type IV collagen a promising marker for postoperative CLM recurrence detection [152].

Overall, the components of the CRC TME present promising potential for targeted therapeutics and diagnostic biomarkers. However, some challenges in regard its poor characterization, toxicity and degradation highlight the need for urgent alternative approaches.

Nanomedicines for enhanced therapy and diagnosis

Cancer diagnosis and therapy improvements in both conventional cancer therapies or modern immunotherapies have been described [153]. However, they remain unsuccessful due to low molecular bio-availabilities, toxicity, molecular instability, short half-time and lack tumor-targeted precision which leads to undesirable side effects [153].

Nanomedicine brings to the healthcare a bright side on the landscape [154]. Advancements in understanding CRC biology and its TME interactions led to the development of nanoparticles (NPs) capable of delivering insoluble drugs to both local and distant tumor sites, thereby minimizing systemic side effects [155]. In this context, NPs brought new possibilities for drug design based on factors like shape, charge, stability, and selective binding capacity, improving stability, pharmacokinetic and pharmacodynamic properties of drugs, mitigating side effects, prolonging drug release, and reducing the dosing frequency [156]. Depending on the chosen biomaterial for NPs design, they can possess attributes such as biocompatibility, non-immunogenicity, non-toxicity, and biodegradability as well as short, tubular or non-rigid physical characteristics associated with higher intratumoral invasion capacity [155].

Poly lactic-co-glycolic acid (PLGA) is a biomaterial, considered the “gold standard” polymer for its biodegradability and biocompatibility [157]. Moreover, PLGA is an FDA approved polymer, extensively employed in controlled release systems, to effectively store cargoes of both small molecules and macromolecules, facilitated by hydrolysis-mediated PLGA degradation, and precisely regulation of their release kinetics [158]. Additionally, depending its monomer ratios (lactide:glycolide: 75:25, 60:40 or 50:50) or molecular weights , PLGA has different degradation rates [159]. In this context, lactide:glycolide copolymer ratios have been described with potential impact on encapsulation, physicochemical properties, stability, and release in lysosomal conditions [160]. Moreover, PLGA offers versatility in manufacturing injectable nanospheres, making it a preferred choice over other polymers for controlled release applications [158]. Additionally, when PLGA is shielded with polyethylene glycol, PEG, FDA and EMA approved enables surface ligands to attach with reduced immunogenicity while maintaining activity [156].Therefore, PEGylated strategies facilitate targeted drug delivery through the selective binding of ligands carrying drugs to receptors on tumor or immune cell surfaces[156]. Moreover,

PEGylation, the attachment of PEG to drugs or nanoparticles, enhances circulation time and reduces host responses since PEG decreases protein adsorption, thereby evading recognition by the mononuclear phagocytic system [161]. PEGylation strategies are typically approached through three distinct processes: PEG adsorption, involving the physical adherence of PEG to NPs via physical adsorption; Covalently bound PEG, where PEG is securely grafted onto the surface of NPs by forming stable chemical bonds and Self-assemble PEG, where PEG can conjugate with hydrophobic molecules to form macromolecules that self-assemble with themselves or other compounds [162]. Therefore, several studies have been reported the impact of increasing PEG's MW, defining MW ranging from 2 to 20 kDa, to prevent aggregation and adsorption to blood components, resulting in extended circulation time in vivo [163]. Furthermore, PEG MW ranging from 20 to 50 kDa has been described for the conjugation of small compounds [163]. Conversely, PEGs with lower MW (1–5 kDa) are preferred for the conjugation of antibodies or NPs, leading to prolonged blood circulation and reduced uptake by the mononuclear phagocytic system [163]. Researchers found that the total amount of protein adsorbed onto NP surfaces significantly decreased as PEG MW increased up to 5 kDa [164]. However, no further decrease in protein adsorption was observed as PEG MW was further increased to 10, 15, and 20 kDa. All PEG MW values ≥ 5 kDa tested provided approximately a 75% decrease in protein adsorption to the PLA-PEG NP surface compared to PLA NPs [164].

Drug delivery nano systems are designed to enhance the accumulation of NPs and the efficacy of drugs or molecules within tumors and their respective TME, mostly achieved through passive or active targeting strategies [155]. Therefore, active targeting involves conjugating targeting moieties, such as aptamers, ligands, and antibodies, onto the surface of nanocarriers to specifically recognize tumor cells [165]. Consequently, ligand-modified NPs binds to overexpressed receptors on the tumor cell surface, and the receptor-mediated endocytosis is triggered, leading to increased internalization of nanocarriers and thus higher therapeutic efficacy with reduced systemic adverse effects [165].Additionally, passive targeting approaches are associated with efficiently extravasation and accumulation in the tumor through the enhanced permeability and retention (EPR) effect, to achieve therapeutic effects in tumor tissues [165].

Stimuli-responsive nanocarriers hold the promise of transforming cancer treatment by facilitating the precise delivery of drugs to disease sites [166]. Employing polymeric nanocarriers with surfaces responsive to triggers like pH, light, temperature, and redox potential enables targeted drug distribution [166]. pH is especially advantageous, as the lower pH in TME can induce alterations in drug release [167]. Recent progress in the advancement of pH-responsive polymeric NPs has demonstrated significant potential for enhanced in vivo drug delivery, mitigated adverse drug reactions, and more accurate drug

distribution [168]. 2,3-dimethylmaleic anhydride, DMMA, is a hydrophilic molecule and can be used for charge-reversal under slightly acidic conditions and is being investigated by several authors for pH-responsive NPs development to achieve effective cancer treatments. Chen et al. reported that pH/redox-responsive NPs to regulate tumor hypoxia, modified with DMMA undergoes a surface charge reversal, resulting in a thick negatively charged shell and a positively charged disulfide cross-linked core [167]. Furthermore, other researchers explored a pH-responsive aggregation nanosystem (Au@PAH-Pt/DMMA), hydrophilic in a normal physiological environment, but with stealthiness loses in the TME due to the breach of the DMMA shed, inducing irreversible self-aggregation of the nanoparticles, a process termed a "charge-reversal-like" strategy [168].

Therefore, NPs loaded with drug-carrying polymers improved drug absorption and exerted increased toxicity on tumor cells, effectively delivering desired molecules to the TME.

Immunomodulatory nanomedicine to improve CRC therapy

Despite the success of the immunotherapy to target the cancer immune system, its applicability is still reduced and restricted to a small subsets of patients, with low survival rates for the most solid cancers [169]. Furthermore, challenges associated with the limited efficacy and significant toxicity are also being faced [170]. Therefore, efforts to develop new immunotherapeutic agents, combined strategies or nanocarriers for their delivery, are being made, in order to increase the number of patients who benefit from this therapy [171].

In fact, nanomedicine can constitute a promising approach to improve the performance of immunotherapy, decreasing its toxicity and refining its efficacy. In 1995 the commercial approval of Doxil, a liposomal nanomedicine, and afterwards of Abraxane, albumin nanoparticles, for cancer treatment led to the development of several nanoformulations [30]. Additionally, those developed nanoformulations were achieved with higher tolerant dosages of chemotherapeutic drugs due to less accumulation at off-target organs and tissues, stimuli-sensitive behavior for safe trafficking and drug release, and prolonged half-lives of bioactive cargo molecules by avoiding degradation by enzymes during blood circulation [172, 173]. Nowadays, preclinical and clinical data, including nanoformulations in clinical trials such mRNA nanovaccines (NCT03313778, NCT02410733) for the treatment of solid tumors and melanoma, have been demonstrating that combining nanomedicine with immunotherapy can boost its therapeutic effect, given its ability to engage immune cells, immunomodulate the tumor, and accumulating at systemic compartments [171].

Nano-immunotherapy has the potential to turning “cold” non-immunoresponsive tumors into “hot” immunoresponsive, due to its facility to target cancer cells or their TME and peripheral immune system, through the delivery of antigens, immunoregulatory agents and adjuvants [170, 174]. Nanomedicines used to target cancer cells can induce immunogenic cell death (ICD), triggering the release of tumor antigens, proteins and adenosine triphosphate (ATP), which prime the activation of more antigen presenting cells (APCs) and consequently, recruit myeloid and lymphoid populations and promote T cells antitumoral activities [175, 176]. Moreover, nanomedicines have the ability to target and inhibit immunosuppressive cells and molecules at the TME, reducing their expression [177]. They can also be employed to target the peripheral immune system, to promote the activity of APCs, of cytotoxic T cells production and to increase the activity of peripheral effector immune cell populations, generating anticancer immunity (Figure 5) [178].

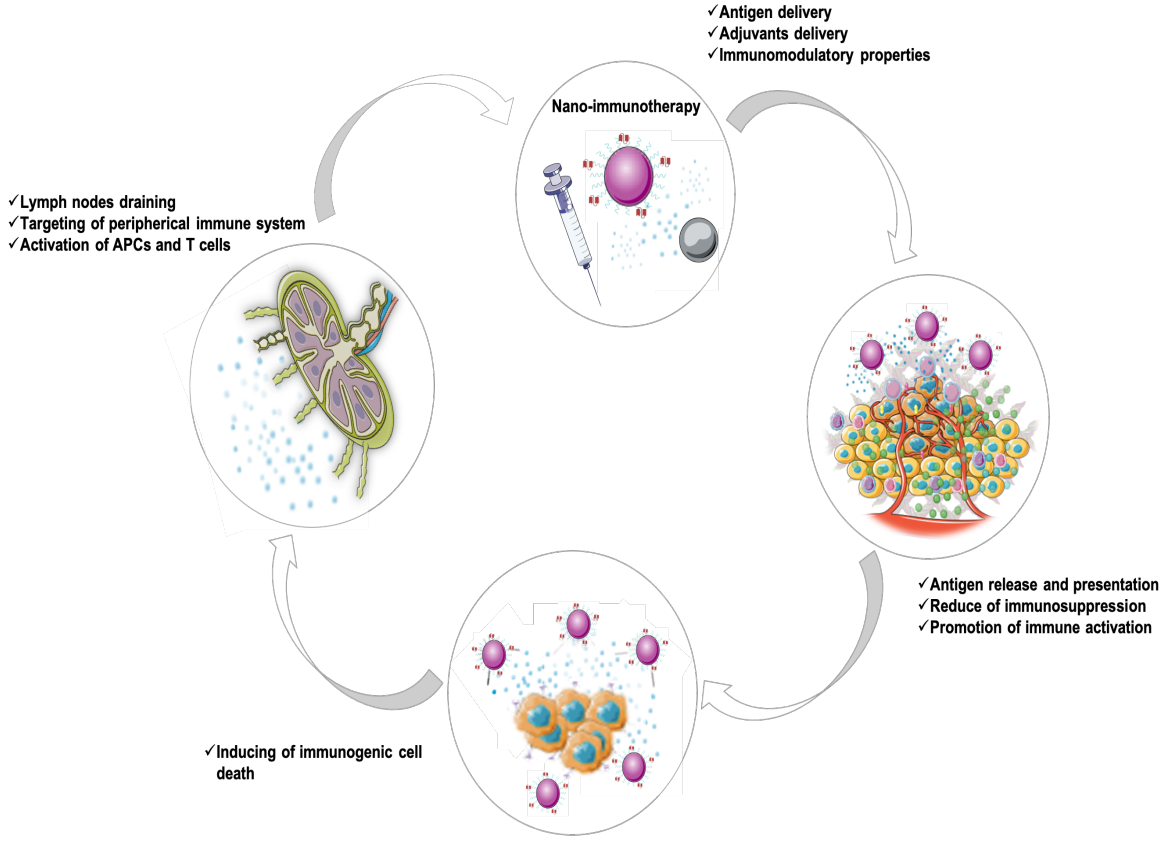


Figure 5 – Schematic illustration of the different targeting strategies in nano-immunotherapy.

Moreover, nanomedicines have also the ability to react with some up-regulated chemical species such, H^+, H_2O_2 and reactive oxygen species (ROS) within the TME, leading to its modulation through its elimination or control [179].

Currently, nano-immunotherapy is included in the majority of the preclinical studies and in emergent clinical trials [180]. Considering the complexity of CRC microenvironment, nano-immunotherapy can offer an opportunity to reverse immunosuppression, induce

immune response and generate memory immune cells for long-term cancer control [181]. Despite the majority of CRC patients are MSS, Mismatch Repair proficient (pMMR) or Mismatch Repair deficiency dMMR, new efforts to revert the immunosuppressive TME from non-responsive T cells into responsive ones have been done [182]

The following sections and table 1 focus and resume the relevance of nano-immunotherapy for CRC treatment.

Table 1: Summary of the nano-immunotherapies being explored to improve CRC immunity and treatment.

NP Composition	NP cargo	Major advances	Immune phenotype Advances	Ref.	Model
iDR-NCs PPT-*g*-PEG to assemble CPG and *Stat3*-silencing shRNA	Neoantigen (AdpgK)	Target delivery Increase of APCs and activation of CD8+ T cells Increase of antitumor immunity	Higher expression of CD80, IL-6, IL-12p40 and TNFα in LNs	[183]	*In vitro* studies: RAW264.7 cell line; *In vivo* studies: C57BL/6 mice bearing MC38 syngeneic colon adenocarcinomas
LPC with DSPE-PEG-Mannose	CpG, 2'3'cGAMP, or 5'pppdsRNA and p-AH1-A5	Efficiently co-encapsulation of phosphorylated peptides/adjuvants Decrease of liver metastasis, Tregs and MDSC population	Higher expression of CD8+. Lower expression of CD4+, FOXP3+, CDllb+, and GR-1+ in primary CRC tumor	[184]	*In vivo* studies: BALB/c mice CRC liver metastasis using the CT-26 model
BanNV with PEG-PLA micelles and CpG-encoding template DNA, microparticles self-assembled with PEG-g-PPT	TLR7/8 agonist (R848); TLR9 agonist; CPG ODNs and a Neoantigen (AdpgK)	Codelivery of adjuvants and neoantigens to LNs and LN-residing APCs Increase in antigen uptake and APCs, therapeutic efficacy and survival rates	Higher expression of CD8+, IL-6, IL-12p40, TNFα. CD80, CD86 and CD11c in LNs	[185]	*In vivo* studies: C57BL/6 mice with MC38 cells injected
TCL@PDA NPs	-	Increase of the Cellular uptake Delay of the tumor progression Increase of activated CD8+ and CD4+ T cells Ability to modulate DC maturation	Higher expression of MHC I, MHC II, CD40, CD86, CD80, CD11c IL-6, IFN-γ and TNF-α, CCR7 in BMDCs and LNs. Higher percentage of CD44Hi CD62LHi cells in CD4+ and CD8+ T cell population in spleen and LNs.	[186]	*In vivo* studies: C57BL/6 mice with MC38 cells injected *In vitro* studies: MTT and Cytotoxicity Assay
PCN@FM	PDT	Increased safety Decreased cytotoxicity	Higher expression of CD86, CD80 and CD3+ in the tumor tissues	[187]	*In vitro* studies: CT26 mouse colon cancer cells *In vivo* studies: BALB/c with injected 4T1cells
NP@FM PEG	-	Biocompatible	Higher expression of CD86 and CD80	[188]	*In vitro* studies: 4T1 cells, 3T3

		Low cytotoxicity Achievement of LNs and APC Increase of T cell activation; CD3+ and CD8+ CTLs	DC, IL-6, TNF-α, CD3+, CD8+ in BMDCs and Higher expression of CD3+, CD8+LNs		cells and CT26 cells *In vivo* studies: BALB/c with injected 4T1cells
AgNP M13@Ag	Anti-PD1 FOLFIRI	APCs activation Increased of the survival	Higher expression of CD86, CD80 and CD11c and CD86-positive M1-phenotype macrophages in BMDCs Higher expression of CD8+ and IFN-γ in spleen and tumor tissues Decrease of Tregs and MDSCs markers as well as IL-10 expression in spleen and tumor tissues	[189]	*In vitro* studies: CT26 cells and 3T3 cells *In vivo* studies: BALB/c mice with injected CT26 cells
sHDL ApoA1	DOX	Stimulation of CD8+ T cell responses Enhancement of the recognition of TAAs, neoantigens and tumor cells	Higher expression of IFN-γ+CD8α+ T cells at the basal level, CD11c+CD11b+Ly6c+ DCs, and CD86+ in TDLNS	[190]	*In vivo* studies: BALB/c mice withCT26 and MC38 colon
PC7A NPs	Anti-PD1	Strong cytotoxic T cell response with low systemic cytokine expression Inhibition of tumor growth Generation of long-term anti-tumor memory	Higher expression of IFN-γ+ and CD8+ T cells in BMDCs and spleen	[191]	*In vivo* studies: C57BL/6 mice with MC38
Ch/γ-PGA	-	T cell activation Decrease of the tumor invasion	Higher expression of CD86, CD40, HLA-DR, TNF-α, CD4+ and CD8+ IL-12p40 and IL-6 in co-cultures. Decrease of CD163 expression in co-cultures	[192]	*In vitro* studies: RKO cell lines
OCD	-	Excellent H_2O_2-eliminating capability Anti-inflamatory activity	Lower expression of MPO, TNF-α, IL-1β, and IL-6	[193]	*In vitro* studies: C26 mouse colon carcinoma cells and Caco-2 human intestinal epithelial cells; RAW264.7 cells

1,2-distearoyl-sn-glycero-3-phosphoethanolamine-N-(polyethyleneglycol)-Mannose (DSPE-PEG-Mannose); Apolipoprotein A1 (ApoA1); Bi-adjuvant nanovaccinne (banNV); Bone marrow dendritic cells

(BMDCs); Chitosan and poly-γ-glutamic acid materials (Ch/γ-PGA NPs); Cytomembranes (FM); DNA-RNA nanocapsules (iDR-NCs); Doxorubicin (DOX); H2O2-eliminating β-CD material (OCD); Lymph nodes (LNs); Lipid Calcium Phosphate Nanoparticles (LPC); Myeloperoxidase [12]; Nanoparticles with cytomembrane (NP@FM); Oligodeoxynucleotides (ODNs); Photodynamic Therapy (PDT); Polydopamine nanoparticles with tumor cell lysate (TCL@PDA NPs); Polyethylene glycol -grafted polypeptide (PPT-g-PEG); Polyethylene glycol-polylactic acid (PEG-PLA); Polymeric NPs and tumor antigens (PC7A NPs); Porphyrin-based Zr-MOF and with FM (PCN@ FM); Silver nanoparticles (AgNP); Surface capsid protein (M13@Ag); Synthetic high density lipoprotein (sHDL) nanodiscs; Tumor associated antigens (TAAs); Tumor-draining lymph nodes (TDLNs); Lipid Calcium Phosphate Nanoparticles (LPC); Polyethylene glycol-polylactic acid (PEG-PLA);

Nanomedicine for antigen and adjuvant delivery in CRC

The use of subunit antigens safer and less immunogenic, stimulate the development efficient adjuvants delivery nanotechnologies [194]. Nanovaccines can be engineered to specifically interact with pattern recognition receptors, like Toll-Like Receptors (TLRs) or mannose receptor (CD206), expressed on APCs surface, to trigger the innate immune response [195]. Alternatively, nanovaccines can passively target APCs, controling antigen release or presentation and prolonging the exposure and duration of the immune response [196]. Moreover, nanocarriers can easily co-deliver TAAs and adjuvants to interact with TLRs on the DCs surface, ensuring their effective activation and antigen presentation [196]. In CRC, Chen's group developed a self-assembled intertwining DNA-RNA nanocapsules (iDR-NCs) to deliver synergistic DNA CpG and *Stat3*-silencing short hairpin RNA (shRNA) – microflowers (MFs) [183]. CPG have the ability to trigger Toll-Like Receptor 9 (TLR9) pathway to activate APCs, such DCs and macrophages [183]. However, STAT3 suppresses CpG-activated immunostimulation being silenced by *Stat3*-silencing shRNA [183]. MFs were shrank into iDR-NCs using PEG-grafted cationic polypeptides to improve the delivery towards the lymph nodes. Moreover, to modulate the immune response in MC38 tumor syngeneic C57BL/6 mice models, a specific CTL neoantigen (AdpgK) was incorporated into the NCs [183]. iDR-NC/AdpgK improved therapeutic efficacy and increase regression rates of the tumor. Furthermore iDR-NCs had the ability to deliver multiple tumor antigens to the Lymph Nodes for a broader spectrum of T cell response, leading to the tumor cell killing and better therapeutic efficacy [183].

Importantly, targeting lymph nodes tissues are being explored to generate effective immunotherapy responses [197]. APCs transport antigen to tumor-draining lymph nodes (TdLNs) are able to prime naïve CD8+ T cells [198]. Moreover, TdLNs are involved in mediating the effects of aCTLA-4 and aPD-1 therapy [199, 200]. The presence of the stem-like CD8+ T cell compartment has been observed in mouse and human LNs, in addition to the TME, suggesting these tissues as a potential source of tumor-infiltrating lymphocytes (TILs) [198]. However, the TME and TdLNs are poorly accessed using systemic drug administration, the predominant route used in both preclinical tumor models and human patients, which may limit drug effects [197]. Nanomedicine can target specifically TdLNs improving the therapy as well demonstrated aforementioned in Chen's work.

Also, a nanovaccine based on mannose-targeted lipid calcium phosphate nanoparticles (NP) co-encapsulating the colon cancer peptide antigen, p-AH1-A5 and each phosphorylated adjuvant, CpG, 2'3'cGAMP, or 5'pppdsRNA, was developed and the efficacy of the three adjuvants to incited similar pro-inflammatory responses was tested in

an orthotopic CRC liver metastasis CT26 model [184]. To assess its pro-inflammatory effect *in vivo*, IFN-γ was measured. The adjuvant 5'pppdsRNA was the only one, able to promote anti-cancer responses due to its ability to maintain low populations of immune suppressive T-reg and MDSCs in TME [184].

Neoantigen vaccines have been also investigated for personalized cancer immunotherapy. Ni *et al*., developed a bi-adjuvant nanovaccine (banNV) which synergistically co-delivered the TLR7/8agonist (R848) and the TLR9 agonist CPG oligodeoxynucleotides (ODNs), as well as a neoantigen (Adpgk) peptide on PEG-PLA micelles to potentiate anti-PD-1 immunotherapy in CRC [185]. The codelivery of these neoantigen with the dual synergistic adjuvants led to a more than 3.65 fold tumor regression in treated mice when compared with the ones that have been treated with a single adjuvant plus the neoantigen [185]. Moreover, on a MC38 orthotopic C57BL/6 CRC model, BanNVs sensitized immune checkpoint PD-1 on T cells and, when combined with anti-PD-1 antibody, induced therapy response with an increased survival rate to 70% on day 48, compared with a 40% of survival rate by BanNVs alone[185].

Biomimetic nanotechnology, mainly cancer-derived membranes, has also being explored for the design of anticancer vaccines to improve the multi-antigenic immune response [201].Therefore, it has been demonstrated that cancer-derived membranes nanoparticles, with an immunostimulatory adjuvant, could facilitate enhanced antigen presentation, leading to the activation of tumor-specific cellular responses [201]. In CRC, Wang *et al*., developed polydopamine nanoparticles (PDA NPs) with tumor cell lysates (TCLs) covalently attached (TCL@PDA NPs) [186]. This biomimetic nanosystem, TCL@PDA NPs, showed a safety improvement and decreased cytotoxicity when compared with TCL and PDA for 48 h [186]. TCL@PDA NPs could promote a 2.6 higher uptake of antigens, enhancing bone marrow dendritic cells (BMDCs) maturation and the expression of surface co-stimulatory molecules and secretion of Th1-related cytokines [186]. The spleen and lymph nodes $CD4^+$ and $CD8^+$ T cell subpopulations were also significantly enhanced, and the production of memory T cells increased, sustain immune surveillance and providing long-term protection against the tumor [186]. Moreover, empty PDA NPs had the ability to modulate DCs maturation by increasing their ability to express MHC II and secrete Th1-related cytokines [186].

Inspired on the development of biomimetic nanotechnology, Lui *et al.*, explored the development of cytomembrane nanovaccines [187]. In this approach fused cytomembranes (FMs) acquired from the fusion of cancer and DCs contributed to APCs activation [187]. This nanosystem was constructed using porphyrin-based Zr-MOF (PCN-224) and FM (PCN@ FM) for the combination of Photodynamic Therapy (PDT) and immunotherapy

(Figure 6a). The targeting effectiveness of the nanosystem was evaluated in 4T1 cell lines and compared with the mouse colon cancer cells CT26. The developed nanosystem exhibited high uptake for 4T1 cell lines due to the tumor antigens expression [187]. Next, in order to generate a cellular nanovaccine, with the ability to offer a powerful immune response towards multiple tumor types, the same team developed nanoparticles-supported stimulatory molecules on cytomembrane (NP@FM) [188]. Therefore, DCs and tumor cells were fused and NPs based in Polyethylene glycol [133] were incorporated as a supporter of FMs [188]. The successful fusion of the DCs and of 4T1cells allowed the antigen peptides-major histocompatibility complex (pMHC) expression on the cytomembrane [188]. Due to the similarity in outer membranes, NP@FM inherits and even amplifies the interfacial biofunctions of the two parent cell lines, such as the lymph node-homing capacity of DCs [188]. This nanosystem was also proved biocompatible and safety with low cytotoxicity *in vitro* for 4T1 cells, normal murine fibroblasts (3T3) and mouse colon cancer CT26 cells [188]. The transcriptome was also investigated in the cells treated with NP@FM and compared with those treated with phosphate buffer solution (PBS). An upregulation of the genes related with the immune system evidences the straight link with the ability to regulate the immune response [188]. *In vivo* assays using BALB/C mice with 4T1cells injected subcutaneously were performed to assess the properties of the nano-cytomembrane in the achievement of lymph nodes, favoring T cell antigen presentation (Figure 6b) [188]. That cytomembrane nanovaccine mimics APCs, and has the ability to directly act on T cell activation (Figure 6c) [188].

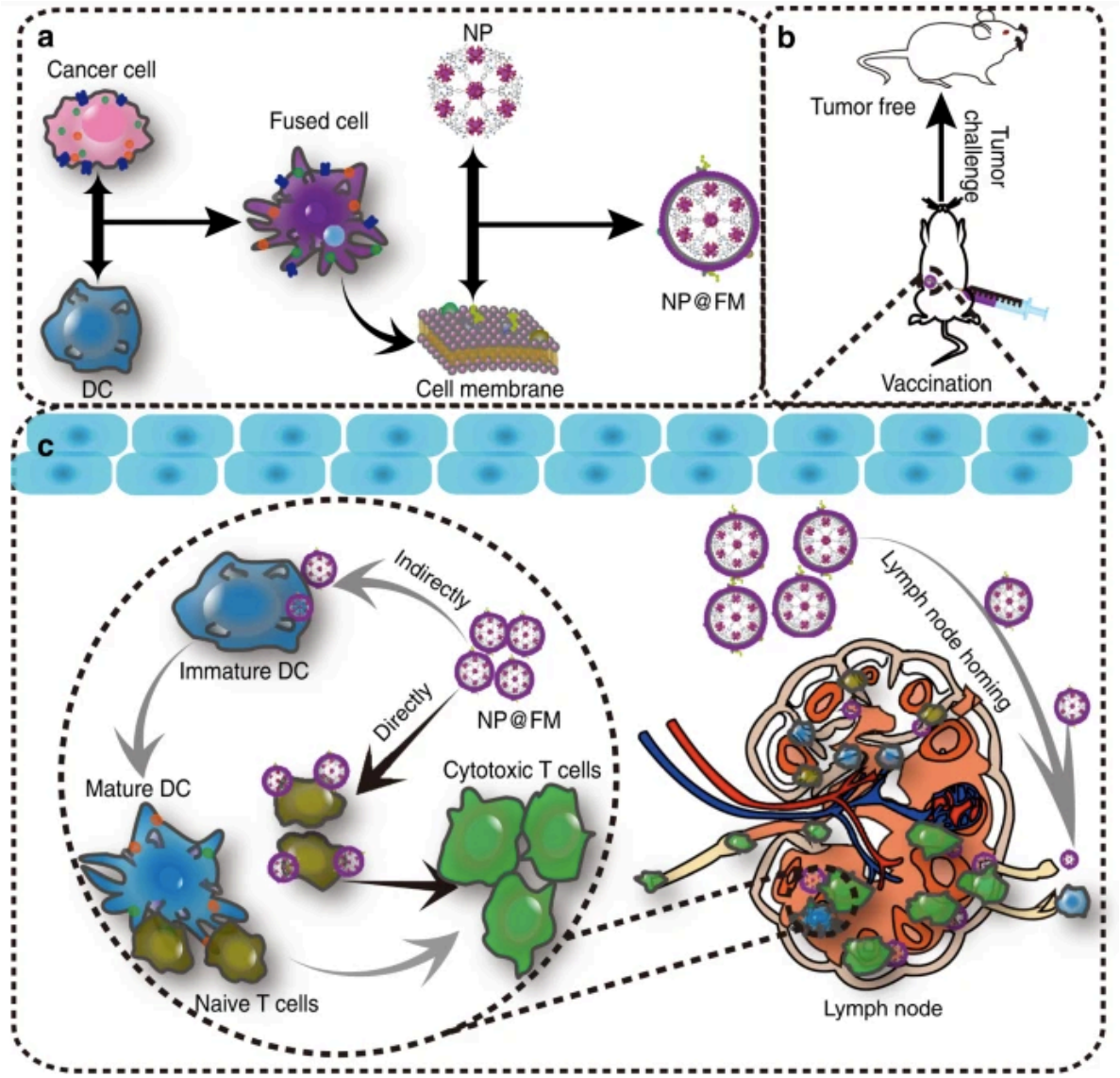


Figure 6 - Schematic illustration of NP@FM for tumor prevention: a) Schematization of the steps to develop NP@FM; b) Vaccination of mice models with the developed NP@FM; c) Mechanisms of NP@FM to induce immune response [188]. Reproduced from Wen-Long Liu et al [188] with permission from Springer Nature, copyright 2019.

In that study, mice were pretreated with cytomembrane-coated nanovaccines and compared with the nanosystem coated with the cancer membrane. Mice submitted to the treatment of cytomembrane-coated nanovaccines reached a tumor-free of 60% for a period of 36 days, compared with 20% of the mice treated with nanosystems coated with cancer membrane [188]. Also, the secretion level of IL-6 and IFN-γ was determined by ELISA, being the levels of secretion of IFN-γ and of IL-6 about 27 and 3 times more than the group treated with PBS [188]. Moreover, the vaccination with MOF@FM led also to a significant increment of $CD3^+$ $CD8^+$ CTLs [188].

Protein-nanoparticles (PNPs) are other approach that are being studied as natural carriers for antigen delivery, and can be obtained by the self-assembly of protein structures [196]. Particularly, PNPs derived from heat-shock proteins (HSPs) can exhibit strong receptor-specific interactions with APCs facilitating antigen presentation and, consequently, the immune stimulation [196]. Previous clinical studies led by Mazzaferro *et al.,* tested cancer vaccines, using antigenic peptides bound to HSP96, in patients with colorectal liver metastases [202]. This study demonstrated an increase in $CD8^{+}$T cells response against colon cancer [202]. Notably, the OS was improved by two-years and the antitumor immune response revealed to be independent from clinical prognostic factors [202]. These results highlight the potential use of HSPs to deliver antigens, which can be further improved when combined with PNPs [202].

CRC development is intimately associated with the gut microbiota. The enriched CRC tissue with bacteria such, *Fusobacterium nucleatum* (*Fn*) are associated with an immunosuppressive myeloid cell, at the TME to further diminish T cell responses. On the other hand, silver nanoparticles (AgNP), an inorganic nanomaterial is known to exhibit excellent antibacterial activity. Therefore, Dong *et al.* developed a phage-based bioinorganic hybridization system to rebuild the tumor-immune microenvironment via manipulation of gut microbiota for CRC suppression. In their study, AgNP were assembled electrostatically having on its surface the capsid protein (M13@Ag) to achieve specific clearance of *Fn* and remodel the TME. Both *in vitro* and *in vivo* studies showed that M13@Ag treatment could scavenge *Fn* in the gut, reducing MDSC infiltration at the tumor site. In addition, antigen-presenting cells (APCs) were activated by M13 phages to further awaken the host immune system. M13@Ag combined with immune checkpoint inhibitors (α-PD1) or chemotherapeutics (FOLFIRI) significantly prolonged overall mouse survival in orthotopic CRC model[189].

Overall, nano-based formulations can potentiate the anticancer effects induced by vaccines, by protecting the antigens and adjuvants from degradation, by increasing its delivery at specific site as well as by activating immune cells through their inherent immunostimulatory properties.

Nanomedicine for immunomodulatory strategies in CRC

The physicochemical properties of the natural or synthetic materials used in the development of the immunomodulatory nanomedicines are extremely important once they can influence the interaction with immune cells and, consequently their biological response [203]. Particularly, molecular weight, degree of acetylation, as well as properties of nano-

based formulations such as size, hydrophobicity, surface charge and coating antigens determine their level of interaction with the TME [204].

Nanomedicines when entering in circulation can adsorb molecules on their surface, causing their deformation, folding and immunogenic response, being recognized as foreign agent by the host immune system [205]. To overcome this, coating NPs with PEG (PEGylation) allow a reduction of protein adsorption avoiding clearance [206]. Moreover, depending on the material and formulation used, when NPs are administrated they can interact with DCs, affecting antigen presentation to T cells and thereby, modulating the adaptive immune response [207]. For example, NPs can be engineered to engage and interact with APCs. or T cells or act in a specific cell surface ligand [180]. Hence, smaller artificial APCs (aAPCs) NPs with about 50 nm are reported as less efficient to activate T cells than those with sizes around 300 nm [208].

Regarding immunostimulatory strategies, Kuai *et al*. demonstrated the efficacy of synthetic high-density lipoprotein (sHDL) nanodiscs to improve, in CRC, DCs antigen presentation [190]. Nanodiscs were produced with a synthetic high-density lipoprotein composed by apolipoprotein A1 (ApoA1) mimetic peptide and by phospholipids, for stimuli-responsive delivery of the chemotherapeutic agent. Afterwards nanodiscs were loaded with doxorubicin (DOX) to induce antitumor T cell responses [190]. Delivery of DOX via nanodiscs triggered immunogenic cancer cell death and exerted antitumor efficacy without any overt off-target side effects, eliciting $CD8^+$ T cell responses, and enhancing the recognition of TAAs, neoantigens and tumor cells [190]. The strategy was also combined with free anti-PD1 therapy in BALB/c mice, inducing a complete regression of established CT26 and MC38 colon carcinomas in 80 to 88% of the animals, and protecting survivors against tumor recurrence [190]. Therefore, engineered stimuli-responsive nanomaterials demonstrate to improve antitumor responses increasing drug delivery effect [209].

Luo *et al.,* developed a minimalist nanovaccine for colon cancer, comprising polymeric NPs (PC7A NPs) and tumor antigens, without incorporation of adjuvants. This vaccine efficiently delivered the antigen to the APCs in lymph nodes, inducing antigen surface presentation and type I interferon-stimulated genes, which was STING-dependent [191]. These PC7A NPs generated strong cytotoxic T cell response with low systemic cytokine expression [191]. Additionally, the PC7A nanovaccine was combined with an anti-PD-1 inhibitor showing great synergy, with 100% survival over 60 days in a MC38 colon cancer in C57BL/6 mice model, and leading to a complete tumor growth inhibition, suggesting the generation of long-term antitumor memory [191]. Therefore, this nanovaccine not only enhances antigen delivery and cross-presentation, but also stimulates the STING pathway to boost antitumor immunity for colon cancer immunotherapy [191].

Other studies showed the inherent immunostimulatory properties of Chitosan and poly-γ-glutamic acid materials in CRC. *Castro et al* demonstrated that empty Ch/γ-PGA NPs have also the ability to reprogram immunosuppressive human macrophages, as well as immature DCs, towards an immunostimulatory profile. This immune cell activation induced $CD4^+$ and $CD8^+$ T cell activation and decreased the invasion of CRC cells *in vitro* [192]. Furthermore, these Ch/γ-PGA NPs also potentiated radiotherapy effects, reinforcing their potential as immune adjuvants to anticancer therapy [210].

To elucidate the impact of nanoparticles on macrophage physiology and cancer growth, Zanganeh *et al.,* investigated the impact of iron oxide nanoparticles compound ferumoxytol *in vitro* and *in vivo* using a MMTV-PyMT-derived cancer cells into the bilateral mammary fat pads of female FVB/N mice [211]. A similar therapeutic effect was also assessed using a KP1-GFP-Luc cells intravenously injected into NOD.Cg-Prkdcscid Il2rgtm1Wjl/SzJ mice [211]. Iron oxide nanoparticles significantly suppressed tumor growth by inducing pro-inflammatory macrophage responses [211]. *In vitro* studies showed that superparamagnetic iron oxides induce a phenotypic shift from M2-like anti-inflammatory macrophages towards a high $CD86^+$, TNFα positive M1-like pro-inflammatory macrophages [211]. This M1 polarization can induce a Fenton reaction which, in turn, can induce cancer cell apoptosis [211]. *In vivo* assays, demonstrated the shift of macrophages polarization towards M1-like phenotypes whereas tissue-resident macrophages lost their M2-like signature [211]. Moreover, pretreatment with ferumoxytol was described to inhibit tumor metastases [211]. Despite this data was not validated or applied to CRC, ferumoxytol could be exploited at the CRC TME as an attempt to modulate the immunosuppressive TME.

A ROS-responsive and H_2O_2-eliminating material was synthesized by Zhang *et al*., confirming the effectiveness of the developed NPs to attenuate oxidative stress and inflammatory response in CRC [193].

Combinatory nanotherapies

Several approaches combining chemotherapy and immunotherapy are being investigated, to boost the immune response and to promote effective therapy. For example, in the CRC, Li *et al.* developed a bilayer system composed by paclitaxel (PTX)-loaded gelatin nanogels (GN) as the inner cores and HT-29 tumor cell membranes (TCM) as the outer shells (TCM/GN/PTX) [212]. This TCM coated GN had the ability of tumor targeting and to effectively accumulate at the tumor site [212]. In that biomimetic cell membranes-coated nanosystems, NPs have the ability to possess the diversity of the surface antigen of the source cell. In particular TCM, presents the natural ability to target homotypic tumor

cells due to the presence of natural and multiple antigens on its surface such homologous proteins and immune escape proteins [212]. The *in vivo* antitumor activity resulted towards HT-29 xenografts mouse models indicating that the TCM/GN/PTX strategy could suppress tumor cells growth through induction of tumor cells necrosis and apoptosis [212]. Moreover, He *et al*. designed a polymer core-shell NP carrying oxaliplatin and the photosensitizer pyropheophorbide-lipid (pyrolipid) [213]. NPs were then combined with the ICIs anti-CTLA4 and anti-PDL-1 to improve its blocking , activating T cells signaling and reducing tumor immune escape [214]. CT26 colorectal cancer model treated with those NPs and immune checkpoint inhibitors (anti-PD-L1), showed a significant reduction of primary and distant tumor cells when comparison to those treated with anti-PD-L1 alone [213].

Wang *et al*. reported the preparation of microneedles (MN) with hyaluronic acid integrated in pH-sensitive dextran NPs encapsulating anti-PD-1 and glucose oxidase to impair CRC tumor progression [214]. Also, mannosylated chitosan (MC) was developed by Kim *et al*. to induce mannose receptor–mediated endocytosis of IL-12 directly into DCs which reside within the tumor. MC was proven to be suitable for IL-12 gene delivery to DCs leading to a clear suppression of CRC growth and angiogenesis [215]. Liu *et al.* developed a non-toxic hybrid nanosystem by self-assembly method, DOTAP/MPEG-PLA-pIL12 (DMP-pIL12), able to inhibit colorectal tumor growth *in vivo* by increasing the secretion of the anti-proliferative and anti-angiogenic mediators IL-12, IFN-γ, and TNF-α, which promoted the increase of cytotoxic T cells [216].

These studies highlighted the importance of the different approaches regarding NPs design and materials composition to modulate the TME and also to deliver immunomodulatory agents, proving immune cells reprograming and an efficient therapeutic response [217].

Challenges and future perspectives

Far from patients with dMMR–MSI-H CRC, single immunotherapy has not evidenced a clinical benefit in patients with pMMR–MSI-L CRC, probably due to the lack of immune players at the tumor site. This feature remains a crucial obstacle to immunotherapy efficacy, being necessary the development of new combinatory strategies. The combination of ICIs with other immunostimulatory agents, able to recruit immune cells to the TME, might be beneficial in patients with pMMR–MSI-L CRC, as reviewed at [20]. Furthermore, colorectal tumors infiltrated with immunosuppressive cells (CSM2 and CSM3) can also be target of immunotherapies, after reprogramming of their immune profile towards an immunostimulatory one. Several agents, like TLR ligands, MDSC inhibitors, and TGF-β modulators might be employed to reeducate the immune cells at the tumor site. Besides the

recruitment and reprograming of the tumor immune compartment, the therapeutic outcome of some immunotherapeutic strategies is still limited. While in cancer vaccines, the antigen and adjuvants delivery can face enzymatic degradation, the delivery of ICIs has also some drawbacks, like unspecificity for the TME, resulting in adverse side-effects. To overcome these limitations, nanomedicine can contribute with formulations that specifically co-deliver antigens, adjuvants, and immunotherapeutic drugs further potentiating immunotherapy efficacy. Despite promising, nanomedicine remains an expensive and time-consuming process. Important issues related to the clinical development of nano-based formulations, including biological challenges, biocompatibility, biosafety as well as large-scale manufacturing and government regulations should be addressed.

References

1. Foster, J.R., *The functions of cytokines and their uses in toxicology.* Int J Exp Pathol, 2001. **82**(3): p. 171-92.
2. GLOBOCAN, *Colorectal cancer*. 2020.
3. Cervantes, A., et al., *Metastatic colorectal cancer: ESMO Clinical Practice Guideline for diagnosis, treatment and follow-up☆.* Ann Oncol, 2023. **34**(1): p. 10-32.
4. Shin, A.E., F.G. Giancotti, and A.K. Rustgi, *Metastatic colorectal cancer: mechanisms and emerging therapeutics.* Trends Pharmacol Sci, 2023. **44**(4): p. 222-236.
5. Silveira, M.J., et al., *Immunomodulatory nanomedicine for colorectal cancer treatment: a landscape to be explored?* Biomater Sci, 2021. **9**(9): p. 3228-3243.
6. Wu, X., et al., *Comprehensive characterization of tumor microenvironment in colorectal cancer via molecular analysis.* eLife, 2023. **12**: p. e86032.
7. Elia, I. and M.C. Haigis, *Metabolites and the tumour microenvironment: from cellular mechanisms to systemic metabolism.* Nat Metab, 2021. **3**(1): p. 21-32.
8. Ogino, S. and A. Goel, *Molecular classification and correlates in colorectal cancer.* J Mol Diagn, 2008. **10**(1): p. 13-27.
9. Guinney, J., et al., *The consensus molecular subtypes of colorectal cancer.* Nat Med, 2015. **21**(11): p. 1350-1356.
10. Kim, J.H., et al., *Clinical significance of carcinoembryonic antigen in peritoneal fluid detected during operation in stage I-III colorectal cancer patients.* Intest Res, 2018. **16**(3): p. 467-474.
11. Tong, G., et al., *The role of tissue and serum carcinoembryonic antigen in stages I to III of colorectal cancer-A retrospective cohort study.* Cancer Med, 2018. **7**(11): p. 5327-5338.
12. Campos-da-Paz, M., et al., *Carcinoembryonic antigen (CEA) and hepatic metastasis in colorectal cancer: update on biomarker for clinical and biotechnological approaches.* Recent Pat Biotechnol, 2018. **12**(4): p. 269-279.
13. Krasteva, N. and M. Georgieva, *Promising Therapeutic Strategies for Colorectal Cancer Treatment Based on Nanomaterials.* Pharmaceutics, 2022. **14**(6).
14. Cisterna, B.A., et al., *Targeted nanoparticles for colorectal cancer.* Nanomedicine (Lond), 2016. **11**(18): p. 2443-56.
15. Jain, A. and S. Jain, *Rising Incidence of Colorectal Cancer in Patients Younger than Age 50 in Hawai'i.* Hawaii J. Med. Public Health, 2019. **78**(6): p. 195-199.

16. Virostko, J., et al., *Recent trends in the age at diagnosis of colorectal cancer in the US National Cancer Data Base, 2004-2015.* Cancer. **0**(0).
17. Society, A.C., *Colorectal cancer facts and figures 2017-2019.* 2017.
18. Dekker, E., et al., *Colorectal cancer.* The Lancet, 2019. **394**(10207): p. 1467-1480.
19. Yu, I.S. and W.Y. Cheung, *Metastatic Colorectal Cancer in the Era of Personalized Medicine: A More Tailored Approach to Systemic Therapy.* Can J Gastroenterol Hepatol, 2018. **2018**: p. 9450754-9450754.
20. Ganesh, K., et al., *Immunotherapy in colorectal cancer: rationale, challenges and potential.* Nat Rev Gastroenterol Hepatol, 2019. **16**(6): p. 361-375.
21. Gorbet, M.-J. and A. Ranjan, *Cancer immunotherapy with immunoadjuvants, nanoparticles, and checkpoint inhibitors: Recent progress and challenges in treatment and tracking response to immunotherapy.* Pharmacol. Ther., 2020. **207**: p. 107456.
22. Bittoni A, S.V., MeletaniBittoni A, Sotte V, Meletani T, Cantini L, Giampieri R, Berardi R. , *Immunotherapy in colorectal cancer treatment: actual landscape and future perspectives.* J Cancer Metastasis Treat 2018. **55**(4).
23. Goldberg, M.S., *Improving cancer immunotherapy through nanotechnology.* Nat Rev Cancer, 2019. **19**(10): p. 587-602.
24. Plundrich, D., et al., *Molecular mechanisms of tumor immunomodulation in the microenvironment of colorectal cancer.* Int J Mol Sci, 2022. **23**(5).
25. Briquez, P.S., et al., *Engineering targeting materials for therapeutic cancer vaccines.* Front. bioeng. biotechnol, 2020. **8**.
26. Nguyen, K.G., et al., *Localized Interleukin-12 for cancer immunotherapy.* Front immunol, 2020. **11**.
27. Jia, Z., et al., *IL12 immune therapy clinical trial review: Novel strategies for avoiding CRS-associated cytokines.* Front Immunol, 2022. **13**: p. 952231.
28. Riley, R.S., et al., *Delivery technologies for cancer immunotherapy.* Nat Rev. Drug discovery, 2019. **18**(3): p. 175-196.
29. Wang, K., et al., *Nano-Drug delivery systems based on different targeting mechanisms in the targeted therapy of colorectal cancer.* Molecules, 2022. **27**(9).
30. Sun, Q., et al., *Cancer nanomedicine meets immunotherapy: opportunities and challenges.* Acta Pharmacol Sin, 2020. **41**(7): p. 954-958.
31. Singh, M.P., et al., *Molecular subtypes of colorectal cancer: An emerging therapeutic opportunity for personalized medicine.* Genes Dis, 2019.
32. Favoriti, P., et al., *Worldwide burden of colorectal cancer: a review.* Updates Surg, 2016. **68**(1): p. 7-11.

33. Carvalho, B., et al., *Colorectal adenoma to carcinoma progression is accompanied by changes in gene expression associated with ageing, chromosomal instability, and fatty acid metabolism.* Cell oncol, 2012. **35**(1): p. 53-63.
34. De Palma, F.D.E., et al., *The Molecular hallmarks of the serrated pathway in colorectal cancer.* Cancers, 2019. **11**(7): p. 1017.
35. Hermsen, M., et al., *Colorectal adenoma to carcinoma progression follows multiple pathways of chromosomal instability.* Gastroenterology, 2002. **123**(4): p. 1109-19.
36. De Rosa, M., et al., *Genetics, diagnosis and management of colorectal cancer (Review).* Oncol Rep, 2015. **34**(3): p. 1087-96.
37. Piccinini, F., *AnaSP: a software suite for automatic image analysis of multicellular spheroids.* Comput Methods Programs Biomed, 2015. **119**(1): p. 43-52.
38. Sousa, A.R., M.J. Oliveira, and B. Sarmento, *Impact of CEA-targeting nanoparticles for drug delivery in colorectal cancer.* J Pharmacol Exp Ther, 2019.
39. Grady, W.M. and S.D. Markowitz, *The molecular pathogenesis of colorectal cancer and its potential application to colorectal cancer screening.* Dig Dis Sci 2015. **60**(3): p. 762-772.
40. Liu, Q., et al., *P-TNM staging system for colon cancer: combination of P-stage and AJCC TNM staging system for improving prognostic prediction and clinical management.* Cancer Manag Res, 2018. **10**: p. 2303-2314.
41. Weiser, M.R., *AJCC 8th Edition: Colorectal Cancer.* Ann Surg Oncol, 2018. **25**(6): p. 1454-1455.
42. Zhou, R., et al., *A robust panel based on tumour microenvironment genes for prognostic prediction and tailoring therapies in stage I;III colon cancer.* EBioMedicine, 2019. **42**: p. 420-430.
43. Galon, J., et al., *Cancer classification using the Immunoscore: a worldwide task force.* JTransl Med, 2012. **10**(1): p. 205.
44. Noack, P. and R. Langer, *Molecular pathology of colorectal cancer.* Memo, 2023. **16**(2): p. 116-121.
45. Wang, R., et al., *Dynamic monitoring of serum CEA and CA19-9 predicts the prognosis of postoperative stage II colon cancer.* Eur J Surg Oncol, 2023. **49**(12).
46. Moretto, R., et al., *CEA increase as a marker of disease progression after first-line induction therapy in metastatic colorectal cancer patients. A pooled analysis of TRIBE and TRIBE2 studies.* Br J Cancer, 2021. **125**(6): p. 839-845.
47. Bhagat, A., et al., *CEA vaccines.* Human vaccines & immunotherapeutics, 2023. **19**(3): p. 2291857.
48. Yu, P., et al., *The dynamic monitoring of CEA in response to chemotherapy and prognosis of mCRC patients.* BMC Cancer, 2018. **18**(1): p. 1076.

49. Mahmoud, N.N., *Colorectal cancer: Preoperative evaluation and staging.* Surg Oncol Clin N Am, 2022. **31**(2): p. 127-141.
50. Tchoupa, A.K., T. Schuhmacher, and C.R. Hauck, *Signaling by epithelial members of the CEACAM family – mucosal docking sites for pathogenic bacteria.* Cell Commun. Signal, 2014. **12**(1): p. 27.
51. Konishi, F., *CEA Doubling Time and CEA Half-life in the Prediction of Recurrences after Colorectal Cancer Surgery.* Jpn J Clin Oncol, 2002. **32**(2): p. 41-42.
52. Sousa, A.R., M.J. Oliveira, and B. Sarmento, *Impact of CEA-targeting nanoparticles for drug delivery in colorectal Cancer.* J Pharmacol Exp Ther, 2019. **370**(3): p. 657-670.
53. Erica A. Golemis, P.S., Tim N. Beck, Eward M. Scolnick, David J. Hunter, Ernest Hawk, and Nancy Hopkins, *Molecular mechanisms of the preventable causes of cancer in the United States.* Genes Dev., 2018. **32**: p. 868-902.
54. Lasry, A., A. Zinger, and Y. Ben-Neriah, *Inflammatory networks underlying colorectal cancer.* Nat Immun, 2016. **17**(3): p. 230-240.
55. Pottier, C., et al., *The importance of the tumor microenvironment in the therapeutic management of cancer.* Expert Rev Anticancer Ther, 2015. **15**(8): p. 943-54.
56. Colangelo, T., et al., *Friend or foe? The tumour microenvironment dilemma in colorectal cancer.* Biochim Biophys Acta Rev Cancer, 2017. **1867**(1): p. 1-18.
57. Hanahan, D. and R.A. Weinberg, *Hallmarks of cancer: the next generation.* Cell, 2011. **144**(5): p. 646-74.
58. Janakiram, N.B. and C.V. Rao, *The Role of inflammation in colon cancer*, in *inflammation and cancer*, Editors. 2014, p. 25-52.
59. Coussens, L.M. and Z. Werb, *Inflammation and cancer.* Nature, 2002. **420**(6917): p. 860-7.
60. Long, A.G., E.T. Lundsmith, and K.E. Hamilton, *Inflammation and colorectal cancer.* Curr Colorectal Cancer Rep, 2017. **13**(4): p. 341-351.
61. Singh, R., et al., *Emerging applications of upconverting nanoparticles in intestinal infection and colorectal cancer.* Int J Nanomedicine, 2019. **14**: p. 1027-1038.
62. Tao, M.Y., et al., *Prognostic value of the systematic immune-inflammation index among patients with operable colon cancer: A retrospective study.* Medicine, 2018. **97**(45): p. e13156.
63. Kather, J.N. and N. Halama, *Harnessing the innate immune system and local immunological microenvironment to treat colorectal cancer.* Br J Cancer, 2019. **120**(9): p. 871-882.

64. Guo, G., et al., *Immune cell concentrations among the primary tumor microenvironment in colorectal cancer patients predicted by clinicopathologic characteristics and blood indexes.* J Immunother Cancer, 2019. **7**(1): p. 179.
65. Fuhr, L., et al., *The interplay between colon cancer cells and tumour-associated stromal cells impacts the biological clock and enhances malignant phenotypes.* Cancers, 2019. **11**(7): p. 988.
66. Pinto, M.L., et al., *The two faces of tumor-associated macrophages and their clinical significance in colorectal cancer.* Front in Immunol, 2019. **10**(1875).
67. Xiong, Y., Y. Wang, and K. Tiruthani, *Tumor immune microenvironment and nano-immunotherapeutics in colorectal cancer.* NBM, 2019. **21**: p. 102034.
68. Fritz, J.M. and M.J. Lenardo, *Development of immune checkpoint therapy for cancer.* JEM, 2019. **216**(6): p. 1244-1254.
69. Xie, Y.-H., Y.-X. Chen, and J.-Y. Fang, *Comprehensive review of targeted therapy for colorectal cancer.* Signal Transduct Target Ther, 2020. **5**(1): p. 22.
70. Havel, J.J., D. Chowell, and T.A. Chan, *The evolving landscape of biomarkers for checkpoint inhibitor immunotherapy.* Nat Rev Cancer, 2019. **19**(3): p. 133-150.
71. Chang, C.-C., et al., *Input of microenvironmental regulation on colorectal cancer: role of the CCN family.* World J Gastroenterol, 2014. **20**(22): p. 6826-6831.
72. Zhang, X., et al., *The functional and prognostic implications of regulatory T cells in colorectal carcinoma.* J Gastrointest Oncol, 2015. **6**(3): p. 307.
73. O'Donnell, J.S., M.W.L. Teng, and M.J. Smyth, *Cancer immunoediting and resistance to T cell-based immunotherapy.* Nat Rev Clin Oncol, 2019. **16**(3): p. 151-167.
74. Chen, D.S. and I. Mellman, *Elements of cancer immunity and the cancer-immune set point.* Nature, 2017. **541**(7637): p. 321-330.
75. Galon, J. and D. Bruni, *Approaches to treat immune hot, altered and cold tumours with combination immunotherapies.* Nat Rev Drug Discov, 2019. **18**(3): p. 197-218.
76. Picard, E., et al., *Relationships between immune landscapes, genetic subtypes and responses to immunotherapy in colorectal cancer.* Front in Immunol, 2020. **11**(369).
77. Sawayama, H., et al., *Investigation of colorectal cancer in accordance with consensus molecular subtype classification.* Ann Gastroenterol Surg, 2020. **4**(5): p. 528-539.
78. Buikhuisen, J.Y., A. Torang, and J.P. Medema, *Exploring and modelling colon cancer inter-tumour heterogeneity: opportunities and challenges.* Oncogenesis, 2020. **9**(7): p. 66.
79. Spallanzani, A., et al., *Immunotherapy in the treatment of colorectal cancer: a new kid on the block.* JCMT, 2018. **4**: p. 28.

80. Bonaventura, P., et al., *Cold Tumors: A Therapeutic challenge for immunotherapy.* Front Immunol, 2019. **10**: p. 168-168.
81. Dienstmann, R., et al., *Relative contribution of clinicopathological variables, genomic markers, transcriptomic subtyping and microenvironment features for outcome prediction in stage II/III colorectal cancer.* Ann Oncol, 2019. **30**(10): p. 1622-1629.
82. Basile, D., et al., *Immunotherapy for colorectal cancer: where are we heading?* Expert Opin Biol Ther, 2017. **17**(6): p. 709-721.
83. McQuade, R.M., et al., *Colorectal cancer chemotherapy: The evolution of treatment and new approaches.* Curr Med Chem, 2017. **24**(15): p. 1537-1557.
84. Awasthi, R., et al., *Nanoparticles in cancer treatment: Opportunities and obstacles.* Curr Drug Targets, 2018. **19**(14): p. 1696-1709.
85. Cisterna, B.A., et al., *Targeted nanoparticles for colorectal cancer.* Nanomedicine, 2016. **11**(18): p. 2443-2456.
86. Coyle, Y., *Chapter 176 - Adjuvant and neoadjuvant therapy for colorectal cancer: Molecular-based therapy*, *Shackelford's Surgery of the Alimentary Tract,* 2019, p. 2126-2136.
87. Damilakis, E., et al., *Immunotherapy in metastatic colorectal cancer: Could the latest developments hold the key to improving patient survival?* Cancers, 2020. **12**(4): p. 889.
88. Zhao, F., et al., *Neoadjuvant radiotherapy improves overall survival for T3/4N+M0 rectal cancer patients: a population-based study of 20300 patients.* Rad Oncol, 2020. **15**(1): p. 49.
89. Hawkins, A.T., et al., *Neoadjuvant radiation for clinical T4 colon cancer: A potential improvement to overall survival.* Surgery, 2019. **165**(2): p. 469-475.
90. Atreya, C.E., R. Yaeger, and E. Chu, *Systemic therapy for metastatic colorectal cancer: From current standards to future molecular targeted approaches.* Am Soc Clin Oncol Educ Book, 2017. **37**: p. 246-256.
91. Marcus, L., et al., *FDA approval summary: TAS-102.* Clin Cancer Res, 2017. **23**(12): p. 2924-2927.
92. Falcone, A., et al., *O-013Safety and efficacy of trifluridine/tipiracil in previously treated metastatic colorectal cancer (mCRC): Preliminary results from the phase IIIb, international, open-label, early-access PRECONNECT study.* Ann Oncol, 2018. **29**(suppl_5).
93. Banerjee, A., et al., *Strategies for targeted drug delivery in treatment of colon cancer: current trends and future perspectives.* Drug Discov Today, 2017. **22**(8): p. 1224-1232.

94. Kotelevets, L., et al., *Nanotechnologies for the treatment of colon cancer: From old drugs to new hope.* Int J Pharm, 2016. **514**(1): p. 24-40.
95. Mishra, J., et al., *Prospective of colon cancer treatments and scope for combinatorial approach to enhanced cancer cell apoptosis.* Crit Rev Oncol Hematol, 2013. **86**(3): p. 232-250.
96. Augestad, K.M., M.A. Merok, and D. Ignatovic, *Tailored treatment of colorectal cancer: surgical, molecular, and genetic considerations.* Oncology, 2017. **11**: p. 1179554917690766-1179554917690766.
97. Kosmidis, C., et al., *Interferon-γ and Colorectal Cancer: an up-to date.* J Cancer, 2018. **9**(2): p. 232-238.
98. Isella, C., et al., *Selective analysis of cancer-cell intrinsic transcriptional traits defines novel clinically relevant subtypes of colorectal cancer.* Nat Commun, 2017. **8**(1): p. 15107.
99. Linnekamp, J.F., et al., *Consensus molecular subtypes of colorectal cancer are recapitulated in in vitro and in vivo models.* Cell Death Differ, 2018. **25**(3): p. 616-633.
100. Piawah, S. and A.P. Venook, *Targeted therapy for colorectal cancer metastases: A review of current methods of molecularly targeted therapy and the use of tumor biomarkers in the treatment of metastatic colorectal cancer.* Cancer, 2019. **125**(23): p. 4139-4147.
101. Lieu, C.H., R.B. Corcoran, and M.J. Overman, *Integrating biomarkers and targeted therapy into colorectal cancer management.* ASCO, 2019(39): p. 207-215.
102. Rawla, P., et al., *Immunotherapies and targeted therapies in the treatment of metastatic colorectal cancer.* Med scienc, 2019. **7**(8): p. 83.
103. *Explaining the unexplainable: discrepancies in results from the CALGB/SWOG 80405 and FIRE-3 studies*. 2019. p. e274-e83.
104. Stintzing, S., et al., *Consensus molecular subgroups (CMS) of colorectal cancer (CRC) and first-line efficacy of FOLFIRI plus cetuximab or bevacizumab in the FIRE3 (AIO KRK-0306) trial.* Ann Oncol, 2019. **30**(11): p. 1796-1803.
105. Mooi, J.K., et al., *The prognostic impact of consensus molecular subtypes (CMS) and its predictive effects for bevacizumab benefit in metastatic colorectal cancer: molecular analysis of the AGITG MAX clinical trial.* Ann Oncol, 2018. **29**(11): p. 2240-2246.
106. Lichtenstern, C.R., et al., *Immunotherapy, inflammation and colorectal cancer.* Cells, 2020. **9**(3): p. 618.
107. Fumet, J.D., et al., *Phase Ib/II trial evaluating the safety, tolerability and immunological activity of durvalumab (MEDI4736) (anti-PD-L1) plus tremelimumab*

(anti-CTLA-4) combined with FOLFOX in patients with metastatic colorectal cancer. ESMO Open, 2018. **3**(4): p. e000375.

108. Tolba, M.F., *Revolutionizing the landscape of colorectal cancer treatment: The potential role of immune checkpoint inhibitors.* Int J Cancer, 2020.
109. Overman, M.J., et al., *Nivolumab in patients with metastatic DNA mismatch repair-deficient or microsatellite instability-high colorectal cancer: an open-label, multicentre, phase 2 study.* Lancet Oncol, 2017. **18**(9): p. 1182-1191.
110. Eng, C., et al., *Atezolizumab with or without cobimetinib versus regorafenib in previously treated metastatic colorectal cancer (IMblaze370): a multicentre, open-label, phase 3, randomised, controlled trial.* Lancet Oncol 2019. **20**(6): p. 849-861.
111. Hollingsworth, R.E. and K. Jansen, *Turning the corner on therapeutic cancer vaccines.* npj Vaccines, 2019. **4**(1): p. 7.
112. Gros, A., et al., *Recognition of human gastrointestinal cancer neoantigens by circulating PD-1+ lymphocytes.* JCI, 2019. **129**(11): p. 4992-5004.
113. Mariathasan, S., et al., *TGFβ attenuates tumour response to PD-L1 blockade by contributing to exclusion of T cells.* Nature, 2018. **554**(7693): p. 544-548.
114. Shelton, S.E., et al., *Engineering approaches for studying immune-tumor cell interactions and immunotherapy.* iScience, 2021. **24**(1): p. 101985.
115. Rus Bakarurraini, N.A.A., et al., *The landscape of tumor-specific antigens in colorectal cancer.* Vaccines, 2020. **8**(3).
116. Kopczynski, M., et al., *Cytotoxic efficacy and resistance mechanism of a TRAIL and VEGFA-peptide fusion protein in colorectal cancer models.* Int J Mol Sci, 2021. **22**(6).
117. Anderson, P., et al., *HLA class I loss in colorectal cancer: implications for immune escape and immunotherapy.* Cell Mol Immunol, 2021. **18**(3): p. 556-565.
118. Deng, H., et al., *New hope for tumor immunotherapy: the macrophage-related "do not eat me" signaling pathway.* Front Pharmacol, 2023. **14**: p. 1228962.
119. Maryam, S., et al., *Interleukins (cytokines) as biomarkers in colorectal cancer: progression, detection, and monitoring.* J Clin Med, 2023. **12**(9): p. 3127.
120. Bhat, A.A., et al., *Cytokine- and chemokine-induced inflammatory colorectal tumor microenvironment: Emerging avenue for targeted therapy.* Cancer Commun, 2022. **42**(8): p. 689-715.
121. *Tumor necrosis factor alfa*, in *meyler's side effects of drugs (Sixteenth Edition)*, J.K. Aronson, Editor. 2016, Elsevier: Oxford. p. 230-232.
122. Tang, P., et al., *Research progress on the carcinogenesis mechanism of inflammation in ulcerative colitis: a narrative review.* Ann Palliat Med, 2021. **10**(11): p. 11994-12002.

123. Alotaibi, A.G., J.V. Li, and N.J. Gooderham, *Tumour necrosis factor-α (TNF-α) enhances dietary carcinogen-induced DNA damage in colorectal cancer epithelial cells through activation of JNK signaling pathway.* Toxicology, 2021. **457**: p. 152806.
124. Stanilov, N., et al., *Colorectal cancer severity and survival in correlation with tumour necrosis factor-alpha.* Biotechnol Biotechnol Equip, 2014. **28**(5): p. 911-917.
125. Kitaura, H., et al., *Role of the interaction of tumor necrosis factor-α and tumor necrosis factor receptors 1 and 2 in bone-related cells.* Int J Mol Sci, 2022. **23**(3).
126. Ham, B., et al., *The diverse roles of the TNF axis in cancer progression and metastasis.* Trends Cancer Res, 2016. **11**(1): p. 1-27.
127. Al Obeed, O.A., et al., *Increased expression of tumor necrosis factor-α is associated with advanced colorectal cancer stages.* World J Gastroenterol, 2014. **20**(48): p. 18390-6.
128. Takasago, T., et al., *Anti-tumor necrosis factor-alpha monoclonal antibody suppresses colorectal cancer growth in an orthotopic transplant mouse model.* PLOS ONE, 2023. **18**(3): p. e0283822.
129. Alotaibi, A.G., J.V. Li, and N.J. Gooderham, *Tumour Necrosis Factor-Alpha (TNF-α)-Induced Metastatic Phenotype in Colorectal Cancer Epithelial Cells: Mechanistic Support for the Role of MicroRNA-21.* Cancers, 2023. **15**(3).
130. Yi, J., et al., *A new strategy for treating colorectal cancer: Regulating the influence of intestinal flora and oncolytic virus on interferon.* Mol Ther Oncolytics, 2023. **30**: p. 254-274.
131. Du, W., et al., *IFNγ signaling integrity in colorectal cancer immunity and immunotherapy.* Cell Mol Immunol, 2022. **19**(1): p. 23-32.
132. Vilček, J. and J. Le, *Interferon γ*, in *Encyclopedia of Immunology (Second Edition)*, P.J. Delves, Editor. 1998, Elsevier: Oxford. p. 1421-1426.
133. Silva, A., et al., *Integrated analysis of biological samples by imaging flow cytometry.* Microsc Microanal, 2015. **21**(S5): p. 95-96.
134. Wang, L., et al., *Deficiency of interferon-gamma or its receptor promotes colorectal cancer development.* J Interferon Cytokine Res, 2015. **35**(4): p. 273-80.
135. Jorgovanovic, D., et al., *Roles of IFN-γ in tumor progression and regression: a review.* Biomark Res, 2020. **8**(1): p. 49.
136. Gong, X.L. and L. Zhao, *[Immune checkpoint inhibitors in the treatment of colorectal cancer: a review of clinical trials].* Zhonghua Wei Chang Wai Ke Za Zhi, 2022. **25**(3): p. 205-213.
137. Zibelman, M., et al., *A phase 1 study of nivolumab in combination with interferon-gamma for patients with advanced solid tumors.* Nat Commun, 2023. **14**(1): p. 4513.

138. Li, J., et al., *The Role of interleukins in colorectal cancer.* Int J Biol Sci, 2020. **16**(13): p. 2323-2339.
139. Justiz Vaillant, A.A. and A. Qurie, *Interleukin*, in *StatPearls*. 2024, StatPearls PublishingCopyright 2024, StatPearls Publishing LLC.: Treasure Island (FL).
140. Briukhovetska, D., et al., *Interleukins in cancer: from biology to therapy.* Nat Rev Cancer, 2021. **21**(8): p. 481-499.
141. Engel, M.A. and M.F. Neurath, *Anticancer properties of the IL-12 family--focus on colorectal cancer.* Curr Med Chem, 2010. **17**(29): p. 3303-8.
142. Ullrich, K.A., et al., *Immunology of IL-12: An update on functional activities and implications for disease.* Excli j, 2020. **19**: p. 1563-1589.
143. Sun, L., et al., *Interleukin 12 (IL-12) family cytokines: Role in immune pathogenesis and treatment of CNS autoimmune disease.* Cytokine, 2015. **75**(2): p. 249-55.
144. Mager, L.F., et al., *Cytokine-Induced Modulation of Colorectal Cancer.* Front Oncol, 2016. **6**: p. 96.
145. Liu, J., et al., *Roles of anoikis in colorectal cancer therapy and the assessment of anoikis-regulatory molecules as therapeutic targets.* JPRP, 2023. **241**: p. 154256.
146. Karlsson, S. and H. Nyström, *The extracellular matrix in colorectal cancer and its metastatic settling – Alterations and biological implications.* Crit Rev Oncol Hematol, 2022. **175**: p. 103712.
147. Tjin, G., et al., *Lysyl oxidases regulate fibrillar collagen remodelling in idiopathic pulmonary fibrosis.* Dis Model Mech, 2017. **10**(11): p. 1301-1312.
148. Liu, C., H. Pei, and F. Tan, *Matrix stiffness and colorectal cancer.* Onco Targets Ther, 2020. **13**: p. 2747-2755.
149. Safaei, S., et al., *Tumor matrix stiffness provides fertile soil for cancer stem cells.* Cancer Cell International, 2023. **23**(1): p. 143.
150. Chen, Y., et al., *Type I collagen deletion in αSMA(+) myofibroblasts augments immune suppression and accelerates progression of pancreatic cancer.* Cancer Cell, 2021. **39**(4): p. 548-565.e6.
151. Liang, Y., et al., *Prognostic significance of abnormal matrix collagen remodeling in colorectal cancer based on histologic and bioinformatics analysis.* Oncol Rep, 2020. **44**(4): p. 1671-1685.
152. Kim, M.S., et al., *Extracellular Matrix Biomarkers in Colorectal Cancer.* Int J Mol Sci, 2021. **22**(17).
153. Nirmala, M.J., et al., *Cancer nanomedicine: a review of nano-therapeutics and challenges ahead.* RSC Adv, 2023. **13**(13): p. 8606-8629.

154. Domingues, C., et al., *Where Is nano today and where Is It headed? A review of nanomedicine and the dilemma of nanotoxicology.* ACS Nano, 2022. **16**(7): p. 9994-10041.
155. Fan, D., et al., *Nanomedicine in cancer therapy.* Signal Transduct Target Ther, 2023. **8**(1): p. 293.
156. Mundekkad, D. and W.C. Cho, *Nanoparticles in clinical translation for cancer therapy.* Int J Mol Sci, 2022. **23**(3).
157. Markowski, A., et al., *Design and development of a new type of hybrid PLGA/Lipid nanoparticle as an ursolic acid delivery system against pancreatic ductal adenocarcinoma cells.* IInt J Mol Sci, 2022. **23**(10): p. 5536.
158. Alsaab, H.O., et al., *PLGA-based nanomedicine: History of advancement and development in clinical applications of multiple diseases.* Pharmaceutics, 2022. **14**(12).
159. Kohno, M., et al., *The effect of PLGA molecular weight differences on risperidone release from microspheres.* Int J Pharm, 2020. **582**: p. 119339.
160. del Moral, M., et al., *Role of the Lactide:Glycolide ratio in PLGA nanoparticle stability and release under lysosomal conditions for enzyme replacement therapy of lysosomal storage disorders.* J Funct Biomater, 2023. **14**(9): p. 440.
161. Bento, C., et al., *Striving for uniformity: A review on advances and challenges to achieve uniform polyethylene glycol.* Org Process Res Dev, 2024.
162. Shi, L., et al., *Effects of polyethylene glycol on the surface of nanoparticles for targeted drug delivery.* Nanoscale, 2021. **13**(24): p. 10748-10764.
163. Padín-González, E., et al., *Understanding the role and impact of Poly (Ethylene Glycol) (PEG) on nanoparticle formulation: Implications for COVID-19 vaccines.* Front Bioeng Biotechnol, 2022. **10**: p. 882363.
164. Suk, J.S., et al., *PEGylation as a strategy for improving nanoparticle-based drug and gene delivery.* Adv Drug Deliv Rev, 2016. **99**(Pt A): p. 28-51.
165. Shi, P., et al., *Active targeting schemes for nano-drug delivery systems in osteosarcoma therapeutics.* J Nanobiotechnology, 2023. **21**(1): p. 103.
166. Bhattacharya, S., B.G. Prajapati, and S. Singh, *A critical review on the dissemination of PH and stimuli-responsive polymeric nanoparticular systems to improve drug delivery in cancer therapy.* Crit Rev Oncol Hematol, 2023. **185**: p. 103961.
167. Morarasu, S., et al., *Targeted cancer therapy via pH-functionalized nanoparticles: A scoping review of methods and outcomes.* Gels, 2022. **8**(4).
168. Zhang, X., et al., *Dual pH-responsive "charge-reversal like" gold nanoparticles to enhance tumor retention for chemo-radiotherapy.* Nano Research, 2019. **12**(11): p. 2815-2826.

169. Zhang, P., et al., *Nanomedicine-based immunotherapy for the treatment of cancer metastasis.* Adv Mater, 2019. **31**(49): p. 1904156.
170. Qiu, H., et al., *Nanomedicine approaches to improve cancer immunotherapy.* Wiley interdisciplinary reviews. Nanomed Nanobiotechnol, 2017. **9**(5).
171. Irvine, D.J. and E.L. Dane, *Enhancing cancer immunotherapy with nanomedicine.* Nat Rev Immunol, 2020. **20**(5): p. 321-334.
172. Brigger, I., C. Dubernet, and P. Couvreur, *Nanoparticles in cancer therapy and diagnosis.* Adv Drug Deliv Rev, 2012. **64**: p. 24-36.
173. Feng, X., et al., *Immunomodulatory Nanosystems.* Adv Sci, 2019. **6**(17): p. 1900101.
174. Matsu-ura, T., S.R. Moore, and C.I. Hong, *WNT takes two to tango: Molecular links between the circadian clock and the cell cycle in adult stem cells.* J Biol Rhythms, 2018. **33**(1): p. 5-14.
175. Martin, J.D., et al., *Improving cancer immunotherapy using nanomedicines: progress, opportunities and challenges.* Nat Rev Clin Oncol, 2020. **17**(4): p. 251-266.
176. Duan, X., C. Chan, and W. Lin, *Nanoparticle-mediated immunogenic cell death enables and potentiates cancer immunotherapy.* Angew Chem Int Ed Engl, 2019. **58**(3): p. 670-680.
177. Shi, Y. and T. Lammers, *Combining nanomedicine and immunotherapy.* Acc Chem Res, 2019. **52**(6): p. 1543-1554.
178. Ma, L., et al., *Enhanced CAR–T cell activity against solid tumors by vaccine boosting through the chimeric receptor.* Science, 2019. **365**(6449): p. 162-168.
179. Huai, Y., et al., *Nanoparticle interactions with the tumor microenvironment.* Bioconjugate Chem, 2019. **30**(9): p. 2247-2263.
180. Liu, Z.-g., et al., *Immunomodulating nanomedicine for cancer therapy.* Nano Lett, 2018. **18**.
181. Rampado, R., et al., *Nanovectors design for theranostic applications in colorectal cancer.* J Oncol, 2019. **2019**: p. 2740923.
182. Roelands, J., et al., *Immunogenomic classification of colorectal cancer and therapeutic implications.* Int J Mol Sci, 2017. **18**(10): p. 2229.
183. Zhu, G., et al., *Intertwining DNA-RNA nanocapsules loaded with tumor neoantigens as synergistic nanovaccines for cancer immunotherapy.* Nat commun, 2017. **8**(1): p. 1482-1482.
184. Goodwin, T.J. and L. Huang, *Investigation of phosphorylated adjuvants co-encapsulated with a model cancer peptide antigen for the treatment of colorectal cancer and liver metastasis.* Vaccine, 2017. **35**(19): p. 2550-2557.

185. Ni, Q., et al., *A bi-adjuvant nanovaccine that potentiates immunogenicity of neoantigen for combination immunotherapy of colorectal cancer.* Sci Adv, 2020. **6**(12): p. eaaw6071.
186. Wang, X., et al., *Polydopamine nanoparticles carrying tumor cell lysate as a potential vaccine for colorectal cancer immunotherapy.* Biomater Sci, 2019. **7**(7): p. 3062-3075.
187. Liu, W.-L., et al., *Expandable immunotherapeutic nanoplatforms engineered from cytomembranes of hybrid cells derived from cancer and dendritic cells.* Adv Mater, 2019. **31**(18): p. 1900499.
188. Liu, W.-L., et al., *Cytomembrane nanovaccines show therapeutic effects by mimicking tumor cells and antigen presenting cells.* Nat Commun, 2019. **10**(1): p. 3199.
189. Dong, X., et al., *Bioinorganic hybrid bacteriophage for modulation of intestinal microbiota to remodel tumor-immune microenvironment against colorectal cancer.* Sci Adv, 2020. **6**(20): p. eaba1590.
190. Kuai, R., et al., *Elimination of established tumors with nanodisc-based combination chemoimmunotherapy.* Sci Adv, 2018. **4**(4): p. eaao1736-eaao1736.
191. Luo, M., et al., *A STING-activating nanovaccine for cancer immunotherapy.* Nat nanotechnol, 2017. **12**(7): p. 648-654.
192. Castro, F., et al., *Pro-inflammatory chitosan/poly(γ-glutamic acid) nanoparticles modulate human antigen-presenting cells phenotype and revert their pro-invasive capacity.* Acta Biomater, 2017. **63**: p. 96-109.
193. Zhang, Q., et al., *A multifunctional nanotherapy for targeted treatment of colon cancer by simultaneously regulating tumor microenvironment.* Theranostics, 2019. **9**(13): p. 3732-3753.
194. Gonzalez-Aramundiz, J.V., et al., *Nanovaccines : nanocarriers for antigen delivery.* Biol Aujourdhui, 2012. **206**(4): p. 249-61.
195. Conniot, J., et al., *Immunization with mannosylated nanovaccines and inhibition of the immune-suppressing microenvironment sensitizes melanoma to immune checkpoint modulators.* Nat Nanotechnol, 2019. **14**(9): p. 891-901.
196. Zhuang, J., et al., *Nanoparticle delivery of immunostimulatory agents for cancer immunotherapy.* Theranostics, 2019. **9**(25): p. 7826-7848.
197. Francis, D.M., et al., *Blockade of immune checkpoints in lymph nodes through locoregional delivery augments cancer immunotherapy.* Sci Transl Med, 2020. **12**(563): p. eaay3575.
198. Rotman, J., et al., *Unlocking the therapeutic potential of primary tumor-draining lymph nodes.* CII, 2019. **68**(10): p. 1681-1688.

199. Fransen, M.F., et al., *Tumor-draining lymph nodes are pivotal in PD-1/PD-L1 checkpoint therapy.* JCI Insight, 2018. **3**(23).
200. Zhou, Z., et al., *Reverse immune suppressive microenvironment in tumor draining lymph nodes to enhance anti-PD1 immunotherapy via nanovaccine complexed microneedle.* Nano Research, 2020. **13**(6): p. 1509-1518.
201. Kroll, A.V., et al., *Nanoparticulate delivery of cancer cell membrane elicits multiantigenic antitumor immunity.* Adv Mater, 2017. **29**(47): p. 10.1002/adma.201703969.
202. Mazzaferro, V., et al., *Vaccination with autologous tumor-derived heat-shock protein Gp96 after liver resection for metastatic colorectal cancer.* Clin Cancer Res, 2003. **9**(9): p. 3235-3245.
203. Madkour, L., *Nucleic acids as gene anticancer drug delivery therapy - 1st Edition*. 2019.
204. Mikelez-Alonso, I., A. Aires, and A.L. Cortajarena, *Cancer nano-immunotherapy from the injection to the target: The role of protein corona.* Int J Mol Sci, 2020. **21**(2).
205. Rezaei, R., et al., *The role of nanomaterials in the treatment of diseases and their effects on the immune system.* Open Access Maced J Med Sci, 2019. **7**(11): p. 1884-1890.
206. Fadeel, B., *Hide and Seek: Nanomaterial interactions with the immune system.* Front Immunol, 2019. **10**(133).
207. Sau, S., et al., *Nanomaterials for tumor immunomodulation and overcoming current clinical challenges.* Nanomedicine, 2019. **14**(12): p. 1515-1519.
208. Hickey, J.W., et al., *Biologically inspired design of nanoparticle artificial antigen-presenting cells for immunomodulation.* Nano lett, 2017. **17**(11): p. 7045-7054.
209. Calmeiro, J., et al., *Biomaterial-based platforms for in situ dendritic cell programming and their use in antitumor immunotherapy.* JITC, 2019. **7**(1): p. 238-238.
210. Castro, F., et al., *Chitosan/poly(γ-glutamic acid) nanoparticles incorporating IFN-γ for immune response modulation in the context of colorectal cancer.* Biomater Sci, 2019. **7**(8): p. 3386-3403.
211. Zanganeh, S., et al., *Iron oxide nanoparticles inhibit tumour growth by inducing pro-inflammatory macrophage polarization in tumour tissues.* Nat Nanotechnol, 2016. **11**(11): p. 986-994.
212. Li, H., et al., *Tumor cell membrane-coated biomimetic nanoplatform for homologous targeted therapy of colorectal carcinoma.* Int J Polym Mater, 2020. **69**(18): p. 1157-1166.

213. He, C., et al., *Core-shell nanoscale coordination polymers combine chemotherapy and photodynamic therapy to potentiate checkpoint blockade cancer immunotherapy.* Nat Commun, 2016. **7**(1): p. 12499.
214. Yan, S., et al., *Current applications and future prospects of nanotechnology in cancer immunotherapy.* Cancer Biol Med, 2019. **16**(3): p. 486-497.
215. Kim, T.H., et al., *Mannosylated chitosan nanoparticle-based cytokine gene therapy suppressed cancer growth in BALB/c mice bearing CT-26 carcinoma cells.* Mol Cancer Ther, 2006. **5**(7): p. 1723-32.
216. Liu, X., et al., *Modified nanoparticle mediated IL-12 immunogene therapy for colon cancer.* Nanomedicine, 2017. **13**(6): p. 1993-2004.
217. Manal Ali Buabeid , E.-S.A.A., and Ghulam Murtaza *Emerging Prospects for Nanoparticle-Enabled Cancer Immunotherapy.* J Immunol Res, 2020.p. 11.

CHAPTER II – OVERVIEW, MOTIVATIONS, OBJECTIVES AND TASKS

Overview and Motivation

CRC presents a significant challenge in healthcare, particularly with a growing incidence observed among young adults [1]. Despite notable progress in CRC diagnosis and treatment, the 5-year survival rate for metastatic patients remains restricted to 14%, solidifying its position as the second deadliest cancer globally [2].

Over the past two decades, the TME has been increasingly recognized for its pivotal role in CRC initiation, progression, and metastasis [3]. Therefore, this TME which comprises the surrounding immune cells, blood vessels, extracellular matrix components, fibroblasts, lymphocytes, bone marrow-derived inflammatory cells, and arrested signaling molecules, contributes to cancer cell immune escape and immune tolerance impacting tumor progression and the therapeutic response [4]. Tumor-associated macrophages (TAMs) constitute a significant portion of immune cells within the colorectal TME [5]. TAMs can polarize into either M1-like macrophages, which act as tumor suppressors, or M2-like macrophages, which promote CRC by suppressing immune responses [5]. Given their plasticity, TAMs have the capability to dynamically adapt in response to signals from cancer cells or from the TME [6]. Therefore, reprogramming TAM polarization holds promise for enhancing tumor immunotherapy and CRC treatment, either through single or combinatory strategies [6].

Currently, the mainstream option for CRC treatment is based on 5-FU chemotherapeutic regimens [7]. However, the severe toxicity of 5-FU renders it unsuccessful with limited local bioavailability and low tumor-specific selectivity [8]. Besides, repeated administrations of 5-FU may impair cytokines levels at the TME [9]. To modulate the immune response and improve treatments in metastatic solid tumors, interleukin-12 (IL-12)-based combined therapies have been investigated in preclinical data, exhibiting anti-tumor response and promoting immune infiltration within the TME [10, 11]. IL-12 has the ability to activate both innate and adaptive immunities, due to its remarkable function to induce IFN-γ expression and production from aforementioned cells, enhancing antigen presentation, attracting T cells and reverting macrophages polarization into a more pro-inflammatory M1-like phenotype [12]. However, IL-12 has been associated with unacceptable levels of side effects and toxicity in early clinical trials [13].

To address these limitations, nanomedicines offer compelling solutions for therapeutic delivery, by effectively overcoming formulation obstacles linked to cargo molecules, such as hydrophobicity, ensuring sustained cargo release, and enhancing molecule stability [14]. Among the array of nanomedicine platforms, targeted NPs have emerged as potential candidates to enhance the safety and efficacy of drug delivery, thereby boosting

bioavailability and mitigating toxic effects [15]. Poly(lactic-co-glycolic acid) (PLGA) NPs have attracted considerable attention because of their biocompatibility and biodegradability within a flexible matrix [15]. Surface modification with polyethylene glycol, PEG, is considered the gold standard method for enhancing PLGA NPs' circulation time, offering a range of possibilities for customizing their surface by functionalizing the PEG outer part [16]. Moreover, surface modification of PLGA NPs with PEG may avoid opsonin adsorption and increase circulation time of intravenously administered NPs [18]. Extensive research has investigated the surface functionalization of NPs with targeting ligands capable of recognizing and binding specific cell transporters, frequently found to be overexpressed or preferentially presented at the desired site [18]. These targeted nanomedicines facilitate increased accumulation and/or likelihood of intracellular transport of therapeutic NPs to the target site, thereby enhancing drug therapeutic efficacy and reducing off-target side effects [16, 19]. Hence, the functionalization of NPs targeted towards specific sites of interest aims to maximize drug delivery to CRC cells and their microenvironment, offering a promising strategy to enhance treatment efficacy.

Carcinoembryonic antigen (CEA) is an overexpressed molecule in CRC patients, playing a crucial role in several biological processes, such inflammation, immune cell transmigration and immune response, promoting the progression and invasion of the tumor [20]. Hence, approaches using anti-CEA antibodies (Ab) or engineered fragments (scFV) are being investigated as theranostics [21]. Also, strategies using anti-CEA antibodies are described to modulate the immune response and to enhance tumor antigen presentation [22, 23].

The colorectal TME, characterized by severe hypoxia, slightly acidic pH, and excessive ROS, presents an opportunity for stimuli-responsive drug delivery systems [24]. Among these, pH-responsive mechanisms are frequently employed, given the lower pH of the tumor microenvironment compared to that of blood and of healthy tissues [25]. pH-responsive polymer carriers have shown potential in enhancing drug delivery efficiency in vivo, facilitating targeted drug delivery, and reducing adverse drug reactions, thus enabling multifunctional and personalized treatment [24]. Consequently, various monomers are being used to design pH-responsive NPs [26]. The 2,3-dimethylmaleic anhydride (DMMA), known as an amino group protector, is being investigated for its ability to undergo reversible cleavage under mild acidic conditions at pH ~6.8, making it suitable for the development of acidic TME-triggered surface charge-reversible nano-therapeutics [25].

Therefore, the need to enhance drug stability and bioavailability while simultaneously targeting CRC and its TME, reducing side effects creates opportunities for the exploration of combinatory targeting strategies.

Aims and Objectives

Main aim

The main goal of this doctoral thesis was to formulate a combinatory nano strategy aimed to simultaneously target CEA-expressing CRC cells and its mildly acidic TME, with the goal of mitigating the immunosuppressive microenvironment and enhance the eradication of CRC cells. The proposed approach involves PLGA-PEG NPs loaded with the chemotherapeutic drug 5-FU, specifically engineered to target CEA-expressing CRC cells for precise and effective action. Additionally, to augment the pro-inflammatory anti-tumor response, this therapeutic strategy was complemented by an immunomodulatory approach, involving the development of PLGA NPs modified with DMMA for pH responsiveness, targeting the slightly acidic TME, and delivering the pro-inflammatory cytokine IL-12. **Therefore, the primary aim of this work can be delineated into three distinct sub-objectives:**

- **Development, characterization, and 2D in vitro assessment of a NP platform containing 5-FU for targeting CEA-expressing CRC cells**, enhancing 5-FU bioavailability and cancer cell specificity. The NPs will comprise a PLGA core with a short-length PEG shielding, combined with an anti-CEA scFv targeting ligand to specifically target CEA-overexpressed MSI and MSS CRC cell lines, improving toxicity in tumor cells while ensuring safety for macrophage administration. CEA is a promising target for CRC therapies due to its well-established overexpression in cancer cells, while being minimally expressed in normal colorectal tissues [27, 28]. The work related with this sub-objective of this doctoral thesis will be presented in **CHAPTER III**.

Specific tasks for the first sub-objective of this doctoral thesis include:

1. Chemical synthesis of the anti-CEA scFv with the polymeric polymer PLGA-PEG-Mal, constituted by PLGA as polymeric matrix of the NPs.
2. Production and characterization of 5-FU-loaded NPs assembled from the previously synthesized polymeric conjugate.
3. Validation of NPs in a 2D *in vitro* models concerning tumor uptake, cytotoxicity, impact on macrophage cell viability, and their effect on macrophage polarization.

- **Development, characterization, and evaluation, in both 2D and 3D *in vitro***

settings, of a pH-responsive NP formulation containing IL-12, designed to target the weakly acidic CRC TME. The goal is to enhance IL-12 stability and minimize side effects. The PLGA core NPs will be chemically modified by conjugating them with an acid-responsive monomer, DMMA, via an amidation process [29]. This involves the reaction of the carboxylate group in DMMA with an amide group (–NH2) present in PLGA (PLGA-NH2), resulting in the formation of an amide bond. Furthermore, under slightly acidic conditions, DMMA will dissociate, leading to a cationic charge reversal property in the NPs [30]. Consequently, IL-12 will be released in a controlled manner, specifically under weakly acidic pH conditions, thereby improving the immune response through the induction of pro-inflammatory IFN-γ production. The work related to this sub-objective of this doctoral thesis will be presented in **CHAPTER IV**.

Specific tasks for the second sub-objective of this doctoral thesis include:

1. Chemical synthesis of the DMMA monomer with the polymeric polymer PLGA-NH2.
2. Manufacturing and characterization of IL-12 encapsulated into the pH-responsive NPs produced from the previously synthesized polymeric conjugate.
3. Validation of NPs in 2D and 3D *in vitro* models regarding macrophages cytotoxicity impact, NO release and IFN-γ secretion as well as macrophages polarization, and the IL-10 anti-inflammatory cytokine production.

- **Assessment of the novel combinatory immunochemotherapeutic strategy in 3D CEA-expressing and non-expressing CRC spheroids**. One of the challenges faced in the clinical translation of immunomodulatory or chemotherapeutic nanomedicines is the lack of suitable *in vitro* models for CEA-expressing (CEA^{high}) and non-expressing (CEA^{low}) MSI CRC, that can precisely mimic the complexity of the disease and predict therapeutic responses. In this study, we propose the use of two multicellular tumor spheroids, based on a heterotypic tumor spheroid-like structure, to replicate the TME and the associated ECM. The CRC 3D spheroids will comprise MSI CEA^{high} or CEA^{low} CRC cell lines, macrophages differentiated from peripheral monocytes from healthy blood donors, and collagen type I.

Specific tasks for the third aim of this doctoral thesis include:

a. High-throughput production of 3D CRC spheroids using agarose micro-molding technology.

b. Morphological and histological characterization of the 3D CRC spheroids.
c. Validation of the ability of 3D CEA^{high} CRC spheroids to respond to therapy, using the single therapy targeting CEA-expressing cells or the combinatory strategy, to act on both cancer cells and its TME and enhance the CRC cell death. The validation involves the investigation of 3D CRC spheroid cell uptake, cytotoxicity, macrophage polarization and cytokines production post-treatment.

The work related with the secondary aim of this doctoral thesis will be presented in **CHAPTER V**.

Collaboration of supervision and institutions

The primary focus of the Nanomedicines & Translational Drug Delivery group at Instituto de Investigação e Inovação em Saúde (i3S) lies in the development and characterization of nanomedicines. These nanomedicines hold promise for diagnostic or therapeutic applications within the pharmaceutical and biomedical domains. Additionally, the group specializes in creating biorelevant *in vitro* cell models that demonstrate excellent correlation between *in vitro* and *in vivo* conditions. These models are helpful in predicting drug bioavailability and elucidating the interactions between cells and nanomaterials. The extensive expertise of the group contributed to tailor a diverse array of nano formulations, including polymer-based formulations, targeting specific tissues to amplify the therapeutic efficacy of drug payloads, and combating high-burden diseases like cancer.
The Tumor Microenvironment Interactions group at i3S focuses primarily on researching the role of the tumor microenvironment for cancer cell immune escape and progression. Specifically, they aim to understand how immune cells and extracellular matrix components influence the modulation of cancer invasion and metastasis. Therefore, the group specializes in creating both *in vitro* and *in vivo* models, using heterotypic spheroids and human decellularized extracellular matrices, derived from cancer patients' surgical resections, to construct 3D-organotypic assays and orthotopic animal models for studying the impact of the tumor microenvironment on gastrointestinal cancers. The generated knowledge may contribute for further biomarkers development and to the design of more efficient anti-cancer therapies.
The Engineered Therapeutics group at the University of Twente operates at the interface of nanomedicine and of the tumor microenvironment. The main goal of the group is to understand and dissect the cellular interactions within the tumor microenvironment, particularly focusing on fibroblasts, macrophages, and extracellular components, with the

aim of developing targeted therapeutic molecules. Therefore, the group holds the expertise of 3D bioengineering technologies development as valuable tools for studying nanomedicine and tumor microenvironments. Moreover, the group employs peptide technologies to reprogram the microenvironment, thereby enhancing the anti-tumor effects of chemotherapy. Additionally, they specialize in advanced targeted nanomedicines, facilitating precise delivery of therapeutic agents to specific cells within the tumor microenvironment, in combination with nanotheranostic methods for personalized medicine.

References

1. Zarour, L.R., et al., *Colorectal cancer liver metastasis: Evolving paradigms and future directions.* Cell Mol Gastroenterol Hepatol, 2017. **3**(2): p. 163-173.
2. Kreidieh, M., et al., *Expanding the scope of immunotherapy in colorectal cancer: current clinical approaches andfFuture directions.* BioMed Res Int, 2020. **2020**: p. 9037217.
3. Chen, X., et al., *The effects of metabolism on the immune microenvironment in colorectal cancer.* Cell Death Discovery, 2024. **10**(1): p. 118.
4. Fuhr, L., et al., *The interplay between colon cancer cells and tumour-associated stromal cells impacts the biological clock and enhances malignant phenotypes.* Cancers, 2019. **11**(7): p. 988.
5. Wang, H., T. Tian, and J. Zhang, *Tumor-associated macrophages (TAMs) in colorectal cancer (CRC): From mechanism to therapy and prognosis.* Int J Mol Sci, 2021. **22**(16).
6. Li, Y., et al., *Functional and Therapeutic Significance of Tumor-Associated Macrophages in Colorectal Cancer.* Front Oncol, 2022. **12**: p. 781233.
7. Cisterna, B.A., et al., *Targeted nanoparticles for colorectal cancer.* Nanomedicine, 2016. **11**(18): p. 2443-56.
8. McQuade, R.M., et al., *Colorectal cancer chemotherapy: The evolution of treatment and new approaches.* Curr Med Chem, 2017. **24**(15): p. 1537-1557.
9. Abdellateif MS, S.S., Badr DM, Shaarawy S, Hussein MM, Zekri AN, Fouad MA. , *The Prognostic Significance of 5-Fluorouracil Induced Inflammation and Immuno-Modulation in Colorectal Cancer Patients.* J Inflamm Res, 2020. **13**: p. 1245-1259.
10. Anwer, K., et al., *Phase I trial of a formulated IL-12 plasmid in combination with carboplatin and docetaxel chemotherapy in the treatment of platinum-sensitive recurrent ovarian cancer.* Gynecol Oncol, 2013. **131**(1): p. 169-73.
11. Strauss, J., et al., *First-in-human phase I trial of a tumor-targeted cytokine (NHS-IL12) in subjects with metastatic solid tumors.* Clin Cancer Res, 2019. **25**(1): p. 99-109.
12. Berraondo, P., et al., *Revisiting interleukin-12 as a cancer immunotherapy Agent.* Clin Cancer Res, 2018. **24**(12): p. 2716-2718.
13. Nguyen, K.G., et al., *Localized interleukin-12 for cancer immunotherapy.* Front Immunol, 2020. **11**(2510).
14. Shi, J., et al., *Cancer nanomedicine: progress, challenges and opportunities.* Nat Rev Cancer, 2017. **17**(1): p. 20-37.

15. *The two directions of cancer nanomedicine.* Nat Nanotechnology, 2019. **14**(12): p. 1083-1083.
16. Martins, C., et al., *Functionalizing PLGA and PLGA derivatives for drug delivery and tissue regeneration applications.* Adv Healthc Mater, 2018. **7**(1): p. 1701035.
17. Silva, A., et al., *Integrated Analysis of Biological Samples by Imaging Flow Cytometry.* Microsc Microanal, 2015. **21**(S5): p. 95-96.
18. Pereira, I., et al., *Carcinoembryonic antigen-targeted nanoparticles potentiate the delivery of anticancer drugs to colorectal cancer cells.* Int J Pharm, 2018. **549**(1-2): p. 397-403.
19. Ahmad, F., et al., *Unique properties of surface-functionalized nanoparticles for Bio-application: Functionalization mechanisms and importance in application.* Nanomaterials, 2022. **12**(8).
20. Rizeq, B., Z. Zakaria, and A. Ouhtit, *Towards understanding the mechanisms of actions of carcinoembryonic antigen-related cell adhesion molecule 6 in cancer progression.* Cancer sci, 2018. **109**(1): p. 33-42.
21. Vigor, K., et al., *Nanoparticles functionalised with recombinant single chain Fv antibody fragments (scFv) for the magnetic resonance imaging of cancer cells.* Biomaterials, 2009. **31**: p. 1307-15.
22. Ellerman, D., *Bispecific T-cell engagers: Towards understanding variables influencing the in vitro potency and tumor selectivity and their modulation to enhance their efficacy and safety.* Methods, 2019. **154**: p. 102-117.
23. Cha, S., et al., *Treatment of CEA-positive solid tumors with anti-CEA chimeric antigen receptor T-cells in CEA transgenic mice.* J Immunol, 2020. **204**(1 Supplement): p. 239.25-239.25.
24. Chu, S., et al., *pH-Responsive polymer nanomaterials for tumor therapy.* Front Oncol, 2022. **12**: p. 855019.
25. Feng, L., et al., *The acidic tumor microenvironment: a target for smart cancer nano-theranostics.* Nat SciRev, 2017. **5**(2): p. 269-286.
26. Morarasu, S., et al., *Targeted cancer therapy via pH-functionalized nanoparticles: A scoping review of methods and outcomes.* Gels, 2022. **8**(4).
27. Moretto, R., et al., *CEA increase as a marker of disease progression after first-line induction therapy in metastatic colorectal cancer patients. A pooled analysis of TRIBE and TRIBE2 studies.* Br J Cancer, 2021. **125**(6): p. 839-845.
28. Elekonawo, F.M.K., et al., *Carcinoembryonic antigen-targeted photodynamic therapy in colorectal cancer models.* EJNMMI Res, 2019. **9**(1): p. 108.
29. Kumar, D., B.A. Eipper, and R.E. Mains, *Amidation☆*, in *Reference Module in Biomedical Sciences*. 2014, Elsevier.

30. Zhang, P., et al., *Charge reversal nano-systems for tumor therapy.* J Nanobiotechnol, 2022. **20**(1): p. 31.

CHAPTER III –TARGETED NANOPARTICLES TO EFFECTIVE TARGETING OF CEA-EXPRESSING COLORECTAL CANCER CELLS

This chapter was based on the following publication:

- **MJ Silveira**; C Martins; T Cruz; F Castro; A Amorim- Costa; K Chester; MJ Oliveira; B Sarmento. "scFv biofunctionalized nanoparticles to effective and safe targeting of CEA- expressing colorectal cancer cells". Journal of Nanobiotechnology 21 1 (2023)

In this original research article, I was responsible for the conceptualization, methodology elaboration, and writing - original draft. The supervisors were responsible for reviewing, editing, and submitting the manuscript. This article was not previously included in another PhD thesis, and it is reproduced in this thesis. The authorization from the journal to reuse the manuscript in this thesis were included in Appendix.

Abstract

Colorectal cancer (CRC) is one of the deadliest cancers worldwide, with the 5-year survival rate in metastatic cases limited to 12%. The design of targeted and effective therapeutics remains a major unmet clinical need in CRC treatment. Carcinoembryonic antigen (CEA), a glycoprotein overexpressed in most colorectal tumors, may constitute a promising molecule for generating novel CEA-targeted therapeutic strategies for CRC treatment. Here, we developed a smart nanoplatform based on chemical conjugation of an anti-CEA single-chain variable fragment (scFv), MFE-23, with PLGA-PEG polymers to deliver the standard 5-Fluorouracil (5-FU) chemotherapy to CRC cells. We confirmed the specificity of the developed CEA-targeted NPs on the internalization by CEA-expressing CRC cells, with an enhance of 3-fold in the cell uptake. Additionally, CEA-targeted NPs loaded with 5-FU induced higher cytotoxicity in CEA-expressing cells, after 24h and 48h of treatment, reinforcing the specificity of the targeted NPs. Lastly, the safety of CEA-targeted NPs loaded with 5-FU was evaluated in donor-isolated macrophages, with no relevant impact on their metabolic activity nor polarization. Altogether, this proof of concept supports the CEA-mediated internalization of targeted NPs as a promising chemotherapeutic strategy for further investigation in different CEA-associated cancers and respective metastatic sites.

Keywords: Cancer therapy; Carcinoembryonic antigen; Drug delivery; Nanomedicine; Single-chain variable fragment functionalization; Targeted therapies

Background

Colorectal cancer (CRC) is the second most lethal cancer worldwide with around 12% of 5-year survival rate in metastatic cases (1, 2). The molecular mechanisms of CRC, associated microbiota, epigenetic and genetic alterations, as well as its tumor microenvironment (TME), confer highly intertumoral and intratumor heterogenicity. Such complexity renders CRC treatment particularly challenging and results in numerous cases of drug resistance and tumor relapse (3). Having in consideration the aforementioned features of CRC, the stratification into four consensus molecular subtypes (CMSs) reflects the molecular and genetic profiles as well as immune infiltrate differences among these tumors (4). In fact, the CMSs classification brought a new paradigm to the CRC treatment, allocating microsatellite instable (MSI) or microsatellite stable (MSS) tumors into different subtypes, allowing a better selection of therapy and its response prediction (5).

The fluoropyrimidine, 5-Fluorouracil (5-FU), an antimetabolite with anticancer effects, remains a mainstream option of chemotherapy to treat high-risk stage II, stage III and IV CRC patients, as single-agent therapy, and multiple-agent regimens (FOLFOX, FOLFIRI, XELOX, and SOX) (6). However, despite multiple benefits, 5-FU-based therapies still hold very low response rates, are frequently associated with chemoresistance, low bioavailability, low drug uptake, lack of tumor targetability and high systemic toxicity (7). Specifically, for patient harboring tumors stratified into CMS1 and CMS4 subtypes, 5-FU adjuvant chemotherapy does not seem to improve overall survival (OS) and significantly decreases the 5-year disease-free survival rate from 83.3% to 30.0%. Whereas, in tumors classified into CMS2 and CMS3, 5-FU treatment is associated with increasing levels of OS and 5-year disease-free survival rates (8).

The TME has been reported as a critical factor, affecting CRC therapeutic outcomes and treatment resistance (9). One of the most important component of the TME are tumor-associated macrophages (TAMs), usually divided into a spectrum of phenotypes between extreme profiles: M1 macrophages (pro-inflammatory) that act as tumor suppressors, and M2 macrophages (anti-inflammatory), which promote cancer progression (10). In patients treated with 5-FU, the increase of TAMs infiltration has been negatively correlated with tumor growth (11). Moreover, some authors have investigated the synergistic effect of 5-FU and M1 macrophages whose findings are associated with higher rates of colorectal cell death (12, 13). However, when TAMs infiltration is enriched with M2 macrophages, they confer CRC resistance to 5-FU, impairing patients OS (14).

Accordingly, the reported limitations in the therapeutic efficacy of 5-FU in regarding its short half-life, high cytotoxicity, macrophages polarization and low bioavailability, elucidate the need for advanced drug delivery systems as potential tools to enhance 5-FU pharmacokinetic properties and pharmacological performance.

Recently, nanotechnology-based strategies have been emerging as promising strategies to revolutionize illness treatments, with remarkable findings in the way how drugs and molecules are delivered and released (15). Different nanotechnology-based strategies have been explored for promoting delivery of 5-FU to tumors (16). However, efforts are required to improve pharmacokinetic aspects and accelerate translation to the clinic (17) Particularly, PEGylated nanoparticles (NPs) based on the poly (lactic-co-glycolic acid) (PLGA) polymer, have gained significant interest due to its biodegradable properties, non-toxicity, and possibility of a targeted cargo delivery by surface modification with targeting moieties directed to the biological site of interest (18, 19).

The carcinoembryonic antigen (CEA) tumor-associated antigen is a membrane-anchored glycoprotein, overexpressed in 90–95% of colorectal primary tumors and respective metastases (20). Moreover, CEA is frequently used for diagnosis and prognosis of CRC, constituting a promising target molecule for CRC therapy (21). Therefore, many monoclonal antibodies have been developed against CEA with diagnosis and therapeutic proposes (22, 23). Recent advantages in antibody engineering have produced different types of antibodies fragments (e.g., single-chain variable (scFv)). Particularly, the MFE-23 scFv has been shown to effectively target CRC in imaging and antibody-directed pro-drug therapy strategies, due to its enhanced tumor cell internalization, prolonged half-life (superior to 4 days at 37ºC), and presence of a binding domain for anti-CEA immunotoxins (24, 25).

The major goal of this work was to develop CEA-targeted NPs of PLGA and PEG as a novel platform to deliver 5-FU to CRC cells, thus increasing 5-FU bioavailability and providing a tumor cell-specific anti-cancer activity. Here, we described the NPs manufacture process and detailed their physicochemical characterization. Moreover, we assessed the specificity and selectively of CEA-targeted NPs loaded with 5-FU in CMS1 and CMS4 CRC cell lines, as well as their effect on cell metabolic activity inhibition. Lastly, we assessed the potential impact of the developed NPs on the metabolic activity and polarization of isolated from healthy blood donor's macrophages.

Methods

To prepare and characterize NPs, PLGA 5004 (50:50 LA:GA; 44K; Purasorb® PDLG 5004A) was kindly provided by Corbion-Purac biomaterials. PLGA (30K)-PEG (5K)-

maleimide (PLGA-PEG-Mal), PLGA (30K)-FITC and PLGA (30K)-Rhodamine B were purchased from RuixiBiotech®; Anti-CEA scFv was kindly developed and provided by Kerry Chester's group at UCL Cancer Institute; 5-FU, Ammonium Hydroxide (NH4OH) and dichloromethane (DCM) were acquired from Sigma-Aldrich®. Tween® 80, sodium chloride, tris(2-carboxyethyl) phosphine (TCEP), and diethyl ether from Sigma-Aldrich®; acetonitrile (ACN), Amicon® Ultra-15 centrifugal filter units (molecular weight cutoff of 100K) were acquired from MERCK® Millipore; dimethylformamide (DMF) and trifluoroacetic acid (TFA) from Acros Organics. XTerra RP-18 column (5 µm, 4.6 × 250 mm) from waters and Zorbax 300SB-C8 Narrow-bore column (5 µm, 2.1 x 150 mm) from Agilent Technologies. Ultrapure water was prepared in-house with a conductivity of 0.055 µS/cm and a resistivity of 18.2 MΩ.cm, using MilliQ® station from Millipore Corporation. For cell cultures, T flasks were acquired from Orange Scientific; Dulbecco's Modified Eagle Medium (DMEM), Roswell Park Memorial Institute (RPMI) 1640 Medium, Trypsin, Fetal Bovine Serum (FBS) and penicillin-streptomycin from Gibco®. Accutase from Thermo Fisher Scientific®. RosetteSep-Human Monocyte Enrichment Cocktail from StemCell Technologies. Histopaque-1077, Resazurin and Triton X-100 and Lipopolysaccharides from Escherichia coli O111:B4 (LPS) were purchased from Sigma-Aldrich®, Macrophage colony-stimulating factor (M-CSF) and Recombinant Human Interleukin-10 (IL-10) obtained from ImmunoTools. Concerning microscopy and flow cytometry staining, CEA Monoclonal Antibody (1106) Alexa Fluor 488-anti mouse, anti-HLA-DR/PB and cell Mask Green Stain (H32714 - CS CellMask Green stain^{TM}) were purchased from Invitrogen. The antibodies anti-CD14/APC and anti-CD86/FITC were obtained from ImmunoTools. The anti-CD206/PE was purchased from BioLegend. Anti-CD163/PE was acquired from BD Biosciences. The anti-PDL1/FITC was acquired from BD-Pharmingen, while the Live/Dead Fixable Viability Dye eFluor™ 780 and 4′,6-diamidino-2-phenylindole (DAPI) from Thermo Fisher Scientific®.

Anti-CEA scFv chemical conjugation to the PLGA-PEG-mal polymer

Anti-CEA scFv containing a disulfide bond molecular weight (MW) ≈ 27K,11.43 mg, 0.42 µmol) was treated with tris(2-carboxyethyl) phosphine (1.5 mg, 13.2 5.23 µmol) in 2mL anhydrous dimethylformamide and stirred for 1h at room temperature (RT) under inert atmosphere. 15 mg of PLGA (30K)-PEG(5K)-Mal (Mn ≈ 35K, 0.43 µmol) in 1 mL anhydrous dimethylformamide were then added to the mixture and allowed to react for 24h at 4°C under inert atmosphere. The reaction mixture was poured into cold diethyl ether (25 mL), washed first time with 40 mL of miliQ water, then with 20 mL of miliQ water

and finally with cold diethyl ether (5 mL). The conjugated polymer (PLGA-PEG-scFv) was then, dried under vacuum, in a vacuum oven overnight at 20ºC.

Characterization of targeted polymer PLGA-PEG-scFv

^{1}H NMR measurements were performed with a BRUKER AVANCE III 600 MHz (Bruker Corporation) spectrometer at 25°C in deuterated dichloromethane. Chemical shifts are reported in ppm (δ units) and were referenced to the residual solvent signal. Mnova software (Mestrelab Research) was used for analysis processing. The conjugation efficiency (CE) of PLGA-PEG-scFv was then calculated by indirect method using HPLC technique, according to the following equation:

$$CE\ (\%) = \frac{initial\ mass\ of\ scFv - recovered\ mass\ of\ scFv}{initial\ mass\ of\ scFv}\ x\ 100$$

Briefly, the amount of scFv in the final conjugated polymer was quantified by indirect method through the difference between the total amount of scFv in the initial reaction and the final amount of scFv detected in the supernatants after the washes, in the purification step of the conjugated polymer, described above. The chromatographic analysis was performed by RP-HPLC with ultraviolet detection using a Hitachi LaChrom Elite® HPLC System (Hitachi High Technologies America, Inc). The RP-C8 column (Zorbax 300SB-C8 Narrow-bore) (5 µm, 2.1 x 150 mm) was used as stationary phase with a mobile phase composed by water with 0.1% of TFA (eluent A) and acetonitrile with 0.1% of TFA (eluent B) in Gradient method. The chromatographic analysis was performed at a flow rate of 0.7 mL/min in a gradient mode started at 30% of eluent B, increasing for to 40% of B in 12 minutes and kept constant at 40% for B for 3 minutes. From 15-15.1, eluent B decreased to 30% and kept constant until 20 minutes. The column oven was kept at 25°C. The absorbance was read at 280 nm. The injection volume was 30µL.

Manufacture of 5-FU loaded CEA-targeted nanoparticles

NPs containing 5-FU, Sigma-Aldrich, were generated by a modified water-in-oil-in-water (w/o/w) double emulsion-solvent evaporation technique. Briefly, 20 mg of polymer of PLGA (Mw ≈ 44K in a 50/50 M ratio of DL-lactide and Glycolide, viscosity midpoint 0.4dl/g viscosity) was mixed with 10% of PLGA-PEG-scFv and dissolved in 4 mL Dichloromethane (Sigma-Aldrich) for 3h. Afterwards 0.2mL of 50mg/mL 5-FU in 1 N

NH4OH was emulsified at 70% amplitude for 30s using a Vibra-CellTM ultrasonic processor in an ice bath. The first emulsion was then, poured into 12mL of 2% Tween 80 (MERCK) aqueous solution and sonicated for 60s, reaching the second emulsion (w/o/w). The final emulsion was then added to 24 mL of the same surfactant. Dichloromethane evaporation from the final solution occurred for 2 h and 30 under magnetic stirring at 600 rpm. Nanoparticles were washed twice with 10 mL of ultrapure water by centrifugation using Amicon® filters of 100K (Millipore Corporation) at 2500xg fr 90 min.

Characterization of nanoparticles

Average particle size, polydispersity index, surface charge and morphology of nanoparticles

Nanoparticles were characterized for their Z-average and polydispersity index (PDI) by dynamic light scattering (DLS), and zeta-potential (ζ-potential) through laser Doppler anemometry (LDA) using a Malvern Zetasizer Nano ZS instrument (Malvern Instruments Ltd). For these measurements, samples were diluted in an ionic solution of 10 mM sodium chloride (NaCl) at a 0.2 mg/mL particle concentration. Values reported are the mean ± standard deviation (SD) of at least three different batches. The morphological features of NPs were analyzed by transmission electron microscopy (TEM) with a JEOL JEM 1400 microscope (JEOL Ltd) at an accelerating voltage of 120 kV. Briefly, 10 µL of each NPs sample were mounted on nickel grids and left to stain for 2 min approximately.

5-FU association efficiency and drug loading

The amount of 5-FU encapsulated into NPs was directly quantified by liquid-liquid phase separation. Briefly, NPs were freeze dried after their purification, and consequently solubilized in 4mL DCM overnight. In the day after, miliQ water in same proportion was added to the first solution to solubilize 5-FU. The presence of this anti-cancer metabolite, 5-FU, was then analyzed by chromatography using a XTerra-C18 column as stationary phase with a mobile phase composed by water (eluent A) and acetonitrile (eluent B) in an isocratic method. The chromatographic analysis was performed with at a flow rate of 0.7 mL/min using 95:5 (eluent A: eluent B) in 10 minutes. The column oven was kept at 25°C. The absorbance was read at 266 nm. The injection volume was 20µL, association efficiency (AE) and drug loading, DL, were calculated using the followed equations:

$$AE\ (\%) = \frac{mass\ of\ encapsulated\ 5-FU}{inital\ mass\ of\ 5-FU}\ x100$$

$$DL(\%)\frac{mass\ of\ encapsulated\ 5-FU}{Total\ mass\ of\ nanoparticles}\ x100$$

Colloidal stability of nanoparticles

The stability of the developed NPs was evaluated during 31 days at 4ºC in a timepoints of 0,1,2,3,7 and 31 days. Afterwards, NPs were evaluated by DLS as previously described.

5-FU in vitro cumulative release

In vitro release behavior of 5-FU encapsulated into anti-CEA PLGA-PEG NPs was performed at 37 °C under gentle stirring rate (150 rpm) in phosphate buffered saline (PBS) pH 7.4 and evaluated in different time points (0, 0.25, 0.5, 1, 1.5,3, 4,72, 120, 140 and 552h). The collected samples were centrifuged at 17000 x g during 15 min (4 °C), and the supernatant was used for HPLC analysis, as previously described.

Cell lines and cell culture

All CRC cell lines were obtained from American Type Culture Collection (ATCC). HCT15, HCT116, HT29, RKO and SW480 CRC epithelial cell lines, were cultured in cell culture flasks in RPMI1640 medium (Gibco) with FBS (10% v/v) (Biowest) and penicillin-streptomycin (1% v/v), (Gibco). SW48, Caco-2 and LS174T CRC epithelial cell lines were cultured in DMEM (Gibco), supplemented with FBS, (10% v/v) and penicillin-streptomycin (1% v/v). Cell culture medium was changed every 2–3 days and cell lines were sub-cultured upon trypsin treatment. Cell cultures were kept in an incubator (Cell Culture CO_2 incubator, ESCO GB Ltd) at 37°C with 5% CO_2 and 95% relative humidity. Mycoplasma detection was routinely performed.

Ethics statement

According to the principles of Declaration of Helsinki, and by the ethical approval of Centro Hospitalar Universitário São João Ethics Committee, protocol reference 90/19, blood donors were informed through a written consent that the products of their blood collections could be used for research purposes. Monocytes were isolated from surplus

buffy coats from healthy blood donors, gently provided by the Immunohemotherapy Department of Centro Hospitalar Universitário São João (CHUSJ), Porto, Portugal.

Human monocytes isolation

As previously reported, human monocytes were isolated from healthy blood donors' buffy coats (27). Briefly, buffy coats were centrifuged and incubated with RosetteSep human monocyte enrichment kit (StemCell Technologies) in order to obtain peripheral blood mononuclear cells (PBMCs). After, each sample was diluted 1:1 with PBS supplemented with 2% FBS and layered over Histopaque-1077(Sigma-Aldrich) to separate blood components from monocytes. The enriched monocyte layer was collected and washed with PBS. For monocyte-macrophage differentiation, 0.5×10^6 monocytes (6-wells plates) and 0.2×10^6 (24-well plates) were cultured and differentiated using 50ng/mL of M-CSF (Immunotools) for 7 days in RPMI1640 medium, supplemented with FBS (10% v/v) and penicillin/streptomycin (1% v/v). Cells were maintained at 37 °C and 5% CO2 humidified atmosphere.

CEA expression evaluation

CRC cell lines (HCT15, HCT116, HT29, RKO, SW480, SW48, Caco-2 and LS174T) were seeded in T25 cm^2 flasks for 48 h. Cells were washed and incubated with accutase (Thermo Fischer) for 5 min at 37 °C and harvested. After, cells were washed and resuspended in FACS buffer (1% BSA in PBS). For staining it were used 0.05 $x10^6$ cells, anti-CEA monoclonal antibody (Invitrogen) diluted 1:100 in FACS buffer, primary antibody, Alexa 488 mouse, secondary antibody, diluted 1:200 in FACS buffer, and the Live/dead stain diluted 1:10,000 in PBS (ebioscience). Each antibody was incubated for 30 min at 4ºC, followed by washing steps with FACS buffer. Cells were fixed with 2% of PFA, 15 min at RT, and washed and resuspended in FACS buffer. Samples were analyzed with a BD FACSCanto™ II flow cytometer (BD Biosciences). Unstained cells and single stained with antibodies were used as control. Median fluorescence intensity was measured for at least 10,000 viable plus single cell gated events per sample, and all data was processed with FlowJo software (Tree Star).

Cell-nanoparticle interaction evaluations

Cellular uptake of anti-CEA-functionalized NPs (F NPs) and non-functionalized NPs (NF NPs) was quantified by imaging flow cytometry and evaluated qualitatively by confocal laser-scanning microscopy.

Imaging flow cytometry

To perform imaging flow cytometry analysis, 1 × 10^6, or 0.5 × 10^6 cells per well were seeded for Caco-2/SW48 and HCT15/SW480 cell lines (6-well plate), respectively. The cells were allowed to attach 24 h, after which media was replaced and 25 μgmL−1 of PLGA-FITC (Excitation maximum, nm:490, Emission maximum, nm:520) labeled F NPs and NF NPs (safety concentration) and free anti-CEA scFv was added. Analysis was done at different time points,1,3, 10 and 24 h at 37 °C. Afterward, cells were washed twice with 500 μL of PBS and detached with 300 μL trypsin (Thermo Fischer) for 5 min. Cells were subsequently washed with PBS at 300g for 5 min, fixed with 200 μL of 2% PFA for 20 min at RT, washed again, and resuspended in 80 μL of PBS for further analysis. Cells were analyzed quantified by imaging flow cytometry (ImageStreamX®, Amnis, EDM Millipore). FITC-NPs fluorescence was assessed by using a laser for excitation and images were acquired in channel 2 (490–560 nm) from the CCD camera using a 40× objective. For brightfield images, a brightfield LED lamp was used, and images were collected on channel 1, 420–480 nm, and at least 150000 events were collected. Image analysis was performed using IDEAS® data analysis software (Amnis, EDM Millipore, version 6.2.64.0), following the Internalization wizard pipeline where the ratio intensity of the FITC-NPs fluorescence signal inside the cell to the intensity of the entire cell was quantified. To discriminate internalized versus membrane-associated NPs, we designed a mask for the whole cell, defined in the brightfield image (Channel 1), darkfield, side scatter (SSC), which provides information about the internal complexity (granularity) of a cell (channel 6) and a cytoplasmic mask (internal) performed by eroding the whole cell mask by 4 pixels. A control based only on cells without NPs was also performed to exclude the possible cellular autofluorescence.

Confocal Laser-Scanning Microscopy

To evaluate the fate of F NPs on the cells, NPs were labelled with 30% of PLGA-Rhodamine B and compared with the control (PLGA- Rhodamine B labeled NF NPs). Briefly, CEA-expressing (Caco-2/SW48) and CEA-non expressing cell lines (HCT15/SW480) were plated in glass coverslips on 24-well plates (0.04 × 10^6 cells per coverslip). Cells were left to adhere for 24 h. After, cells were washed with PBS and treated with 25 μg mL−1 of F NPs or NF NPs, for 1, 3, 10 and 24 h at 37ºC. Cells were fixed with 4% PFA for 15 min at RT, and permeabilized with 0.1% Triton-X100 for 15 min at RT. For cell staining it was used DAPI (1:100) for nuclei, and Green Stain (HCS CellMask Green stain™) with initial concentration of 0,01 μg/mL (1:1000 dilution), for cell membrane, and Vectashield (Vector laboratories) used as mounting media. Cells were

imaged with a SP5 confocal microscope (Leica Microsystems, Germany) and image analysis was performed with the LAS AF Lite software (Leica). Green fluorescence was obtained from the green channel (excitation wavelength: 493 nm, emission wavelength: 516 nm), representing the cell membrane and cytoplasm with HCS cell Mask. The blue fluorescence is from the blue channel (excitation wavelength: 365 nm, emission wavelength: 470 nm), which shows blue stained cell nucleic acid with DAPI. The red fluorescence is from the red channel (excitation wavelength: 633, emission wavelength: 690 nm), which shows the red-stained of F NPs and NF NPs with rhodamine B.

Cell metabolic activity

Resazurin assay was used to analyze cell metabolic activity. Therefore, 0.002×10^6 cells of Caco-2/SW48 and 0.004×10^6 cells of HCT15/SW480 were seeded in 96-well plates and allowed to attach during 24h. 2×10^5 of monocytes, were differentiated in 24 well plates for 7 days, as described above. Subsequently, in both, the medium was removed, cells were washed with PBS, and different concentrations of free 5-FU or NPs (2.5, 5, 10, 50, 75, 100, 500μM regarding the drug) in medium (200 μL) were incubated for 24h, 48 h and 72 h, at 37 °C. NH_4OH was added as a negative control and cells without treatment as a positive control. At each timepoint, resazurin redox dye (0.01 mg/mL, Sigma-Aldrich) was added (1/10 of the total volume of culture medium) to cell culture, incubated for 4 h at 37 °C and 5% CO2, and the fluorescence intensity was measured at 530/590 nm using a SynergyMx MultiMode microplate reader (BioTek). All data were normalized using, background medium, negative and positive (cells without treatment) controls, which were considered 0% and 100% metabolic activity, respectively. The cell metabolic activity was analyzed using as a threshold of 70% cell viability according to the ISO 10993-5 standard (28)

Impact of NPs on macrophage polarization

As described above, 0.5×10^6 monocytes were plated in 6-well plates and differentiated into macrophages. After 7 days of differentiation, RPMI 1640 medium was removed, and macrophages were washed. As a controls of polarization, macrophages were incubated with 10 ng/mL of LPs (M1- like) or 10 ng/mL of IL-10 (M2 – like), for 4 h. M0 macrophages, were incubated without any addiction of exogenous factors. After, 75 μM of free drug and NPs (in regard of drug concentration) were added for 72h. To evaluate macrophage polarization, macrophages were detached with accutase at 37 °C during 30 min and harvested by gently scrapping. Cells were washed and resuspended in FACS buffer containing appropriate conjugated antibodies, and stained in the dark for 40 min at 4 °C.

Briefly, macrophages were stained with the following antibodies: anti-human CD14/APC (ref 620926) (1:50), anti-HLA-DR/PB (ref 2437643) (1:250), anti-CD86/FITC (ref 277175) (1:50) , anti-CD206/PE (ref B353712) (1:50) , anti-CD163/PE (ref. 1260877) (1:50) and anti-PDL1-FITC (ref.1055403) (1:50). After 40 min of incubation, cells were washed twice and incubated with Live/Dead stain (1:10000) in PBS for 30 min at 4ºC. Cells were washed twice and fixed with 2% PFA for 15 min at RT, washed again, and placed into cytometer tubes for further analysis. Samples were analyzed with a BD FACSCanto™ II flow cytometer (BD Biosciences). To define background, unstained controls were used and to compensate staining overlaps beads-matched antibodies were used. Median fluorescence intensity was measured for at least 50,000 viable plus single cell gated events per sample, and all data was processed with the FlowJo software (Tree Star). All experiments were performed, at least, in triplicate.

Statistical analysis

Results were expressed as mean ± standard deviations (SD) of minimum three independent experiments. Data was analyzed using Student's t-test for comparison between two independents groups and ANOVA for comparison among three or more groups, in GraphPad Prism 8.0 software (GraphPad, USA). The level of significance was set at probabilities of $*p < 0.05$; $**p < 0.01$ and $****p < 0.001$.

Results

Chemical synthesis of Anti-CEA scFv with PLGA-PEG-mal polymer

The sulfhydryl group of the anti-CEA scFv, MFE-23, was chemically conjugated with the maleimide group of the PLGA-PEG-Mal polymer to obtain the CEA-targeted PLGA-PEG-scFv polymeric conjugate (24, 29). A PLGA-PEG-Mal polymer containing a PEG of 5K was selected since this molecular weight has been associated with a prolonged blood circulation time due to lower absorption of serum proteins and interaction with macrophages reduced kidney's clearance, therefore increasing the probability of a successful anti-tumor therapy (30, 31). The conjugation protocol herein used was previously optimized by our group (32, 33), allowing us to obtain an anti-CEA scFv conjugation efficiency (CE) of around 90%. Additionally, ^{1}H NMR confirmed the successful reaction between the anti-CEA scFv and PLGA-PEG-Mal, revealing characteristics peaks of the polymer (δ = 5.20, 4.91, 3.50 and 1.46 ppm) (32, 33) and of

the scFv (δ = 8.11, 7.95, 7.22, 6.81, 6.61 ppm) (34) in the spectrum of the final polymeric conjugate (Figure 1).

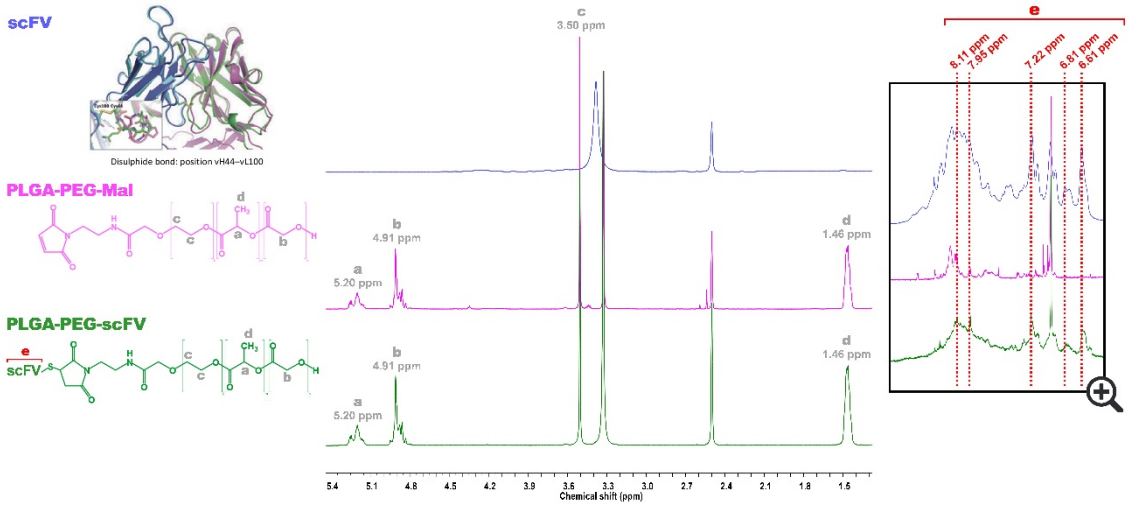


Figure 1. [1]H NMR analysis of the chemical conjugation between anti-CEA scFv and PLGA-PEG co-polymer. [1]H NMR characterization of PLGA-PEG-anti CEA scFv polymer: characteristic peaks of a, d) glycolic acid, b) lactic acid; c) PEG and e) anti-CEA scFv in the final PLGA-PEG - scFv polymer (right).

Manufacture and characterization of 5-FU-loaded CEA-targeted NPs

Despite the clinical significance of 5-FU, its systemic toxicity, low bioavailability, short half-life, and frequent drug resistance, are still limiting its therapeutic effect. Therefore, to overcome these drawbacks, the development of sustained release formulations of 5-FU such as NP systems may have an important impact in the improvement of the therapeutic response, providing effective tumor regression with minimal side effects in comparison with the native form of the drug (35). However, 5-FU encapsulation into NP systems is characterized by several drawbacks, including the drug's hydrophilic properties and small size (MW 130.08 Da). Consequently, the challenging weak interactions with NP system matrices such as PLGA, lead to low encapsulation efficiency, undesired leakage, and initial burst release (36). In this work, 5-FU was encapsulated in a functionalized anti-CEA targeted PLGA-PEG-scFv NPs, (F NPs), by double emulsion technique (Figure 2), achieving a drug loading (DL) of 8.3 ± 3.85 % (Table 1). This finding is in agreement with the solubility profile of 5-FU as well as its hydrophilicity which leads to 5-FU diffusion to the aqueous external phase during the encapsulation process (37).

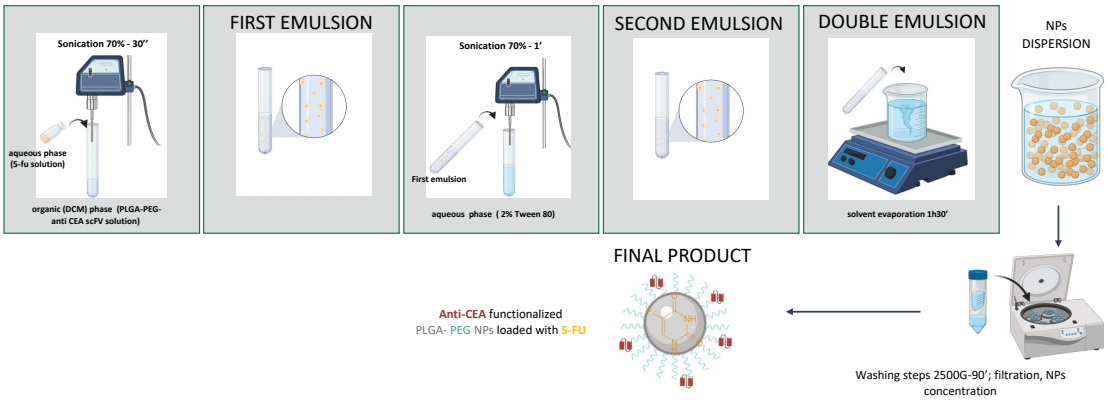


Figure 2. Schematic illustration of the methodology of nanoparticles production.

Regarding the physicochemical properties of NPs, Z-average size of 5-FU-loaded F NPs and respective controls ranged from approximately 130 and 170 nm, with a relatively monodisperse size distribution characterized by a polydispersity index of around 0.2. Additionally, a decreasing ζ-Potential of nanoparticles with scFv was observed due to the net negative charge on their surface from the scFv moiety (38).

Table 1. Physicochemical properties of functionalized and 5-FU loaded nanoparticles as well as respective controls, with mean size (Z-average size), polydispersity index, surface charge (ζ-Potential), and DL (%). Values are represented as mean values ± SD (N = 6). Non applicable (-).

	Size (nm)	Polydispersity Index	Surface charge (mV)	Drug Loading (%)
EMPTY PLGA NPs	164.6 ± 5.1	0.21 ± 0.01	-7.46 ± 0.30	-
5-FU LOADED PLGA NPs	169.9 ± 2.9	0.19 ± 0.01	-6.62 ± 0.38	4.7 ± 2.3
EMPTY NF NPs	142.4 ± 6.8	0.25 ± 0.03	-5.55 ± 0.81	-
EMPTY F NPs	136.8 ± 2.1	0.22 ± 0.01	-9.22 ± 0.84	-
5-FU-LOADED F NPs	133.7 ± 1.3	0.25 ± 0.01	-12.53 ± 0.37	8.3 ± 3.9

Furthermore, NPs revealed a spherical shape with relatively smooth surfaces and uniform size distribution in all samples as shown through TEM analysis. The nanoparticles stability was assessed over 1 month with a relatively constant size (Figure 3 A and B). Moreover, the 5-FU cumulative release had 2 phases (Figure 3 C): (i) an initial burst release, in accordance of described for several authors due to the initial dissolution of entrapped drug attached to the NPs surface, and some particular properties of the nano system, such size, porosity, MW and drug hydrophilicity (39); and (ii) a second release step, with slow drug diffusion from the PLGA matrix, being associated with the erosion and/or swelling of PLGA in release medium (40, 41). Nevertheless, these data were obtained from an *in vitro* mimicking analytical assay which

may not allow extrapolation of conclusions regarding the initial burst release in *in vivo* conditions.

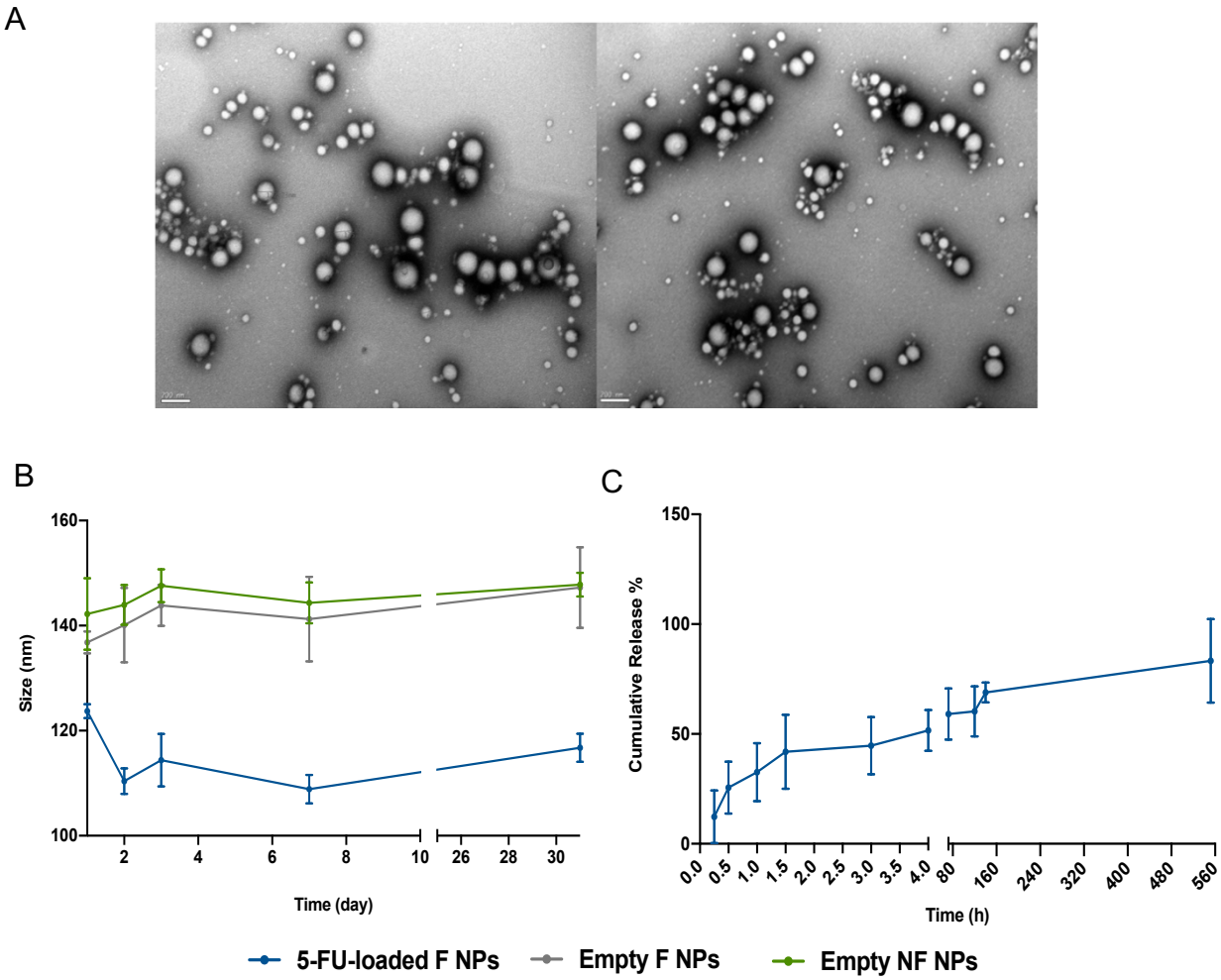


Figure 3. Nanoparticles physicochemical characterization and in vitro release of 5-FU. A) Image of empty F NPs (left) and of 5-FU-loaded F NPs (right) obtained by Transmission Electron Microscopy (TEM). Scale bar: 200nm. B) Stability of empty nanoparticles (NF NPs), functionalized unloaded NPs (empty F NPs) and of 5-FU-loaded F NPs, in cell culture medium at 4°C for 1 month. C) in vitro release profile of 5-FU from F NPs in PBS pH 7.4 at 37 °C during 552h. C). All measurements were done in triplicate and results are presented as mean ± SD.

CEA expression analysis in colorectal cancer cell lines

To assure that the develop NPs could hold maximum specificity, a full screening of CEA expression in a number of CRC cell lines from different CMSs was performed by flow cytometry. The obtained results showed different levels of CEA expression, with lower expression levels in SW480, HCT-15, HCT-116 and RKO cell lines. The higher values were achieved in Caco-2, HT-29, LS174T and SW48 cell lines, though from different CMSs (Figures S1 and S2). These findings are in concordance with recent reports

referring that, despite the transversal CEA expression in CRC stages, CRC's intratumor and intertumoral heterogenicity with different activated molecular pathways leads to distinctive CEA levels of plasticity and expression (42). Additionally, the efficacy of 5-FU treatments is being correlated with CMSs and molecular subtypes (43). Therefore, to conduct NPs efficacy studies in different CMS and (MSI or MSS, MSI cell lines from CMS1, representing the CRC subpopulation where 5-FU has less efficacy and immunotherapy is illegible, were selected as CEA ^{high} (SW48) and CEA ^{low} (HCT-15). Moreover, MSS cell lines from CMS4, representing the CRC subpopulation with inactivated immune infiltrate, immunosuppressive TME and where 5-FU has been correlated with no significance in OS, were also selected and included cell lines CEA ^{high} (Caco-2) and CEA ^{low} (SW480). The selection of each cell line, categorized as MSI or MSS in the respective CMS, had in consideration the work published by Berg K. et al. (44).

Targeting capacity of anti-CEA scFv functionalized NPs towards CEA^{high} and CEA^{low} CRC cells

To evaluate the specificity and selectivity of the developed CEA-targeted NPs, interaction with the aforementioned CRC cell lines was investigated. Therefore, to understand the impact of the targeted strategy on cell-NP interaction, a protocol for image flow cytometry evaluation was established with prior detachment of the cells with trypsin, that allowed to remove the majority of non-internalized NPs, present on the surface of the cells and have accurate results. To infer their specificity to target cells, the ImageStream flow cytometry technology was used, since it allows simultaneous evaluation of a given molecule of interest expression and localization, allowing the acquisition of multiple images of each cell in flow. Brightfield images were recorded to differentiate cell membrane and cytoplasm (Channel 1). NPs were tracked in Channel 2, where significant differences in the degree of cellular interaction between empty non-functionalized (NF NPs) and CEA-targeted NPs (F NPs) were observed in CEA-expressing cells (Figure 4). In addition, channel 6 provided information about the granularity of the cells (internal complexity). Unstained cells were included as controls (brightfield in channel 1 and darkfield (SSC) in channel 6).

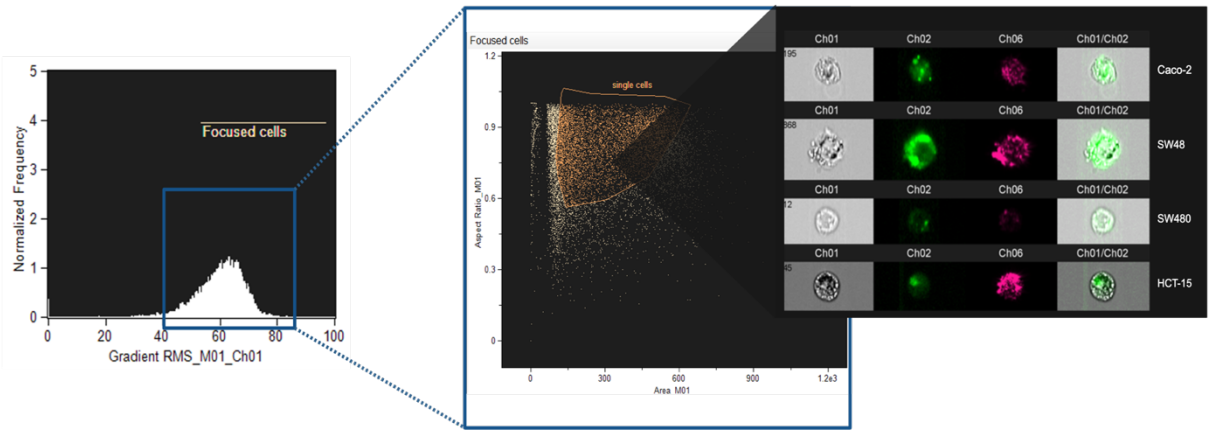


Figure 4. Gating strategy used to select cells in focus and separate them from the doublets and non-focused events in untreated cells (left image). Gating strategy for single cells from focused cells in the middle. Features for the bivariate dot plot are calculated based on a Brightfield image and using the mask that covers the whole cell (channel 1, ch1). Proof of successful separation of the cells from the non-focused and doublets verified in imaging gallery with respective fluorescence in each channel (Caco-2; SW48; SW480 and HCT-15 cell lines incubated with F NPs along 24h) (right image).

The F NPs showed 2-3-fold higher internalization in CEA^{high} expressing MSS and MSI CRC cell lines, indicating the specificity of the developed targeted nanosystem. As shown in Figure 5A, Caco-2 cell line (MSS CEA^{high} cell line) presented a significant increase in the internalization rate of F NPs comparing to NF NPs (p = 0.0106, p = 0.0320, p = 0.0350 and p = 0.0411), along the different times of incubation (1, 3, 10 and 24h), respectively. Importantly, the incubation of NF NPs with the free anti-CEA scFv (NF NPs + scFv) did not result in an improvement of internalization rate by the Caco-2 cell line, highlighting the importance of anti-CEA scFv functionalization on the surface of NPs. Additionally, equivalent results were found in the SW48 cell line (MSI CEA^{high} cell line) with critical differences between F NPs and NF NPs as well as F NPs and NF NPs incubated with free scFv at time point 1h (p = 0.0056 and p = 0.0067) respectively. Moreover, changes in the internalization rate of F NPs vs NF NPs were maintained along 24h of incubation (p values of 0.0283 for 3h, 0.0278 for 10h and 0.0142 for 24 h). Similar results comparing F NPS vs NF NPS + scFv from 3h, 10h and 24h of incubation (p = 0.0308; 0.0330 and <0.0001, respectively) were obtained. The higher cell internalization of F NPs compared to NF NPs was reflected by an increase of up to three times in the percentage of focused positive cells, over 24 h (Figure 4). In fact, our results corroborated the previously reported tumor cell specificity of the anti-CEA scFv, when used to functionalize Superparamagnetic iron oxide nanoparticles (22, 45). In addition, we had also confirmed the CEA-targeting specificity of our system by evaluating the same NPs conditions in MSI and MSS CEA^{low} expressing CRC cell lines. The results

presented non-significant changes between NP testing conditions (Figure 5B), being the cellular uptake independent on the presence of the anti-CEA scFv in the NPs surface. Therefore, our results confirmed the specific targeting of CEA-targeted NPs for MSI/MSS CEA^{high}.

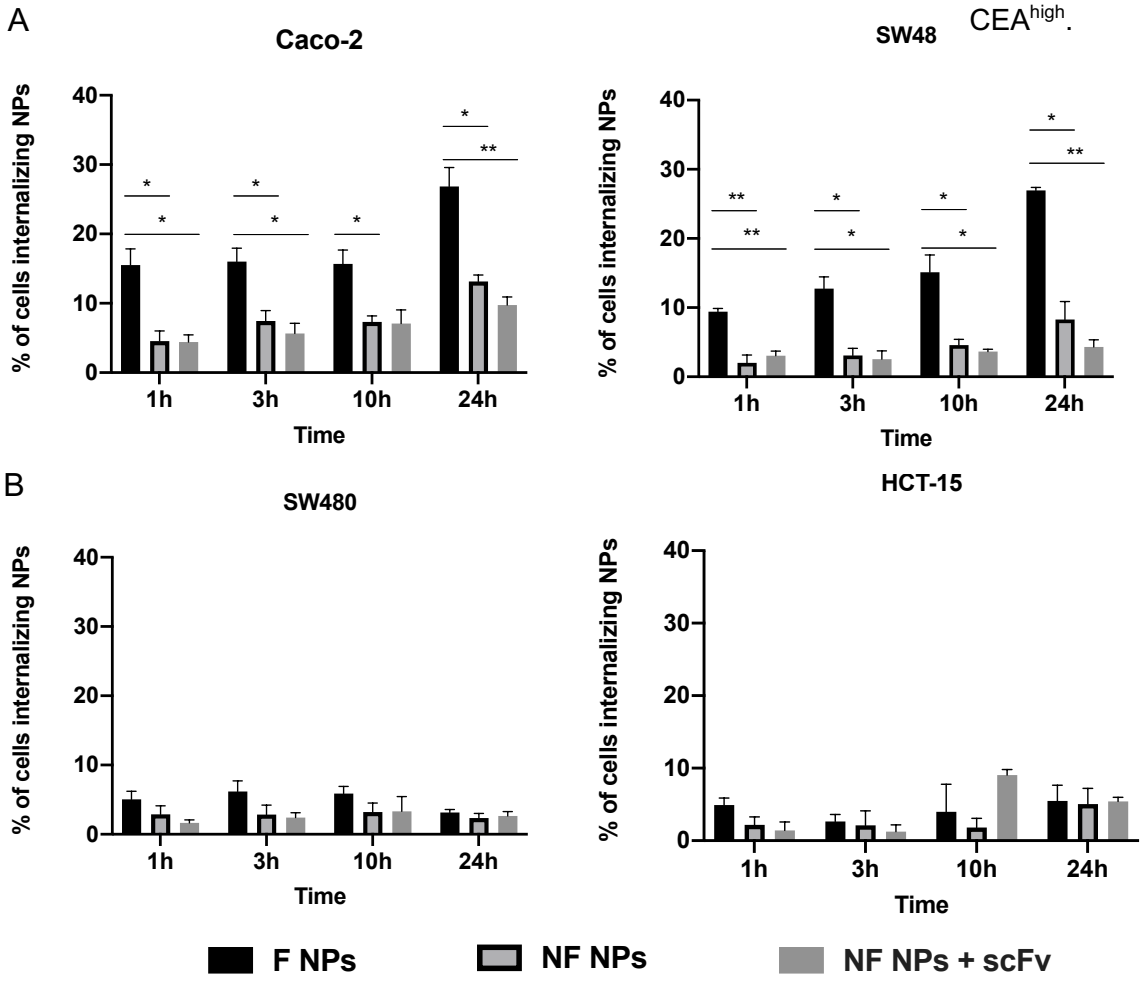


*Figure 5. Imaging Flow cytometry analysis of cell internalization of F and NF NPs or NF NPs incubated with free anti-CEA (NF NPs + scFv) into A) CEA ^{high} cell lines (Caco-2 MSS cell line on the left and Sw48 MSI cell line on the right) and into B) CEA-non expressing cell lines (SW480, MSS cell line, on the left and, HCT-15, MSI cell line, on the right). Expression values were normalized to the unstained control. Statistical comparison of functionalized with non-functionalized NPs. *p < 0.05, **p < 0.01, ***p < 0.001 or ****p < 0.0001.*

To improve our knowledge about a possible intracellular localization of the developed NPs, we examined the fluorescent signal of F NPs and NF NPs after incubation with MSI and MSS CEA^{high} and CEA^{low} CRC cells during 24 h, using confocal microscopy (Figure S3). F NPs were observed to have a much higher cell affinity to Caco-2 and Sw48 cells (CEA^{high}) than NF NPs, which did not demonstrate an evident interaction with these cancer cells. Moreover, we observed that some of the NF NPs pools were localized outside the cell membrane (Figure S3B and S3C), while F NPs were effectively found inside the cells, as demonstrated through overlay's orthogonal projections in XZ and YZ in SW48 cells (Figure S3D). In fact, in solid tumors, high-affinity antibodies have been

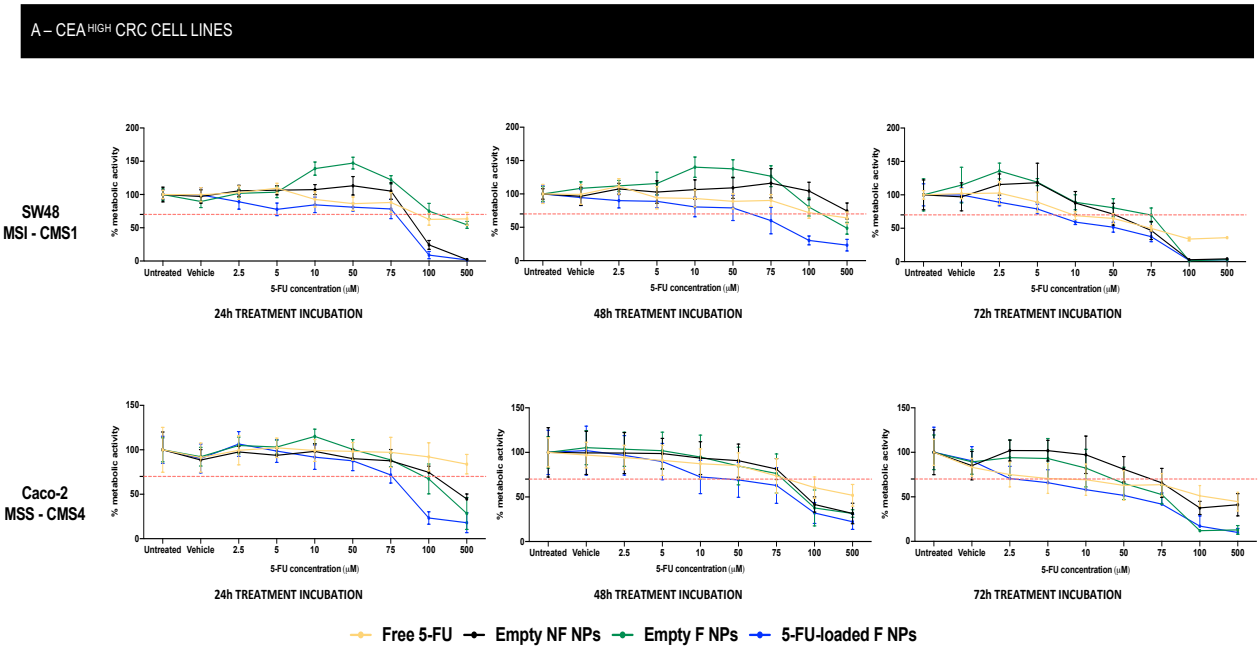
described to bind to the antigen of interest, but their lengths affect their retention at the tumor cell surface. In particular, CEA was reported as a non-internalizing antigen (46). However, recent studies suggested CEA as an internalizing antigen, being the anti-CEA antibody penetration into the cells caused by the metabolic turnover of the CEA of around 16 h and associated with alternative transport pathways not involving clathrin (47, 48). Therefore, since the internalization of anti-CEA antibodies is reported as faster than receptor-mediated endocytosis, the alternative endocytic pathway may involve a similar mechanism of non-clathrin-coated vesicle pathway (49). Moreover, as presented in Figure 5, when comparing F NPs with NF NPs + scFv, F NPs had no evidence of scFv absorption to NF NPs. Hence, our data reinforced the potential of CEA as a promising target for anti-CRC therapies, favoring the internalization of drug-loaded NP systems.

Effect of 5-FU-loaded CEA-targeted NPs in the metabolic activity of CRC cells

The ability of the developed NPs to compromise the metabolic activity of CRC cells was assessed *in vitro* through resazurin assays in the selected CEA ^{high} and CEA ^{low} CRC cell lines (Figure 6). The metabolic activity was evaluated over 24 h, 48 h and 72 h using 5-FU doses ranging from 2.5 to 500 μM. For both CEA ^{high} CRC cell lines (Caco-2 and SW48), the metabolic activity of the cells treated with 5-FU-loaded anti-CEA functionalized NPs (5-FU loaded F NPs) significantly decreased when compared with the free 5-FU, after 24 h of incubation. Moreover, in SW48 cells, the reduction on the metabolic activity was significantly affected from 5 μM ($p < 0.0001$) when compared with the 5-FU free drug, after 24h. Over 48 h, the metabolic activity was only impacted from 75 μM ($p = 0,0086$). Moreover, the respective controls, consisting of unloaded NF NPs and F NPs, were considered safe until 75 μM after 48 h, and until 50 μM after 72 h with above 70% of viable cells (28). Despite the improvements in the reduction of cell metabolic activity from 10 μM in 24h, in CRC CEA ^{high} MSS - CMS4 cell line, Caco-2, the statistical significance was only reflected from 75 μM ($p < 0.0001$). In similarity with SW48 cells, the controls using unloaded NF NPs and F NPs showed safety until 75 μM in 48 h. No significant values of lower metabolic activity, indicating cell death, were found at 72h. These findings revealed the capability of the targeted NPs to induce higher cell death rates in CRC CEA-expressing MSI and MSS cells within 24h, in contrast with free 5-FU, which takes 72 h to impact cancer cell in the same way (IC50 = 75μM) (Figure 6B) (50, 51) (52). Accordingly, treatments in the same range of concentrations were added to the selected CEA ^{low} MSS and MSI cell lines and, despite the lower expression of CEA, the nanosystems showed better pharmacological performances with a significant impact in

cell metabolic activity in 48 h. For SW480, MSS cell line $p < 0.001$ as found from 2.5 µM to 500 µM. Moreover, despite the reduction in cell viability in HCT-15, MSI cell line, no significant statistical values were found until 75 µM ($p < 0.0001$ for 100 and 500 µM). Additionally, in both CEA ^{low} cell lines, unloaded NF NPs and F NPs exhibited safety until 75 µM after 72h (Figure 6C). The same experiment was done in primary human macrophages, isolated from healthy blood donors. No differences in macrophages metabolic activity were obtained until 75 µM after 72h (Figure 6D).

According to the literature, the IC50 of ~60 µM and ~300 µM for free 5-FU drug, after 72h of incubation with SW48 and SW480 5-FU resistant cell lines, respectively, are in accordance with our findings, suggesting that our cells lines spontaneously generated 5-FU resistance as described by other authors (50, 52). Moreover, similar IC50 ~10 µM for free 5-FU drug and 5-FU loaded F NPs incubation with Caco-2 and HCT15 5-FU sensitive cell lines was found in this work (51, 53). Therefore, the obtained results agreed with the reported IC50 for 5-FU free drug, showing a potent efficacy of the 5-FU-loaded F NPs within 24h of incubation with CEA ^{high} cell lines, in comparison with the free drug. Additionally, reported studies are describing an enhancing cytotoxic potential when NPs were surface modified with a targeting ligand (19), as well as an increase of toxic effects when polymeric nanoparticles repeated-dose exposure, inducing a certain osmotic pressure on the cells, which may justify our results(54).



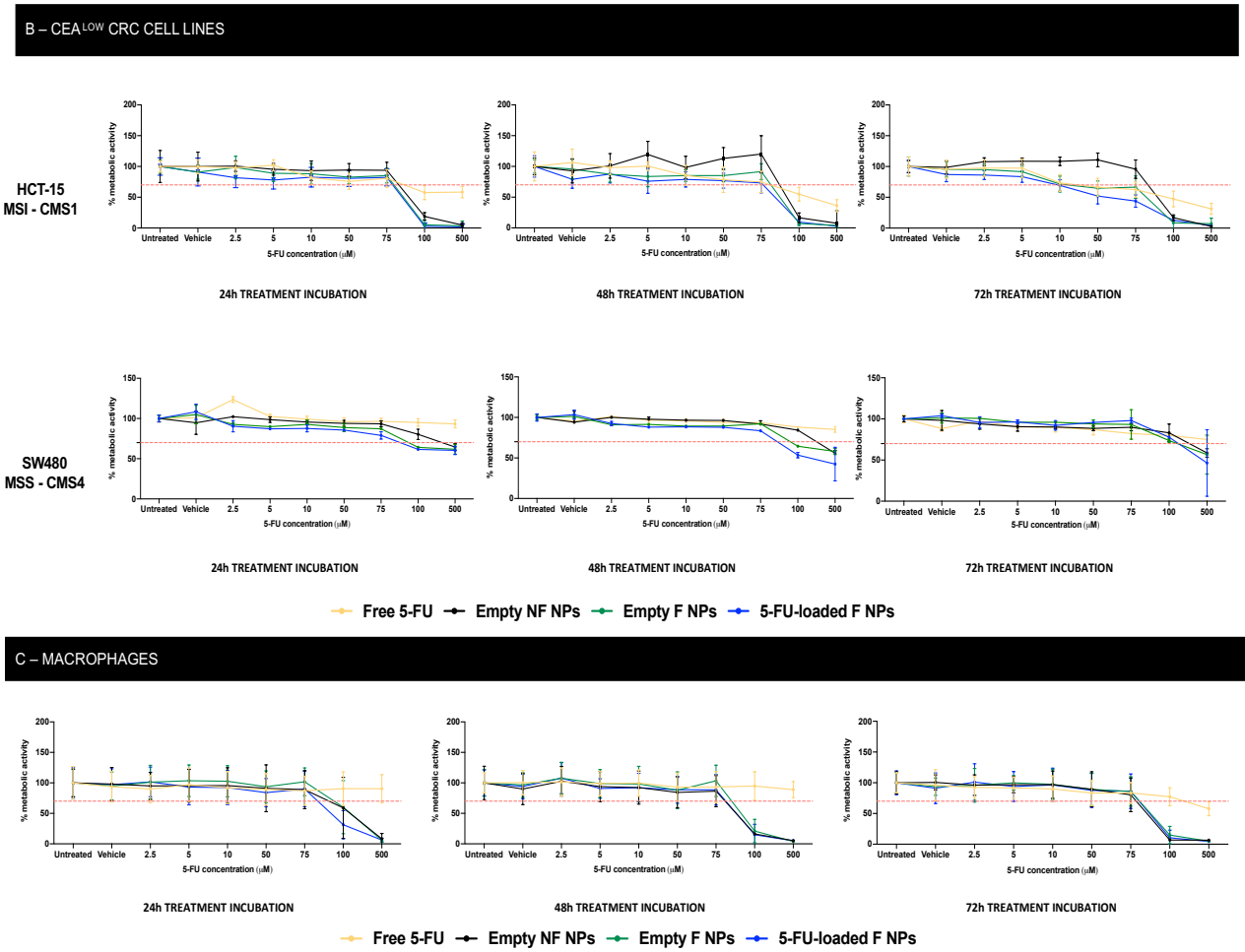


*Figure 6. Evaluation of metabolic activity in CRC MSI and MSS cell lines when incubated with free 5-FU, empty NF NPs, F NPs and 5-FU loaded F NPs at 24h, 48h and 72h. A) Metabolic activity assessment of CEA ^{high} cells. B) Cell viability evaluation in CEA ^{low} cells. C) Macrophages metabolic activity. Statistical comparison of 5FU-loaded F NPs with the free drug 5-FU, within each dose range. *p < 0.05, **p < 0.01, ***p < 0.001 or ****p < 0.0001*

Impact of 5-FU-loaded F NPs on the polarization of macrophages

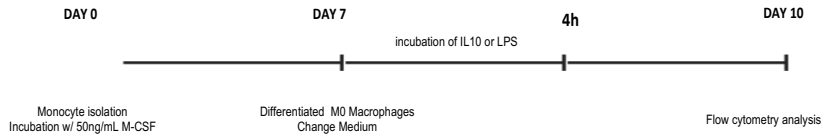
TAMs are described as controversial in CRC progression and treatment response prediction, according to their polarization status (55). $CD206^{+}$ TAMs have been positively correlated with recurrence-free interval duration (56) and described as able to mediate resistance to 5-FU chemotherapy (9). Here, we evaluated the potential impact of the developed NPs on macrophage polarization, since 5-FU-based chemotherapy has been reported as a critical factor for macrophages polarization, consequently resulting in divergent treatment responses.

Experimentally, we first stimulated macrophages with IL-10 or LPS to confirm their polarization capacity into a M2 or M1-like macrophages, respectively. Their phenotype was evaluated by the surface expression of CD86 and CD163 as M1 and M2 markers,

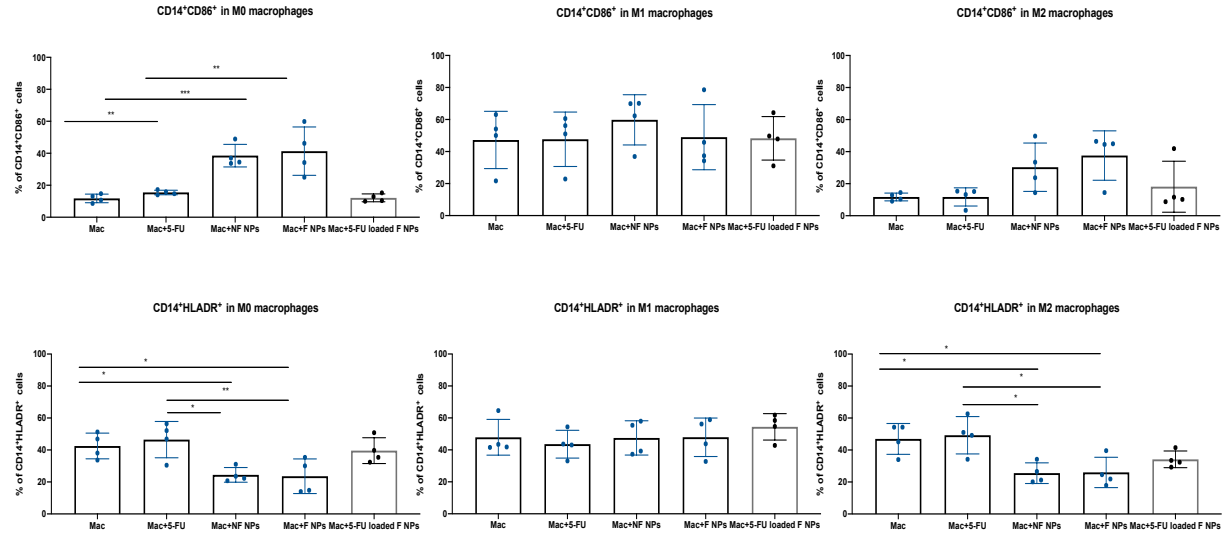
respectively, confirming their capacity to polarize when compared with the non-stimulated macrophages (Figure 7). As expected, LPS stimulation decreased the expression of $CD163^+$ cells and increased the expression of $CD86^+$ cells, while IL-10 stimulation had the opposite effect.

To determine whether unloaded NF NPs, F NPs and 5-FU-loaded F NPs had a similar impact of free 5-FU on macrophages polarization, 75 μM of NPs (safe concentration observed above) was added to unstimulated, LPS or IL-10-stimulated macrophages. When unstimulated macrophages were incubated with NF NPs, the percentage of $CD86^+$ cells increased, whereas the percentage of HLA-DR+ cells decreased ($p< 0.01$, Figure 7B). However, when the anti-inflammatory surface markers (CD163 and CD206) were evaluated, no significant changes were observed. Additionally, when compared with the administration of free 5-FU drug, the administration of NF NPs could sustain the initial levels of untreated and unstimulated macrophages (Figure 7C). When macrophages were stimulated with LPS, acquiring a M1-like phenotype, no changes in the percentage of cells expressing pro-inflammatory markers (CD86 and HLA-DR) were found, despite the tendency to decrease the percentage of cells expressing anti-inflammatory markers (CD163 and CD206), comparing with free 5-FU treated macrophages (Figures 7B and 7C). Lastly, in the M2- like macrophages stimulated with IL-10, a slight decrease of HLA-DR expression levels was achieved but with no significant differences in the percentage of $CD86^+$ expressing cells. No changes were obtained in the percentage of cells expressing the anti-inflammatory markers CD163 and CD206. Moreover, in unstimulated and LPS-stimulated macrophages, a tendency in keeping the initial expression of CD206 surface levels was observed when compared with the impact of free 5-FU in this marker. Overall, no significant changes were achieved on the macrophages' polarization, despite the tendency to maintain the initial expression of surface markers in untreated macrophages. Moreover, the immunogenicity of associated antibody fragments shown no effect on macrophages, proving a safe administration of the developed NPs.

A. TREATMENT SCEDULE



B. PRO-INFLAMATORY MARKERS



C. ANTI-INFLAMATORY MARKERS

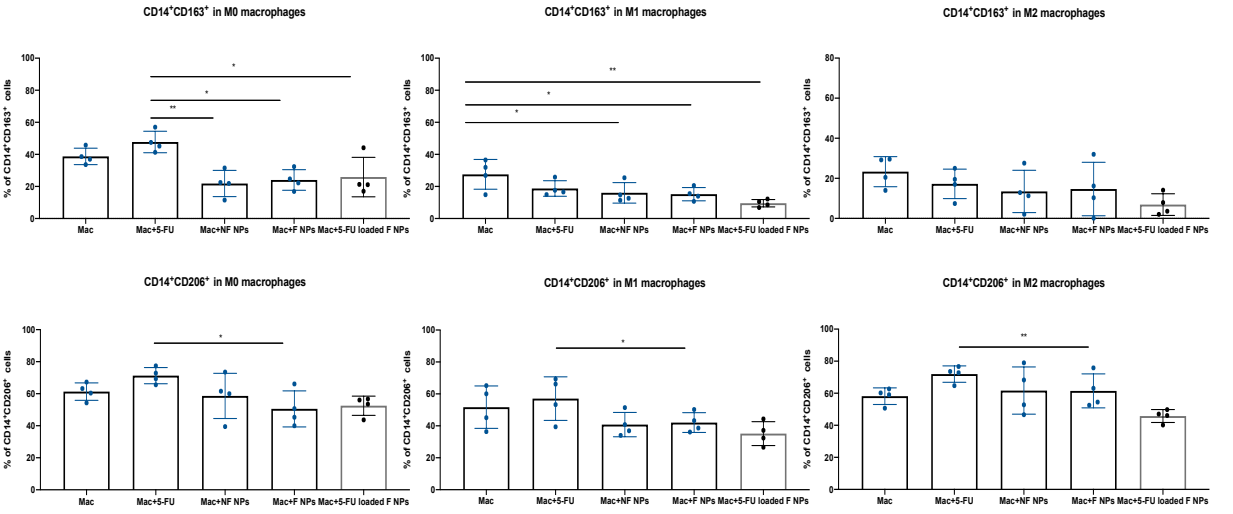


Figure 7. Impact of NPs on macrophages polarization. A) Experiment schedule B) Percentage of cells expressing pro-inflammatory markers (CD86, HLA-DR) on unstimulated, M1-like and M2-like macrophages surface B) Percentage of cells expressing anti -inflammatory markers (CD163, CD206) on unstimulated, M1-like and M2-like macrophages surface.

Conclusions

We developed an innovative nanoplatform to deliver 5-FU to CRC, based on the functionalization of a PLGA and PEG polymer with an anti-CEA scFv, namely MFE-23. To our best knowledge, this is the first proof-of-concept using an anti-CEA scFv chemically conjugated with PLGA-PEG polymers for nano-chemotherapeutic applications, facilitating the delivery of a conventional drug to treat CRC. Here, we observed the ability of CEA-targeted NPs to provide a specific targeting to CEA-expressing cells with 3-times enhanced rates of internalization when compared with NF NPs. Furthermore, the developed strategy was able to significantly decrease the metabolic activity of CEA-expressing cells in 24h and 48h, conferring better anti-cancer activity to the delivered drug. Moreover, the CEA-targeted NPs loaded with 5-FU were considered safe for macrophages, with no relevant biological impact on macrophages polarization, proving the suitability of the strategy for further application in a more complex 3D model with associated TAMs mimicking the surrounding TME. The developed therapy might bring a new perspective of investigation to explore the advanced delivery system with higher loading capacity and minimum adverse effects on CEA-expressing CRC tumors. Additionally, CEA-targeted NPs may also offer an opportunity for further targeted therapy applied to different types of cancer and metastatic sites of CRC, normally expressing CEA. Altogether, we developed a targeted strategy that could constitute a new outlook of chemotherapy employment in association with combinatory immunotherapeutic strategies.

Supporting Information

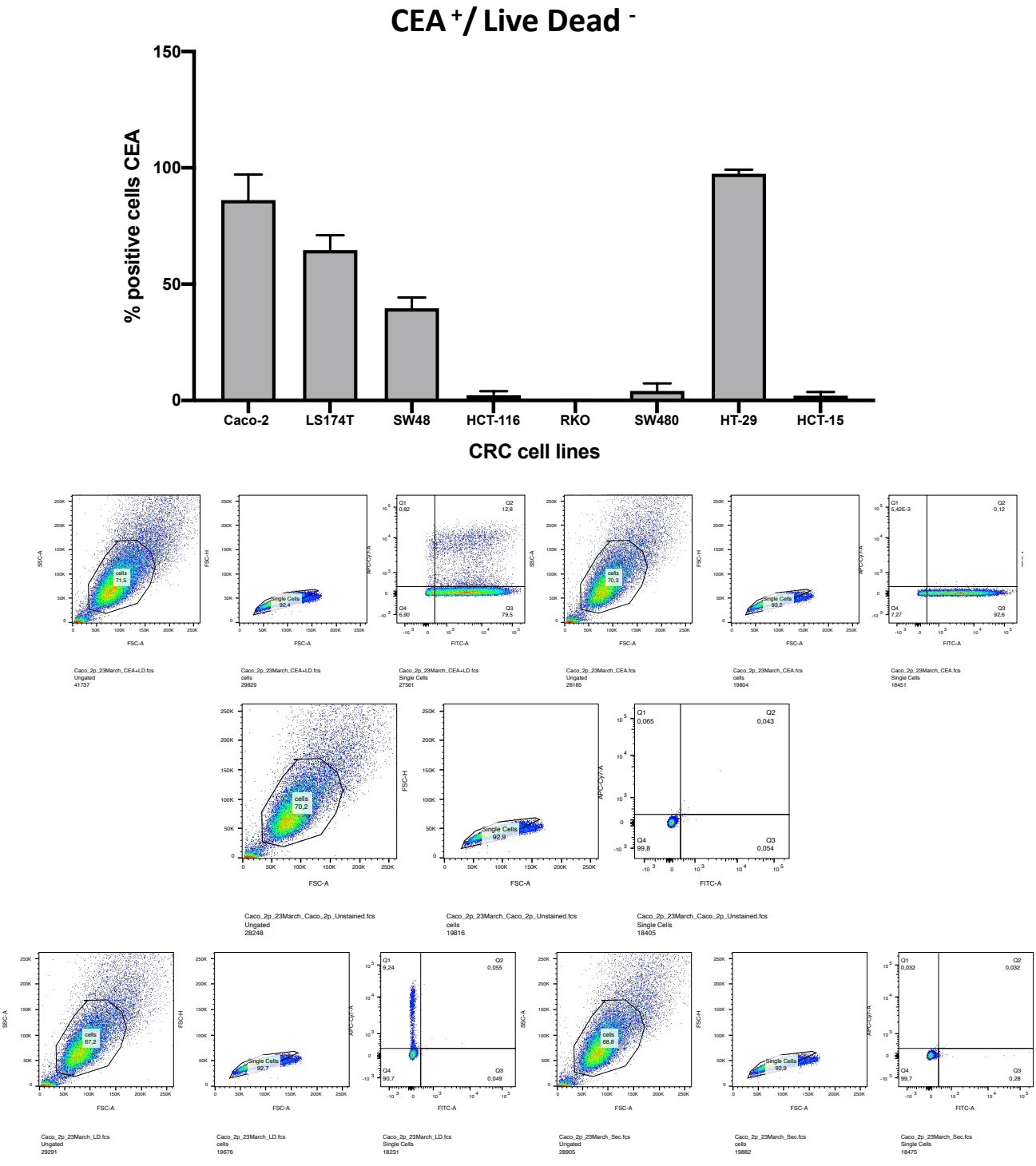


Figure S1. Evaluation of surface CEA expression levels in live CRC cell lines. A) percentage of CEA positive cells within live cell, analyzed by flow cytometry. B) Gating strategy applied during the analysis in Flow Jo software The scatter plots exhibit a representative image of the gating strategy created with FlowJo software for flow cytometry analysis. FSC-A/SSC-A exemplifies the distribution of cells in the light scatter based on cell size and granularity, respectively; FSC-A/FSC-H represents the single cells of the previously selected population.

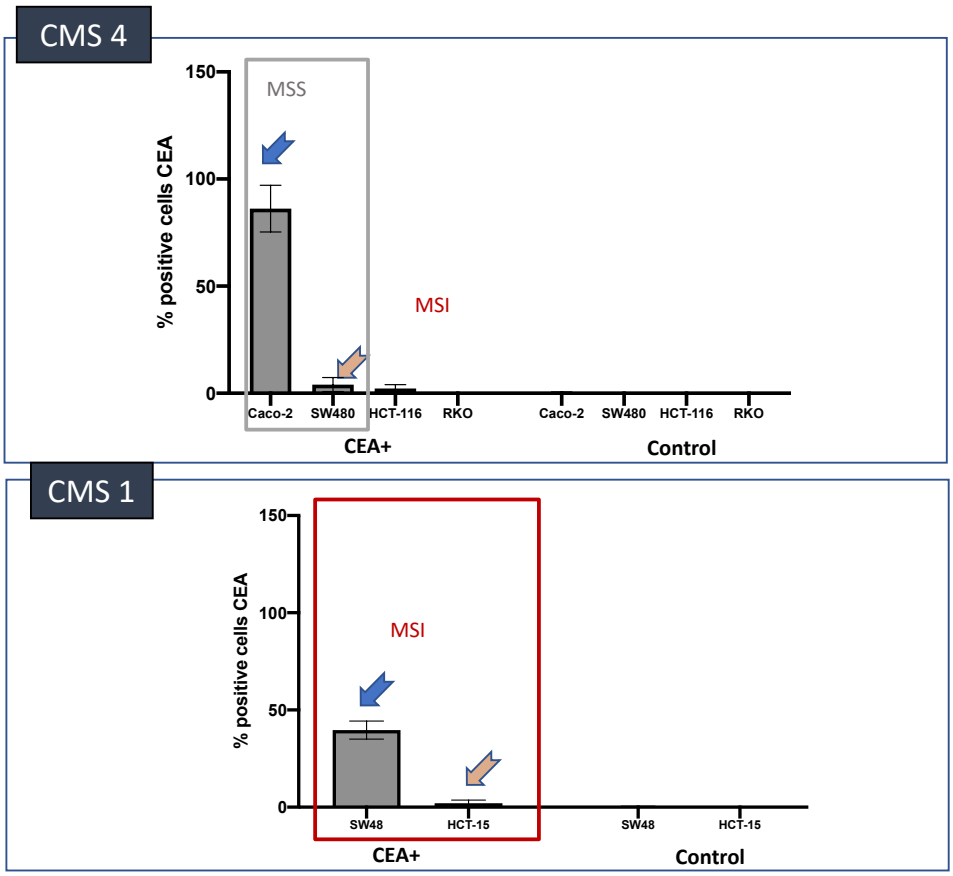


Figure S 2. Expression levels of CEA, determined by flow cytometry in the selected MSS and MSI CRC cell lines and their subclassification according to CMS. The control is presenting the autofluorescence of cells in each respective unstained selected cells.

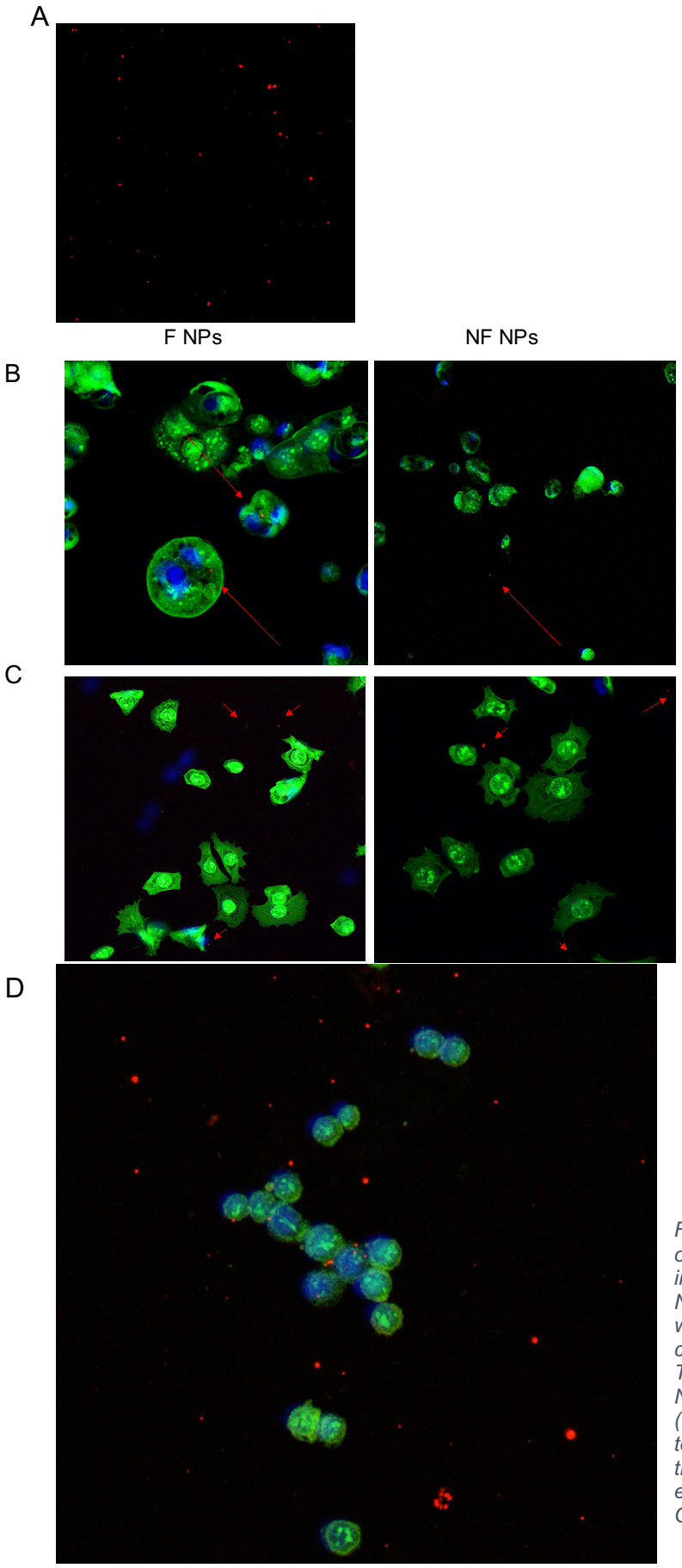


Figure S 3. Confocal microscopy analysis of cell internalization of NF NPs and F NPS into same cell lines at 24h of incubation. A) NPs are stained in red. B) Green Cell mask was used to stain and define the cytoplasm cell area; nucleus are stained in blue. Therefore, (B) is representing F NPS and NF NPs interaction with Caco-2 cells and (C) with SW480 cells. The red arrows point to the NPs. D) 3D projection is reproducing the overlap between XZ and XY axis, evidencing F NPs inside Sw48 CEA ^{high} Cells. Scale bars represent 60 µm.

References

1. Colorectal cancer [Internet]. 2020 [cited June 2023]. Available from: https://gco.iarc.fr/today/data/factsheets/cancers/10_8_9-Colorectum-fact-sheet.pdf.

2. Siegel RL, Wagle NS, Cercek A, Smith RA, Jemal A. colorectal cancer statistics, 2023. CA: Cancer J Clin. 2023;73(3):233-54.

3. Sobral D, Martins M, Kaplan S, Golkaram M, Salmans M, Khan N, et al. Genetic and microenvironmental intra-tumor heterogeneity impacts colorectal cancer evolution and metastatic development. Commun Biol. 2022;5(1):937.

4. Guinney J, Dienstmann R, Wang X, de Reyniès A, Schlicker A, Soneson C, et al. The consensus molecular subtypes of colorectal cancer. Nat Med. 2015;21(11):1350-6.

5. Valenzuela G, Canepa J, Simonetti C, Solo de Zaldívar L, Marcelain K, González-Montero J. Consensus molecular subtypes of colorectal cancer in clinical practice: A translational approach. World J Clin Oncol. 2021;12(11):1000-8.

6. Silveira MJ, Castro F, Oliveira MJ, Sarmento B. Immunomodulatory nanomedicine for colorectal cancer treatment: a landscape to be explored? Biomater Sci. 2021;9(9):3228-43.

7. Sethy C, Kundu CN. 5-Fluorouracil (5-FU) resistance and the new strategy to enhance the sensitivity against cancer: Implication of DNA repair inhibition. Biomed Pharmacother. 2021;137:111285.

8. ten Hoorn S, de Back TR, Sommeijer DW, Vermeulen L. Clinical value of consensus molecular subtypes in colorectal cancer: A systematic review and meta-analysis. J Natl Cancer Inst. 2021;114(4):503-16.

9. Li Y, Chen Z, Han J, Ma X, Zheng X, Chen J. Functional and therapeutic significance of tumor-associated macrophages in colorectal cancer. Front Oncol. 2022;12:781233.

10. Wang H, Tian T, Zhang J. Tumor-associated macrophages (TAMs) in colorectal cancer (CRC): From mechanism to therapy and prognosis. Int J Mol Sci. 2021;22(16).

11. Blondy S, David V, Verdier M, Mathonnet M, Perraud A, Christou N. 5-Fluorouracil resistance mechanisms in colorectal cancer: From classical pathways to promising processes. Cancer Sci. 2020;111(9):3142-54.

12. Kate W, Weng N, Tara Laurine R, Therese MB, Stephanie Hui-Su L, Wei C, et al. Tumour immune microenvironment biomarkers predicting cytotoxic chemotherapy efficacy in colorectal cancer. J Clin Pathol. 2021;74(10):625.

13. Malesci A, Bianchi P, Celesti G, Basso G, Marchesi F, Grizzi F, et al. Tumor-associated macrophages and response to 5-fluorouracil adjuvant therapy in stage III colorectal cancer. OncoImmunol. 2017;6(12):e1342918.

14. Wei C, Yang C, Wang S, Shi D, Zhang C, Lin X, et al. M2 macrophages confer resistance to 5-fluorouracil in colorectal cancer through the activation of CCL22/PI3K/AKT signaling. Onco Targets Ther. 2019;12:3051-63.

15. Alsaab HO, Alharbi FD, Alhibs AS, Alanazi NB, Alshehri BY, Saleh MA, et al. PLGA-Based Nanomedicine: History of advancement and development in clinical applications of multiple diseases. Pharmaceutics. 2022;14(12).

16. Entezar-Almahdi E, Mohammadi-Samani S, Tayebi L, Farjadian F. Recent advances in designing 5-Fluorouracil delivery systems: A stepping stone in the safe treatment of colorectal cancer. Int J Nanomedicine. 2020;15:5445-58.

17. Valencia-Lazcano AA, Hassan D, Pourmadadi M, shamsabadipour A, Behzadmehr R, Rahdar A, et al. 5-Fluorouracil nano-delivery systems as a cutting-edge for cancer therapy. Eur J Med Chem. 2023;246:114995.

18. Fahmy SA, Mahdy NK, Al Mulla H, ElMeshad AN, Issa MY, Azzazy HME-S. PLGA/PEG Nanoparticles loaded with cyclodextrin-peganum harmala alkaloid complex and ascorbic acid with promising antimicrobial activities. Pharmaceutics. 2022;14(1):142.

19. Chiu HI, Samad NA, Fang L, Lim V. Cytotoxicity of targeted PLGA nanoparticles: a systematic review. RSC Adv. 2021;11(16):9433-49.

20. Aldilaijan AF, Kim YI, Kim CW, Yoon YS, Park IJ, Lim S-B, et al. Clinical implication of tissue carcinoembryonic antigen expression in association with serum carcinoembryonic antigen in colorectal cancer. Sci Rep. 2023;13(1):7616.

21. Elekonawo FMK, Bos DL, Goldenberg DM, Boerman OC, Rijpkema M. Carcinoembryonic antigen-targeted photodynamic therapy in colorectal cancer models. EJNMMI Res. 2019;9(1):108.

22. Vigor KL, Kyrtatos PG, Minogue S, Al-Jamal KT, Kogelberg H, Tolner B, et al. Nanoparticles functionalised with recombinant single chain Fv antibody fragments (scFv) for the magnetic resonance imaging of cancer cells. Biomaterials. 2010;31(6):1307-15.

23. Jin S, Sun Y, Liang X, Gu X, Ning J, Xu Y, et al. Emerging new therapeutic antibody derivatives for cancer treatment. Signal Transduct Target Ther. 2022;7(1):39.

24. Graff CP, Chester K, Begent R, Wittrup KD. Directed evolution of an anti-carcinoembryonic antigen scFv with a 4-day monovalent dissociation half-time at 37°C. Protein Eng Des Sel. 2004;17(4):293-304.

25. Begent RHJ, Verhaar MJ, Chester KA, Casey JL, Green AJ, Napier MP, et al. Clinical evidence of efficient tumor targetting based on single–chain Fv antibody selected from a combinatorial library. Nat Med. 1996;2(9):979-84.

26. Eide PW, Moosavi SH, Eilertsen IA, Brunsell TH, Langerud J, Berg KCG, et al. Metastatic heterogeneity of the consensus molecular subtypes of colorectal cancer. npj Gen Med. 2021;6(1):59.

27. Cardoso AP, Pinto ML, Pinto AT, Oliveira MI, Pinto MT, Gonçalves R, et al. Macrophages stimulate gastric and colorectal cancer invasion through EGFR Y(1086), c-Src, Erk1/2 and Akt phosphorylation and smallGTPase activity. Oncogene. 2014;33(16):2123-33.

28. ISO 10993-5: 2009 Biological Evaluation of Medical Devices-Part 5: Tests for in Vitro Cytotoxicity; ISO: Phoenix, USA 2009 [Internet]. 2007 [cited June 2023]. Available from: https://www.iso.org/standard/36406.html

29. Lee YC, Boehm MK, Chester KA, Begent RHJ, Perkins SJ. Reversible Dimer Formation and Stability of the Anti-tumour Single-chain Fv Antibody MFE-23 by Neutron Scattering, Analytical Ultracentrifugation, and NMR and FT-IR Spectroscopy. J Mol Biol. 2002;320(1):107-27.

30. Wang J-L, Du X-J, Yang J-X, Shen S, Li H-J, Luo Y-L, et al. The effect of surface poly(ethylene glycol) length on in vivo drug delivery behaviors of polymeric nanoparticles. Biomaterials. 2018;182:104-13.

31. Hoang Thi TT, Pilkington EH, Nguyen DH, Lee JS, Park KD, Truong NP. The Importance of Poly(ethylene glycol) alternatives for overcoming PEG immunogenicity in drug delivery and bioconjugation. Polymers. 2020;12(2).

32. Garizo AR, Castro F, Martins C, Almeida A, Dias TP, Fernardes F, et al. p28-functionalized PLGA nanoparticles loaded with gefitinib reduce tumor burden and metastases formation on lung cancer. J Control Release. 2021;337:329-42.

33. Martins C, Araújo M, Malfanti A, Pacheco C, Smith SJ, Ucakar B, et al. Stimuli-responsive multifunctional nanomedicine for enhanced glioblastoma chemotherapy augments multistage blood-to-brain trafficking and tumor targeting. Small. 2023;19(22):2300029.

34. Yuasa N, Koyama T, Subedi GP, Yamaguchi Y, Matsushita M, Fujita-Yamaguchi Y. Expression and structural characterization of anti-T-antigen single-chain antibodies (scFvs) and analysis of their binding to T-antigen by surface plasmon resonance and NMR spectroscopy. J Biochem. 2013;154(6):521-9.

35. Haggag YA, Osman MA, El-Gizawy SA, Goda AE, Shamloula MM, Faheem AM, et al. Polymeric nano-encapsulation of 5-fluorouracil enhances anti-cancer activity and ameliorates side effects in solid Ehrlich Carcinoma-bearing mice. Biomed Pharmacother. 2018;105:215-24.

36. Li Q, Li X, Zhao C. Strategies to obtain encapsulation and controlled release of small hydrophilic molecules. Front bioeng biotechnol. 2020;8.

37. El-Hammadi MM, Delgado ÁV, Melguizo C, Prados JC, Arias JL. Folic acid-decorated and PEGylated PLGA nanoparticles for improving the antitumour activity of 5-fluorouracil. Int J Pharm. 2017;516(1):61-70.

38. Boehm MK, Corper AL, Wan T, Sohi MK, Sutton BJ, Thornton JD, et al. Crystal structure of the anti-(carcinoembryonic antigen) single-chain Fv antibody MFE-23 and a model for antigen binding based on intermolecular contacts. Biochem J. 2000;346 Pt 2(Pt 2):519-28.

39. Yoo J, Won Y-Y. Phenomenology of the initial burst release of drugs from PLGA microparticles. ACS Biomater Sci Eng. 2020;6(11):6053-62.

40. Shao L, Shen S, Liu H. Recent advances in PLGA micro/nanoparticle delivery systems as novel therapeutic approach for drug-resistant tuberculosis. Front bioeng biotechnol. 2022;10.

41. Ding D, Zhu Q. Recent advances of PLGA micro/nanoparticles for the delivery of biomacromolecular therapeutics. Materials science & engineering C, Mater Sci Eng C. 2018;92:1041-60.

42. Gonzalez-Exposito R, Semiannikova M, Griffiths B, Khan K, Barber LJ, Woolston A, et al. CEA expression heterogeneity and plasticity confer resistance to the CEA-targeting bispecific immunotherapy antibody cibisatamab (CEA-TCB) in patient-derived colorectal cancer organoids. J Immunother Cancer. 2019;7(1):101.

43. Tian J, Zhang D, Kurbatov V, Wang Q, Wang Y, Fang D, et al. 5-Fluorouracil efficacy requires anti-tumor immunity triggered by cancer-cell-intrinsic STING. Embo j. 2021;40(7):e106065.

44. Berg KCG, Eide PW, Eilertsen IA, Johannessen B, Bruun J, Danielsen SA, et al. Multi-omics of 34 colorectal cancer cell lines - a resource for biomedical studies. Mol Cancer. 2017;16(1):116.

45. Bhatia J, Sharma SK, Chester KA, Pedley RB, Boden RW, Read DA, et al. Catalytic activity of an in vivo tumor targeted anti-CEA scFv::carboxypeptidase G2 fusion protein. Int J Cancer. 2000;85(4):571-7.

46. Schmidt MM, Thurber GM, Wittrup KD. Kinetics of anti-carcinoembryonic antigen antibody internalization: effects of affinity, bivalency, and stability. Cancer Immunol Immunother. 2008;57(12):1879-90.

47. Ackerman ME, Pawlowski D, Wittrup KD. Effect of antigen turnover rate and expression level on antibody penetration into tumor spheroids. Mol Cancer Ther. 2008;7(7):2233-40.

48. Shinmi D, Nakano R, Mitamura K, Suzuki-Imaizumi M, Iwano J, Isoda Y, et al. Novel anticarcinoembryonic antigen antibody–drug conjugate has antitumor activity in the existence of soluble antigen. Cancer Med. 2017;6(4):798-808.

49. Ford CH, Tsaltas GC, Osborne PA, Addetia K. Novel flow cytometric analysis of the progress and route of internalization of a monoclonal anti-carcinoembryonic antigen (CEA) antibody. Cytometry. 1996;23(3):228-40.

50. Suetsugu T, Mori R, Futamura M, Fukada M, Tanaka H, Yasufuku I, et al. Mechanism of acquired 5FU resistance and strategy for overcoming 5FU resistance focusing on 5FU metabolism in colon cancer cell lines. Oncol Rep. 2021;45(4).

51. Koch J, Mönch D, Maaß A, Gromoll C, Hehr T, Leibold T, et al. Three dimensional cultivation increases chemo- and radioresistance of colorectal cancer cell lines. PLoS One. 2021;16(1):e0244513.

52. Sakatani A, Sonohara F, Goel A. Melatonin-mediated downregulation of thymidylate synthase as a novel mechanism for overcoming 5-fluorouracil associated chemoresistance in colorectal cancer cells. Carcinogenesis. 2019;40(3):422-31.

53. Doello K, Mesas C, Cabeza L, Gandara MJ, Quiñonero F, Ortiz R. 34P Molecular markers of response to different chemotherapeutic agents in RAS / BRAF mutated colon cancer cell lines. Ann Oncol. 2020;31:S254-S5.

54. Fonseca-Gomes J, Loureiro JA, Tanqueiro SR, Mouro FM, Ruivo P, Carvalho T, et al. In vivo bio-distribution and toxicity evaluation of polymeric and lipid-based nanoparticles: A potential approach for chronic diseases treatment. Int J Nanomedicine. 2020;15:8609-21.

55. Zhang Y, Zhao Y, Li Q, Wang Y. Macrophages, as a promising strategy to targeted treatment for colorectal cancer metastasis in tumor immune microenvironment. Front Immunol. 2021;12:685978.

56. Konstantinov AS, Kovaleva OV, Samoilova DV, Shelekhova KV. Role of macrophages in progression of colorectal cancer: a contrast with the traditional paradigm. Int J Clin Exp Pathol. 2022;15(10):403-11.

CHAPTER IV – IL-12 PH-RESPONSIVE NANOPARTICLES TO MODULATE THE TUMOR MICROENVIRONMENT

This chapter was based on the following publication:

- **MJ Silveira**; C Martins; AP Cardoso; MJK Ankone; MJ Oliveira; B Sarmento, J Prakash. "Precision Therapy in Colorectal Cancer: Harnessing IL-12 pH-Responsive Nanoparticles to Modulate the Tumor Microenvironment" (Manuscript under review)

In this original research article, my roles included the conceptualization, methodology development, and the writing of the initial draft. The supervisory team was tasked with the review, editing, and submission of the manuscript. This article has not been previously included in any other PhD thesis and is reproduced in full in this thesis.

Abstract

The dismal 5-year survival rate of 14% for metastatic colorectal cancer (CRC) underscores the need for more effective treatments. Within CRC, the immunosuppressive tumor microenvironment (TME) with a weakly acidic pH (~6.5) significantly impacts treatment efficacy. Although IL-12 shows promise in solid tumor immunotherapy by stimulating IFN-γ expression, its clinical application is hindered by side effects. Here, we developed a pH-responsive nanoparticles (NPs) encapsulating IL-12 (IL-12 pH-responsive NPs) to enhance efficacy without triggering unwanted immune responses. IL-12 pH-responsive NPs exhibited activity at pH ~6.5, inducing antitumoral inflammation, by increasing IFN-γ and NO release, without impacting macrophage metabolic activity. Additionally, to validate the NPs' specificity, CRC 3D spheroids resembling tumor spatial organization and extracellular matrix were generated. The interaction of IL-12 pH-responsive NPs with CRC 3D spheroids confirmed pH-responsiveness with minimal impact on metabolic activity. Furthermore, the strategy induced macrophage polarization, reducing M2-like markers while increasing pro-inflammatory M1-like counterparts. Moreover, IL-12 pH-responsive NPs elevated IFN-γ levels and reduced IL-10 secretion. Overall, this study demonstrates the potential of pH-responsive NPs to precisely deliver IL-12 to the slightly acidic CRC TME, eliciting an anti-tumoral and pro-inflammatory immune response, encouraging further exploration in other solid cancers.

Keywords: IL-12; pH-responsiveness; Nanomedicine; 3D spheroid; Immunomodulation

Background

Colorectal cancer (CRC) is the world's third most common cancer type, while it is ranked second in cancer-related deaths [2]. The metastasis of CRC to distant sites significantly contributes to its high mortality rate, with up to 50% of localized disease progressing to metastases [3, 4]. Moreover, metastatic CRC remains a lethal disease with a 5-year survival rate of 14%, highlighting a substantial unmet need in disease management [5].

The tumor microenvironment (TME) plays a pivotal role in regulating metastasis and facilitating intricate mechanisms that promote the invasion of cancer cells [5]. In CRC, the ever-changing makeup of the TME underscores the significance of tumor-associated macrophages (TAMs) as one of the most abundant immune cell populations [6]. TAMs play a crucial role in generating chemokines, growth factors, and immunosuppressive cytokines that contribute to the suppression of T cells, promotion of angiogenesis, and metastasis [7]. In fact, depending on their microenvironment, TAMs can be activated with different features, being categorized as M1-like (promoting an inflammatory response against tumors) or M2-like (supporting tumor advancement through an immunosuppressive phenotype) [8]. Furthermore, recent discoveries have emphasized the importance of activated immune cells in generating and releasing growth factors and cytokines that modulate the inflammatory environment in CRC [9]. In this context, several immunomodulatory therapies focusing on cytokine secretion are being explored for cancer treatment [10].

Among various cytokines, interleukin 12 (IL-12) has been proposed as a crucial component for immune responses, serving as a key factor in tumor immunotherapy [11, 12]. The primary role of IL-12 involves the differentiation of naïve T cells and activation of Natural Killer (NK) cells and macrophages by triggering a signaling cascade employing tyrosine kinases JAK and STAT pathways, for IFN-γ cytokine-induced gene expression [13, 14]. Furthermore, IL-12 receptors identified in macrophages contribute to polarization towards M1-like macrophages through IFN-γ induction, fostering the development of a pro-inflammatory microenvironment [15]. Despite its potent antitumor effects in mouse models and initial clinical trials against solid tumors, the benefit-to-toxicity ratio for IL-12 was unfavorable due to IFN-γ-associated toxicity [12]. In addition, susceptibility of IL-12 to protease-mediated degradation resulted in short half-life and sub-therapeutic concentrations in the bloodstream [16].

Nanomedicine offers a promising solution to improve half-life of protein-based therapeutics and thereby extend their therapeutic effects [16]. TME-responsive drug delivery systems in nanomedicine, activated by stimuli from the TME, have gained

enormous interests to achieve tumor-specific drug release [17]. To enhance tumor-specific responsiveness, factors such as size, surface charge, and other physicochemical properties, triggered by internal stimuli such as pH, redox conditions, and enzymes can be modified [18]. Specifically, pH-sensitive nanomaterials remain inactive until reaching the TME, enabling targeted and selective payload release [17]. These nanomaterials act through acid-triggered processes, including functional group protonation and linker cleavage [19]. The 2,3-dimethylmaleic amide (DMMA) has been identified as a potent charge conversion molecule and pH-sensitive compound, which undergoes acid-triggered linker cleavage [20]. Modifying PLGA, a FDA approved polymer known for its excellent biodegradable properties, safety, and controlled drug release capabilities, with DMMA produces pH-responsive nanoparticles (NPs) for targeted release in the mildly acidic TME (pH ~ 6.5) [20, 21]. The stable amide bond under neutral and alkaline conditions promptly cleaves upon encountering the weakly acidic TME, revealing positive-charge amino groups, inducing a surface charge shift from negative to positive and promoting accumulation into the TME [22].

The main goal of this study is to develop pH-responsive PLGA NPs as a novel platform to deliver IL-12 within the mildly acidic CRC TME. With the release of IL-12, we aim to stimulate a robust pro-inflammatory immune response, characterized by increased IFN-γ production and decrease of the immunosuppressive IL-10 secretion. Here, we detailed the NPs manufacturing process and provided a comprehensive physicochemical characterization. Additionally, we investigated the specificity and selectivity of IL-12-loaded NPs, by assessing their capability to release IL-12 under mildly acidic pH conditions. Furthermore, we assessed the impact of NPs on the metabolic activity in 2D cell culture models, including the mouse RAW 264.7 macrophagic cell line or the human primary monocyte-derived macrophages isolated from healthy blood donors. Moreover, a 3D cell culture model was established to better replicate the *in vivo* complexity of the disease, detaining tumor heterogeneous cell populations, extracellular matrix (ECM), and dynamic cell-cell and cell-ECM interactions. The 3D assembled multicellular tumor model (spheroid) incorporated the CRC cell line SW48, blood donor monocyte-derived macrophages and exogenous collagen type I as major ECM component. This setup allowed us to assess the impact of NPs on the spheroids' metabolic activity, macrophage polarization, and production of nitric oxide (NO), IFN-γ, and IL-10.

Materials and Methods

PLGA 5004 (50:50 LA: GA; 44 K; Purasorb® PDLG 5004A) was kindly provided by Corbion-Purac biomaterials. PLGA-NH2 (LA:GA- 50:50; 30K) was purchased from

RuixiBiotech® and PLGA-FKR648 was acquired from Akina (USA). Reagents such 2,3-Dimethylmaleic anhydride (DMMA), resazurin, Polyvinyl alcohol (PVA), dichloromethane (DCM), paraformaldehyde (PFA), Sulfanilamide, dimethyl sulfoxide (DMSO), Phosphoric acid, N-naphthylethylenediamine, neutral buffered formalin, trypsin, xylene, Histopaque-1077, a graded alcohol series, hematoxylin and eosin staining solution, Tris, EDTA and sodium citrate were obtained from Sigma-Aldrich (USA). RPMI 1640 and high glucose Dulbecco's Modified Eagle (DMEM) GlutaMAX medium were purchased from Alfagene, Lda. SeaKem® LE agarose was purchased from Lonza (Switzerland). Accutase® and BCA Protein Assay Kit were obtained from Thermo Fisher Scientific (USA), and Triton X-100 from Spi-Chem (USA). The RosetteSep-Human Monocyte Enrichment Cocktail was procured from StemCell Technologies, murine and human IL-12, interferon-γ (IFN-γ), IL-4, IL-13, and bacterial lipopolysaccharide (LPS) were acquired from PeproTech, M-CSF, IL-10 from ImmunoTools (Germany) and Collagen type I (COL-I) from Corning (UK). Alexa Fluor 488-anti rabbit, and Alexa Fluor 594-anti mouse antibodies were sourced from Invitrogen (Belgium). Ultrapure water was prepared in-house with a conductivity of 0.055 µS/cm and a resistivity of 18.2 MΩ.cm, using MilliQ® station from Millipore Corporation. For cell cultures, T flasks were acquired from Orange Scientific. Fetal bovine serum and penicillin-streptomycin were acquired from Gibco (USA). IFN-γ and IL-12 ELISA Kit were obtained from BioLegend while IL-10 ELISA KIT from was purchased from PeproTech. The total protein content analysis kit (Dc Protein kit, USA) was acquired from Bio-Rad. Antibodies, including anti-CD14/APC and anti-CD86/FITC were obtained from ImmunoTools. The anti-CD206/PE was purchased from BioLegend. Anti-CD163/PE was acquired from BD Biosciences. The anti-HLA-DR/ PB and anti-EPCAM/PB, Live/Dead Fixable Viability Dye eFluor™ 780 and 4′,6-diamidino-2-phenylindole (DAPI) from Thermo Fisher Scientific®. The antibody, anti-collagen type I (Anti-COL-I) rabbit was acquired from Rockland Immunochemicals. Dialysis membranes of 10k, 100K, N-2-hydroxyethylpiperazine-N-2-ethane sulfonic acid (HEPES) and DMSO-d6 were acquired from Merck (USA). Mouse macrophages RAW 264.7 and the human colon cells SW-48 cell lines were purchased from American Type Culture Collection (Rockville, MD).

Chemical conjugation and characterization of the DMMA and PLGA polymer composite

The DMMA and PLGA polymer composite (PLGA-DMMA) was prepared in anhydrous conditions, through an amidation process where the carboxylate group present in DMMA reacted with an amide group (–NH2) present in PLGA (PLGA-NH_2) resulting in an amide

[23]. Briefly, 25 mg of PLGA-NH_2 (Mn ≈ 30 K, 0.83 μmol) was dissolved in 1 mL of DMSO, and 10 equiv (to amino groups) of DMMA (Mn ≈ 126.11 Da,1.05 mg, 8.3 μmol), previously dissolved in 1 mL of DMSO were added. The reaction was stirred for 24h at 40ºC under inert atmosphere [24, 25].The final solution was transferred into a dialysis bag with 10K molecular weight cutoff and dialyzed for 48h against 200 mL of distilled water to remove excess DMMA. The composite polymer was then dried under vacuum, in a vacuum oven, overnight at 25ºC. ^{1}H NMR measurements were performed with a Varian Inova 400 MHz 1H NMR spectrometer, at room temperature (RT), in deuterated DMSO. Chemical shifts are reported in ppm (δ units) and were referenced to the residual solvent signal. DMSO residual solvent at 2.50ppm was removed after the analysis using GSD Mnova software (Mestrelab Research) which was used for analysis processing.

Manufacture of IL-12 loaded pH responsive nanoparticles

NPs containing IL-12 (MW ≈ 75K), were produced using a modified water-in-oil-in-water (w/o/w) double emulsion-solvent evaporation technique [26]. In this process, 20 mg of non-modified PLGA (Mw ≈ 44 K, 50/50 ratio of lactide and glycolide, viscosity midpoint 0.4 dl/g viscosity) was mixed with 40% PLGA-DMMA (regarding total polymer concentration) in 4 mL dichloromethane for 3h at RT. Subsequently, 0.2 mL of 25ug/mL IL-12 in PBS was emulsified at 70% amplitude for 30 s using a Vibra-CellTM ultrasonic processor in an ice bath. The initial emulsion was then poured into 4 mL of 2% PVA (aqueous solution) and sonicated for 60 s, resulting in the formation of the second emulsion (w/o/w). The final emulsion was added to 50 mL of PVA. Dichloromethane evaporation from the solution occurred overnight under magnetic stirring at 400 rpm. The NPs were subjected to two rounds of washing with 20 mL of ultrapure water using ultracentrifugation at 8,000 *g* for 30 min at 4ºC.

Characterization of nanoparticles

Average particle size, polydispersity index, surface charge and morphology of nanoparticles

NPs undertook characterization for their Z-average and polydispersity index (PDI) using dynamic light scattering (DLS), while zeta-potential (ζ-potential) was determined through laser Doppler anemometry (LDA) employing a Malvern Zetasizer Nano ZS instrument (Malvern Instruments Ltd). The measurements were conducted on samples diluted in a 10 mM sodium chloride (NaCl) ionic solution, maintaining a particle concentration of 0.2 mg/mL. The reported values represent the mean ± standard deviation (SD) obtained from

at least three distinct batches. The morphological analysis of the NPs was performed using scanning Electron Microscopy [27] (JSM-IT100, JEOL, Tokyo, Japan) at an accelerating voltage of 5 kV and a probe current of 38 and 23 respectively.

Evaluation of nanoparticles pH responsiveness

PLGA-DMMA features a pH-responsive amide linker that remains stable under normal physiological conditions. However, upon exposure to a slightly acidic environment, the amide linker undergoes rapid hydrolysis, revealing positively charged amino groups. To validate this pH responsiveness of PLGA-DMMA, NPs were subjected to buffer solutions of different pH, ranging from 8 to 5, and alterations in both their average size and ζ-potential were assessed using DLS/DLA after 24h of incubation.

IL-12 association efficiency and drug loading

The amount of IL-12 encapsulated into NPs was directly quantified by liquid–liquid phase separation. Briefly, NPs were freeze dried after their purification, and subsequently solubilized in 4 mL DCM overnight. In the day after, PBS1x in same proportion was added to the first solution to solubilize IL-12. The presence of this cytokine, IL-12, was then measured by enzyme-linked immunosorbent assay (ELISA) as commercially recommended. The association efficiency (AE) was calculated using the following equation:

$$AE\ (\%) = \frac{mass\ of\ encapsulated\ IL-12}{inital\ mass\ of\ IL-12}\ x100$$

IL-12 in vitro cumulative release

The drug release profile of IL-12 from PLGA-DMMA NPs in an *in vitro* setting was assessed through the dialysis diffusion method. The release media comprised potassium phosphate (pH 6.5), phosphate buffer (pH 7.4), citrate buffer (pH 5), and HEPES buffer (pH 8). A volume of 100 mL of dissolution media was placed in a flask and maintained at 37°C ± 2°C on an orbital shaker. A dialysis membrane with a 100K molecular weight cutoff, containing 1 mL nano-suspension of IL-12, was suspended in the release media. The flask with release media was stirred at 60 ± 2 rpm. At specified time intervals (0.5, 1, 4, 14, and 24h), 0.2 ml samples were withdrawn, and the amount of drug release was determined using the BCA Protein Assay kit (Tecan plate reader, 562 nm wavelength measurements). The BCA Protein kit was followed according to the supplier's recommendations. The volume of release media was adjusted to the original volume

after each sampling, and the temperature was kept constant. Average percentage release and standard deviations (SD) were calculated (n = 3).

Cell lines and cell culture reagents

The SW48 CRC epithelial cell line was cultured in DMEM supplemented with 10% v/v FBS and 1% v/v penicillin-streptomycin. The cell culture medium was changed every 2–3 days, and trypsin treatment was employed for subculturing the cell lines. Cells were housed in a Cell Culture CO2 incubator (ESCO) at 37°C with 5% CO2 and 95% relative humidity. Routine mycoplasma detection was conducted. Additionally, mouse macrophages RAW 264.7 were cultured in RPMI1640 medium supplemented with 10% v/v FBS, 100 U/ml penicillin, 0.1 mg/ml streptomycin, and 2 mM L-glutamine in a CO_2 incubator at 37 °C.

Ethics statement

In accordance with the guidelines set forth in the Declaration of Helsinki and with ethical approval granted by the Centro Hospitalar Universitário São João Ethics Committee (protocol reference 90/19), blood donors were duly informed and provided written consent for the utilization of their blood collections for research purposes. Monocytes were isolated from excess buffy coats generously supplied by the Immunohemotherapy Department of Centro Hospitalar Universitário São João (CHUSJ) in Porto, Portugal, sourced from healthy blood donors.

Human monocytes isolation

Human monocytes were isolated from healthy blood donors' buffy coats, as previously reported [28]. In summary, the buffy coats underwent centrifugation and were incubated with the RosetteSep human monocyte enrichment kit (StemCell Technologies) to isolate peripheral blood mononuclear cells (PBMCs). Subsequently, each sample was diluted 1:1 with PBS supplemented with 2% FBS and layered over Histopaque-1077 (Sigma-Aldrich) to separate monocytes from other blood components. The enriched monocyte layer was collected and washed with PBS.

2D Macrophages differentiation

Mouse RAW264.7, M1 macrophages were differentiated using murine recombinant 20 ng/ml IFN-γ and 100 ng/ml LPS. RAW264.7, M2 macrophages were differentiated

using 10 ng/mL murine recombinant IL-4 and 10 ng/ml IL-13. For the differentiation of monocytes isolated from blood donors into macrophages, 0.2 × 10^6 monocytes (in 24-well plates) were cultured and differentiated using 50 ng/mL M-CSF for a period of 7 days, in RPMI1640 medium over glass coverslips. Following a 7-day differentiation period, the medium was aspirated, and the macrophages were subjected to a washing step. To serve as controls for polarization, human macrophages were exposed to 10 ng/mL LPs (to differentiate as M1-like) or 10 ng/mL IL-10 (to differentiate as M2-like). M0 macrophages, on the other hand, were cultured without the addition of any exogenous factors. The cells were maintained in a humidified atmosphere at 37 °C and 5% CO2.

Assessment of the metabolic activity in 2D macrophages cells

Resazurin assay was used to analyze cell metabolic activity. For murine RAW264.7 macrophages, 0.15x10^6 cells were seeded in 96-well plates for 24h and for human monocytes 0.2 x 10^6 cells, were differentiated in 24 well plates for 7 days, as described above. Subsequently, after 24h and 7 days, respectively, the medium was removed, cells were washed with PBS, and different concentrations of free IL-12 or NPs (62,5, 125, 250, 500 pg/mL regarding drug content) in medium (200 µL) were incubated for 24h, at 37 °C. Afterwards, resazurin redox dye (0.01 mg/mL) was added (1/10 of the total volume of culture medium) to cell culture, incubated for 4 h at 37 °C and 5% CO2, and the fluorescence intensity was measured at 530/590 nm using a SynergyMx MultiMode microplate reader (BioTek). All data were normalized using a background control and positive control (M0 cells without treatment, 100% metabolic activity). The cell metabolic activity was analyzed using as a threshold of 70% cell viability according to the ISO 10993-5 standard [29]. The pH responsiveness of the NPs was confirmed using the phenol red indicator.

Nitric oxide (NO) release bioassay in 2D macrophages

The impact of the developed NPs on inducing M1 proinflammatory polarization in both murine and human macrophages was evaluated by assessing NO release, a stable metabolite produced by M1-like macrophages. Macrophages isolated from healthy blood donors were cultured as mentioned above. RAW264.7 cells (0.15x10^6 cells/well) were seeded in 96-well plates and cultured for 24h. Subsequently, the medium was replaced, and varying concentrations of free IL-12 or different NPs (62.5, 125, 250, 500 pg/mL with respect to the drug) in medium (200 µL) were incubated for an additional 24h at 37 °C. Controls for M1 polarization were performed using IFN-γ (20 ng/mL) and LPS (100

ng/mL), while M2 polarization controls involved incubation with 10 ng/mL IL-4 and IL-13. For macrophages isolated from healthy blood donors, following a 7-day differentiation period, both free IL-12 and NPs in the same concentrations as aforementioned were added. In parallel, controls for polarization were conducted using 10 ng/mL LPs (M1-like) or 10 ng/mL IL-10 (M2-like). In both cases, M0 macrophages were cultured without the addition of any exogenous factors. After 24 hours, 100 µL of the culture supernatant was combined with 100 µL of Griess reagent (1% sulfanilamide, 0.1% naphthyl ethylenediamine dihydrochloride, 3% phosphoric acid), and the absorbance at 540 nm was measured using a microplate reader. NO release assays were conducted in triplicate across three independent experiments. The pH responsiveness was confirmed using the phenol red indicator.

In vitro efficacy studies in 2D macrophages by IFN-γ production

To initiate the differentiation of RAW macrophages, cells were seeded at a density of $0.15x10^6$ cells per well in 96-well plates and incubated for 24h. Following this incubation, the medium was replaced, and the IL-12 pH-responsive nanoparticles (NPs), free IL-12, and respective controls were added at concentrations of 62.5, 125, 250, and 500 pg/mL (with respect to the drug) for a 24-hour incubation period. M1 or M2 polarization controls were implemented by exposing the cells to LPS (100 ng/mL) and IFN-γ (20 ng/mL) for M1 differentiation, and IL-4 (10 ng/mL) and IL-13 (10 ng/mL) for M2 differentiation, also for 24 hours. In the case of human macrophages, after a 7-day differentiation period, both free IL-12 and NPs at the aforementioned concentrations were introduced. Furthermore, polarization controls were conducted using either 10 ng/mL of LPs (M1-like) or 10 ng/mL of IL-10 (M2-like). M0 macrophages in both scenarios were cultured without the addition of any exogenous factors. Subsequently, IFN-γ concentration in the supernatants was determined by ELISA using a commercially available kit according to the manufacturer's instructions. All efficacy studies were independently conducted independently at least three times. The pH responsiveness was confirmed using the phenol red indicator.

3D colorectal cancer spheroid establishment

Multicellular colorectal spheroid, comprising SW48 cells, human macrophages, and COL-I, were generated using commercially available molds (3D Petri Dish®, MicroTissues, USA). Agarose was dissolved at a concentration of 2% (w/v) in 0.9% NaCl (w/v) and poured into 3D Petri Dish® molds to create hydrogel micro-molds featuring 81

uniform circular recesses. Each micro-mold was filled with 190µL of medium and placed in a well of a 12-well plate containing 2 mL of medium [30, 31].For monoculture, SW48 cells (0.0025×10^6, 0.005×10^6, or 0.01×10^6 cells per spheroid) were added to the micro-molds (190 µL) and allowed to settle for 30 minutes before supplementing each well with complete DMEM medium (2 mL). In the case of dual culture control spheroid (SW48 and human monocytes), the total number of cells per spheroid was maintained at 0.005×10^6. Additionally, three different ratios were explored for SW48: human monocytes double culture (75:25, 65:35, and 50:50), and a defined concentration of COL-I (8µg/mL) was incorporated to mimic the presence of the extracellular matrix (ECM). Macrophage differentiation within the spheroids, originated from human peripheral monocytes, occurred spontaneously in situ without the need for colony-stimulating factors or other exogenous agents, as previously reported by our group [31]. The medium was refreshed every two days.

Characterization of the average diameter, metabolic activity, and circularity of 3D colorectal spheroids

3D spheroids images were captured at specified time intervals (1, 4, and 7 days) using brightfield microscopy (ZOE™ Fluorescent Cell Imager, Bio-Rad Laboratories, USA). The 3D spheroids' average diameter, circularity, and compactness were randomly assessed in three distinct spheroids per micro-mold core through the AnaSP open-source software [32]. For metabolic activity measurements on days 1, 4, and 7, 3D spheroids were incubated with DMEM complete medium containing resazurin (20% v/v) and incubated in the dark at 37 °C for 4h. Following incubation, the fluorescence of was measured at the excitation and emission wavelengths of 530 nm and 590 nm, respectively, using a SynergyMx™ MultiMode microplate reader (BioTek™, USA). All analysis were conducted on samples from three independent blood donors, with each analysis performed in triplicate.

Histological analysis of the 3D colorectal spheroids

On day 7, the medium was extracted from micro-molds, and the 3D spheroids were fixed in neutral buffered formalin (10% v/v) for 24h at RT. Subsequently, the micro-molds underwent a PBS 1X wash, and a sealing layer of 2% w/v agarose was applied to the top of each micro-mold. The micro-molds were then embedded in paraffin using an automated embedding system (Thermo Scientific™ STP 120 Spin Tissue Processor, USA). Paraffin-embedded samples were sectioned into 3 µm sections, deparaffinized in

xylene, and rehydrated in a graded alcohol series. Staining was carried out using hematoxylin and eosin (H&E), Sirius Red (SR), and Masson's Trichrome (MT) [33].

3D colorectal spheroids immunofluorescence analysis

At day 7, the fixed paraffin-embedded samples, prepared as outlined earlier, underwent sectioning into 5 µm sections, followed by deparaffinization in xylene and rehydration in sequentially decreasing ethanol concentrations. Prior to staining, sections were subjected to antigen retrieval by treatment with Tris-EDTA (TE) (pH 9) or sodium citrate buffer (pH 6) at 96 °C for 30 min. Subsequently, the samples underwent three washes by immersing sections in PBS 1X (pH 7.4) for 5 min each [30]. For sample permeabilization, sections were immersed in 0.25% (v/v) Triton for 10 min and then washed three times, as previously described. Before the addition of antibodies, samples were blocked with 10% FBS in PBS for 1h at RT. Primary human antibodies diluted in block solution (Anti-EpCAM 1:100, Anti-CD68 1:100, and Anti-COL-I 1:100) were introduced to the samples and incubated overnight in a wet chamber at 4 °C. Following three washes, secondary antibodies (at a 1:400 dilution) diluted in block solution were incubated in a wet chamber, in the dark, for 1h at RT. Subsequently, samples were stained with DAPI (1:25,000) solution for 20 min and after washed for 5 min in PBS 1X. Finally, sections were mounted with VectaShield and imaged using a Zeiss AxioImager Z1 microscope (Carl Zeiss, Germany) equipped with an AxioCam MR ver. 3.0.

Characterization 3D colorectal spheroids through flow cytometry analysis

Following a 7-day culturing period, 3D colorectal spheroids were gathered into a 15 mL Falcon tube, centrifuged (300 g, 5 min, 20°C), and the medium was collected. The samples were then washed once with PBS 1X through centrifugation under the same conditions, followed by the removal of the supernatant. Dissociation of the 3D colorectal spheroids into a single-cell suspension was achieved by incubating with Accutase for 15 min at 37 °C, with periodic pipetting every 5 min during the incubation. Subsequently, cold PBS 1X (1.5 mL) was added to inactivate the Accutase, and the cells were centrifuged (300 g, 5 min, 4°C) and washed with PBS 1X. Next, 200,000 cells per staining were resuspended in FACS Buffer containing PBS 1X, 2% BSA, and 0.01% azide and centrifuged again. Following that, conjugated antibodies (anti-EpCAM/PB, anti-CD14/APC, anti-CD86/FITC, anti-CD163/PE, anti-CD206/PE, and anti-HLA/DR/PB), previously diluted 1:50 in FACS buffer, were incubated for 40 min at 4 °C in the dark. After incubation, cells were washed twice with FACS buffer and incubated with Live Dead

(1:10,000) diluted in PBS 1X for 20 min. Following washing with FACS buffer, samples were incubated with 2% PFA for 15 min at RT. Finally, samples were washed again in FACS buffer and filtered through a 70 µm pore filter membrane. Cell counting beads were used to absolute cell count of each sample in the concentration of 9.7×10^{-4} particles/mL. The acquisition of samples was performed using the BD FACS Canto™ II flow cytometer (BD Biosciences, USA), and all analysis were performed with FlowJo software (Tree Star, Inc., USA). Cells submitted to the same protocol with only FACS buffer were the unstained control. Experiments were conducted at least in triplicate.

Uptake of NPs into 3D colorectal cancer spheroids

On the 6^{th} day of 3D spheroid development, empty FKR648-labeled NPs in DMEM without FBS (100 µg/mL) were introduced to each micro-mold and incubated for 24h. Following incubation, the medium was collected, and the 3D spheroids were washed with PBS 1X. Subsequently, the spheroids were transferred to a 15 mL plastic tube. Within each tube, spheroids were subjected to trypsin incubation for 15 minutes at 37 °C, followed by vigorous pipetting for dissociation into single cells. The isolated cells were then washed twice with PBS 1X, fixed with 2% PFA for 20 min at room temperature (RT), washed again, and placed into cytometer tubes for subsequent analysis. BD FACS Canto™ II flow cytometer was employed for cytometry acquisition. Cells incubated solely with cell culture medium served as the unstained control, and all cell constituents were grouped into a single gate. All data was processed using FlowJo software. Experiments were conducted at least in triplicate.

Effect of NPs on macrophages polarization and anti-proliferative effect of 3D colorectal cancer spheroids

At day 6, each micro-mold was washed with PBS 1X, and different concentrations of IL-12 or NPs (62.5, 125, 250, and 500 pg/mL, in regard to the IL-12) in medium without FBS (190 µL per micro-mold, and 2 mL per each 12 well-plate well where the micro-mold was placed) were added and incubated for 24 h, at 37 °C. Afterwards, the flow cytometry staining protocol was applied as described above. The cells acquisition was performed in BD FACS Canto™ II flow cytometer and analyzed with the FlowJo software. The pH responsiveness was confirmed using the phenol red indicator.

Effect of NPs on NO, IFN-γ and IL-10 levels of 3D colorectal cancer spheroids

Following the incubation of nanoparticles (NPs) and their respective controls, 3D colorectal spheroids were evaluated for nitric oxide (NO) release and their capacity to generate pro- or anti-inflammatory cytokines as IFN-γ or IL-10, respectively. The evaluation of NO release was conducted as previously described, while cytokine production was determined using ELISA Kits from the selected manufacturers. The pH responsiveness was confirmed using the phenol red indicator.

Statistical analysis

The findings were presented as mean ± standard deviations (SD) derived from a minimum of three independent experiments. Statistical analysis involved two-sided unpaired Student's t-test for comparing two independent groups and one- or two-way ANOVA for comparing three or more groups, conducted using GraphPad Prism 8.0 software (GraphPad, USA). Significance levels were established at probabilities of *$p < 0.05$, **$p < 0.01$, and ****$p < 0.001$.

Results

Production and characterization of the pH-responsive NPs

IL-12, a potent pro-inflammatory cytokine, is hindered by dose-limiting toxicities [34]. The intricate nature of the TME poses challenges to cancer therapy, but comprehending its complexity and specific traits offers an opportunity to create innovative and more effective therapeutics [35]. We used pH as a tumor-responsiveness factor because the TME is more acidic than blood and healthy tissues. pH-responsive polymer carriers can enhance *in vivo* drug delivery efficiency, facilitating targeted delivery and minimizing adverse reactions, enabling multifunctional and personalized treatment (Fig. 1A) [36]. We first chemically synthesized a pH-responsive DMMA-PLGA composite polymer. A PLGA counterpart of 30K LA:GA-50:50 was selected since lower than that molecular weight and LA/GA ratios have been associated with an accelerated hydrolysis and erosion, and thus accelerated drug release [30, 31]. ^{1}H NMR confirmed the successful reaction between the carboxylate group of the DMMA and PLGA-NH_2, revealing characteristics peaks of PLGA (δ = 5.20, 4.95 and 1.46 ppm) [4], -NH_2 (δ = 3.05, 1.2 ppm) [37] and DMMA (δ = 1.99 ppm) [32]. The appearance of a distinct peak at δ=2.54 ppm in the spectrum of the final polymeric conjugate is associated with the C=O

stretching vibration of the carboxylic acid on DMMA [33]. This observation strongly suggests the successful integration of DMMA into PLGA (Fig. 1B). Following the polymer conjugation, pH-responsive NPs with a polymer content of 40% PLGA-DMMA were produced by double emulsion technique (Fig. 1C). In addition, to address the reported drawbacks of IL-12, it was encapsulated in pH-responsive nanoparticles with an association efficacy of 46.8 $\pm$ 5.4% (Table 1). This finding aligns with the protein's solubility profile and molecular weight, indicating part of its diffusion into the aqueous external phase during the encapsulation process [16, 38].

Table 1 Physicochemical characteristics of empty pH-responsive NPs, IL-12-loaded pH-responsive NPs, and their respective controls were assessed, including mean size (Z-average size), polydispersity index, surface charge (ζ-Potential), and association efficacy (AE %). Values are presented as mean ± SD (N = 8). Non-applicable values are denoted by (-).

	Size (nm)	Polydispersity index	Surface charge (mV)	Association efficiency (%)
Empty PLGA NPs	245.8 ± 10.1	0.15 ± 0.06	0.89 ± 1.08	-
Empty pH-responsive NPs	195.8 ± 1.6	0.06 ± 0.04	0.79 ± 0.65	-
IL-12 pH-responsive NPs	211.6 ± 4.4	0.06 ± 0.03	0.64 ± 1.17	46.8 ± 5.4
IL-12 PLGA NPs	200.6 ± 4.4	0.10 ± 0.05	0.55 ± 2.60	40.1 ± 3.6

Concerning the physicochemical attributes of NPs, the Z-average size for both NPs and their corresponding controls fell within the range of approximately 200 to 250 nm. They exhibited a uniform size distribution, indicated by a polydispersity index of around 0.1. Furthermore, the ζ-Potential of the NPs approached neutrality, attributed to the presence of -NH2 groups in the NPs and the adsorption of some negatively charged IL-12 molecules [39, 40]. Furthermore, NPs exhibited a spherical morphology with smooth surface, and a uniform size distribution across all samples, as evidenced by SEM analysis (Fig. 1C). The self-aggregation of NPs is being reported as a process that is facilitated by hydrophobic and electrostatic interactions, involving the negatively charged unhydrolyzed particles and positively protonated amidogen through DMMA dissociation at pH 6.5 [41].

Furthermore, NPs were subjected to incubation at different pH solutions (5, 6.5, 7.4, and 8) to assess the influence on their surface charge, assessed by the ζ-Potential values. Hence, notable distinctions in the surface charge of NPs were observed after 24h of incubation. Specifically, significant differences were identified between pH 8 and 7.4 ($p=0.0016$), pH 8 and 6.5 ($p < 0.0001$), pH 7.4 and 5 ($p=0.0003$), as well as pH 6.5 and 5 ($p=0.0423$), affirming the specific cationic charge reversal characteristics of the developed NPs (Fig. 1D). This investigation was conducted because DMMA has been reported as a monomer capable of inducing a cationic charge reversal property in NPs under slightly acidic conditions [42]. Moreover, DMMA-based NPs have been described

to exhibit a capacity for size alteration following incubation at pH 5, 6.5, 7.4, and 8 [43]. Thus, following a 24h incubation period, significant variations in the size of NPs were observed between NPs incubated at pH 8, 7.4, 6.5, and 5.

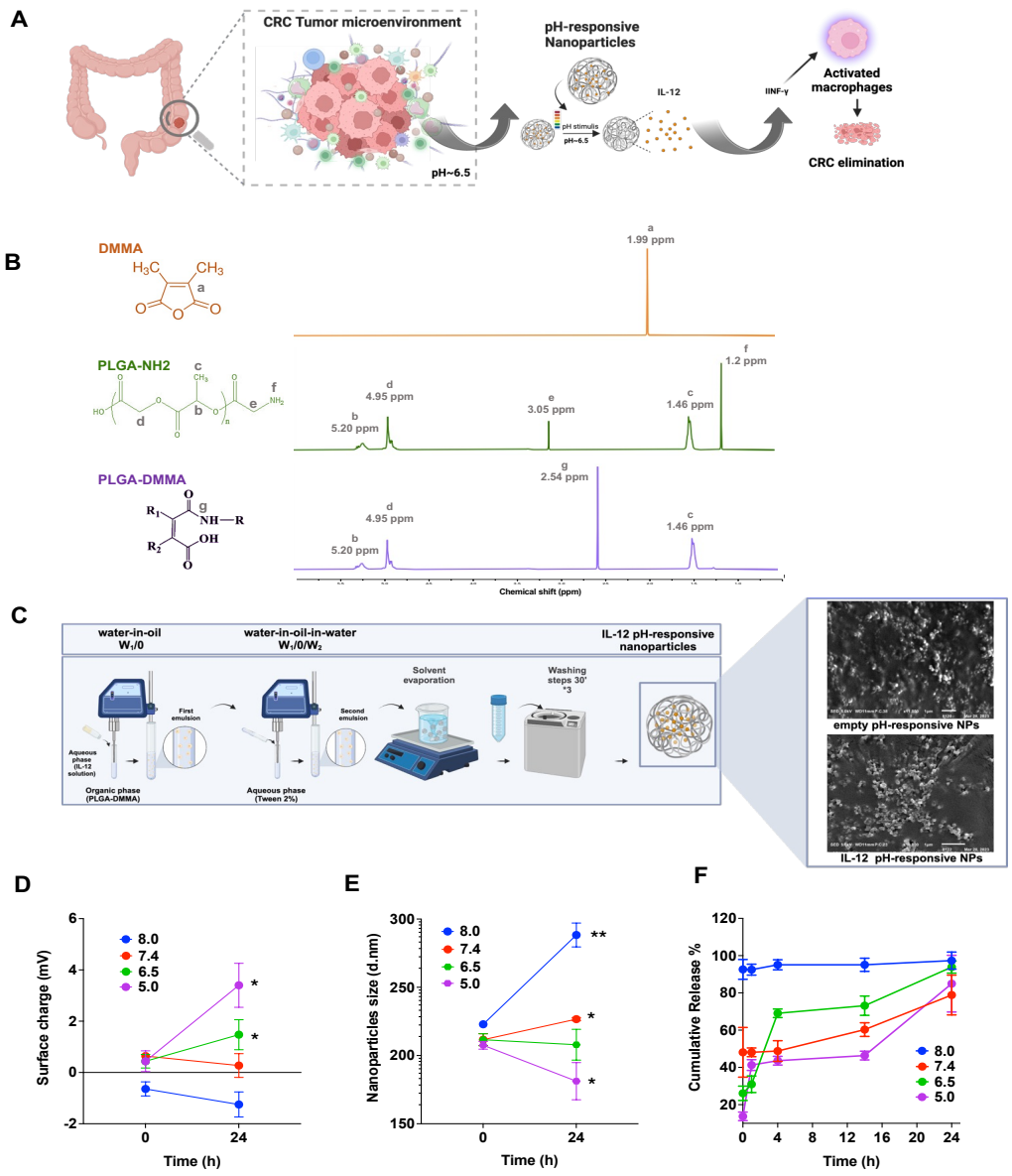


Fig. 1: Schematic illustration of the primary objectives of the developed strategy and its physicochemical characterizations. *A) Illustration outlining the intended objective of NPs. B) ^{1}H NMR characterization of PLGA-DMMA polymer performed in DMSO-d6: characteristic peaks of glycolic acid (δ= 5.21, 1.47 ppm), (δ = 4.89 ppm) lactic acid, and δ= 2.54 ppm of DMMA in the final PLGA-DMMA polymer. C) Demonstration of the double emulsion technique used in the manufacturing of NPs, along with SEM images illustrating empty pH-responsive NPs and IL-12-loaded pH-responsive NPs. Scale bar: 1μm. D and E) Assessment of the surface charge and size of NPs submitted at different pH (8, 7.4,6.5 and 5), respectively and F) In vitro release profile of IL-12 from pH-responsive NPs at pH 8, 7.4, 6.5 and 5 at 37°C, over 24h. All measurements were conducted in triplicate, and results are presented as mean ± SD. Statistical comparison of IL-12-loaded pH-responsive NPs when submitted at different pH, *p < 0.05, **p < 0.01, ***p < 0.001 or ****p < 0.0001.*

Additionally, significant differences were noted between NPs incubated at pH 7.4 and 6.5 , pH 7.4 and 5 as well as pH 6.5 and 5. The decrease in the size of NPs as the pH decreases is linked to the degradation of DMMA in a slightly acidic environment (Fig. 1E) [43]. Additionally, to demonstrate the responsiveness of the NPs, the cumulative release of encapsulated IL-12 was examined across diverse pH solutions (pH 5, 6.5, 7.4, and 8) (Fig. 1F) and timepoints (0.5, 1, 4, 14, and 24 h). Despite the two-step cumulative release pattern observed under conditions of pH 7.4, 6.5, and 5, which involved an initial burst release followed by a slower diffusion from the PLGA matrix in the release medium, notable distinctions were identified between NPs incubated at pH 8 and 6.5 (representative of the CRC TME pH) [48]. When comparing NPs after 30 min of incubation at different pH solutions, all conditions exhibited significant differences with p values < 0.001. Furthermore, after 1 h of incubation, comparisons between NPs at pH 5 and 6.5 revealed significant differences in IL-12 cumulative release ($p < 0.0001$). Following 4 h of incubation, differences in IL-12 release were observed between NPs at pH 5 and pH 6.5 and pH 6.5 vs. pH 7.4 ($p < 0.0001$). A 14 h incubation period resulted in differences across all conditions ($p < 0.0001$), and after a total release of the protein at 24 h of incubation at pH 8, nearly all NPs were capable of releasing over 80% of IL-12. At this time point, the most significant differences were noted when comparing NPs at pH 8 and pH 5 ($p=0.0038$), pH 6.5 and 7.4 ($p=0.0003$), and pH 7.4 and 8 ($p < 0.0001$). Consequently, these observed variations led to the conclusion that IL-12 encapsulated in pH-responsive NPs was released in accordance with the specific pH and over the course of time, confirming NPs' responsiveness to the mildly acidic pH. At pH 8, IL-12 exhibited a burst release, with approximately 90% of the total protein released into the medium in the initial 30 min of incubation.

Therapeutic effect of the IL-12-loaded pH-responsive NPs in 2D *in vitro* models of macrophages

IL-12 is a cytokine that can activate macrophages potently, and this activating effect is mediated primarily through its effect on macrophage IFN-γ release [44, 45]. To investigate the therapeutic effects on macrophages, the metabolic activity was assessed over a 24 h period. This involved employing IL-12 doses ranging from 62.5 to 500 pg/mL in murine macrophages as well as in human macrophages isolated from healthy blood donors (Fig. 2A and B, respectively). Therefore, as expected, there were no disparities in the metabolic activity of both mouse or human macrophages after 24h of contact with IL-12-loaded pH-responsive nanoparticles or the mentioned controls. Additionally, no

significant impact of the distinct NPs on the metabolic activity, were observed, of already polarized mouse and human macrophages, as the pro-inflammatory M1-like or the anti-inflammatory M2-like macrophages (Fig. S1). IL-12's primary role is to induce the secretion of IFN-γ, which serves as the classical trigger for establishing M1 polarization by activating the expression of inducible NO synthase [46]. Therefore, to confirm the polarization of macrophages toward an inflammatory (M1-like) phenotype, the release of NO from macrophages was investigated (Fig. 2C and D). As presented in Fig. 2C, macrophages treated with higher concentrations of IL-12 pH-responsive NPs

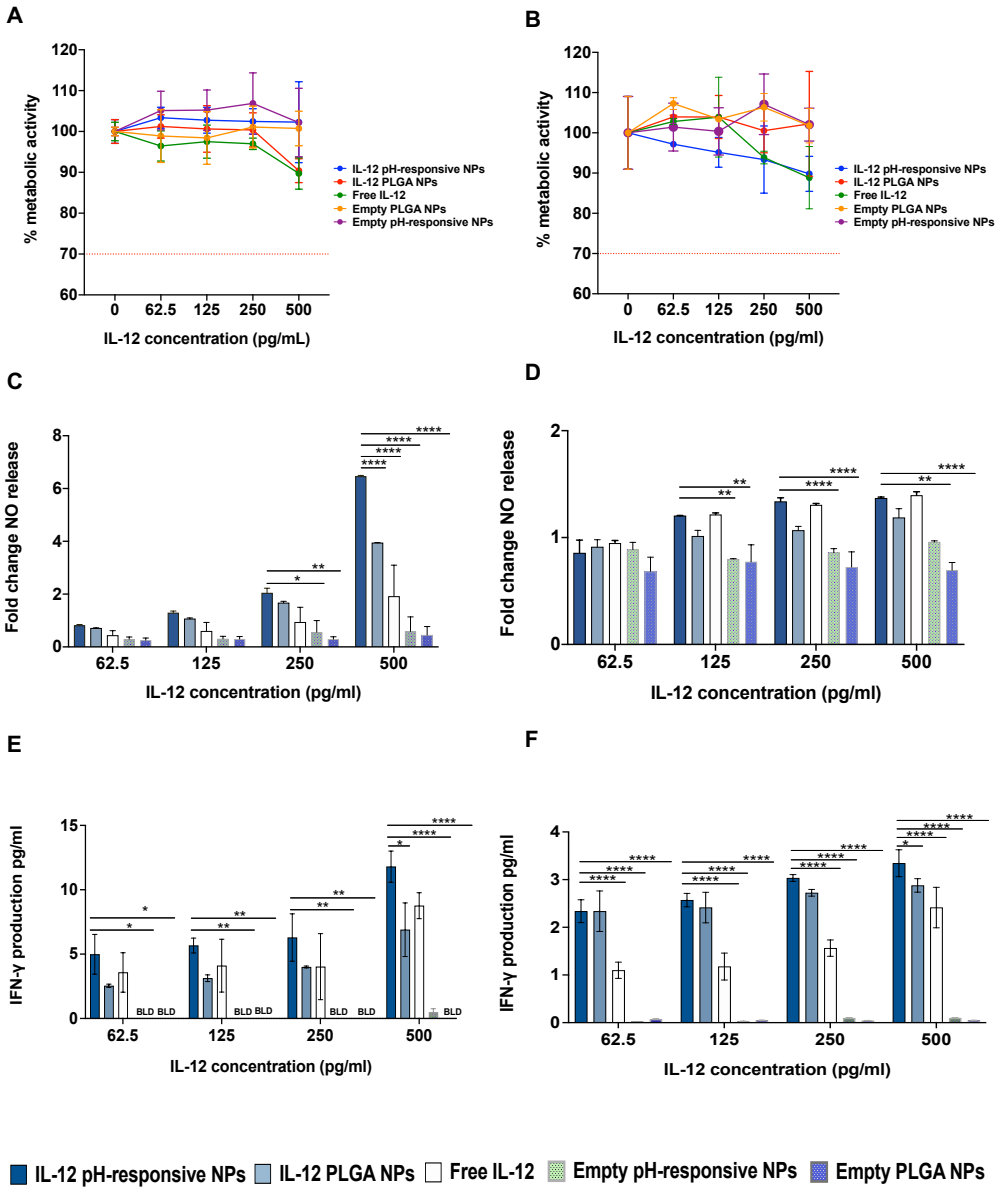


Fig. 2: Evaluation of the impact of IL-12 pH-responsive NPs in macrophages. *A and B) Metabolic activity assessment in murine RAW264.7 macrophages (left panel) or human macrophages (right panel) after 24h incubation with free IL-12, empty PLGA NPs, pH-responsive NPs, and IL-12-loaded pH-responsive NPs. C and D) Impact evaluation of different IL-12 pH-responsive NPs concentrations and corresponding controls on NO release in 2D RAW264.7 macrophages or human macrophages, respectively. D and F) Influence of*

IL-12 pH-responsive NPs on IFN-γ production in RAW264.7 macrophage cell line or human macrophages, respectively. Statistical comparison of IL-12-loaded pH-responsive NPs with free IL-12 in each dose range.

(250 pg/mL and 500 pg/mL) demonstrated significant differences in NO release from RAW264.7 murine macrophages. Notably, at a concentration of 250 pg/mL, significant differences in NO release were observed between IL-12 pH-responsive NPs and the corresponding empty pH-responsive NPs ($p=0.0330$), as well as with non-responsive empty NPs (empty PLGA NPs) ($p=0.0071$). Furthermore, macrophages exhibited ~3 times higher amount of NO release when exposed to IL-12 pH-responsive NPs compared to empty NPs ($p<0.0001$), and ~2 times more than those associated to free IL-12 and IL-12 loaded non-responsive NPs (IL-12 PLGA NPs) ($p<0.0001$). Additionally, in the human macrophages (Fig. 2D), no significant differences were found between IL-12 pH-responsive NPs and free IL-12. However, despite differences in the sensitivity of macrophages isolated from healthy blood donors, IL-12 pH-responsive NPs were able to induce ~2 times more NO release from macrophages treated with the concentrations of 125, 250 and 500 pg/mL (in terms of IL-12 concentration) compared to empty NPs (Fig. 2 D). The presented results clearly demonstrate that both, macrophages cell line and isolated from healthy blood donors, react to elevated IL-12 levels by acquiring an inflammatory M1-like phenotype, as evident in the NO released from the induced M1 polarized macrophages (Fig. S2). To further confirm the M1 polarization of macrophages and the primary objective of IL-12 to induce IFN-γ secretion, the impact of the developed NPs on the production of IFN-γ from macrophages was evaluated. As presented in Fig. 5, IL-12 pH-responsive NPs effectively triggered substantial levels of IFN-γ in both the RAW264.7 macrophage cell line (Fig. 2E) and human macrophages (Fig. 2F) across all concentrations, compared to the empty NPs.

Notably, at a higher concentration of IL-12 (500 pg/mL), significant differences were observed between IL-12 pH-responsive NPs and IL-12 PLGA NPs, affirming the specificity of the developed system and the immunomodulatory ability of NPs (Fig. 2E). Furthermore, in macrophages isolated from healthy blood donors, IL-12 pH-responsive NPs induced higher IFN-γ levels across all tested concentrations compared to all controls (Fig. 2F). Despite variability introduced by the isolation of macrophages from different blood donors, significant differences, particularly at the higher concentration of 500 pg/mL, were noted between IL-12 pH-responsive NPs and IL-12 PLGA NPs, underscoring the specificity of the developed NPs (Fig. 2F). Additionally, significant differences were evident at all concentrations between IL-12 pH-responsive NPs and free IL-12, suggesting internalization of the IL-12 and reduced cytokine degradation from NPs, thereby enhancing the overall response. In summary, at the elevated concentration of 500 pg/ml, the developed IL-12 pH-responsive NPs were deemed safe for

administration to macrophages. Moreover, they exhibited the capability to enhance NO release and increase IFN-γ levels. Collectively, these findings support their ability to drive macrophage polarization towards an M1-like phenotype.

Refinement and characterization of heterotypic CRC 3D spheroids

To evaluate the impact of the developed NPs in a more intricate 3D structure that mimics the TME, providing a valuable platform for predicting the therapeutic efficacy of novel immunomodulatory treatments, a novel CRC 3D spheroid model was established. The primary objective of this model was to closely replicate the 3D structure of the tumor and the interactions established among three key components of the CRC TME i.e. SW48 CRC cells, human monocytes, and an exogenous ECM constituent, collagen type I (COL-I) [47, 48]. This setup endorsed the assessment of the efficacy and biocompatibility of NPs with anticancer and/or immunomodulatory properties. The CRC 3D spheroids were constructed using microwell array technology by seeding cells into high-throughput 81-well agarose hydrogel micro-molds [30]. The agarose hydrogel prevented cell-surface adhesion, promoting cell-cell interaction and aggregation. This approach resulted in the large-scale production of CRC spheroids with excellent reproducibility in terms of shape and size [30, 31]. The optimization of CRC spheroids involved an initial step with the SW48 cell line in a tumor core monoculture. Subsequently, human monocytes from peripheral blood and COL-I were incrementally added, refining the structure of the CRC spheroids (Fig. 3A).

Establishment and optimization of the CRC monospheroid 3D model

To assemble the SW48 CRC mono-culture 3D spheroids, cells were seeded at three different densities (2500, 5000, and 10,000 cells per spheroid) on agarose micro-molds. Brightfield microscopy revealed the formation of cell aggregates for all cell densities by day 1 (Fig. 3B). Over the subsequent 7 days, the integration of cell-cell interactions in a 3D cellular structure was observed in the higher cell densities, resulting in a more compact and circular structures (Fig. 3E, 3F) [49]. This characteristic was not achieved in the lower cell density. Additionally, for the intermediate cell density (5000 cells/spheroid), the metabolic activity of CRC spheroids remained stable from day 4 to day 7 at approximately 2500 R.F.U with a consistent average size of around 650 μm (Fig. 3C and 3D). Therefore, the observed nearly constant levels of metabolic activity were aligned with the typical steady growth rate of a 3D spheroid structure [30].

Brightfield microscopy also confirmed this size-related feature from day 4 to 7, along with the emergence of irregular protuberances on the spheroid surface (Fig. 3B).

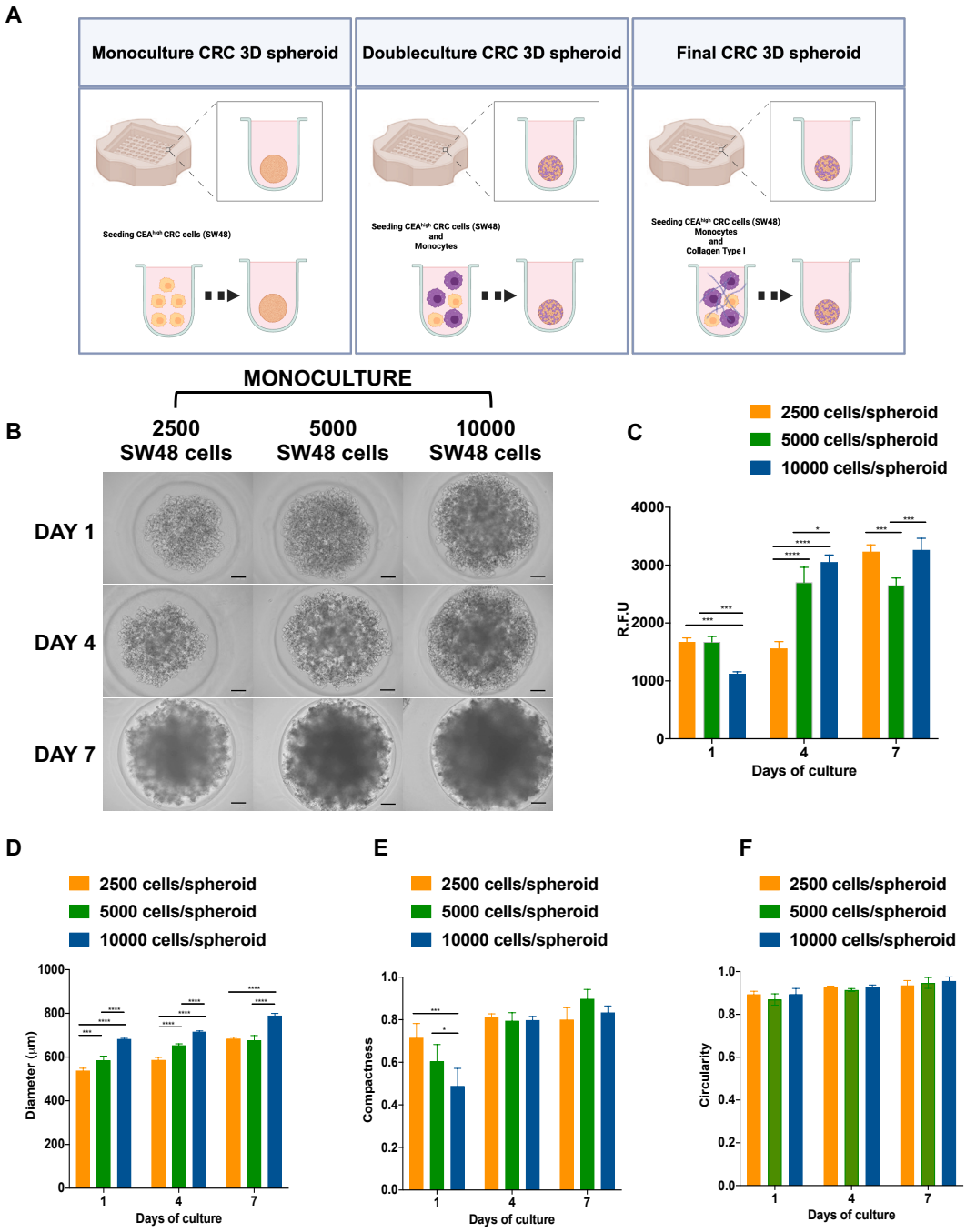


Fig. 3: Establishment and characterization of SW48 monoculture 3D spheroids over a 7-day period. *A) Diagram depicting the proposed final CRC spheroid 3D model containing SW48 CEA+ CRC cells, macrophages differentiated in situ from peripheral blood monocytes, and collagen Type I. Representative illustration of the formation of CRC spheroid 3D models by liquid overlay technique. Generated using BioRender.com. B) Brightfield microscopy images illustrating the progression of 3D spheroids' morphology over time, with three distinct initial cultured cell densities. The scale bar indicates 100 µm. C) Dynamics of the 3D spheroids' metabolic activity; D) Changes in average diameter; E) Progression of compactness and F) Evaluation of circularity over time based on the initial seeding cell density. Values represent mean ±*

standard deviation (n ≥ 3). Statistical comparison performed between each cell concentration and days of culture.

In contrast, the highest cell density exhibited increasing metabolic activity and average size (approximately 600–800 nm) over the culture period, consistent with typical proliferation rates in cellular 2D culture. Considering the aforementioned results for the higher densities and as there were no major differences in spheroid self-assembling and no significant characteristics between the tested initial cell densities, we standardized the density at 5000 cells per spheroid for subsequent studies. Moreover, to create a compact 3D model with guaranteed cell-cell interaction, representing a more advanced tumor stage, seven days of culturing was deemed the optimal condition for all further experiments. Additionally, SW48 was previously noted for lacking α-catenin expression, a factor revealed to be crucial for cell adhesion [50]. Therefore, in order to ensure cell-cell interaction and matrix-dependent cluster formation, 8μg/ml of COL-I, an ECM matrix constituent, was incorporated into the CRC spheroids (Fig. S3) [51] .

Establishment of heterotypic immunospheroid as a screening therapeutic platform

To generate a more intricate representation of the TME, a dual-culture system involving human blood donor isolated peripheral monocytes and SW48 tumor cells was established in three different ratios, namely 75:25, 65:35, and 50:50 (monocytes: tumor cells). To facilitate cell-cell interaction within the spheroids, 8μg/ml COL-I was mixed with the cell components. Spheroids' compactness, circularity, diameter, and metabolic activity were investigated (Fig. 4). On day 1, similar to mono-culture observations through brightfield microscopy, dual-culture 3D spheroids exhibited cell aggregates for all tested ratios, both with and without COL-I (Fig. 4A and B). However, by day 7, an enhancement in cell compactness and the formation of a spherical 3D structure were achieved. For the 3D spheroids with COL-I, in all ratios, the spheroids metabolic activity (R.F.U) increased over time from day 1 to day 7 (Fig. 4C). In the case of the 3D spheroids with COL-I, metabolic activity (R.F.U) increased over time for all ratios from day 1 to day 7 (Fig. 4C). Conversely, spheroids without COL-I showed a stabilization in metabolic activity (R.F.U) (Fig. 4C). This difference may be attributed to the presence of ECM which provides grow factors and sustain cell metabolic activity and due to the interaction and penetration of monocytes and tumor cells through the collagen network in the first case, while excessive

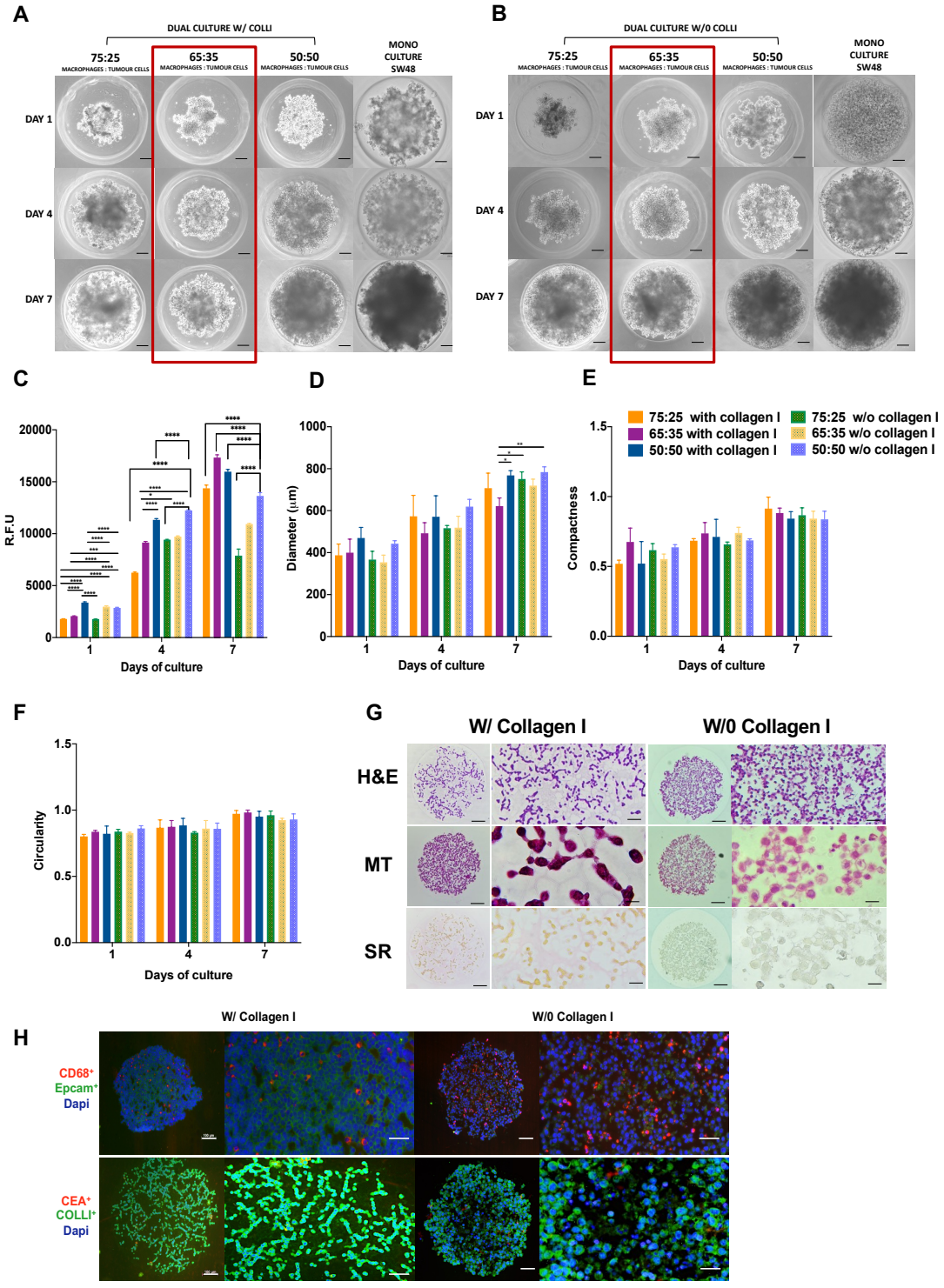


Fig. 4: Temporal evolution and assessment of CRC 3D spheroids in co-culture with human macrophages, at various ratios, in the presence or absence of COL-I. *A and B) Brightfield microscopy depicting morphological changes in CRC 3D spheroids over time with different macrophage-to-tumor cell ratios with or without COL-I, respectively. Scale bar: 100 µm. C) Analysis of the impact of COL-I in CRC 3D spheroids metabolic activity, D) diameter, E) compactness and F) circularity over a 7-day period compared to initial seeding cell density. Values are mean ± standard deviation (n ≥ 3). Statistical comparison performed between each cell concentration w/ or w/o collagen I and days of culture. G) H&E staining at 20× magnification (scale bar: 100 µm) and 40× magnification (scale bar: 50 µm) revealing the structure of the selected final ratio of CRC 3D spheroids on day 7. H) Immunofluorescence microscopy on day 7 displaying cellular organization (SW48-EpCAM in green, macrophages–CD68 in red) and co-localization of SW48-CEA expression (red) and ECM-COL-I [1]. Nuclei were counterstained with DAPI (blue). Scale bars: 100 µm.*

monocytes in the latter case may have been not able to infiltrate and constitute the 3D structure. Moreover, the self-assembled cells without COL-I seemed to not be able to interact to the same extent, compromising their ability to proliferate and possibly causing secretion of factors that impair immune cell viability [52]. Regarding average size, the 3D spheroids expanded in size over time across all ratios (Fig. 4D). However, when comparing 3D spheroids with COL-I to those without, the 65:35 ratio (monocytes: tumor cells) exhibited a smaller size (~500 µm v*ersus* ~650 µm). Additionally, compactness and circularity showed no biologically relevant differences between the different ratios with COL-I, at day 1, 4, and 7 (averaging 0.5-1, Fig. 4E and Fig. 4F). However, spheroids without COL-I displayed slightly lower values of compactness and circularity (averaging 0.5-0.8, Fig. 4E and 4F). Thus, the presence of the ECM component, collagen type I, reinforces cell-cell interaction and promotes a more compacted 3D structure.

Considering the observed results, the ratio of 65:35 (monocytes: tumor cells) with COL-I was chosen as the optimal condition for subsequent studies. To confirm the presence and co-localization of COL-I, histological analyses including H&E, Masson trichrome [33] and Sirius Red (SR) staining, were conducted (Fig. 4). The H&E histological analysis revealed a well-organized structure at day 7, with better compactness of the cells and spherical shape when COL-I was present (Fig. 4G).

Additionally, the absence of COL-I led to a more irregular 3D spheroid exhibiting surface protuberances and lacking ECM support to sustain the structure (Fig.4G). As expected, MT and SR stainings allowed to successfully confirm the presence of collagen fibers as an exogenous ECM counterpart in the final dual-culture model (Fig. 4G). SR is typically described as a technique to distinguish collagen type I, which is usually stained in yellow, orange, or red colors, from collagen type III, which appears in green [53]. Also, as depicted in Fig. 4G, collagen fibers in the 3D spheroid with the addition of COL-I were stained using MT.

Immunofluorescence studies were further performed to investigate the cellular location of SW48 tumor cells ($EPCAM^+$), CEA expression in SW48 cells (CEA^+), macrophages ($CD68^+$), and the ECM component ($COL\text{-}I^+$), as presented in Fig. 4H. The spatial organization of the spheroids demonstrated that macrophages are widely distributed throughout the 3D structure, rather than accumulating solely at the surface, with or without COL-I. Moreover, macrophages were surrounded by SW48 tumor cells, which were associated with CEA expression, in accordance with our previous work [26]. The presence of COL-I was found to be homogeneous throughout the spheroids, contributing to increased compactness of the structure (Fig. 4H). In 3D spheroids without COL-I addition, collagen type I was still identified, albeit in considerably lower amounts,

suggesting minimum endogenous production of this ECM component by the cells of the spheroids. In summary, this 3D spheroids successfully recapitulate part of the immune-tumoral TME of CRC, serving as a promising tool for drug and NP testing.

Effect of NPs on cellular interactions and metabolic activity of 3D CRC spheroids

The developed pH-responsive NPs were designed to provide a controlled release of IL-12 in the CRC TME. Previously, it was demonstrated that the NPs' ability to respond to pH changes and induce INF-y production by macrophages. Usually, cellular effects and interactions are examined in 2D *in vitro* culture, lacking key components of the TME). The absence of the ECM, responsible for creating physical barriers and diffusion gradients in tissues, might impact NPs interactions and potentially compromise their overall effectiveness, influencing the reliability of the results obtained [54]. To validate these findings in a more complex 3D model of CRC, the 3D CRC spheroids were challenged with the NPs, which were assessed in terms of cellular uptake and their potential to induce anti-proliferative effects. In cellular uptake studies, pH responsiveness did not affect cellular uptake of the NPs, with no significant differences found between non-responsive and pH-responsive NPs (Fig. S4). The results obtained are consistent with previously reported findings, affirming minimal cellular uptake of the nanoparticles and thereby confirming the specificity of the nanoparticles to pH responsiveness. Afterwards, the ability of IL-12 pH-responsive NPs to inhibit CRC 3D spheroids cell viability was assessed and compared to free IL-12 and empty/loaded non-responsive NPs after an uninterrupted period of treatment of 24 h with IL-12 doses ranging from to 62.5 pg/ml to 500 pg/mL (Fig. S5). The NPs did not impact the metabolic activity of the CRC 3D spheroids at any tested concentration, consistent with observations in the macrophages 2D assays (Fig. S5). Furthermore, no significant differences were noted between the developed NPs and free IL-12. Overall, as seen previously, the NPs were deemed safe for administration.

Impact of the NPs in the polarization of macrophages

Macrophages play a pivotal role in driving CRC advancement and influencing treatment outcomes by facilitating tumor proliferation, invasion, and migration [55]. These cells exhibit plasticity, allowing them to differentiate to different subsets with unique biological roles. The M1-like subtype induces pro-inflammatory effects, while the M2-like subtype elicits immunosuppressive effects, influencing the progression and treatment of CRC

[56]. In this study, we explored the effects of varying concentrations of IL-12 pH-responsive NPs on CRC 3D spheroids macrophage polarization after a 24-hour treatment. Additionally, the analysis of the CD14+ macrophage population in CRC 3D spheroids was focused on assessing the expression of CD163 (anti-inflammatory M2 markers) and CD86 (a pro-inflammatory M1 marker), as illustrated in Fig. 5.

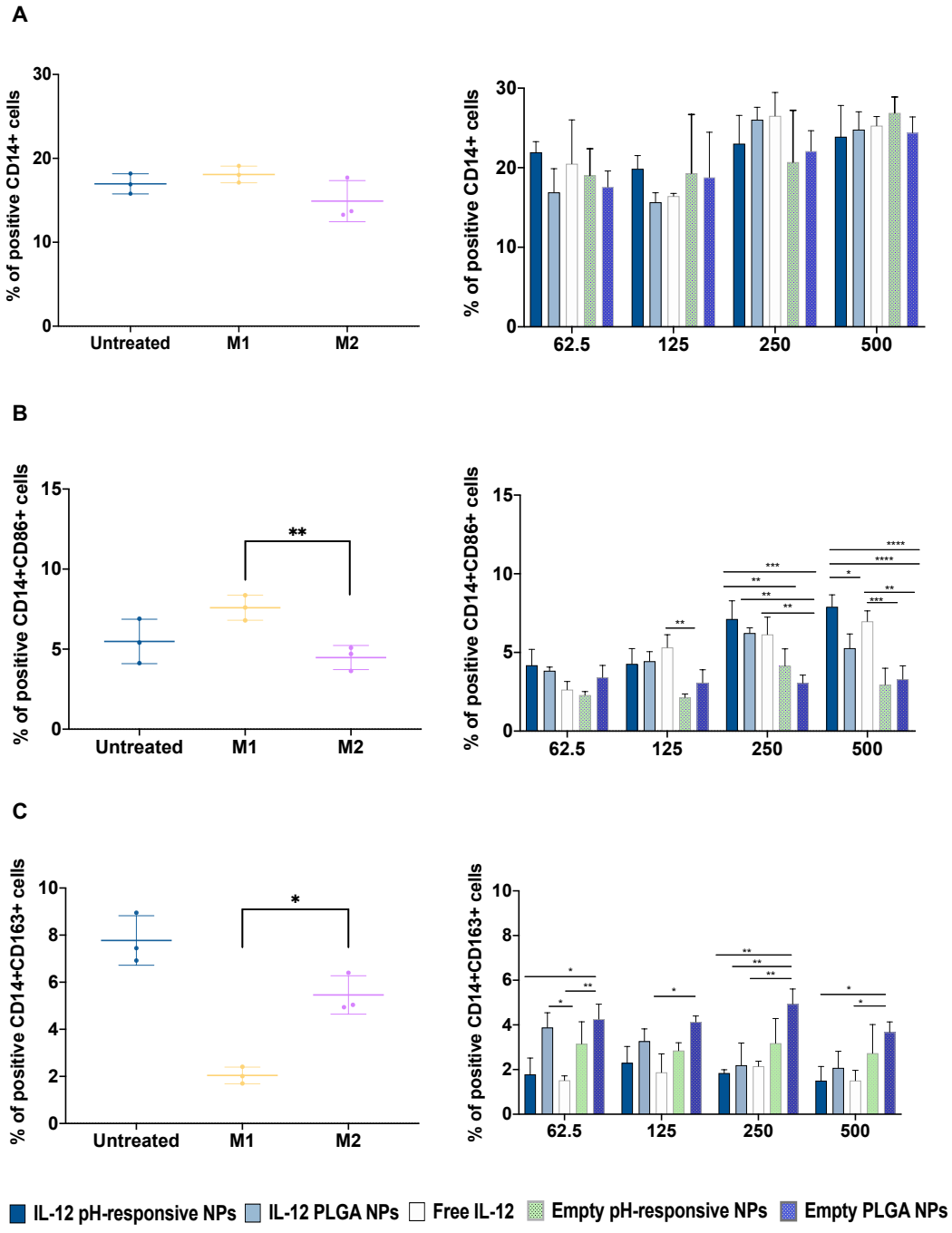


Fig. 5: Evaluation of macrophage polarization profile in the CRC 3D spheroids before and post-treatment analyzing the CD14+ macrophage population. *The analysis included assessing the expression of CD163 (M2-like marker) and CD86 (M-like marker), presented as a percentage of expressing positive cells. The CRC 3D spheroids were incubated with various treatments, such as cell culture medium (untreated), unloaded PLG NPs and pH-responsive NPs, free IL-12, and IL12-loaded PLGA NPs and IL-12*

*pH-responsive NPs for a duration of 24 hours. Statistical comparison between IL-12-loaded pH-responsive NPs and the respective control groups was conducted within each dose range. Significance levels are denoted as *p < 0.05, **p < 0.01, ***p < 0.001 or **** p<0.0001.*

As depicted in Fig. 5A, there were no significant variations in the expression of the CD14+ macrophage population across all experimental groups, maintaining a consistent level of approximately 19.3 ± 0.7%. Despite the notable difference from the initially seeded cell ratios (65% monocytes to 19% macrophages), which can be explained by the non-proliferative nature inherent to macrophages, this final ratio aligns with the in vivo context of CRC, characterized by ~18.21% TAMs [57]. Concerning the polarization of the CD14+ macrophage population, higher concentrations of IL-12-loaded pH-responsive NPs and free IL-12 (250 pg/mL and 500 pg/mL), resulted in increased CD86+ expression levels (pro-inflammatory marker) compared to the IL-12 PLGA NPs and empty NPs controls (Fig. 5B). This observation further confirms the responsiveness of NPs under pH<6.6, as validated through the phenol red pH indicator. Additionally, similar levels of CD86+ expression were observed between the control M1-like stimulated macrophages (LPS and IFN-γ stimulation) and macrophages treated with IL-12 pH-responsive NPs and free IL-12 (7 ± 0.5% *vs* 7.5 ± 0.5% *vs* 6.5 ± 0.6%, respectively; Fig. 5B). However, despite the increased CD86+ levels in 3D spheroids treated with 250 pg/mL or 500 pg/mL of IL-12 pH-responsive NPs versus those treated with equivalent concentrations of free IL-12, no significant differences between them were observed (Fig. 5B). Regarding the polarization of the CD14+ macrophage population towards the M2-like phenotype, a reduction in CD163+ expression levels was observed in the conditions treated with IL-12 pH-responsive NPs and free IL-12 (Fig. 5C). The M2-like macrophage polarization was evaluated in comparison to the control M2-like stimulated macrophages (IL-10 stimulation). In summary, the developed NP strategy clearly demonstrated the specificity in inducing a pro-inflammatory M1-like profile in macrophages, characterized by higher CD86+ and lower CD163+ expression levels. Importantly, the released IL-12 from the pH-sensitive NPs was fully effective similar the free IL-12.

Effect of pH-responsive NPs containing IL-12 on the production of IFN-γ and IL-10

To validate the hypothesis that the developed NPs induce a macrophagic M1-like phenotype, cytokines such as IFN-γ, recognized as an inducing factor for the M1-like phenotype, were assessed (Fig. 6A and 6B). Whereas, to confirm the pro-inflammatory polarization of macrophages in CRC 3D spheroids, the evaluation of anti-inflammatory cytokines such as IL-10 was conducted, as its secretion is associated with M2-like

macrophages and tends to decrease during the opposite M1-like polarization (Fig. 6C and 6D) [55]. Hence, the intrinsic ability of CRC 3D spheroids to independently secrete signaling mediators was confirmed through untreated controls of M1 or M2-like stimulated macrophages (6B and 6D). Changes in the secretion levels of IFN-γ and IL-10 were analyzed after a 24-hour treatment of 3D CRC spheroids with unloaded pH-responsive NPs, PLGA NPs, free IL-12, IL-12-loaded PLGA NPs, and IL-12-loaded pH-responsive NPs. As depicted in Fig. 6A, in all tested concentrations, IL-12 pH-responsive NPs were able to induce INF-y production by macrophages, with significant differences when comparing IL-12 pH-responsive NPs and the remaining controls. Moreover, although there are no statistically significant difference observed in the levels of IFN-γ secreted between conditions treated with IL-12 pH-responsive NPs and free IL-12, the conditions treated with IL-12 pH-responsive NPs exhibited higher cytokine levels (Fig. 6A). The pH as confirmed by the phenol red indicator, as previously mentioned. Furthermore, the pro-inflammatory potential of the strategy was evaluated by assessing the reduction in secreted anti-inflammatory cytokines from the 3D spheroids, as shown in Fig. 6C. While statistical significance was found between conditions treated with IL-12 pH-responsive NPs and the other controls, lower levels of IL-10 were achieved, particularly in the higher treatment concentrations (250 pg/ml and 500 pg/ml). Significant differences were observed when comparing IL-12 pH-responsive NPs with IL-12 PLGA NPs and the empty controls, Fig.6C. In summary, the developed IL-12 pH-responsive NPs successfully induced IFN-γ production, suggestive of the polarization of macrophages towards an M1-like phenotype. This hypothesis is supported by the lower levels of IL-10 secreted by CRC 3D spheroids after treatment. Altogether, these results provide evidence that the developed IL-12 loaded pH-responsive NPs enhance, under low pH conditions similar to those at the TME, the release of IL-12. The burst of this cytokine is, on its turn, able to drive macrophages into a more pro-inflammatory phenotype, enhancing the expression of CD86 and the secretion of IFN-γ, while reducing the expression of CD163 and the secretion of IL-10.

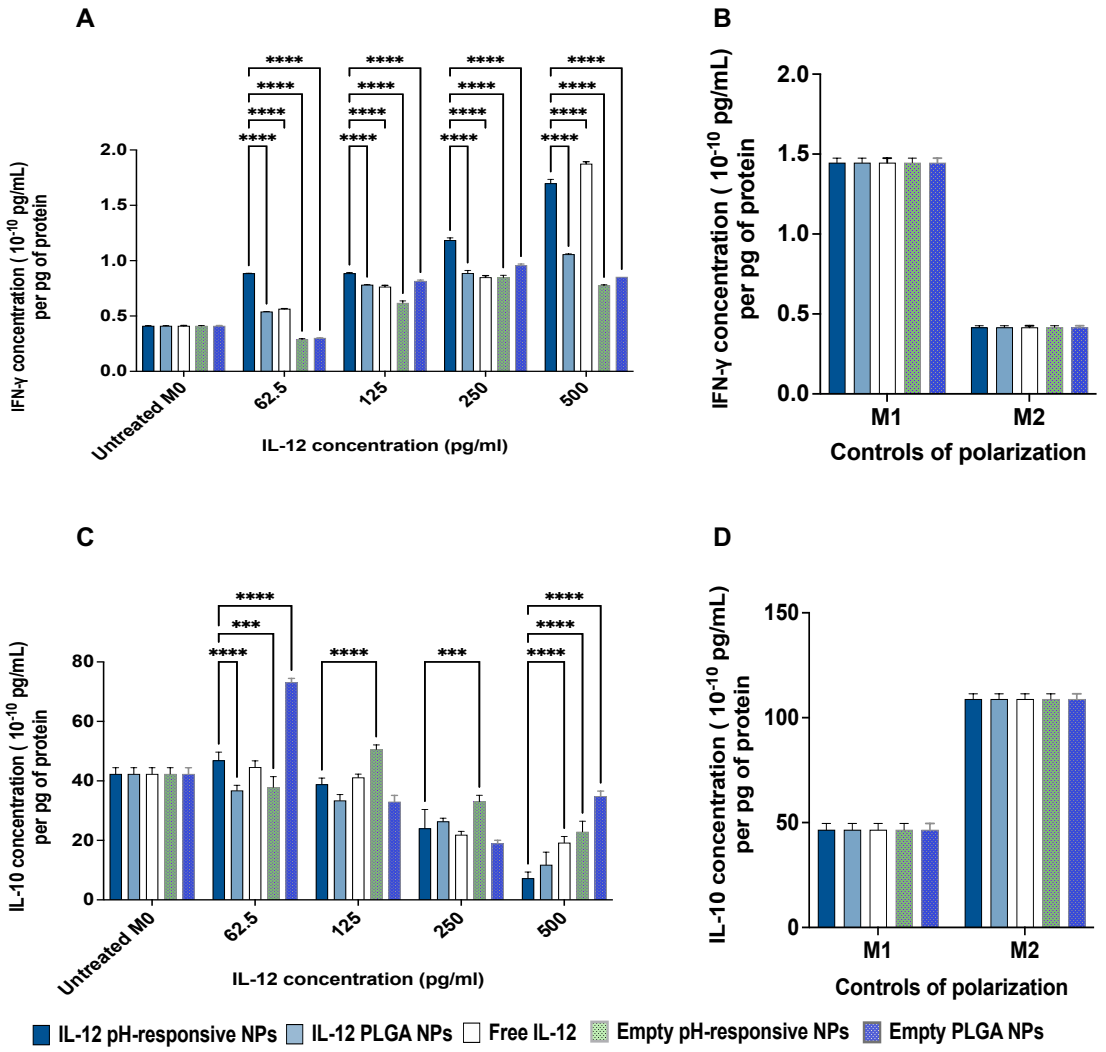


Fig. 6: Evaluation of the potential of the developed strategy to induce pro-inflammatory and anti-inflammatory cytokine production *in a CRC 3D spheroid after a 24-hour treatment, untreated conditions, unloaded pH-responsive NPs and PLGA NPs, free IL-12, IL-12-loaded PLGA NPs, and IL-12 pH-responsive NPs. A) Assessment of the potential of the developed NPs to induce IFN-γ production. B) Assessment of the IFN-γ production in the controls of M1 or M2-like stimulated macrophages. C) Analysis of the secretion of the anti-inflammatory cytokine IL-10 induced by the treatments. D) Assessment of the IL-10 production in the controls of M1 or M2-like stimulated macrophages Statistical comparisons were performed between the different testing groups, denoted as *p < 0.05, **p < 0.01, ***p < 0.001, or p < 0.0001.*

Conclusions

In this study, we have successfully developed novel pH-responsive NPs encapsulating IL-12 and demonstrate their functionality in 2D and complex 3D models mimicking the TME features. The manufacturing strategy for these pH-responsive NPs involved the surface functionalization of the PLGA polymer with a pH-responsive monomer, namely DMMA, whose hydrolysis under weakly acidic pH exposes positively charged amino groups. IL-12 was effectively encapsulated into these pH-responsive NPs, and its release confirmed under slightly acidic pH conditions, similar to those at the TME. Moreover, IL-12-loaded pH-responsive NPs were found to stimulate IFN-γ secretion in 2D mouse macrophage cell lines and human macrophages isolated from healthy blood donors and increase NO release levels by 2-3-fold. These data suggested that IL-12-loaded pH-responsive NPs trigger the stimulus for M1-like macrophages polarization. Furthermore, a novel CRC 3D spheroid model was developed, composed by SW48 cancer cells, macrophages differentiated *in situ* from peripheral blood monocytes, and an exogenous ECM-like non-cellular constituent, COL-I. The CRC 3D spheroids demonstrated the ability to mimic cellular and structural features of the tumor, such as cell spatial organization, the presence of ECM, and a pro-tumor and anti-inflammatory M2-like macrophage phenotype. The effect of the IL-12-loaded pH-responsive NPs was then investigated in this 3D model, evidencing that NPs reduced the expression of anti-inflammatory macrophage markers while increasing the levels of pro-inflammatory macrophage markers. These data confirm their ability to reeducate the tumor immune microenvironment within the CRC 3D spheroids. Accordingly, IL-12-loaded pH-responsive NPs caused a reduction in the secretion of a key anti-inflammatory cytokine, IL-10, and an increase of the IFN-γ pro-inflammatory cytokine. Overall, the IL-12 pH-responsive NPs presented responsiveness to the slightly acidic pH of the CRC TME (~6-5), were deemed safe for macrophage administration and capable of inducing IFN-γ production. Moreover, the established CRC 3D spheroid contributed to better recapitulate the biological architecture and composition of the native tumor, making it a promising *in vitro* technology for the testing of newly developed (nano-)drugs and improve the *in vivo* predictability.

Supporting Information

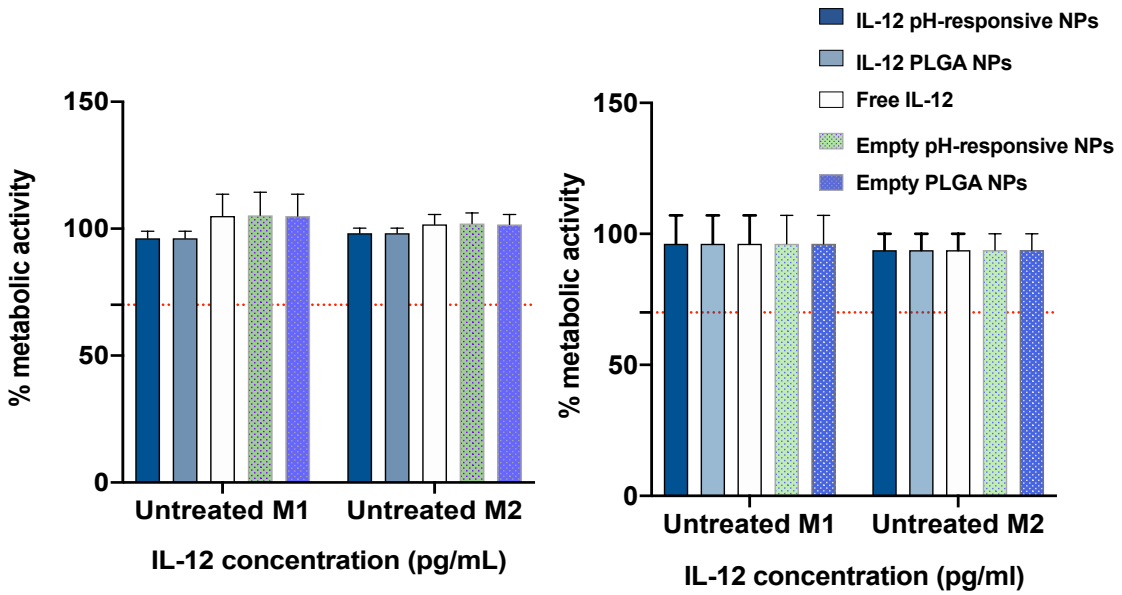


Figure S1: Effect of stimuli employed in the polarization of macrophages towards M1 or M2-like phenotypes on the metabolic activity.

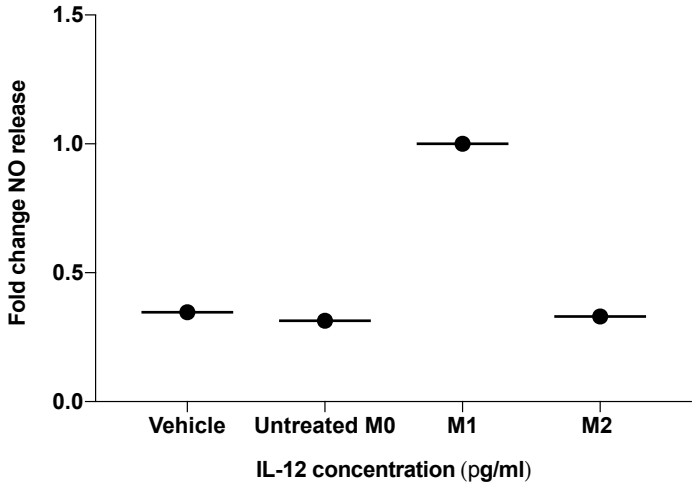
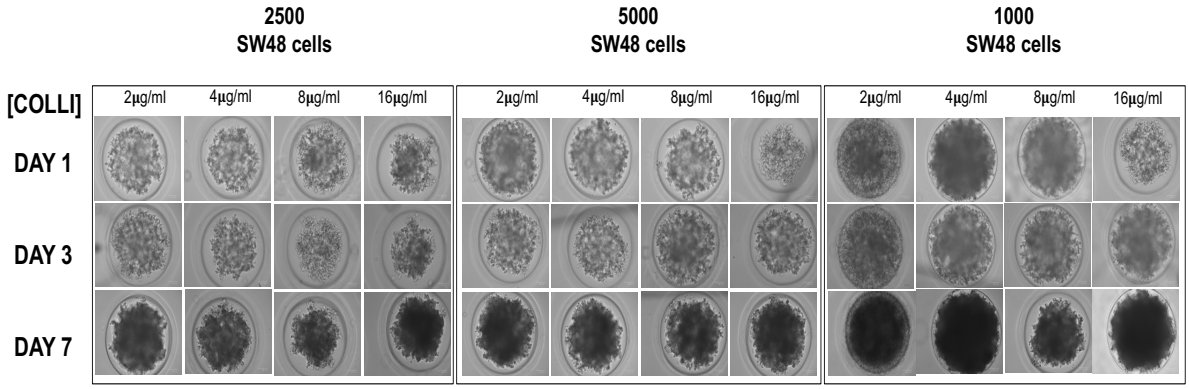


Figure S2: Controls for evaluating the fold change in nitric oxide (NO) release in M1 or M2-like macrophage



polarization.

Figure S3: Evaluation of the optimal concentration of collagen I within three different cell ratios in monocultures CRC 3D spheroids. Diameter size assessment was conducted over the course of 7 days of culture.

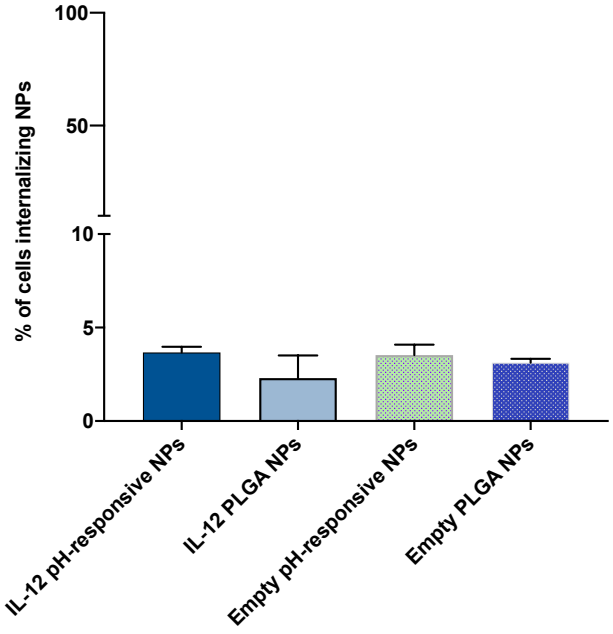


Figure S4: Flow cytometry analysis of the percentage of cells internalization IL-12 pH-responsive NPs and the respective controls into CRC 3D spheroids.

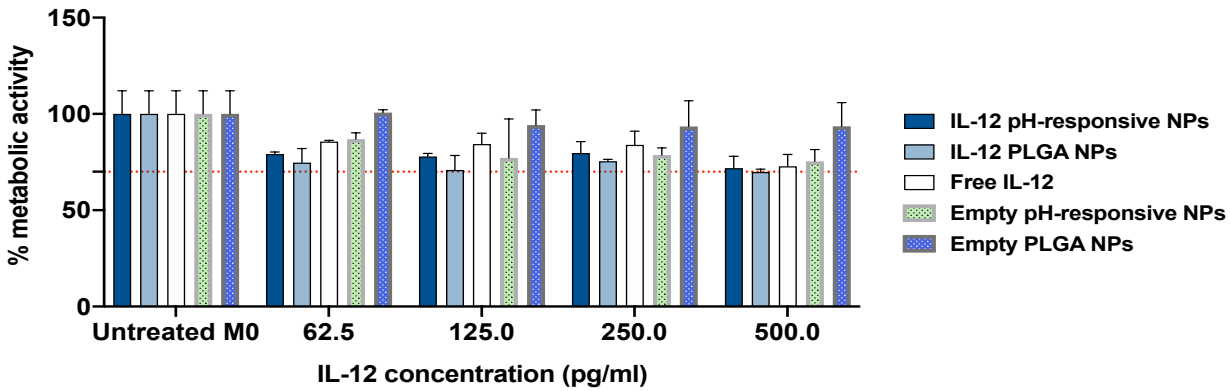


Figure S5: Evaluation of the impact of IL-12 pH-responsive NPs, Free IL-12, and the corresponding controls of NP formulations on the proliferation of CRC 3D spheroids.

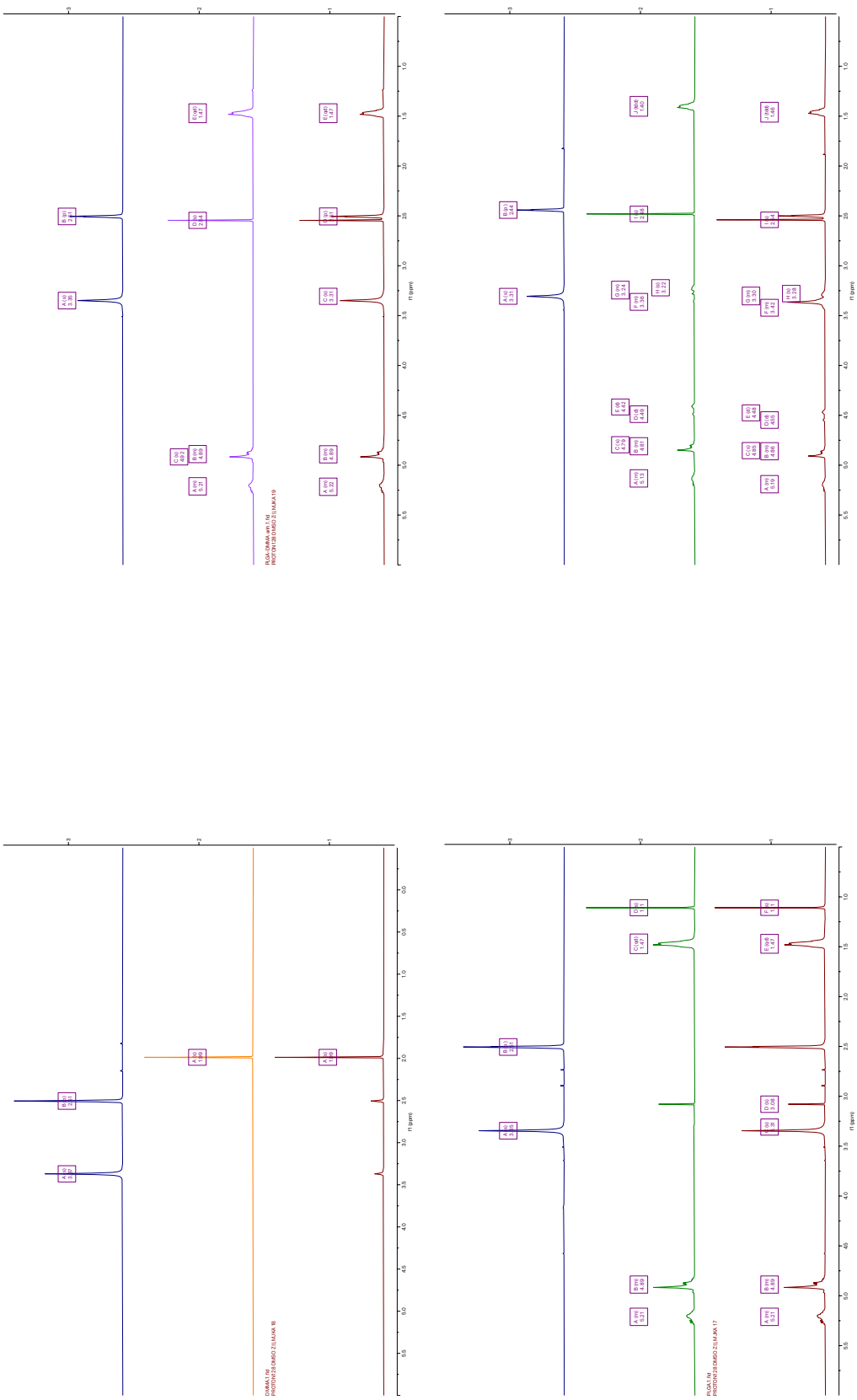


Figure S6: Complete NMR spectra of DMMA, PLGA-NH2 an PLGA-DMMA.

References

1. Begent, R.H.J., et al., *Clinical evidence of efficient tumor targetting based on single–chain Fv antibody selected from a combinatorial library.* Nat Med, 1996. **2**(9): p. 979-984.
2. Cervantes, A., et al., *Metastatic colorectal cancer: ESMO Clinical Practice Guideline for diagnosis, treatment and follow-up☆.* Ann Oncol, 2023. **34**(1): p. 10-32.
3. Chandra, R., et al., *The colorectal cancer tumor microenvironment and its impact on liver and lung metastasis.* Cancers, 2021. **13**(24).
4. Ciardiello, F., et al., *Clinical management of metastatic colorectal cancer in the era of precision medicine.* CA Cancer J Clin, 2022. **72**(4): p. 372-401.
5. Shin, A.E., F.G. Giancotti, and A.K. Rustgi, *Metastatic colorectal cancer: mechanisms and emerging therapeutics.* Trends Pharmacol Sci, 2023. **44**(4): p. 222-236.
6. Zhang, H., et al., *Roles of tumor-associated macrophages in anti-PD-1/PD-L1 immunotherapy for solid cancers.* Mol Cancer, 2023. **22**(1): p. 58.
7. Gallo, G., et al., *Therapeutic Targets and Tumor Microenvironment in Colorectal Cancer.* J Clin Med, 2021. **10**(11).
8. Lin, Y., J. Xu, and H. Lan, *Tumor-associated macrophages in tumor metastasis: biological roles and clinical therapeutic applications.* J Hematol. Oncol, 2019. **12**(1): p. 76.
9. Mager, L.F., et al., *Cytokine-induced modulation of colorectal cancer.* Front Oncol, 2016. **6**: p. 96.
10. Jia, Z., et al., *IL12 immune therapy clinical trial review: Novel strategies for avoiding CRS-associated cytokines.* Front Immunol, 2022. **13**: p. 952231.
11. Habiba, U.e., et al., *The multifaceted role of IL-12 in cancer.* Adv Cancer Biol, 2022. **5**: p. 100053.
12. Cirella, A., et al., *Novel strategies exploiting interleukin-12 in cancer immunotherapy.* Pharmacol Ther, 2022. **239**: p. 108189.
13. Kerneur, C., C.E. Cano, and D. Olive, *Major pathways involved in macrophage polarization in cancer.* Front Immunol, 2022. **13**: p. 1026954.
14. Dutta, P. and B. Bishayi, *IL-10 in combination with IL-12 and TNF-α attenuates CXCL8/CXCR1 axis in peritoneal macrophages of mice infected with*

Staphylococcus aureus through the TNFR1-IL-1R-NF-κB pathway. Int Immunopharmacol, 2023. **120**: p. 110297.

15. Grohmann, U., et al., *Positive Regulatory Role of IL-12 in macrophages and modulation by IFN-γ1.* J Immunol, 2001. **167**(1): p. 221-227.
16. Zeng, L., et al., *Poly(lactic-co-glycolic acid) nanoparticle-mediated interleukin-12 delivery for the treatment of diabetic retinopathy.* Int J Nanomedicine, 2019. **14**: p. 6357-6369.
17. Mendes, B.B., et al., *Nanomedicine-based strategies to target and modulate the tumor microenvironment.* Trends Cancer, 2021. **7**(9): p. 847-862.
18. Li, S., et al., *Tumor microenvironment-oriented adaptive nanodrugs based on peptide self-assembly.* Chem Sci, 2020. **11**(33): p. 8644-8656.
19. He, Q., et al., *Tumor microenvironment responsive drug delivery systems.* Asian J Pharm Sci, 2020. **15**(4): p. 416-448.
20. Hu, Y., et al., *Activated charge-reversal polymeric nano-system: The promising strategy in drug delivery for cancer therapy.* Polymers, 2016. **8**(4): p. 99.
21. Hines, D.J. and D.L. Kaplan, *Poly(lactic-co-glycolic) acid-controlled-release systems: experimental and modeling insights.* Crit Rev Ther Drug Carrier Syst, 2013. **30**(3): p. 257-76.
22. Wang, W., et al., *pH-Sensitive and charge-reversal polymeric nanoplatform enhanced photothermal/photodynamic synergistic therapy for breast cancer.* Front bioeng biotechnol, 2022. **10**.
23. Kumar, D., B.A. Eipper, and R.E. Mains, *Amidation☆*, in *Reference Module in Biomed Sci*. 2014, Elsevier.
24. Li, S., et al., *Dual pH-responsive micelles with both charge-conversional property and hydrophobic–hydrophilic transition for effective cellular uptake and intracellular drug release.* Polymer Chem, 2016. **7**(12): p. 2202-2208.
25. Wu, W., et al., *Tumor-acidity activated surface charge-conversion of polymeric nanocarriers for enhanced cell adhesion and targeted drug release.* Macromol Rapid Commun, 2014. **35**(19): p. 1679-1684.
26. Silveira, M.J., et al., *scFv biofunctionalized nanoparticles to effective and safe targeting of CEA-expressing colorectal cancer cells.* J Nanobiotechnol, 2023. **21**(1): p. 357.
27. Gonzalez-Exposito, R., et al., *CEA expression heterogeneity and plasticity confer resistance to the CEA-targeting bispecific immunotherapy antibody cibisatamab (CEA-TCB) in patient-derived colorectal cancer organoids.* J Immunother Cancer, 2019. **7**(1): p. 101.

28. Cardoso, A.P., et al., *Macrophages stimulate gastric and colorectal cancer invasion through EGFR Y(1086), c-Src, Erk1/2 and Akt phosphorylation and smallGTPase activity.* Oncogene, 2014. **33**(16): p. 2123-33.
29. A, *ISO 10993-5: 2009 Biological evaluation of medical devices-part 5: Tests for in Vitro Cytotoxicity; ISO: Phoenix, USA 2009*. 2007.
30. Bauleth-Ramos, T., et al., *Colorectal cancer triple co-culture spheroid model to assess the biocompatibility and anticancer properties of polymeric nanoparticles.* J Control Release, 2020. **323**: p. 398-411.
31. Martins, C., et al., *Glioblastoma immuno-endothelial multicellular microtissue as a 3D in vitro evaluation tool of anti-cancer nano-therapeutics.* J Control Release, 2023. **353**: p. 77-95.
32. Piccinini, F., *AnaSP: a software suite for automatic image analysis of multicellular spheroids.* Comput Methods Programs Biomed, 2015. **119**(1): p. 43-52.
33. Kosmidis, C., et al., *Interferon-γ and Colorectal Cancer: an up-to date.* J Cancer, 2018. **9**(2): p. 232-238.
34. Nguyen, K.G., et al., *Localized Interleukin-12 for Cancer Immunotherapy.* Front Immunol, 2020. **11**.
35. Sas, Z., et al., *Tumor microenvironment of hepatocellular carcinoma: Challenges and opportunities for new treatment options.* Int J Mol Sci, 2022. **23**(7).
36. Chu, S., et al., *pH-Responsive polymer nanomaterials for tumor therapy.* Front Oncol, 2022. **12**: p. 855019.
37. Da Silva, H.C. and W.B. De Almeida, *Theoretical calculations of 1H NMR chemical shifts for nitrogenated compounds in chloroform solution.* Chem Physics, 2020. **528**: p. 110479.
38. Li, J., et al., *Dual-target IL-12-containing nanoparticles enhance T cell functions for cancer immunotherapy.* Cell Immunol, 2020. **349**: p. 104042.
39. Chen, P., et al., *An IL-12-based nanocytokine safely potentiates anticancer immunity through spatiotemporal control of inflammation to eradicate advanced cold tumors.* Adv Sci, 2023. **10**(10): p. 2205139.
40. Yoon, C., et al., *Charged residues dominate a unique interlocking topography in the heterodimeric cytokine interleukin-12.* Embo j, 2000. **19**(14): p. 3530-41.
41. Zhang, P., et al., *Charge reversal nano-systems for tumor therapy.* J Nanobiotechnol, 2022. **20**(1): p. 31.
42. Zhang, X., et al., *Dual pH-responsive "charge-reversal like" gold nanoparticles to enhance tumor retention for chemo-radiotherapy.* Nano Research, 2019. **12**(11): p. 2815-2826.

43. Li, Z., et al., *Charge-reversal nanomedicines as a smart bullet for deep tumor penetration.* Smart Mater Med, 2022. **3**: p. 243-253.
44. Xing, Z., A. Zganiacz, and M. Santosuosso, *Role of IL-12 in macrophage activation during intracellular infection: IL-12 and mycobacteria synergistically release TNF-alpha and nitric oxide from macrophages via IFN-gamma induction.* J Leukoc Biol, 2000. **68**(6): p. 897-902.
45. Puddu, P., et al., *IL-12 induces IFN-gamma expression and secretion in mouse peritoneal macrophages.* J Immunol, 1997. **159**(7): p. 3490-7.
46. Xie, C., et al., *Effects of IRF1 and IFN-β interaction on the M1 polarization of macrophages and its antitumor function.* Int J Mol Med, 2016. **38**(1): p. 148-60.
47. Wei, R., et al., *Cellular and extracellular components in tumor microenvironment and their application in early diagnosis of cancers.* Anal Cell Pathol, 2020: p. 6283796.
48. Li, J., D. Chen, and M. Shen, *Tumor microenvironment shapes colorectal cancer progression, metastasis, and treatment responses.* Front Med, 2022. **9**.
49. Kanton, S. and S.P. Paşca, *Human assembloids.* Development, 2022. **149**(20).
50. Ilyas, M., et al., *β-Catenin mutations in cell lines established from human colorectal cancers.* Proc Natl Acad Sci, 1997. **94**(19): p. 10330-10334.
51. Förster, S., et al., *Differential effects of α-catenin on the invasion and radiochemosensitivity of human colorectal cancer cells.* Int J Oncol, 2018. **52**(4): p. 1117-1128.
52. Murphy, R.J., et al., *Mechanical cell competition in heterogeneous epithelial tissues.* Bull Math Biol, 2020. **82**(10): p. 130.
53. Junqueira, L.C.U., W. Cossermelli, and R. Brentani, *Differential staining of collagens type I, II and III by sirius red and polarization microscopy.* Arch Histol Jpn, 1978. **41**(3): p. 267-274.
54. Munir, M.U., *Nanomedicine penetration to tumor: Challenges, and advanced strategies to tackle this issue.* Cancers, 2022. **14**(12).
55. Wang, H., T. Tian, and J. Zhang, *Tumor-associated macrophages (TAMs) in colorectal cancer (CRC): From mechanism to therapy and prognosis.* Int J Mol Sci, 2021. **22**(16).
56. Lu, L., et al., *Macrophages play a role in inflammatory transformation of colorectal cancer.* World J Gastrointest Oncol, 2021. **13**(12): p. 2013-2028.
57. Li, C., et al., *A Higher Frequency of CD14+ CD169+ Monocytes/Macrophages in Patients with Colorectal Cancer.* PLoS One, 2015. **10**(10): p. e0141817.

CHAPTER V – COMBINATORY STRATEGY TO IMPROVE COLORECTAL CANCER THERAPY

This chapter was based on the following publication:

- **MJ Silveira**; MJ Oliveira; B Sarmento. " Enhancing CRC Therapy: Combinatorial Strategy Targeting CEA-Expressing Cells and Eliciting Anti-Tumoral Markers and Cytokines (Manuscript in preparation).

Abstract

The alarming 5-year survival rate of only 14% for metastatic colorectal cancer (mCRC) underscores the urgent need for more effective treatments. Although immunotherapy agents have gained approval for CRC treatment in recent years, their efficacy is limited to benefit a small fraction of CRC patients with MSI-H/dMMR tumors. Consequently, there has been growing interest in investigating combinatorial strategies to improve the prognosis of the disease and overcome the limitations of monotherapies. In this study, we developed a novel combinatorial strategy using NPs designed to target not only CRC cells expressing CEA but also the surrounding immunosuppressive tumor microenvironment (TME). To validate the specificity of the NPs, we generated MSI CRC 3D spheroids that mimic the spatial organization and extracellular matrix of tumors. The combinatorial approach exhibited increased toxicity against CEA^{high} CRC 3D spheroids, leading to antitumoral inflammation by elevating IFN-γ levels and decreasing IL-10, a pro-tumoral cytokine. Moreover, our investigation revealed that IL-12 pH-responsive NPs interacted with CRC 3D spheroids, demonstrating pH-responsiveness with minimal impact on metabolic activity. Conversely, CEA targeted-NPs loaded with 5-FU showed specificity in targeting CEA-expressing tumors, significantly affecting their metabolic activity. Furthermore, the combinatorial strategy induced macrophage polarization, reducing M2-like markers while increasing pro-inflammatory M1-like counterparts. Additionally, the strategy elevated IFN-γ levels and reduced IL-10 secretion. Overall, this study highlights the potential of combinatorial strategies to precisely target desired cells while eliciting an anti-tumoral and pro-inflammatory immune response for macrophages' cancer cell recognition and elimination, paving the way for further explorations in other solid cancers.

Keywords: combinatorial treatment; Nanomedicine; MSI 3D spheroid; chemotherapy, Immunomodulation.

Background

Colorectal cancer (CRC) presents a significant global public health challenge due to its widespread occurrence, impact, and high mortality rates [1]. Moreover, the metastatic CRC (mCRC), exhibits a median 5-year overall survival rate of only 14%, highlighting the urgent need of more effective therapeutic options [2].

The tumor microenvironment (TME), composed by tumor cells, stromal cells, fibroblasts, endothelial cells, immune cells, and non-cellular components of the extracellular matrix (ECM), has been identifying as a pivotal factor, to impact therapeutic outcomes in CRC [3]. One of the most important component of the TME are tumor-associated macrophages (TAMs), typically categorized into a spectrum of phenotypes ranging from M1-like macrophages (pro-inflammatory), which exert tumor-suppressive effects, to M2-like macrophages (anti-inflammatory), which foster cancer progression [4].

The carcinoembryonic antigen (CEA) tumor-associated antigen is a membrane-anchored glycoprotein, overexpressed in 90–95% of both primary colorectal tumors and their respective metastases [5]. Moreover, CEA is commonly used for the diagnosis and prognosis of CRC, constituting a promising targeting molecule for therapeutic approaches in CRC therapy [6].

The fluoropyrimidine, 5-fluorouracil (5-FU), an antimetabolite with anticancer effects, remains a mainstream option of chemotherapy for managing high-risk stage II, III and IV CRC patients, being frequently administrated as single-agent therapy, and as part of multiple-agent regimens [7]. Additionally, cytokines such interleukin 12 (IL-12) has been recognized as a crucial element in immune responses, contributing to the polarization of macrophages towards M1-like phenotypes by IFN-γ induction, thereby fostering an inflammatory microenvironment and playing a central role in tumor immunotherapy [14].

CRC treatment is classically guided by their classification or stratification [8]. Consequently, tumors exhibiting a hypermutant phenotype, known as microsatellite instability high (MSI-H) status, are associated with the inactivation of mismatch repair (MMR) genes, resulting in MMR deficiency (dMMR) [9]. The aforementioned deficiency results in widespread mutations across the genome and subsequent release of numerous mutation-associated neoantigens, which bolster the immune response and contributes for the high responsiveness to the immunotherapeutic agents [10]. Therefore, currently, all immunotherapy agents approved for CRC treatment are limited to MSI-H/dMMR mCRC [8]. However, combined strategies are being employed to improve overall survival of patients combining the immunotherapeutics, ipilimumab and nivolumab, after treatment with fluoropyrimidine, oxaliplatin, and irinotecan treatment [11]. Furthermore, pembrolizumab

and nivolumab, either individually or in conjunction with CTLA-4 inhibitors like ipilimumab, have garnered approval from the US FDA for clinical application in managing mCRC with dMMR/MSI-H [12].

Numerous clinical trials have been exploring the combination of chemotherapy and immunotherapy such NCT04008030 where the effectiveness of three treatment protocols: nivolumab monotherapy, combined nivolumab and ipilimumab therapy, and chemotherapy are being assessed [13]. Therefore, the number of treatment options for mCRC patients has been growing, especially, with combination therapy showing promise in enhancing the prognosis of the disease and overcome the insufficient efficacy or resistance by monotherapy [14].

Despite efforts to design co-administration of two or more drugs to achieve greater therapeutic effect than the individual drug treatments, the administration of small drugs such 5-FU or biological molecules like cytokines presents certain drawbacks, including low bioavailability, toxicity, and off-target effects resulting in diminished therapeutic potential [15]. Therefore, nanoparticle-mediated drug delivery systems hold significant promise in combinatorial therapy, offering enhanced drug solubility, reduced systemic toxicity, prolonged circulation times in the bloodstream, controllable release profiles, and potential to target specific cells while avoiding rapid drug clearance [16]. Particularly, for CRC several authors are demonstrating nanoparticles (NPS) as tools with the ability to enhance the efficacy of traditional chemotherapies and the development of immunomodulatory therapeutic strategies [8, 17].

Previous efforts, performed by our group in the development of targeted strategies for 5-FU delivery specifically to CEA-expressing CRC cells (5-FU-CEA-NPs) and IL-12 for its tumor microenvironment (IL-12 pH-responsive NPs) had presented better pharmacological performances and potential to improve M1-like polarization of macrophages [18]. Therefore, in this work we propose to evaluate the potential of developed targeted polymeric nano strategies as a combinatory strategy using an *in vitro* 3D spheroid model able to recapitulate the *in vivo* complexity and predict the therapeutic response in a clinical setting. Therefore, a 3D CRC spheroid model was established detaining tumor heterogeneous cell populations, extracellular matrix (ECM), and dynamic cell-cell and cell-ECM interactions. Moreover, two 3D CRC spheroids representatives of CEA-expressing (CEA ^{high}) and non-expressing (CEA ^{low}) models were developed incorporating the CRC cell line CEA ^{high}, SW48, or CEA ^{low}, HCT-15, blood donor monocyte-derived macrophages and exogenous collagen type I ECM. This setup allowed us to assess the impact of the combinatory strategy of NPs on the spheroids' metabolic activity, cellular uptake, macrophage polarization, and production of nitric oxide (NO), IFN-γ, and IL-10.

Methods

PLGA 5004 (50:50 LA:GA; 44 K; Purasorb® PDLG 5004A) was generously provided by Corbion-Purac biomaterials. PLGA-NH2 (LA:GA- 50:50; 30K) was procured from RuixiBiotech®, while PLGA-FKR648 was sourced from Akina (USA). Reagents such as 2,3-Dimethylmaleic anhydride (DMMA), resazurin, Polyvinyl alcohol (PVA), dichloromethane (DCM), paraformaldehyde (PVA), Sulfanilamide, dimethyl sulfoxide (DMSO), Phosphoric acid, N-naphthylethylenediamine, neutral buffered formalin, trypsin, xylene, Histopaque-1077, a graded alcohol series, hematoxylin and eosin staining solution, Tris, EDTA, Tween 80 and sodium citrate were obtained from Sigma-Aldrich (USA). RPMI 1640 and high glucose Dulbecco's Modified Eagle (DMEM) GlutaMAX medium were purchased from Alfagene, Lda. SeaKem® LE agarose was acquired from Lonza (Switzerland). Accutase® and BCA Protein Assay Kit were obtained from Thermo Fisher Scientific (USA), while Triton X-100 was sourced from Spi-Chem (USA). The RosetteSep-Human Monocyte Enrichment Cocktail was procured from StemCell Technologies, human IL-12, interferon-γ (IFN-γ), IL-4, and bacterial lipopolysaccharide (LPS) were acquired from PeproTech, M-CSF, IL-10 from ImmunoTools (Germany), and Collagen type I (COL-I) from Corning (UK). Alexa Fluor 488-anti rabbit, and Alexa Fluor 594-anti mouse antibodies were sourced from Invitrogen (Belgium). Ultrapure water was prepared in-house with a conductivity of 0.055 µS/cm and a resistivity of 18.2 MΩ.cm, using MilliQ® station from Millipore Corporation. For cell cultures, T flasks were acquired from Orange Scientific. Fetal bovine serum and penicillin-streptomycin were acquired from Gibco (USA). IFN-γ and IL-12 ELISA Kit were obtained from BioLegend, while IL-10 ELISA KIT was purchased from PeproTech. The total protein content analysis kit (Dc Protein kit, USA) was acquired from Bio-Rad. Antibodies, including anti-CD14/APC and anti-CD86/FITC were obtained from ImmunoTools. The anti-CD206/PE was purchased from BioLegend. Anti-CD163/PE was acquired from BD Biosciences. The anti-HLA-DR/ PB and anti-EPCAM/PB, Live/Dead Fixable Viability Dye eFluor™ 780 and 4′,6-diamidino-2-phenylindole (DAPI) were obtained from Thermo Fisher Scientific®. The antibody, anti-collagen type I (Anti-COL-I) rabbit, was acquired from Rockland Immunochemicals. Dialysis membranes of 10k, 100K, N-2-hydroxyethylpiperazine-N-2-ethane sulfonic acid (HEPES), and DMSO-d6 were acquired from Merck (USA). Human colon cells SW-48 and HCT-15 cell lines were purchased from American Type Culture Collection (Rockville, MD).

Cell lines and culture supplies

The SW48 CRC epithelial cell line was cultured in DMEM supplemented with 10% v/v FBS and 1% v/v penicillin-streptomycin. Furthermore, HCT-15 CRC epithelial cell line was cultured in RPMI1640 medium supplemented with 10% v/v FBS and 1% v/v penicillin-streptomycin. Cell culture mediums was refreshed every 2–3 days, and trypsin treatment was utilized for subculturing the cell lines. Cells were maintained in a Cell Culture CO2 incubator at 37°C with 5% CO2 and 95% relative humidity. Regular mycoplasma testing was performed.

Ethical Considerations

Following the principles outlined in the Declaration of Helsinki and with ethical clearance obtained from the Ethics Committee of Centro Hospitalar Universitário São João (protocol reference 90/19), blood donors were informed and consented in writing for the use of their blood samples for research. Monocytes were isolated from excess buffy coats provided by the Immunohemotherapy Department of Centro Hospitalar Universitário São João (CHUSJ) in Porto, Portugal, obtained from healthy blood donors.

Isolation of human monocytes

Human monocytes were isolated from buffy coats obtained from healthy blood donors, following established procedures [19]. Briefly, the buffy coats were centrifuged, and the resulting cell pellet was incubated with the RosetteSep human monocyte enrichment kit (StemCell Technologies) to isolate peripheral blood mononuclear cells (PBMCs). The PBMCs were then diluted 1:1 with PBS supplemented with 2% FBS and layered over Histopaque-1077 to facilitate the separation of monocytes from other blood components. The enriched monocyte layer was collected and subsequently washed with PBS.

CEA^{high} and CEA^{low} 3D CRC spheroids development

Multicellular colorectal spheroid, comprising HCT-15 or SW48 cell, human macrophages, and COL-I, were generated using commercially available molds (3D Petri Dish®, MicroTissues, USA), as reported previously [20, 21]. Briefly, hydrogel micro-molds featuring 81 uniform circular recesses were created thought the use of agarose (2% w/v in 0.9% NaCl). Afterwards, each micro-mold was hydrated with medium for 2 hours. $CEA^{low/high}$ monocultures from HCT-15/SW48 cell lines (0.0025 × 106, 0.005 × 106, or 0.01 × 106 cells per spheroid) were added to the micro-molds (190 µL), settled for 30 minutes, and then

supplemented with 2 mL of complete medium. For dual culture control spheroid (SW48 or HCT-15 and human monocytes), the total cell number was maintained at 0.005 × 106 per spheroid, with different ratios of SW48 or HCT-15: human monocytes (75:25, 65:35, and 50:50) and COL-I (8µg/mL) was incorporated to mimic the presence of ECM. Macrophage differentiation from human peripheral monocytes occurred spontaneously within the spheroids without additional agents. The medium was refreshed every two days.

Characterization of the average diameter, metabolic activity, and circularity of 3D colorectal spheroids

As described before, 3D spheroids were imaged at specified intervals (1, 4, and 7 days) using brightfield microscopy (ZOE™ Fluorescent Cell Imager, Bio-Rad Laboratories, USA). Furthermore, for the 3D spheroids' average diameter, circularity, and compactness were randomly assessed in three per micro-mold core using AnaSP software [32]. Additionally, metabolic activity was assessed on days 1, 4, and 7, spheroids, by incubation with the medium containing resazurin (20% v/v) at 37°C for 4h. Fluorescence was measured at 530 nm and 590 nm using a SynergyMx™ Microplate Reader (BioTek™, USA). Triplicate analyses were conducted on samples from three independent blood donors.

Histological and immunofluorescence analysis of the 3D colorectal spheroids

As previously explained for CEA^{high} 3D spheroids, on day 7, CEA^{low} 3D spheroids were histologically analyzed and characterized by immunofluorescence. Briefly, the medium of CEA^{low} 3D spheroids, comprising HCT-15 cell lines, was removed and the spheroids were fixed in 10% neutral buffered formalin for 24h at RT. After a PBS 1X wash, a 2% w/v agarose sealing layer was applied atop each micro-mold. Then, micro-molds were embedded in paraffin using Thermo Scientific™ STP 120 Spin Tissue Processor. Paraffin-embedded samples were sectioned (3 µm), deparaffinized, and stained with H&E, Sirius Red, and Masson's Trichrome. For immunofluorescence characterization, on day 7, the paraffin-embedded samples, as prepared previously, were sectioned into 5 µm slices and subjected to deparaffinization and rehydration. Antigen retrieval was performed using Tris-EDTA (pH 9) or sodium citrate buffer (pH 6) at 96 °C for 30 min. After three PBS 1X washes, sections were permeabilized with 0.25% Triton and blocked with 10% FBS in PBS for 1h at RT. Primary antibodies (Anti-EpCAM, Anti-CD68, Anti-COL-I) were applied overnight at 4 °C. After three washes, secondary antibodies were added for 1h at RT. DAPI staining followed by a PBS 1X wash was performed before mounting with VectaShield. Imaging was

conducted using a Zeiss AxioImager Z1 microscope equipped with an AxioCam MR ver. 3.0.

Characterization 3D colorectal spheroids through flow cytometry analysis

For flow cytometry analysis of the 3D CRC spheroids, same protocol optimized and described before was used. Briefly, after a 7-day culturing period, 3D colorectal spheroids were collected, centrifuged (300 g, 5 min, 20°C), and the medium was collected. The samples were then washed once with PBS 1X, centrifuged again, and the supernatant was discarded. Spheroids were dissociated into single-cell suspension using Accutase at 37°C for 15 min with periodic pipetting. After inactivating Accutase with cold PBS 1X, cells were centrifuged, washed, and resuspended in FACS Buffer containing PBS 1X, 2% BSA, and 0.01% azide. Next, FACS Buffer Conjugated antibodies (anti-EpCAM/PB, anti-CD14/APC, anti-CD86/FITC, anti-CD163/PE, anti-CD206/PE, and anti-HLA/DR/PB), previously diluted 1:50 in FACS buffer, were added to 200,000 cells resuspended in FACS buffer and incubated for 40 min at 4°C. Following washing, cells were incubated with Live Dead (1:10,000) diluted in PBS 1X for 20 min, fixed with 2% PFA for 15 min at RT, and filtered through a 70 µm pore filter membrane. Cell counting beads were utilized for absolute cell count. Samples were acquired using BD FACS Canto™ II flow cytometer and analyzed with FlowJo software. Unstained cells served as controls. Experiments were conducted in triplicate.

Uptake of 5-FU-CEA-NPs by 3D CRC spheroids

On the 6th day of 3D spheroid development, empty FKR648-labeled NPs (400 µg/mL) in DMEM or RPMI without FBS were added to each micro-mold and incubated for 24h. Following incubation, the medium was discarded, 3D spheroids, washed and transferred to a 15 mL plastic tube. Within each tube, spheroids were subjected to trypsin incubation for 15 minutes at 37 °C, by pipetting for cell dissociation. The isolated cells were then washed, fixed with 2% PFA for 20 min at room temperature (RT), washed again, and analyzed using BD FACS Canto™ II flow cytometer. All data was processed using FlowJo software. Experiments were conducted in triplicate with unstained medium controls.

Effect of 5-FU-CEA-NPs and IL-12 pH-responsive on the metabolic activity of 3D colorectal cancer spheroids

At day 6, each micro-mold was washed with PBS 1X, and different concentrations of 5-FU-CEA-NPs (50, 100, 200 a 400 µg/mL, in regard to 5-FU) or IL-12 pH-responsive NPs (62.5, 125, 250, and 500 pg/mL, in regard to IL-12) in medium without FBS (190 µL per micro-mold, and 2 mL per each 12 well-plate well where the micro-mold was placed) were added and incubated for 24 h, at 37 °C.

Effect of the IL-12 pH-responsive NPs monotherapy or combinatory NPs strategy on the polarization of macrophages

On day 6, each micro-mold was rinsed with PBS 1X, followed by a 24-hour incubation period with the chosen combination of NPs (5FU-CEA-NPs: 400 µg/mL and IL-12 pH-responsive NPs: 250 pg/mL), or the monotherapy IL-12pH-responsive NPs 62.5, 125, 250, and 500 pg/mL, in regard to IL-12), along with their corresponding controls. Subsequently, 3D colorectal spheroids were analyzed to elucidate the impact of the developed combination strategy or the IL-12 pH responsive monotherapy on macrophage polarization. To induce M1 or M2 polarization controls, the cells were treated with either 10 ng/mL of LPS (to mimic M1 polarization) or 10 ng/mL of IL-10 (to mimic M2 polarization). M0 macrophages in both experimental setups were cultured without the introduction of any external factors. The flow cytometry staining protocol, as described previously, was employed. Conjugated antibodies for polarization assessment (anti-CD14/APC, anti-CD86/FITC, and anti-CD163/PE), diluted at 1:50 in FACS buffer, were added to 200,000 cells suspended in FACS buffer and then incubated for 40 minutes at 4°C. Cell acquisition was conducted using the BD FACS Canto™ II flow cytometer, and analysis was performed using FlowJo software.

Effect of the combinatory NPs on NO, IFN-γ and IL-10 levels of 3D colorectal cancer spheroids

Following a 24-hour incubation period with the selected combination of NPs (5FU-CEA-NPs: 400 µg/mL and IL-12 pH-responsive NPs: 250 pg/mL) and their respective controls, 3D colorectal spheroids were examined for their capacity to produce pro- or anti-inflammatory cytokines (IFN-γ or IL-10). M1 or M2 polarization controls were established by treating the cells with 10 ng/mL of LPS (M1-like) or 10 ng/mL of IL-10 (M2-like). M0 macrophages in both scenarios were cultured without the addition of any exogenous

factors. Subsequently, the concentration of IFN-γ in the supernatants was quantified via ELISA using a commercially available kit according to the manufacturer's instructions.

Statistical analysis

The results are presented as mean ± standard deviation (SD) from at least three independent experiments. Statistical analysis utilized two-sided unpaired Student's t-test for comparing two independent groups, and one- or two-way ANOVA for comparing three or more groups, performed with GraphPad Prism 8.0 software. Significance was denoted by *$p < 0.05$, **$p < 0.01$, and ****$p < 0.001$.

Results

Development and characterization of the CEA^{low} mono spheroids

As described in our previous study for CEA^{high} CRC spheroids, we generated CEA^{low} 3D CRC spheroids by culturing HCT-15 MSI cell line in monoculture at three different densities (2500, 5000, and 10,000 cells per spheroid). Over a 7-day period, we evaluated the morphology, size, and metabolic activity of these spheroids. Brightfield microscopy revealed the formation of cell aggregates for all densities by day 1 (Fig. 1A). By day 7, cell-cell interactions resulted in the formation of compact and circular structures across all densities (Fig. 1D and 1E) [22]. Additionally, for spheroids at the intermediate density (5000 cells/spheroid), metabolic activity remained stable from day 4 to day 7 at approximately 4000 R.F.U, with an average size of around 450 µm (Fig. 1B and 1C). This consistent metabolic activity aligns with the slow proliferation rates typical of compact cellular tissues [20]. Furthermore, brightfield microscopy revealed size-related changes from day 4 to 7, including the emergence of irregular protuberances on the spheroid surface (Fig. 1A). In contrast, spheroids at all densities exhibited increasing metabolic activity and average size (approximately 200–400 µm) over the culture period, akin to typical proliferation rates in 2D cellular culture. Considering, the similar self-assembling and no significant differences between initial cell densities, we standardized the density at 5000 cells per spheroid for subsequent studies. Furthermore, to establish a compact 3D model with strong cell-cell interactions, mimicking an advanced tumor stage, we concluded that culturing for 7 days, along with the incorporation of COL-I at 8µg/ml as an extracellular matrix component, was the optimal condition for all subsequent experiments.

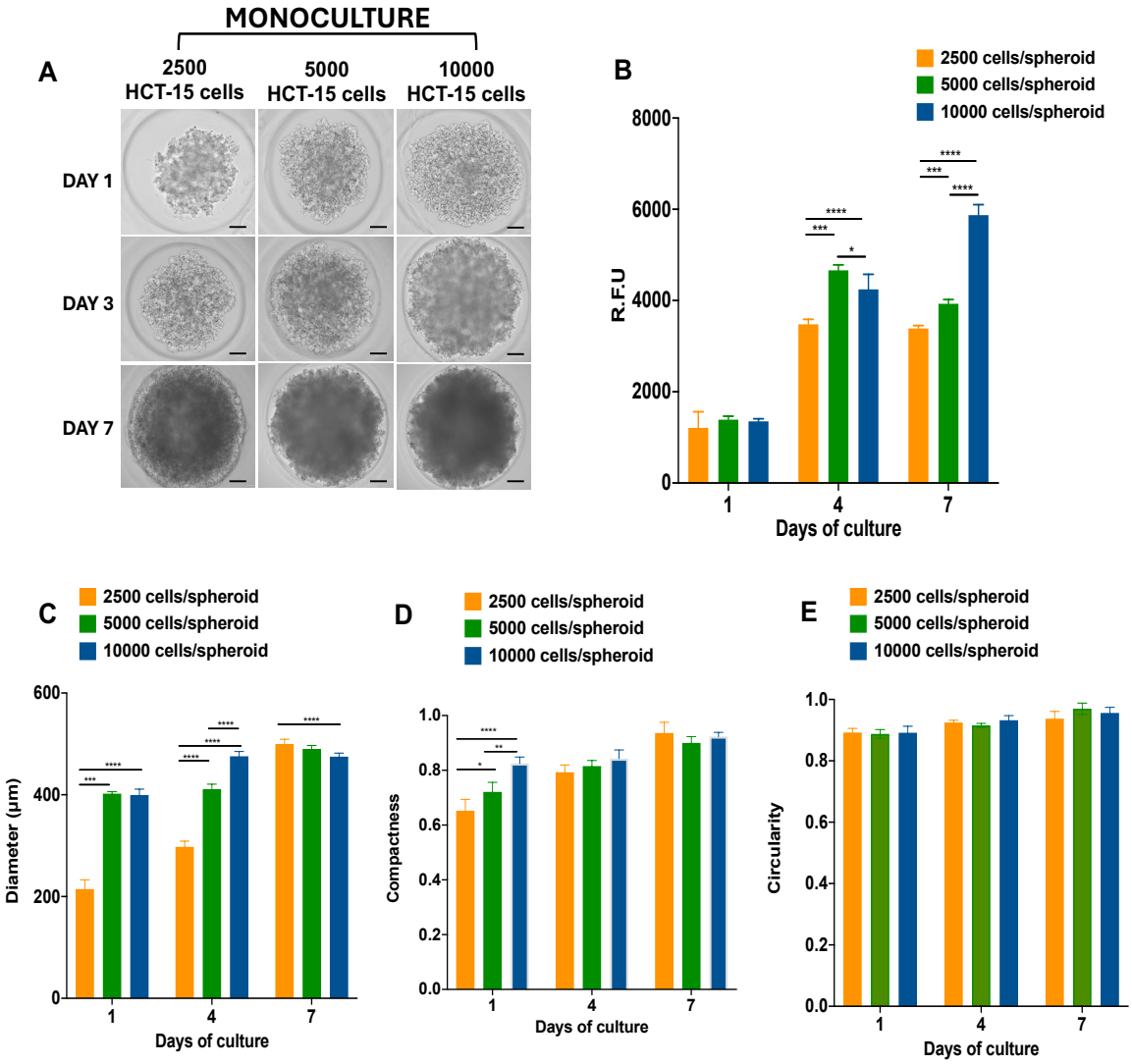


Figure 1: Establishment and characterization of HCT-15 monoculture 3D spheroids over a 7-day period. A) Brightfield microscopy images depicting the evolution of 3D spheroid morphology over time, initiated at three distinct cell densities. Scale bar: 100 µm. B) Dynamics of the 3D spheroids' metabolic activity.C) Changes in average diameter. D) Progression of compactness.E) Evaluation of circularity over time based on the initial seeding cell density. Values represent mean ± standard deviation (n ≥ 3). Statistical comparisons were conducted between each cell concentration and days of culture.

Establishment and characterization of the heterotypic 3D CRC immunospheroids

Similarly, for the generation of dual-culture CEA^{high} 3D spheroids in our previous work, a CEA^{low} 3D system was established, comprising human blood donor isolated peripheral monocytes, mimicking TAMs at the TME, and HCT-15 tumor cells, in three different ratios: 75:25, 65:35, and 50:50 (monocytes: tumor cells). Moreover, to promote cell-cell interaction within the spheroids, 8 µg/ml COL-I was mixed with the cell components. The compactness, circularity, diameter, and metabolic activity of the spheroids were assessed (Fig.2).

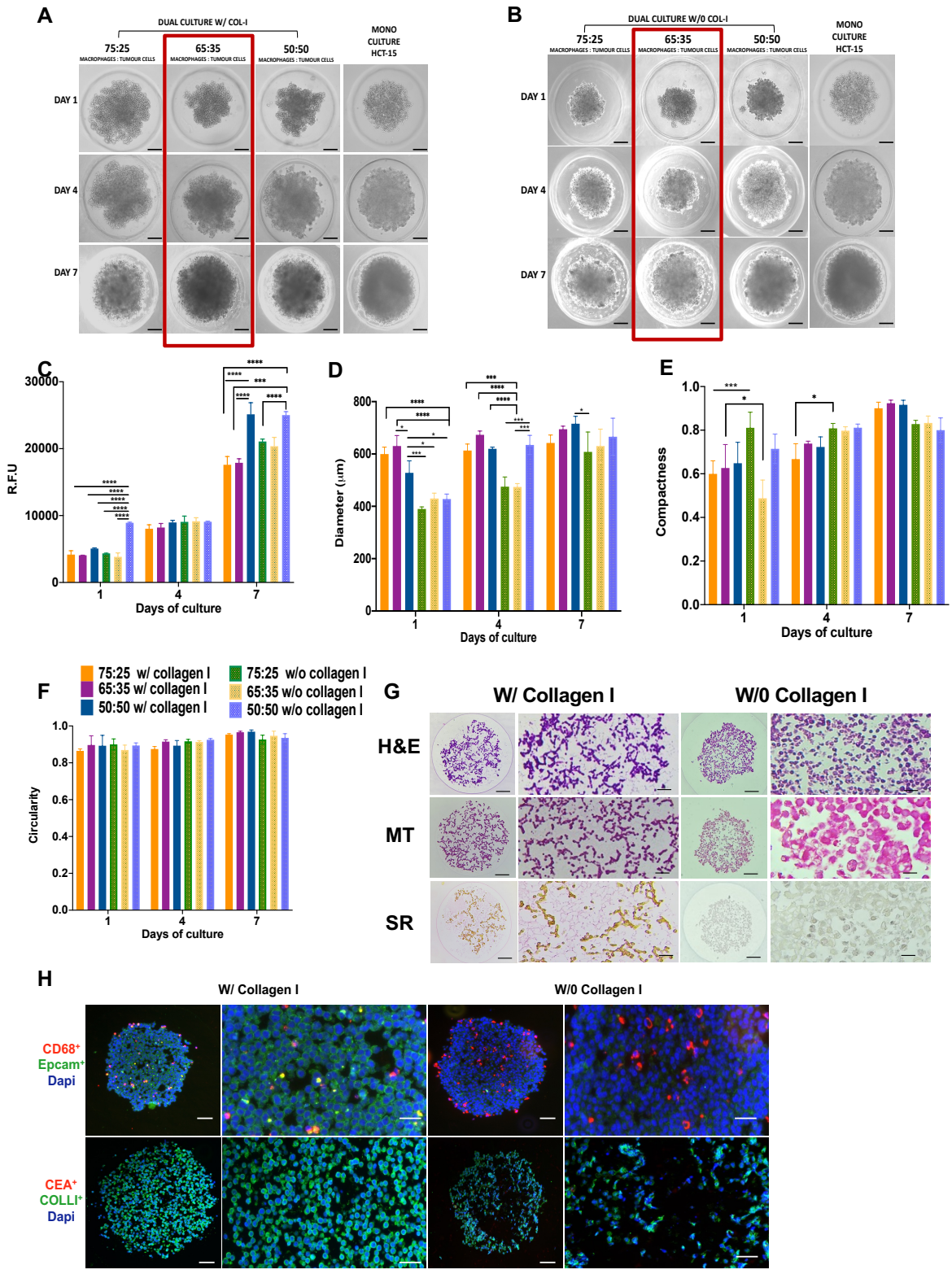


Figure 2: Temporal progression and evaluation of CRC 3D spheroids in co-culture with human macrophages, at varying ratios, in the presence or absence of COL-I. A and B) Brightfield microscopy images illustrating the changing morphology of CRC 3D spheroids over time with different macrophage-to-tumor cell ratios, with or without COL-I, respectively. Scale bar: 100 µm. C) Assessment of the influence of COL-I on the metabolic activity of CRC 3D spheroids. D) Evaluation of diameter changes. E) Measurement of compactness. F) Analysis of circularity over a 7-day period compared to initial seeding cell density. Values are presented as mean ± standard deviation (n ≥ 3). Statistical comparisons were conducted between each cell concentration with or without collagen I and different culture days. G) H&E staining at 20× magnification (scale bar: 100 µm) and 40× magnification (scale bar: 50 µm) revealing the structure of the selected final ratio of CRC 3D spheroids on day 7. H) Immunofluorescence microscopy on day 7 depicting cellular organization (SW48-EpCAM in green, macrophages–CD68 in red) and the co-localization of SW48-CEA expression (red) and ECM-COL-I (green). Nuclei were counterstained with DAPI (blue). Scale bars: 100 µm.

On day 1, similar to observations in 3D monoculture through brightfield microscopy, dual-culture 3D spheroids displayed cell aggregates for all tested ratios, with and without COL-I (Fig. 2A and B). However, by day 7, an enhancement in cell compactness and the formation of a spherical 3D structure was observed. Moreover, in spheroids with COL-I, metabolic activity (R.F.U) increased over time from day 1 to day 7 across all ratios (Fig. 2C). However, in the case of 3D CRC spheroids without COL-I, at the highest density of tumor cells: macrophages (50:50), a maintenance of metabolic activity was observed. This discrepancy may be attributed to the presence of ECM, which provides growth factors and sustains cell metabolic activity, and the interaction and penetration of monocytes and tumor cells through the collagen network in the spheroids with COL-I, while excessive monocytes in the latter case may have been unable to infiltrate and establish the 3D structure, in spheroids without COL-I. Moreover, self-assembled cells without COL-I seemed to have a reduced ability to interact to the same level, compromising their proliferation and potentially leading to the secretion of factors impairing immune cell viability, as observed on day 7 in Figure 2B. Regarding average size, the 3D spheroids enlarged over time across all ratios (Fig. 2D). However, in the 3D spheroids without COL-I, small differences in size were observed from day 1 to day 4.

Comparison between spheroids with and without COL-I revealed less compaction in the 65:35 ratio for those lacking COL-I on day 1 (Fig. 2E). Additionally, by day 7, all ratios with COL-I exhibited higher compactness compared to those without COL-I. Moreover, circularity did not show any biologically significant differences between the different ratios with or without COL-I on days 1, 4, and 7, averaging between 0.8 and 1 (Fig. 2F). However, spheroids without COL-I displayed slightly lower values of compactness and circularity (see Fig. 2E and 2F). Thus, the presence of the ECM component, collagen type I, reinforces cell-cell interaction and promotes a more compacted 3D structure. To validate the presence and co-localization of COL-I, histological analyses including H&E, Masson trichrome (MT, and Sirius Red (SR) staining were performed (Fig. 2G). The H&E histological analysis at day 7 revealed a well-organized structure, demonstrating enhanced cell compactness and a spherical shape in the presence of COL-I (Fig. 2G). Conversely, the absence of COL-I resulted in a more irregular 3D spheroid with surface protrusions, lacking ECM support necessary to maintain its structure (Fig. 2G). As anticipated, Masson trichrome, MT, and Sirius Red (SR) staining effectively confirmed the presence of collagen fibers as an exogenous ECM component in the final dual-culture model (Fig. 2G). SR is commonly employed to differentiate collagen type I, typically stained in yellow, orange, or red hues, from collagen type III, which appears green [23]. Additionally, as shown in Fig. 2G, collagen fibers in the 3D spheroid supplemented with COL-I were stained using MT.

Immunofluorescence studies were conducted to investigate the cellular localization of HCT-

15 tumor cells (EPCAM+), CEA expression in HCT-15 cells (CEA+), macrophages (CD68+), and the ECM component (COL-I+), as illustrated in Fig. 2H. The spatial arrangement of the spheroids revealed that in spheroids with COL-I, macrophages are distributed widely throughout the 3D structure, rather than being concentrated solely at the surface, along with COL-I. Furthermore, macrophages were found to be surrounded by HCT-15 tumor cells, consistent with findings from previous research. However, a tendency in macrophages to be localized at the periphery of the spheroid was observed in the absence of COL-I addition. Moreover, the presence of COL-I was uniformly distributed throughout the spheroids with COL-I, contributing to increased compactness of the structure (Fig. 2H). In 3D spheroids without COL-I supplementation, collagen type I was still detected, although in significantly lower quantities, indicating minimal endogenous production of this ECM component by the spheroid cells. Notably, Epcam expression was widely observed in CRC 3D spheroids with COL-I, reinforcing the regulation of cell adhesion and its reported association with advanced stages [24, 25]. This underscores the role of Col I remodeling in modulating tumor growth and metabolism [26]. As expected, CEA expression was not detected in CEA^{low} 3D CRC spheroids as previously reported [18]. To supplement this analysis, CEA^{high} (Sw48) and CEA^{low} (HCT-15) CRC 3D spheroids were evaluated in terms of metabolic activity, cell composition, and expression of pro- and anti-inflammatory markers (Fig. 3). Our findings revealed no disparities in metabolic activity on day 7 of spheroid formation, whether with or without COL-I (Fig. 3A). Furthermore, the amounts of macrophages and tumor cells showed no significant discrepancies between spheroids with or without COL-I, with the CD14+ macrophage population remaining consistently around 20% across all conditions (Fig 3B). Moreover, despite the notable deviation from the initially seeded cell proportions (65% monocytes to 19% macrophages), attributable to the non-proliferative nature inherent in macrophages, this final ratio aligns with the in vivo CRC context, typified by ~18.21% TAMs [27]. Additionally, a consistent pattern in the preservation of percentages in the expression of M1-like and M2-like markers between conditions with or without COL-I, was observed (Fig. 3C and 3D). Lastly, both CEA^{high} and CEA^{low} 3D CRC spheroids were associated with higher levels of M2-like macrophage polarization profile, consistent with reported analyses of the CRC TME [28]. In summary, the developed 3D CRC spheroids successfully recapitulate aspects of the immune-tumoral TME of CRC, making them a promising tool for drug and nanoparticle testing.

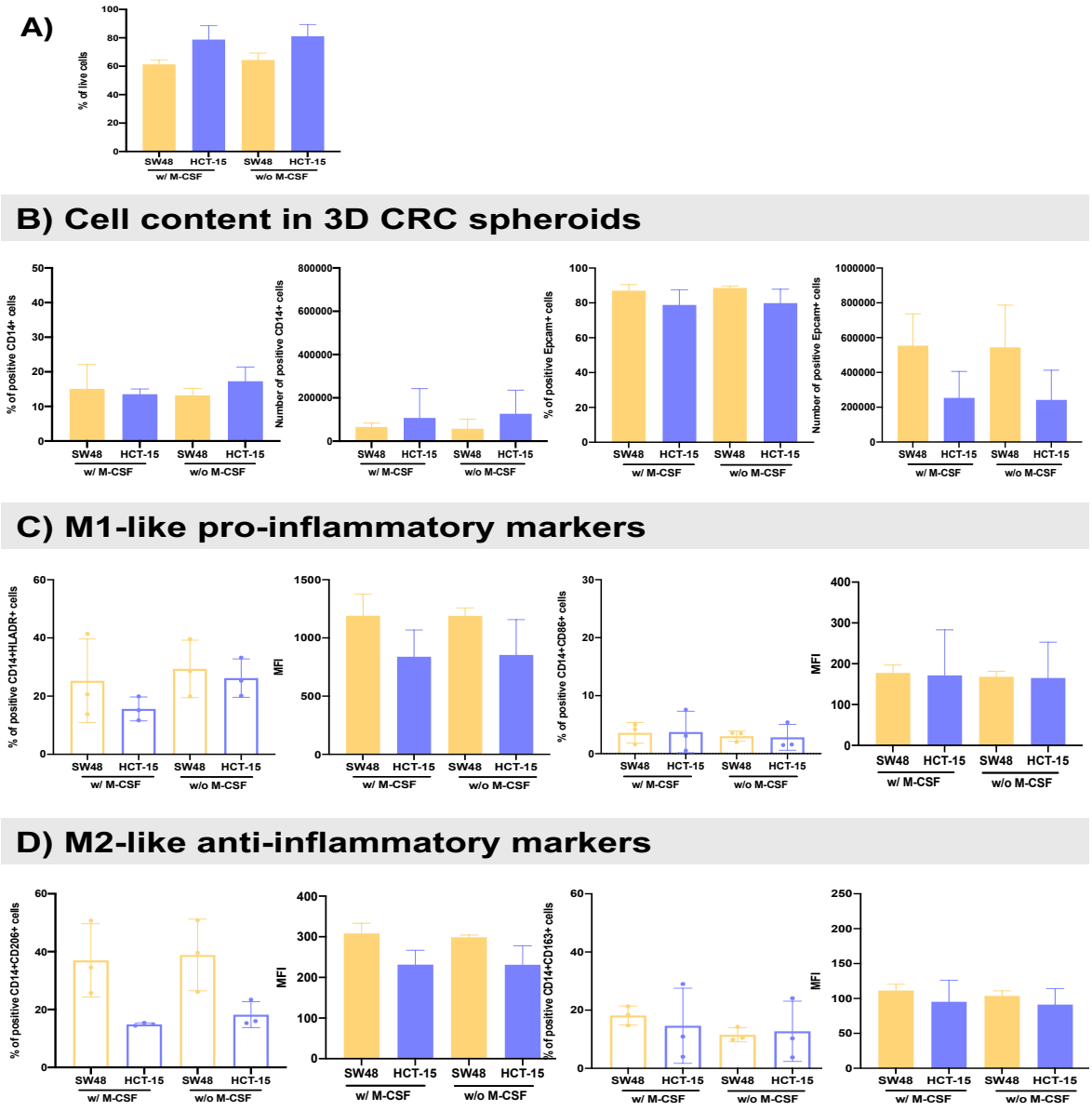


Figure 3: Assessment of the cellular composition of the developed CEA^{high} (SW48) and CEA^{low} (HCT-15) 3D CRC spheroids after 7 days of culture, comparing spheroids with or without COL-I. A) Metabolic activity evaluation. B) Examination of cellular components within the 3D CRC spheroids. C) Assessment of M1-like expression markers in macrophages. D) Evaluation of M2-like expression markers in macrophages.

Assessing the effects of 5-FU-CEA-NPs and IL-12 pH-Responsive NPs as Monotherapies on CEA^{high} and CEA^{low} 3D CRC spheroids

To assess the efficacy of our developed strategies as monotherapies in CEA^{high} and CEA^{low} 3D CRC spheroids, we investigated the ability of NPs to target CRC cells expressing CEA (5-FU-CEA-NPs) and the surrounding tumor microenvironment (IL-12-pH-responsive NPs). An essential consideration in developing NPs for anticancer purposes is their capacity to be taken up by tumor cells [29]. Therefore, in our previous work, we evaluated the cellular

interactions of our developed nanomaterials in 2D culture monolayers in vitro, although these lack crucial components of the tumor environment [18, 30]. Consequently, the use of 3D models, which can replicate various aspects of the tumor microenvironment, is becoming increasingly relevant in preclinical testing to enhance predictive outcomes and facilitate clinical translation. In line with this, we examined the interaction of the developed 5-FU-CEA-NPs with CEA-expressing CRC cells in 2D in vitro models, as previous described in our recent work [18] and, within the developed 3D CRC spheroids, comparing them with their respective controls using flow cytometry (Fig. 4A and 4B).

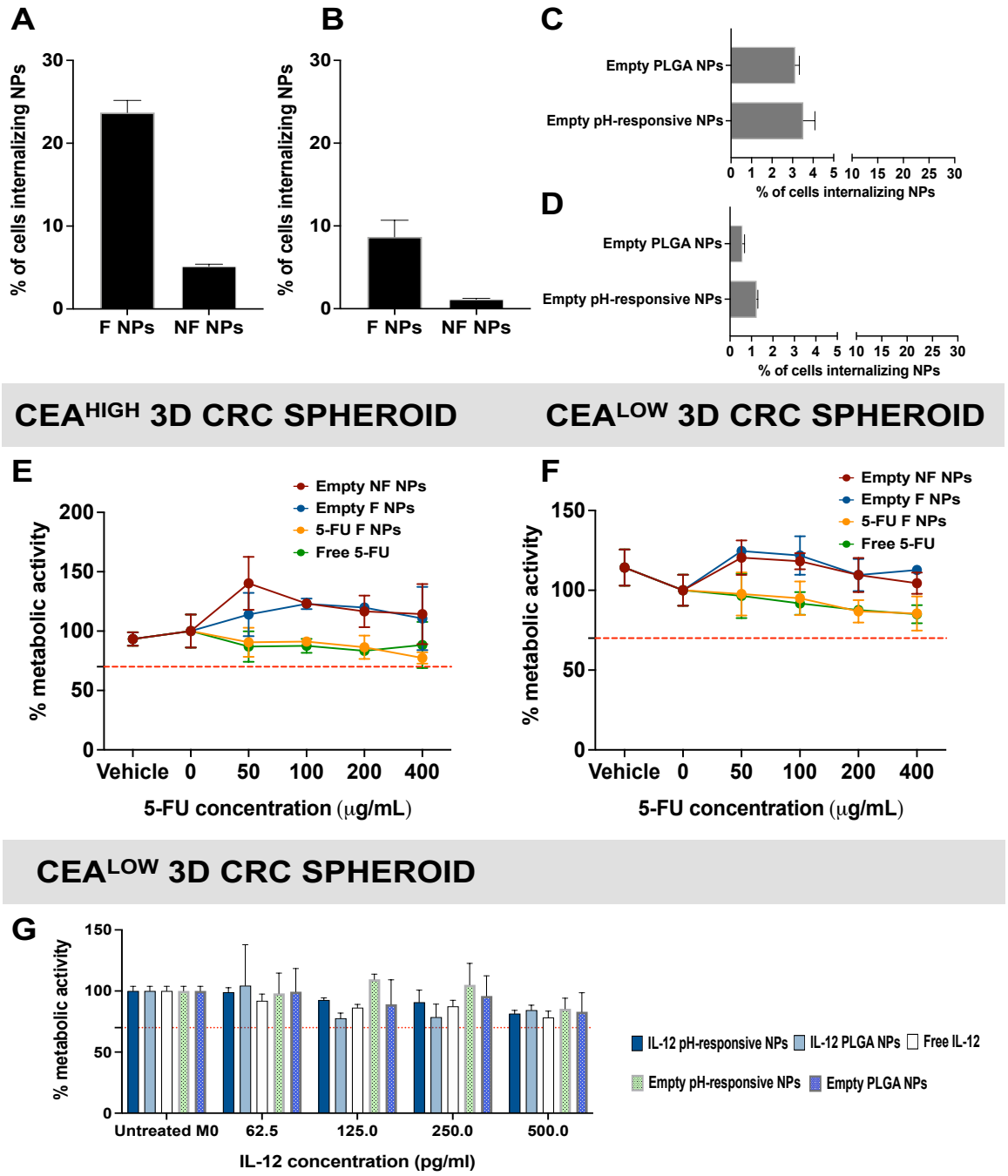


Figure 4: Assessment of the Impact of developed NPs as Monotherapies in 3D CRC Spheroids. A) Evaluation of CEA-functionalized NPs (F NPs) cellular uptake by CEA ^{high} 3D CRC spheroids and B) CEA^{low} 3D CRC spheroids. C) Examination of pH-responsive NPs cellular uptake by CEA^{high} 3D CRC spheroids and D) CEA^{low} 3D CRC spheroids. E) Assessment of the impact on metabolic activity of 5-FU F NPs and respective controls in CEA^{high} 3D CRC spheroids and F) CEA^{low} 3D CRC

spheroids. G) Evaluation of the impact in metabolic activity of IL-12 pH-responsive NPs and respective controls in CEA^{low} 3D CRC spheroids.

FKR648-labeled NPs were incubated with the CEA^{high} or CEAl^{ow} 3D CRC spheroids, and after a 24-hour incubation period, the cells were collected, and fluorescence intensity was measured via flow cytometry. As expected, our findings demonstrated higher internalization by CEA^{high} 3D CRC spheroids of CEA functionalized NPs (F NPs) (~25%) (Fig. 4A), approximately twice as much as by CEA l^{ow} 3D CRC spheroids (Fig. 4B), underscoring the specificity of the developed NPs. Moreover, F NPS were ~3 times more internalized by both 3D CRC spheroids when comparing with the non-functionalized NPs (NF NPs) (Fig. 4A and 4B). However, despite these significant findings, a two-fold decrease in the percentage of CEA-expressing cells internalizing F NPs compared to data previously obtained from cellular uptake studies in 2D in vitro models was observed [18]. This discrepancy in cellular association between the 2D and 3D models can be attributed to the conformation of the 3D model, where cells are densely packed and surrounded by extracellular matrix, more closely resembling an organotypic structure. Furthermore, to confirm the pH-responsiveness of the strategy targeting the CRC TME within a more intricate 3D CRC model, 3D CRC spheroids were exposed to the NPs and evaluated their cellular uptake. Therefore, after 24h incubation, cellular uptake was evaluated presenting no impact of the pH-responsiveness NPs in their cellular uptake, with no significant differences observed between non-responsive and pH-responsive NPs (Fig. 4 C and D). These results align with previously reported findings, indicating minimal cellular uptake of the NPs and thereby validating them specificity to pH responsiveness. Moreover, the potential of developed monotherapies to induce antiproliferative effects was evaluated (Figs. 4E, 4F and 4G). Therefore, after a 24-hour incubation 5-FU F NPs demonstrated enhanced cell toxicity compared to the free drug at the maximum concentration of 400 µg/mL in CEA^{high} 3D CRC spheroids (Fig. 4E), reducing to 70% the metabolic activity. Additionally, 5-FU F NPs showed a similar effect to the free drug on the metabolic activity of CEA^{low} 3D CRC spheroids (Fig. 4F). Subsequently, we evaluated the ability of IL-12 pH-responsive NPs to inhibit CEA^{low} CRC 3D spheroid cell viability and compared them to free IL-12 and empty/loaded non-responsive NPs after an uninterrupted 24-hour treatment period with IL-12 doses ranging from 62.5 pg/mL to 500 pg/mL (Fig. 4G). Furthermore, no significant differences were observed between the developed NPs and free IL-12. Overall, consistent with previous findings, the IL-12 pH-responsive NPs were found to be safe for administration. The primary function of IL-12 is to stimulate the production of the cytokine IFN-γ, recognized for its role in promoting the M1-like phenotype [4]. Hence, akin to prior research, pH-responsive NPs were evaluated for their ability to stimulate the pro-inflammatory cytokine IFN-γ production and consequently

induce the M1-like macrophage phenotype, while concurrently diminishing the anti-inflammatory cytokine IL-10 in CEA^{low} 3D CRC spheroids (Fig. 5).

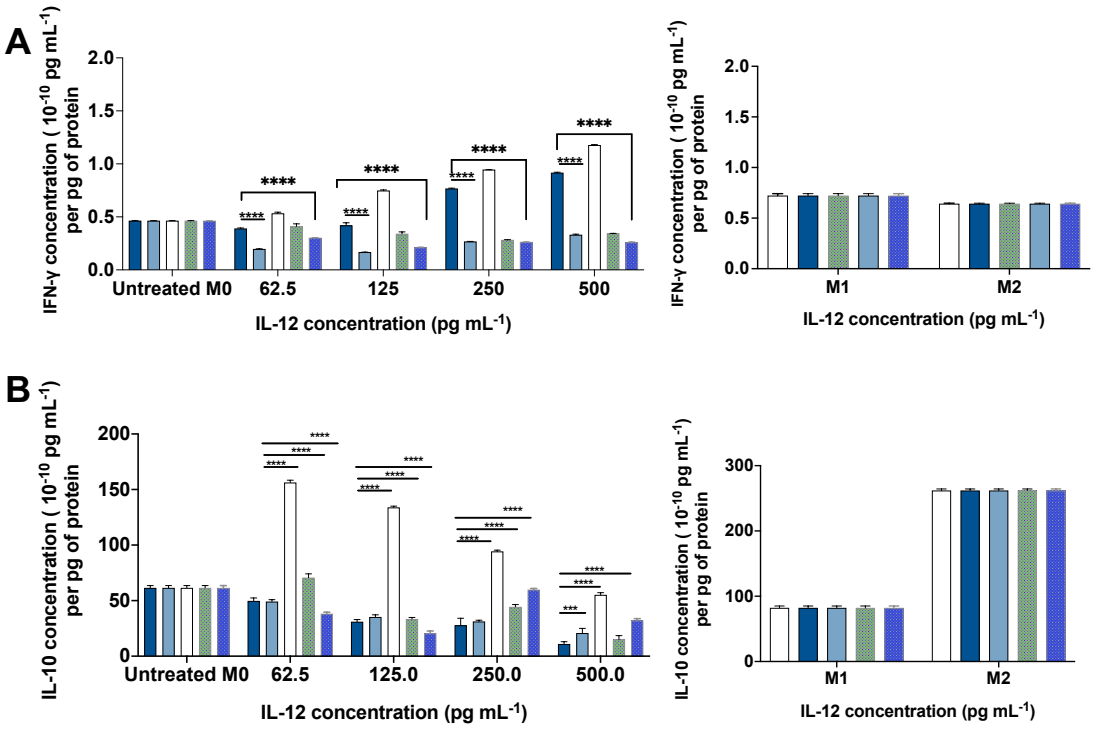


*Figure 5: Assessing the capability of the developed strategy to stimulate pro-inflammatory and anti-inflammatory cytokine production in CRC 3D spheroids after a 24-hour treatment involved comparing untreated conditions with various treatments, including unloaded pH-responsive NPs and PLGA NPs, free IL-12, IL-12-loaded PLGA NPs, and IL-12 pH-responsive NPs..A) Assessment of IFN-γ production in the controls of M1 or M2-like stimulated macrophages.B) Analysis of the secretion of the anti-inflammatory cytokine IL-10 induced by the treatments. Statistical comparisons were made between the different testing groups, denoted as *p < 0.05, **p < 0.01, ***p < 0.001, or p < 0.0001.*

Therefore, secretion levels of IFN-γ and IL-10 were examined after 24-hour treatment of 3D CRC spheroids with unloaded pH-responsive NPs, PLGA NPs, free IL-12, IL-12-loaded PLGA NPs, and IL-12-loaded pH-responsive NPs. Moreover, our findings shown that IL-12 pH-responsive NPs induced significant IFN-γ production compared to controls across all concentrations (Fig. 6A). Additionally, the ability of strategy to induce pro-inflammatory cytokines levels was also assessed by examining the decrease in secreted anti-inflammatory cytokines from CEA^{low} 3D spheroids (Fig. 5B). Statistically significant differences were noted between IL-12 pH-responsive NPs and other controls, across all tested concentrations. Furthermore, to validate the strategy's potential to induce M1-like macrophage polarization, polarization markers were evaluated in the same CEA low 3D CRC spheroids via flow cytometry (Fig. S1), confirming that the developed IL-12 pH responsive NPs had no impact on the expression of CD14+ marker related-macrophages comparing with the non-stimulated 3D spheroids (Fig. S1A). Moreover, macrophages derived from 3D spheroids treated for 24 hours exhibited heightened CD86+ expression in CD14+ macrophages compared to controls (Fig. S1B), confirming NP responsiveness under pH<6.6. Moreover, IL-12 pH-responsive NP treatment reduced CD163+ expression (Fig. S1C), indicating suppression of M2-like macrophage polarization. Overall, the NP

strategy effectively induced a pro-inflammatory M1-like profile in macrophages, with pH-sensitive NPs releasing IL-12 effectively at CRC TME. Moreover, IL-12 pH-responsive NPs reinforced IFN-γ production, indicating macrophage polarization towards an M1-like phenotype, and reduced IL-10 secretion by CRC 3D spheroids. This suggests that IL-12 loaded pH-responsive NPs promote a pro-inflammatory macrophage phenotype under low pH conditions, enhancing CD86 expression and IFN-γ secretion, and decreasing CD163 expression and IL-10 secretion.

Impact of Combinatorial Strategy on Metabolic Activity, IFN-γ, and IL-10 Production in 3D CRC Spheroids, and Subsequent Stimulus for M1-like Polarization Profile

Combination strategies utilizing chemotherapy and immunotherapy have been investigated within precision medicine as a synergistic approach [31, 32]. The rationale of this works is to target CEA-expressing CRC cells effectively while simultaneously addressing the immunosuppressive TME, thereby enhancing anti-tumor immunity and promoting enhanced CRC cell death. Therefore, we evaluated the impact of the combination approach utilizing 400 µg/mL of 5-FU-CEA-NPs alongside 250 pg/mL of IL-12 pH-responsive NPs on the metabolic activity of CEA^{high} or $CEAl^{ow}$ 3D CRC spheroids over a 24-hour period (Fig. 6A and Fig. 6B).Consequently combined strategy significantly influenced the metabolic activity of CEA^{high} 3D CRC spheroids, resulting in approximately 45% less cell viability after 24 hours of treatment (Fig. 6A). Furthermore, the combined strategy exhibited 1.5 times lower metabolic activity values when its therapeutic impact was compared with CEA^{low} 3D CRC spheroids (Fig. 6B), supporting the specificity of the developed strategy to target CEA-expressing cells. Moreover, the observed effect may be attributed to the enhanced cellular uptake of CEA^{high} 3D CRC spheroids facilitated by CEA-functionalized NPs, leading to a more pronounced chemotherapeutic effect of 5-FU in conjunction with IL-12 release at the TME, thereby promoting the recognition of cancer cells by TAMs. This effect was particularly notable given that at a concentration of 400 µg/mL, 5FU-CEA-NPs failed to induce significantly higher toxicity, bellow 70%, as previously demonstrated.

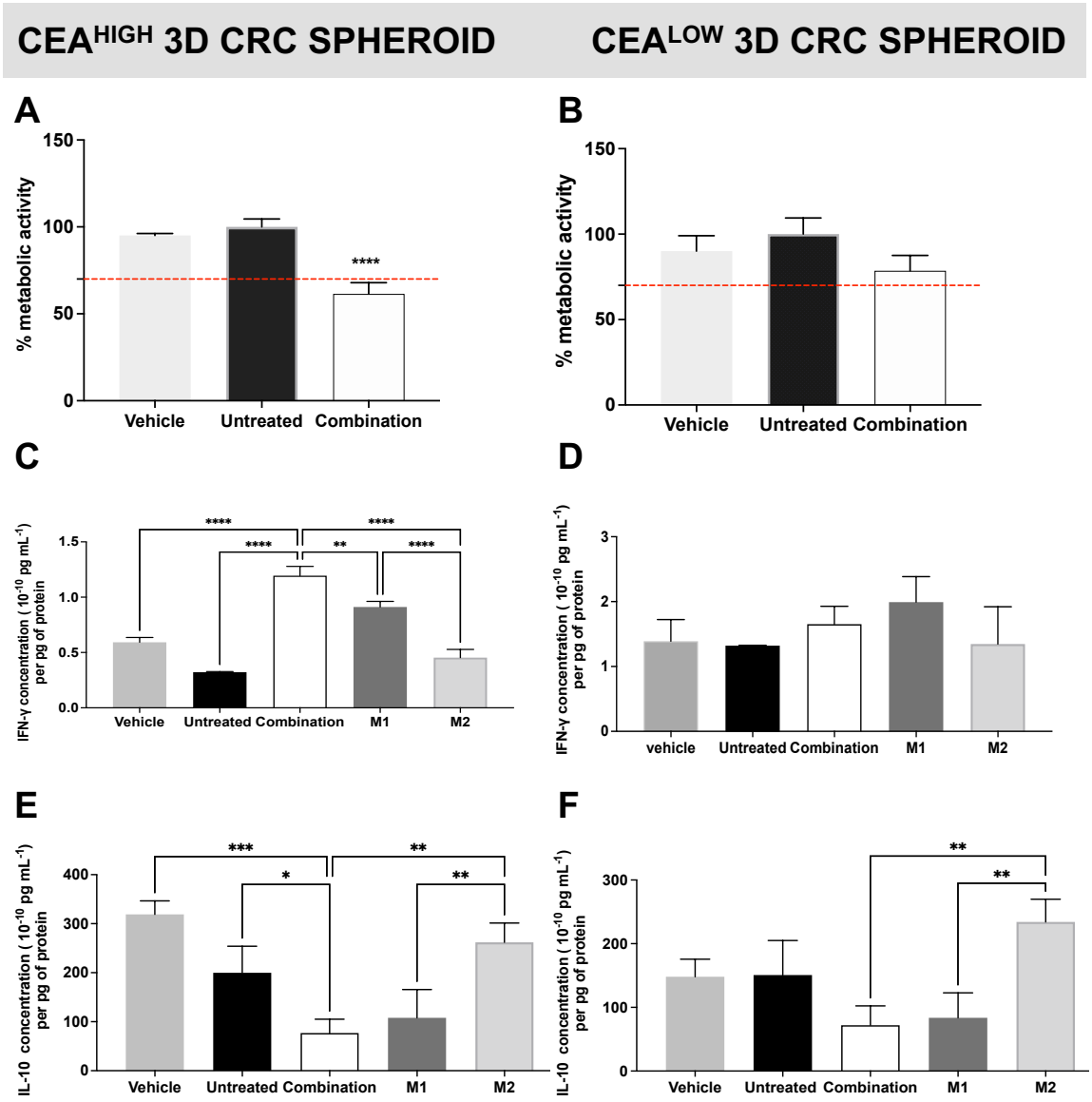


Figure 6: Assessment of the impact of the combinatorial strategy on both CEA^{high} and CEA^{low} 3D CRC spheroids including A) Evaluation of the effect of the strategy on metabolic activity in CEA^{high} 3D CRC spheroids and B) CEA^{low} 3D CRC spheroids. C) Analysis the impact of the combination on the secretion levels of the pro-inflammatory cytokine IFN-γ in CEA^{high} 3D CRC spheroids and D) CEA^{low} 3D CRC spheroids. E) Examination of the effect of the strategy on the secretion levels of the anti-inflammatory cytokine IL-10 in CEA^{high} 3D CRC spheroids and F) CEA^{low} 3D CRC spheroids.

To validate the hypothesis that the developed combinatorial strategy enhanced the chemotherapeutic effect by stimulating IL-12 release, thereby inducing IFN-γ secretion and subsequently promoting M1 polarization, levels of the pro-inflammatory cytokine IFN-γ were investigated. Hence, there were significant increases in IFN-γ secretion observed in CEA^{high} 3D CRC spheroids, along with an enrichment in its detection in CEA^{low} 3D CRC spheroids (Fig. 6C and 6D). Additionally, the pro-inflammatory potential of the strategy was assessed by measuring the reduction in secreted anti-inflammatory IL-10 cytokine from the 3D CRC spheroids, as depicted in Fig. 6E and 6F. In this context, statistically significant differences were found between untreated and treated spheroids, with lower levels of IL-10 observed in both CEA^{high} and CEAl^{ow} 3D CRC spheroids after the 24h period of the combinational treatment. In summary, the devised combinatory NP strategy effectively induced IFN-γ

production, suggesting the polarization of macrophages towards an M1-like phenotype. This idea is supported by the decreased levels of IL-10 secreted by CRC 3D spheroids post-treatment. However, while no statistically significant change in macrophage polarization within the 3D CRC spheroids was observed after 24 hours of combinatorial strategy treatment, a tendency towards increased expression of the M1-like pro-inflammatory marker CD86+ in both CEA^{high} and CEA^{low} 3D CRC spheroids, was observed (see Fig S2 A and S2 C). Furthermore, lower levels of CD163+ marker expression were noted in both CEA^{high} and CEA^{low} 3D CRC spheroids following treatment with the combinatorial strategy (Fig. S2 B and S2 D), suggesting a pro-inflammatory M1-like profile of macrophages with continued administration. Altogether, these findings collectively provide evidence that the developed strategy enhances CRC cell death by heightening cytotoxic sensitivity through CEA-targeted NPs and IL-12 release at the CRC TME. This process of IL-12 release at TME, propels macrophages toward a more pro-inflammatory phenotype, boosting CD86 expression and IFN-γ secretion, while diminishing CD163 expression and IL-10 secretion, thus facilitating the recognition and elimination of CRC cells.

Conclusions

This study introduces a novel combinatorial NP strategy designed to target both CRC cells expressing CEA and the immunosuppressive TME, through nanoencapsulation of 5-FU and IL-12, demonstrated functionality in complex 3D models that mimic MSI and TME features. Moreover, as monotherapies, IL-12-loaded pH-responsive NPs were shown to stimulate IFN-γ secretion in 3D CEAlow CRC spheroids, while 5-FU-loaded CEA-targeted NPs specifically targeted CEA-expressing cells, leading to a reduction in their metabolic activity. Additionally, a CRC 3D spheroid model was developed, comprising HCT-15 MSI CRC cells, macrophages differentiated in situ from peripheral blood monocytes, and an exogenous ECM-like non-cellular constituent, COL-I. These CRC 3D spheroids successfully mimic cellular and structural tumor features, including cell spatial organization, ECM presence, and a pro-tumor, anti-inflammatory M2-like macrophage phenotype. Moreover, the combinatorial strategy was assessed in CEAhigh or CEAlow 3D CRC models, revealing a reduction in the expression of anti-inflammatory macrophage markers and an increase in pro-inflammatory markers. These results confirm the ability of the strategy to reeducate the tumor immune microenvironment within CRC 3D spheroids. The combinatorial strategy NPs decreased the secretion of the anti-inflammatory cytokine IL-10 while enhancing the levels of the IFN-γ pro-inflammatory cytokine, thereby improving macrophages recognition of CRC cells and toxicity of 5-FU. The CRC 3D spheroid models established in this study offer improved replication of the biological architecture and composition seen in native tumors, rendering them a promising *in vitro* platform for testing new nanotherapeutics, thereby enhancing the predictability of *in vivo* outcomes

Supporting Information

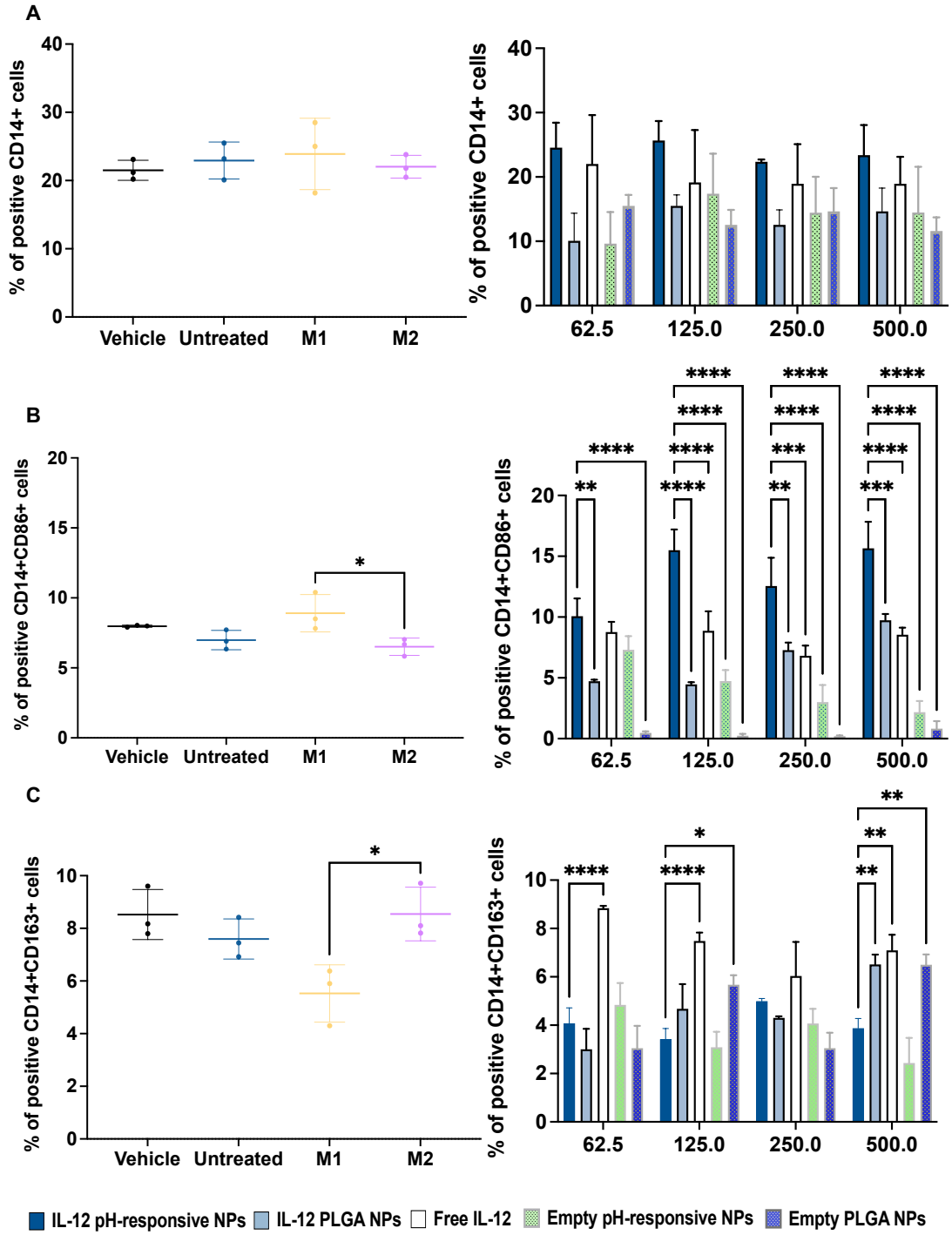


*Figure S 1: Assessment of macrophage polarization in CRC 3D spheroids pre- and post-treatment, focusing on the A) CD14+ macrophage population. B) Evaluation of the expression of CD86+ (M1-like marker) and C) CD163+ (M2-like marker). Spheroids received various treatments: untreated medium, unloaded PLG NPs, pH-responsive NPs, free IL-12, and IL-12-loaded PLGA NPs and pH-responsive NPs for 24 hours. Statistical comparisons between IL-12-loaded pH-responsive NPs and controls were made within each dose range, with significance denoted as *p < 0.05, **p < 0.01, ***p < 0.001, or ****p < 0.0001.*

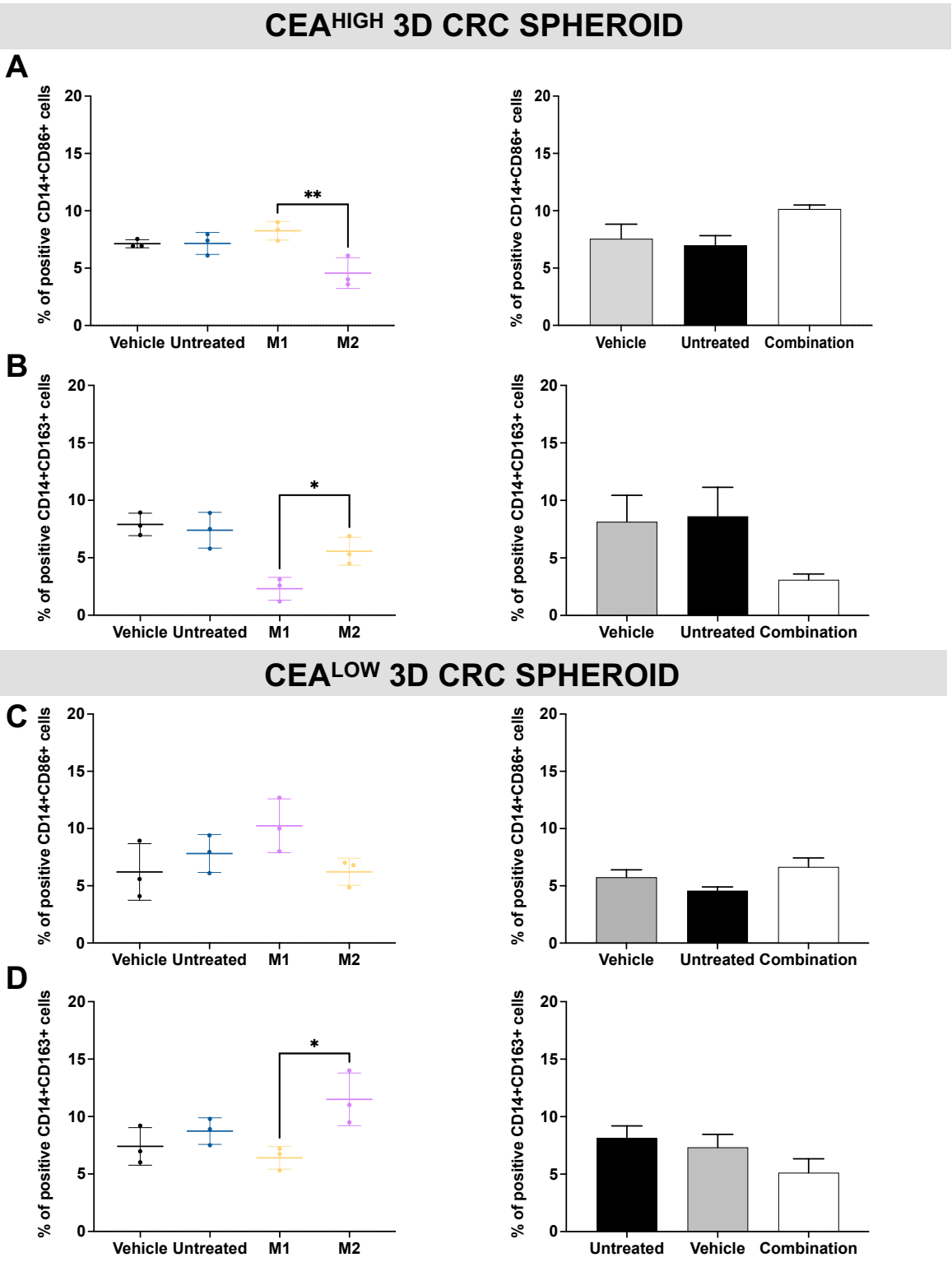


*Figure S 2: Examination of macrophage polarization in CRC 3D spheroids before and after treatment focused on: A) Assessing the expression of CD86+ (M1-like marker) and B) CD163+ (M2-like marker) in CEA^{high} 3D CRC spheroids. C) Evaluation the expression of CD86+ (M1-like marker) and D) CD163+ (M2-like marker) in CEA^{low} 3D CRC spheroids. Spheroids underwent the combinatory treatment over 24h period and were compared with untreated, and vehicle controls. Significance was indicated as *p < 0.05 or **p < 0.01*

References

1. Guo, L.W., et al., Current status of global colorectal cancer prevalence, prevention and control.CAMPH, 2024. 46(1): p. 57-65.
2. Leowattana, W., P. Leowattana, and T. Leowattana, Systemic treatment for metastatic colorectal cancer. World J Gastroenterol, 2023. 29(10): p. 1569-1588.
3. Li, Y., et al., Functional and therapeutic significance of tumor-associated macrophages in colorectal cancer. Front Oncol, 2022. 12: p. 781233.
4. Wang, H., T. Tian, and J. Zhang, Tumor-associated macrophages (TAMs) in colorectal cancer (CRC): From mechanism to therapy and prognosis. Int J Mol Sci, 2021. 22(16).
5. Aldilaijan, A.F., et al., Clinical implication of tissue carcinoembryonic antigen expression in association with serum carcinoembryonic antigen in colorectal cancer. Sci Reports, 2023. 13(1): p. 7616.
6. Elekonawo, F.M.K., et al., Carcinoembryonic antigen-targeted photodynamic therapy in colorectal cancer models. EJNMMI Res, 2019. 9(1): p. 108.
7. Vodenkova, S., et al., 5-fluorouracil and other fluoropyrimidines in colorectal cancer: Past, present and future. Pharmacol Therap, 2020. 206: p. 107447.
8. Silveira, M.J., et al., Immunomodulatory nanomedicine for colorectal cancer treatment: a landscape to be explored? Biomater Sci, 2021. 9(9): p. 3228-3243.
9. Mulet-Margalef, N., et al., Challenges and therapeutic opportunities in the dMMR/MSI-H colorectal cancer landscape. Cancers, 2023. 15(4).
10. Gandini, A., et al., The role of immunotherapy in microsatellites stable metastatic colorectal cancer: state of the art and future perspectives. Front Oncol, 2023. 13: p. 1161048.
11. Chen, S.Y., et al., Chapter 12 - The clinical application of immuno-therapeutics, in Clinical Immuno-Oncology, J.E. Niederhuber, Editor. 2024, Elsevier: New Delhi. p. 237-288.e7.
12. Li, J. and X. Xu, Immune checkpoint inhibitor-based combination therapy for colorectal cancer: An Overview. Int J Gen Med, 2023. 16: p. 1527-1540.
13. Ros, J., et al., Advances in immune checkpoint inhibitor combination strategies for microsatellite stable colorectal cancer. Front Oncol, 2023. 13.
14. Kano, Y., M. Suenaga, and H. Uetake, Strategic Insight into the Combination Therapies for Metastatic Colorectal Cancer. Current Oncol, 2023. 30(7): p. 6546-6558.

15. Li, X., et al., Multifunctional nanoparticle-mediated combining therapy for human diseases. Signal Transd Target Ther, 2024. 9(1): p. 1.
16. Ma, L., M. Kohli, and A. Smith, Nanoparticles for combination drug therapy. ACS Nano, 2013. 7(11): p. 9518-25.
17. Gogoi, P., G. Kaur, and N.K. Singh, Nanotechnology for colorectal cancer detection and treatment. World J Gastroenterol, 2022. 28(46): p. 6497-6511.
18. Silveira, M.J., et al., scFv biofunctionalized nanoparticles to effective and safe targeting of CEA-expressing colorectal cancer cells. J Nanobiotechnol, 2023. 21(1): p. 357.
19. Cardoso, A.P., et al., Macrophages stimulate gastric and colorectal cancer invasion through EGFR Y(1086), c-Src, Erk1/2 and Akt phosphorylation and smallGTPase activity. Oncogene, 2014. 33(16): p. 2123-33.
20. Bauleth-Ramos, T., et al., Colorectal cancer triple co-culture spheroid model to assess the biocompatibility and anticancer properties of polymeric nanoparticles. J Control Release, 2020. 323: p. 398-411.
21. Martins, C., et al., Glioblastoma immuno-endothelial multicellular microtissue as a 3D in vitro evaluation tool of anti-cancer nano-therapeutics. J Control Release, 2023. 353: p. 77-95.
22. Kanton, S. and S.P. Paşca, Human assembloids. Development, 2022. 149(20).
23. Junqueira, L.C.U., W. Cossermelli, and R. Brentani, Differential staining of collagens type I, II and III by sirius red and polarization microscopy. Arch Histol Jpn, 1978. 41(3): p. 267-274.
24. Huang, L., et al., Functions of EpCAM in physiological processes and diseases (Review). Int J Mol Med, 2018. 42(4): p. 1771-1785.
25. Dai, M., et al., Relationship between epithelial cell adhesion molecule (EpCAM) overexpression and gastric cancer patients: A systematic review and meta-analysis. PLoS One, 2017. 12(4): p. e0175357.
26. Su, H., et al., Collagenolysis-dependent DDR1 signalling dictates pancreatic cancer outcome. Nature, 2022. 610(7931): p. 366-372.
27. Li, C., et al., A Higher Frequency of CD14+ CD169+ monocytes/macrophages in patients with colorectal cancer. PLoS One, 2015. 10(10): p. e0141817.
28. Wang, X., et al., A new method for predicting the prognosis of colorectal cancer patients through a combination of multiple tumor-associated macrophage markers at the invasive front. Heliyon, 2023. 9(2): p. e13211.
29. Anisimov, R.A., D.A. Gorin, and A.A. Abalymov, 3D cell spheroids as a tool for evaluating the effectiveness of carbon nanotubes as a drug delivery and photothermal therapy agents. C, 2022. 8(4): p. 56.

30. Castro, F., et al., Advances on colorectal cancer 3D models: The needed translational technology for nanomedicine screening. Adv Drug Deliv Rev, 2021. 175: p. 113824.
31. Karthika, C., et al., Multiple strategies with the synergistic approach for addressing colorectal cancer. Biomed Pharm, 2021. 140: p. 111704.
32. Gmeiner, W.H., Recent advances in therapeutic strategies to improve colorectal cancer treatment. Cancers, 2024. 16(5): p. 1029.

CHAPTER VI – GENERAL DISCUSSION AND FUTURE PERSPECTIVES

General Discussion

Colorectal cancer (CRC), standing as the second foremost cause of cancer-related mortality worldwide, remains a substantial threat, with metastatic CRC (mCRC) exhibiting a mere 14% five-year survival rate [1]. Although treatments have advanced, therapeutic options are restricted to specific CRC subtypes and can induce severe side effects [2]. This underscores the urgency for novel therapeutic modalities to address metastatic cases more effectively, while complementing existing treatment protocols. A crucial element in crafting effective treatments for CRC patients involves comprehending the dynamics within the tumor microenvironment (TME), given its proven role in fostering drug resistance and treatment ineffectiveness *in vivo* [3]. Therefore, the development of novel *in vitro* methodologies, such as advanced 3D models of CRC, holds clinical significance in expediting the evaluation and translation of new drugs. These models can effectively mimic the complexities of the TME *in vitro*, bridging the gap between 2D cultures and *in vivo* investigations [4]. Additionally, 3D models not only aim to minimize dependance on animal models but also facilitates the optimization of cellular and extracellular interactions within the CRC TME happening *in vivo* context and thereby enhancing the development of more clinically applicable treatment options for patients [5].

The development of new therapeutic approaches hinges on designing systems capable of effectively targeting CRC cells to amplify drug therapeutic efficacy. In this context, the carcinoembryonic antigen (CEA) stands out as an appealing target for colorectal cancer due to its prevalent expression in nearly all colorectal tumors and minimal expression in healthy adult tissues [6, 7]. Moreover, it is also crucial to engineer systems with the capacity to precisely target the CRC TME, thereby inducing modulation of immune responses, reducing cancer cell immune evasion and thus, enhancing the outcomes of chemotherapeutic treatments.

To address these unmet needs, which have contributed to recent clinical trial failures, this work proposes the use of CEA-targeted nanoparticles (NPs) for delivering the chemotherapeutic 5-FU. Despite its widespread use in CRC treatment, 5-FU is associated with severe side effects, low bioavailability, and limited tumor specificity. Additionally, to target the slightly acidic CRC TME, a pH-responsive NPs were proposed to deliver the potent IL-12 cytokine, known for its efficacy, but hindered by its unacceptable systemic toxicity. Leveraging the overexpression of CEA, these NPs aim to enhance drug delivery specifically to CRC cells, while pH responsiveness ensures targeted release of IL-12 in the acidic TME, potentially improving treatment outcomes. Likewise, the advancement of new *in vitro* tools to support CRC drug testing requires the establishment of high-throughput co-

cultures that closely mimic the TME and include extracellular matrix (ECM) components, capable of accurately replicate the native features and the complexity of the tumor. In this context, this doctoral thesis gathered expertise from diverse fields including chemistry, materials science, pharmaceutical nanotechnology, cancer biology and cancer immunology, aiming the development of innovative anti-CRC strategies by employing a combination of CEA-targeted therapy and a stimulus-responsive immunomodulatory strategy.

The outlined strategies underwent evaluation utilizing CEA^{high} or CEA^{low} 3D CRC models, regardless as monotherapies or as combinatorial strategy. Regarding, the CEA-targeted NPs for 5-FU delivery (**CHAPTER III**), polymeric conjugate, using PLGA-PEG modified with anti-CEA single-chain variable fragment (scFv), MFE-23 moiety was chemically synthesized to act as matrix for the proposed targeted NPs. Confirmation of successful chemical reactions was done using techniques like 1H NMR and FTIR, showing a conjugation efficiency of around 90% by RT-HPLC. Moreover, NPs loaded with 5-FU were prepared through double emulsion technique, resulting in sizes ranging from 130 to 170 nm, with a polydispersity index of 0.2, and zeta-potential ranging from -5 to -12 mV. Furthermore, CEA-targeted NPs demonstrated a specific affinity for 2D CEA-expressing cells, with a threefold increase in internalization rates compared to non-targeted NPs. Moreover, this strategy significantly reduced the metabolic activity of CEA-expressing cells after 24h and 48h, enhancing the anticancer efficacy of the delivered drug[1]. Additionally, CEA-targeted NPs loaded with 5-FU were found to be safe for macrophages, exhibiting no significant biological impact on macrophage polarization, underscoring the potential of the strategy for further application in more complex 3D models mimicking the TME with associated tumor-associated macrophages (TAMs).

Regarding the formulation aiming to target TME (**CHAPTER IV**) a significant milestone was achieved by developing innovative pH-responsive NPs that encapsulate IL-12 and demonstrating their efficacy in both 2D and complex 3D models that mimic features of the TME. Our manufacturing approach for these pH-responsive NPs involved chemical modification of the PLGA polymer with a pH-responsive monomer, DMMA, which, when exposed to weakly acidic pH, reveals positively charged amino groups. IL-12 was efficiently encapsulated within the pH-responsive NPs, by double emulsion technique with an association efficacy of around 50%, average size ranging from 200 to 250 nm, 0.1 polydispersity index and confirmed release under similar pH found in the CRC TME. Furthermore, IL-12-loaded pH-responsive NPs were observed to induce IFN-γ secretion in 2D mouse macrophage cell lines and human macrophages isolated from healthy blood donors, along with a notable 2-3-fold increase in NO release levels, suggesting a significant

stimulus for polarization towards M1-like macrophages. Moreover, we developed a pioneering 3D spheroid model of CRC, containing of CEA-expressing MSI cancer cells (SW48 cells), macrophages that were in situ differentiated from peripheral blood monocytes, and an exogenous ECM-like non-cellular component, collagen type I(COL-I). This innovative CRC 3D spheroid model accurately replicated cellular and structural characteristics of the tumor, including cell spatial organization, the presence of ECM, and a mixed phenotype of pro-tumor and anti-inflammatory M2-like macrophages. Therefore, the impact of IL-12-loaded pH-responsive NPs was investigated in the developed 3D model, revealing a reduction in the expression of anti-inflammatory macrophage marker CD163 alongside an elevation in pro-inflammatory macrophage marker, CD86, confirming the ability of NPs to reshape the tumor immune microenvironment within the CRC 3D spheroids. Likewise, NPs demonstrated responsiveness to the slightly acidic pH of the CRC TME (~6-5), were considered safe for macrophage administration, and were capable of inducing IFN-γ production and a reduction in the secretion of a key anti-inflammatory cytokine, IL-10.

Concerning the combinatorial strategy (**CHAPTER V)** to target both CRC cells expressing CEA and the immunosuppressive TME involving encapsulating 5FU and IL-12, was assessed in terms of its efficacy in the aforementioned CEA^{high} or CEA^{low} 3D models mimicking MSI and TME characteristics, using SW48 and HCT-15 cells as CEA-expressing or non-expressing, respectively. Consequently, the developed nano formulations were assessed as single treatments, demonstrating that IL-12-loaded pH-responsive NPs were able to stimulate IFN-γ secretion also in 3D CEA^{low} CRC spheroids, while 5-FU-CEA-NPs specifically targeted 2 times more CEA-expressing cells, leading to a decrease in their metabolic activity after 24h of treatment. Furthermore, the impact of the combinatorial strategy was assessed in CEA^{high} or CEA^{low} 3D CRC models, inducing after 24h of treatment a reduction in the expression of the anti-inflammatory macrophage marker CD163, a scavenger receptor, and an increase in the pro-inflammatory marker, CD86, a T cell co-receptor, in both 3D spheroid models. Furthermore, the combination strategy NPs induced a decrease in the secretion of the anti-inflammatory cytokine IL-10 while simultaneously boosting the levels of the pro-inflammatory cytokine IFN-γ. This modulation led to a shift in macrophage polarization towards an M1-like phenotype, resulting in enhanced recognition of CRC cells and increased toxicity of 5-FU.

Overall, our developed innovative therapy opens up avenues for exploring advanced delivery systems with higher drug loading capacities and minimal adverse effects on CEA-expressing CRC tumors. Additionally, CEA-targeted NPs show promise for targeted therapy in various cancer types and metastatic CRC sites, where CEA expression is prevalent.

Moreover, to the best of our knowledge, the synthesized pH-responsive NPs releasing IL-12 represent a pioneering effort in releasing IL-12 at pH levels similar to those of the CRC TME, with the ability to induce IFN-γ production and polarization of M1-like macrophages.

In conclusion, our combinatory strategy presents a novel approach to chemotherapy, emerging as an immunomodulatory strategy to be combined with other available therapies to improve CRC cancer cells recognition and elimination by the immune system. Furthermore, the novel, developed, CRC 3D spheroid models, offered improved replication of the biological architecture and composition observed in native tumors, making them a promising *in vitro* platform for testing new nanotherapeutics and enhancing the predictability of *in vivo* outcomes.

The research undertaken in this doctoral thesis has significantly advanced therapeutic approaches for managing the burden of CRC. This progress is evidenced by the development of two distinct and promising strategies for treating mCRC: first, with the development of a CEA-targeted nanotherapy designed to precisely deliver therapeutic payloads to CEA-expressing CRC cells and metastatic sites; and second, with the innovation of a pH-responsive nanosystem for efficient delivery and release of biological molecules within the slightly acidic TME with a pH of ~ 6.6. Additionally, the establishment of a novel CRC 3D in vitro model has emerged as a promising asset for accelerating the translation of newly developed anti-cancer nanomedicines.

Future Perspectives

New approaches for mCRC treatment as well as combinatory strategies are being explored by several authors [8-10]. Therefore, as future perspectives both strategies as single or combinatorial NPs treatment regimens needs to be validated in more advances *in vitro* systems and in *in vivo* efficacy studies.

Murine models of CRC, including azoxymethane (AOM)/dextran sulfate sodium (DSS) model is predominantly utilized for studying colitis-associated cancer due to its reproducibility, low cost, and ease of use [11]. However, despite de expertise of our group in the handling of and inducement of this model, the lack of standardization in the AOM/DSS model, with varying doses and exposures to AOM and DSS across different studies, complicates data analysis and comparison [11, 12]. Therefore, hybrid model combining human CEA transgenic mice (H-2Kb) with Apc1638N (H-2Kb) knockout mice has been proposed, spontaneously developing gastrointestinal tumors that express CEA, progressing from adenomatous polyps to invasive carcinomas over several months [13]. Furthermore,

the Apc1638N/CEA mice provide a valuable tool for evaluating CEA-targeted vaccines, NPs and other immunotherapies in a context where tumor growth and CEA expression coincide. [14]. Thus, the murine model previously described have been proved to be useful in better understanding the normal host response to CEA and guiding the continued development strategies for human CRC. Moreover, looking ahead in the use of mice models, as future perspectives might be important to select appropriate endpoints for colon excision and to analyze key markers of tumor progression and treatment efficacy, such as cleaved caspase-3 and Ki67. Moreover, should also be included mass spectrometry studies to precisely quantify the biodistribution of 5-FU and IL-12 in the colon and other major organs. Additionally, *in vivo* validation methods should be explored to assess the effectiveness of combinatory nanoparticles (NPs). In this context, considering the development of a human tumor xenograft model using immunocompetent mice may also be advantageous, as it offers a more accurate reflection of the clinical environment, including the influence of immune cells on NP efficacy.

Despite, animal-based testing has long been the benchmark for research, and it continues to be a crucial step in confirming the safety and efficacy of products entering the market today [15]. Traditional preclinical models often fail, letting toxic drugs enter clinical trials despite their intended protective role [16]. This flaw leads to wasted time and resources on unsuccessful drugs, highlighting the need for better testing processes, using advanced technologies like Organ-on-a-Chip to boost safety and efficacy in drug development [16].

Therefore, recent advances in *in vitro* culture systems have been employed not only to understand the unique futures of cell-cell and ECM interactions but also to improve the newly nano-drug discovery using 3D microfluidic organ-on a chip [17]. In this context, researchers had developed CRC-on-chip that integrates fluid flow with peristalsis-like cyclic stretching to allow the examination of CRC progression and to serve as an adaptable, human-relevant model system, highly useful for investigating early invasive cancer processes and for conducting drug tests [18, 19].

Furthermore, the models mentioned earlier accurately reflect the architecture and functions of organs and cells, along with the in vivo expression, localization, and activity of key intestinal drug transporters, as critical aspects for studying drug transport, metabolism, and interactions [20].Consequently, the CRC-on-chip offers a promising tool for investigating CRC drug metabolizing enzymes and drug-drug interactions, which are crucial for understanding pharmacokinetics, safety, and efficacy.

References

1. Silveira, M.J., et al., scFv biofunctionalized nanoparticles to effective and safe targeting of CEA-expressing colorectal cancer cells. J Nanobiotechnol, 2023. **21**(1): p. 357.
2. Shin, A.E., F.G. Giancotti, and A.K. Rustgi, Metastatic colorectal cancer: mechanisms and emerging therapeutics. Trends Pharmacol Sci, 2023. **44**(4): p. 222-236.
3. Reidy, E., et al., A 3D view of colorectal cancer models in predicting therapeutic responses and resistance. Cancers, 2021. **13**(2): p. 227.
4. Abbas, Z.N., et al., Comparative analysis between 2D and 3D colorectal cancer culture models for insights into cellular morphological and transcriptomic variations. Sci Reports, 2023. **13**(1): p. 18380.
5. Mu, P., et al., Newly developed 3D in vitro models to study tumor–immune interaction. J Exp Clin Cancer Res, 2023. **42**(1): p. 81.
6. Sandberg, M.L., et al., A carcinoembryonic antigen-specific cell therapy selectively targets tumor cells with HLA loss of heterozygosity in vitro and in vivo. Sci Transl Med, 2022. **14**(634): p. eabm0306.
7. Sousa, A.R., M.J. Oliveira, and B. Sarmento, Impact of CEA-targeting nanoparticles for drug delivery in colorectal cancer. J Pharmacol Exp Ther, 2019. **370**(3): p. 657-670.
8. Gmeiner, W.H., Recent advances in therapeutic strategies to improve colorectal cancer treatment. Cancers, 2024. **16**(5): p. 1029.
9. Ohishi, T., et al., Current targeted therapy for metastatic colorectal cancer. Int J Mol Sci, 2023. **24**(2).
10. Freitas, S.C., et al., New frontiers in colorectal cancer treatment combining nanotechnology with photo- and radiotherapy. Cancers, 2023. **15**(2).
11. Dzhalilova, D., et al., Murine models of colorectal cancer: the azoxymethane (AOM)/dextran sulfate sodium (DSS) model of colitis-associated cancer. PeerJ, 2023. **11**: p. e16159.
12. Almeida, A., et al., Oral delivery of camptothecin-loaded multifunctional chitosan-based micelles is effective in reduce colorectal cancer. J Control Release, 2022. **349**: p. 731-743.
13. Hörig, H., et al., A new mouse model for evaluating the immunotherapy of human colorectal cancer. Cancer Res, 2001. **61**(23): p. 8520-6.

14. Hance, K.W., H.E. Zeytin, and J.W. Greiner, Mouse models expressing human carcinoembryonic antigen (CEA) as a transgene: evaluation of CEA-based cancer vaccines. Mutat Res, 2005. **576**(1-2): p. 132-54.
15. Nuwer, R., US agency seeks to phase out animal testing. Nature, 2022.
16. Ewart, L., et al., Performance assessment and economic analysis of a human Liver-Chip for predictive toxicology. Commun Med, 2022. **2**(1): p. 154.
17. Sarvestani, S.K., et al., A Tissue engineering approach to metastatic colon cancer. iScience, 2020. **23**(11): p. 101719.
18. Kasendra, M., et al., Duodenum intestine-chip for preclinical drug assessment in a human relevant model. Elife, 2020. **9**.
19. Strelez, C., et al., Human colorectal cancer-on-chip model to study the microenvironmental influence on early metastatic spread. iScience, 2021. **24**(5).
20. Strelez, C., et al., Integration of patient-derived organoids and organ-on-chip systems: Investigating colorectal cancer invasion within the mechanical and GABAergic tumor microenvironment. bioRxiv, 2023.

APPENDIX – DOCTORAL THESIS SUPPLEMENTARY DOCUMENTS

The complete version of the publication that was partially reproduced in this doctoral thesis will be presented as appendix information in the following pages. The included publication is:

• **MJ Silveira**; F Castro; MJ Oliveira; B Sarmento. “Immunomodulatory Nanoparticles for Colorectal Cancer Treatment, a landscape to be explored?” Biomaterials Science, 9, 3228-3243 (2021). (CHAPTER I)

In the following pages, permission for the full reproduction and integration of the publication that forms the basis of CHAPTER III in this doctoral thesis will also be included. CHAPTER III was based on the following publication:

• **MJ Silveira**; C Martins; T Cruz; F Castro; A Amorim- Costa; K Chester; MJ Oliveira; B Sarmento. "scFv biofunctionalized nanoparticles to effective and safe targeting of CEA-expressing colorectal cancer cells". Journal of Nanobiotechnology 21 1(2023).

Biomaterials Science

ROYAL SOCIETY OF CHEMISTRY

REVIEW

View Article Online
View Journal | View Issue

Published on 04 March 2021. Downloaded by Universidade do Porto (UP) on 5/5/2024 9:05:19 PM.

Check for updates

Cite this: *Biomater. Sci.*, 2021, **9**, 3228

Immunomodulatory nanomedicine for colorectal cancer treatment: a landscape to be explored?

Maria José Silveira, [a,b,c] Flávia Castro, [a,b] Maria José Oliveira [a,b,d] and Bruno Sarmento *[a,b,e]

Colorectal cancer (CRC) is one of the deadliest cancers in the world mainly due to metastasis events. Despite improvements, the available treatment modalities for metastatic cases are limited, being generally associated with poor prognosis. As is well known, the immunosuppressive tumor microenvironment (TME) plays a key role in tumorigenesis, promoting cancer cell immune escape and disease progression. In addition, accumulating evidence indicates that the immunosuppressive microenvironment is a critical barrier for antitumor immunity in CRC, being extremely important to modulate the immune microenvironment to inhibit the tumor-promoting immune response. Therefore, new and effective cancer immunotherapeutic approaches demand a better control over the TME to reverse these immunosuppressive conditions. According to the features of different nanomedicines, nanoparticles can constitute a promising strategy, using different materials with the inherent ability to modulate TME and also with the potential to target immunosuppressive cells, to deliver antigens or immunomodulatory agents to eliminate this tumor. In this review, we summarize the importance of the TME in the progression and treatment response of CRC, exploring the potential of the nanotechnology for the development of immunomodulatory therapeutic strategies.

Received 24th January 2021,
Accepted 28th February 2021

DOI: 10.1039/d1bm00137j

rsc.li/biomaterials-science

1. Introduction

Colorectal cancer (CRC) is an alarming problem in health care with an increasing incidence among young adults.[1–3] Despite the significant advances in the pathophysiological understanding, diagnosis and treatment of CRC, the overall survival (OS) of metastatic patients remains poor, making it the second deadliest cancer in the world.[4]

Available treatments for CRC are largely based on the tumor stage.[5] However, factors such as molecular events and genetic and epigenetic alterations can play a crucial role in deciding the treatment.[6] The most important therapeutic approach for patients with local CRC is the surgical resection of the tumor.[7] However, in metastatic CRC (mCRC), surgery is not recommended due to the physical damage of the tumor mass, which can spark some metastasis.[8,9] Chemotherapy constitutes one of the frequent therapeutic approaches, especially in advanced cases, relying on three main drugs: 5-fluorouracil (5-FU), oxaliplatin and irinotecan.[7] These drugs are often combined in therapeutic regimens named FOLFOX, FOLFIRI and FOLFOXIRI which are applied specifically in different CRC stages.[10–13]

To personalize therapy and maximize the cancer cell target, a new modality for the treatment of mCRC was approved. It involves the combination of chemotherapy and targeted monoclonal antibodies, such as anti-epidermal growth factor receptor (EGFR) or anti-vascular endothelial growth factor (VEGF) antibodies, extending the survival to 2 years and longer.[14] However, despite the results, the survival rates remain low.[15]

Cancer immunotherapy has emerged to treat otherwise untreatable solid tumors, such as lung cancer and melanoma, changing the paradigm and achieving long-term durable responses.[16] This alternative approach has the ability to efficiently and specifically target immune cells, altering the tumor microenvironment (TME), of high tumor mutation burden and immune cell infiltration, the main markers of responsiveness to immunotherapy.[17] Specifically, pembrolizumab, an immunotherapeutic drug that blocks the signaling axis PD-1/PD-L1, was approved in 2017 for mCRC.[18] However, this treatment is limited to tumors with high mutational rates classified as mismatch-repair-deficient (dMMR) or with high levels of microsatellite instability (MSI-H).[19] This phenotype of CRC is molecularly

[a]*i3S – Instituto de Investigação e Inovação em Saúde, Universidade do Porto, Rua Alfredo Allen 208, 4200-135 Porto, Portugal. E-mail: bruno.sarmento@ineb.up.pt; Tel: +351 226074949*
[b]*INEB – Instituto de Engenharia Biomédica, Universidade do Porto, Rua Alfredo Allen 208, 4200-135 Porto, Portugal*
[c]*ICBAS – Instituto de Ciências Biomédicas Abel Salazar, Universidade do Porto, Rua de Jorge Viterbo Ferreira 228, 4050-313 Porto, Portugal*
[d]*FMUP – Departamento de Anatomia Patológica, Faculdade de Medicina, Universidade do Porto, Al. Prof. Hernâni Monteiro, 4200-319 Porto, Portugal*
[e]*CESPU – Instituto de Investigação e Formação Avançada em Ciências e Tecnologias da Saúde, Rua Central de Gandra 1317, 4585-116 Gandra, Portugal*

This journal is © The Royal Society of Chemistry 2021

Published on 04 March 2021. Downloaded by Universidade do Porto (UP) on 5/5/2024 9:05:19 PM.

classified as immune subtype (CMS-1), which corresponds to 15% of the total of diagnosed cases. The majority of the tumors are microsatellite stable (MSS), being subclassified into 3 subtypes: the canonical type (CMS-2), the metabolic type (CMS-3), and the mesenchymal type (CMS-4).[20,21] Therefore, immunotherapeutics displays low response rates for the majority of CRC tumors and limited efficacy when used as monotherapy.[22,23] Additionally, challenges in the immunotherapeutic index are being associated with limited dosing, renal clearance and low potential penetration through biological barriers.[24] Furthermore, one of the major limitations in the implementation of these therapeutics remains in its severe side effects which can promote autoimmunity and nonspecific inflammation.[25]

To overcome these drawbacks, nanotechnology provides new approaches that can improve the safety and efficacy of the delivery of immunotherapeutic agents counteracting the pharmacokinetic shortages.[24] The combination of nanomedicine and immunotherapy in preclinical studies revealed promising results, reinforcing the cancer–immunity cycle, through the key steps in the immune reaction cascade namely in antigen release, processing, presentation, and immune cell-mediated killing.[26] The nano-immune therapeutic combination has the potential to target cancer cells, immune microenvironment and peripheral immune system, which expand significantly the applicability of immunotherapy in cancer therapy.[26]

This review summarizes the importance of the TME in CRC progression and treatment response, exploring the potential of the nanotechnology for the development of immunomodulatory therapeutic approaches with the ability to regulate the TME. An overview of therapies based on nanotechnology with immunomodulatory effects is presented, as well as the available data on preclinical studies.

2. Understanding the TME and immune system in CRC

In a few percentages of patients, CRC can be associated with hereditary mutations. However, most of them are developed due to errors during normal cell division, environmental exposure, or a chronic inflammation condition.[27,28] Thus, in the last decade, CRC was started to be understood, not only due to the genetic alterations but also due to its interactions with the microenvironment which is composed of multiple distinct cell types derived from the neighboring mesenchymal stroma.[29–31]

The tumor microenvironment (TME), composed not only of cancer cells but also of resident and recruited inflammatory immune cells, fibroblasts, endothelial cells, inflammatory cytokines, growth factors, stromal cells, stellate cells and adipocytes, plays a key role in host immune system's fight against cancer cells.[32] Inflammatory cells, as well as their cytokines and chemokines, promote and regulate tumor growth, producing an attractive environment by the migration and differentiation of all cell types in the TME, facilitating genomic instability and promoting angiogenesis.[33] As is known, inflammation when controlled contributes for the maintenance of homeostasis.[34] However, chronic uncontrolled inflammation creates an environment with immunosuppressive activity, such as immature or dysfunctional dendritic cells (DCS), anti-inflammatory macrophages, myeloid-derived suppressor cells (MDSCs) and regulatory T cells (Tregs), which favors immune escape and tumor progression.[35–38] Moreover inflammatory signals, such as nuclear factor-κB (NF-κB) and signal transducer and activator of transcription 3 (STAT3), can promote angiogenesis and suppress immune-mediated tumor elimination.[32] Besides, tumor cells produce transforming growth factor-β (TGF-β), interleukin-10 (IL-10) and other immunosuppressive cytokines leading to a permissive TME.[39] Colorectal tumors are also able to recruit Tregs that can further produce immunosuppressive cytokines to suppress the cytotoxic T cell response and maintain immune tolerance.[39] Tumor-associated macrophages (TAMs) play also an important role in CRC tumorigenesis, due to its ability to polarize into an anti-inflammatory and pro-invasive phenotype (M2-like).[40] Furthermore, several immune checkpoint inhibitors are expressed on the surface of cancer cells but also of immune cells, binding to the programmed cell death 1 (PD-1), Fas type I transmembrane protein or cytotoxic T lymphocyte antigen 4 (CTLA-4), receptors expressed on the surface of T cells, suppressing their immune response.[41] Immune tolerance of T cells can also occur through anergy, deletion, suppression or death induced by host regulatory cells, or when T cells ignore antigen-positive cells due to inadequate affinity for the host complex of histocompatibility (MHC) molecules (Fig. 1).[42]

Similarly, immune escape of tumor cells is connected with three main factors: secretion of immunosuppressive factors, recruitment of immunosuppressive cells, loss of the immunogenicity *via* down regulation of MCH-I or impairment of T cell activity through the expression of PD-1 or of PDL-1 immune checkpoints.[43,44] Hence, tumor cells also regulate the immune response being important modulators of the immunosuppressive TME, and crucial orchestrators of the escape to immune surveillance.[45]

At the CRC microenvironment, infiltrating B and T cells were found, in tissues and related lymph nodes, both *in vitro* and *in vivo*.[46] $CD4^+$ Tregs are, generally, the most abundant lymphoid subpopulation, having the ability to suppress the activation and function of other immune cells.[46] Moreover, MHCI-loss-detecting natural killer (NK) cells were also found in CRC, leading to an ineffective tumor elimination.[43] Additionally, the immune infiltrated tumors with a high amount of $CD8^+$ and $CD4^+$ T cell infiltration within the tumor tissue and surrounding stroma have been associated with favorable outcomes in CRC, suggesting a possible role for immunoediting in the control of tumor growth.[18,47] Thus, in order to predict the treatment outcome, recurrence risk and prognosis, CRC tumors are classified into two main subtypes based on their immunoscore: immunogenic, inflamed or hot and non-immunogenic or cold tumors.[48]

Currently, the terms 'hot' and 'cold' are routinely used to classify tumors according to the T cell-infiltration: immune activated with a huge amount of T-cell infiltrated (CMS1),

Published on 04 March 2021. Downloaded by Universidade do Porto (UP) on 5/5/2024 9:05:19 PM.

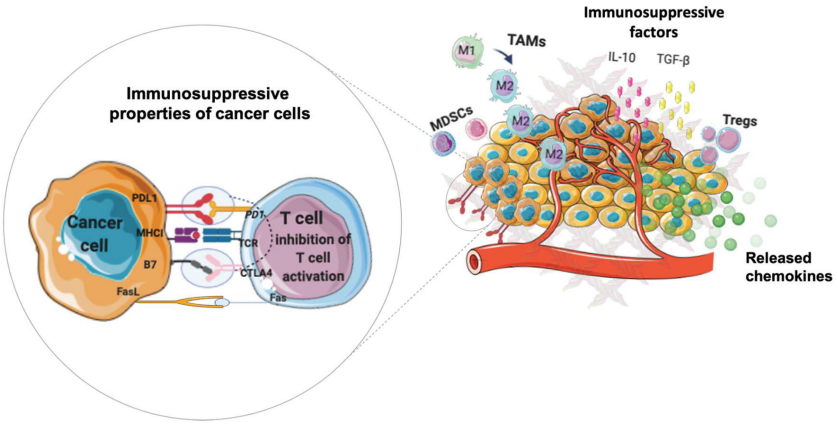


Fig. 1 Summary of the immunosuppressive mechanisms in the CRC TME: (i) production and secretion of immunosuppressive factors into the microenvironment (such as TGF-β and IL-10); (ii) recruitment of immunosuppressive cells (Tregs, MDSCs and TAMs); (iii) release of chemokines by the tumor which triggers the accumulation of Tregs and of MDSCs at the tumor sites; (iv) expression of immunosuppressive molecules on the surface of the tumor cells (Co-inhibitory signals such PD-L1 and PD-L2) promoting T cell inhibition. The ligands of the B7 co-stimulator family (CD80 or CD86) bound to CTLA-4, inactivating T cells. Similarly, membrane-bound programmed cell death ligand 1 (PD-L1) or Fas ligand (FasL) can engage PD-1 or Fas, respectively, of T cells leading to its inactivation or apoptosis.

inflamed but non-infiltrated (CMS4), and non-inflamed tumors (CMS2 and CMS3), reflecting well the higher and lower immunoscore category (Fig. 2).[49] Hence, T cells are currently recognized as the key population to fight against tumors, making use of the immunoscore an attractive option to complement prognosis and to help in guiding treatment selection.[49]

Efforts to overcome and define strategies to convert non-immunogenic cold CRC tumors (CMS-2 and CMS-3) into immunogenic inflamed ones and to restore a "CMS-1 like" immune microenvironment in the immunosuppressive CMS-4 subtype tumors are being made through many clinical trials exploiting new or combined therapies.[53] In that way, the use of the CMS classification model is very helpful to define potential therapeutic options for activating host immune responses taking into account the different strategies to treat hot tumors (CMS1 and CMS4) or to treat the ones with a lack of immune activation, termed cold tumors (CMS2 and CMS3).[54]

In a retrospective analysis, Dienstmann R. and co-workers evaluated the ratios of $CD8^+$ cytotoxic lymphocytes and cancer-associated fibroblast (CAF) infiltration in the tumor tissue confirming the linkage of the therapy resistance and the poor outcome of the treatment with the CAF content existing at the tumor microenvironment between different CMS CRC subtypes.[55]

Therefore, the immunosuppressive TME exerts a strong impact on the therapeutic response, limiting the success of standard therapies as well as of the novel immunotherapeutic approaches. Thus, immune TME targeting and modulation could be the key for the improvement of current therapeutics along with the development of more effective innovative strategies.[56–59]

3. Colorectal cancer therapy

The treatment of CRC is largely based on the stage of the disease.[60] Therefore, the assessment of the tumor stage, presence of malignant lymph nodes and distant metastases as well as of specific molecular markers help to direct the treatment and to predict the therapy response. In early stages, surgery is the first-line treatment mostly applied.[60] In colon cases, the use of adjuvant chemotherapy can dramatically improve the clinical outcome. However, in rectal cases the use of the neoadjuvant chemotherapy in non-metastatic cancers or stage III is an integral part of the successful treatment.[60] For mCRC, standard treatment mainly includes chemotherapy, surgery, targeted therapies and immunotherapy which can be managed alone or in combination with other therapeutic options.[61] Moreover, those therapies can be combined with radiotherapy in the treatment of rectal cancer.[62] Briefly, the current therapeutics for CRC are discussed below.

3.1. Radiotherapy

CRC is a complex disease which can be divided into two major subtypes: colon (CC) and rectal cancer (RC).[62] In early stages, due to the close proximity of the rectum to the pelvic structures and organs, radiotherapy (RT) is indicated as a neoadjuvant or adjuvant therapy option for RC, in order to improve the patient OS rates.[62] Chemoradiotherapy can also be associated with the treatment of RC stages II and III as a neoadjuvant therapy, providing a significant reduction of local recurrences.[62] Zhao F. *et al.*, suggested that neoadjuvant RT can be also adopted for T3/4N + M0 RC with lymph node infiltration

 This journal is © The Royal Society of Chemistry 2021

Published on 04 March 2021. Downloaded by Universidade do Porto (UP) on 5/5/2024 9:05:19 PM.

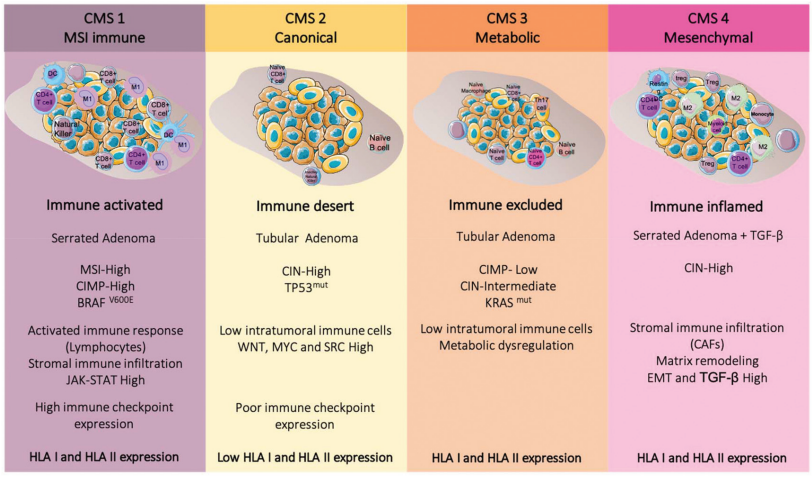


Fig. 2 Schematic illustration of the classification according to the colorectal cancer consensus molecular subtypes with the genetic modifications and intratumoral immune phenotypes. CMS1 and CMS4 are considered hot tumors due to the intense immune cell infiltration conferring a specific functional immune landscape. CMS1 tumors are enriched with activated CD4 and CD8 T cells, express high levels of HLA and immune checkpoints and have a high neoantigen load, being highly immunogenic; CMS4 tumors display an unfavorable immunosuppressive inflamed immune environment characterized by the high expression of TGF-β, VEGF, complement components and infiltration by immunosuppressive cells (Tregs, M2 macrophages, MDSCs). However, CMS2 and CMS3 are termed cold tumors due to their similar immune phenotype with poor or low immune cell infiltration. However, CMS3 tumors maintain the HLA and IC expression which differs from the CMS2.[50–52]

but without distant metastasis.[62] In CC, Hawkins A. T. *et al.*, studied the use of RT as a neoadjuvant treatment for T4 colon cancer patients and demonstrated its impact on improving patients' OS, suggesting also that neoadjuvant RT in those patients should be assessed case-by-case, to clearly define its risks and benefits.[63]

3.2. Chemotherapy

In CRC chemotherapeutic treatment, 5-fluorouracil (5-FU) can be used as a monotherapy or in combination with one or several drugs such as leucovorin (folinic acid), irinotecan, oxaliplatin and capecitabine.[64–66] These drugs are administered in adjuvant doublet or triplet chemotherapy regimens named FOLFOX (oxaliplatin plus infusion 5-FU/leucovorin), FOLFIRI (irinotecan plus infusion 5-FU/leucovorin) or FOLFOXIRI (5-FU/leucovorin infusion plus oxaliplatin and irinotecan) and CAPOX/XELOX (oral capecitabine plus oxaliplatin) to treat patients in stage III and IV.[7] In the first line therapy, the single agent-based therapy is given to the patients with poor performance or low risk of deterioration while the combined regimes remain the mainstream.[43] In metastatic cases, the use of chemotherapy improved for 20 months patients' OS, becoming the backbone of CRC treatment.[43] However, chemotherapy is associated with systemic toxicity, unsatisfactory response rates, unpredictable innate and acquire resistance and low tumor-specific selectivity.[67–69] Consequently, in order to refine or even to replace the existing chemotherapy, new approaches were developed taking into account all prognostic markers and factors (genetic profiles, molecular biomarkers and anatomic variances) for a better treatment with minimal adverse effects (Fig. 3).[70]

In the sense of the CMS stratification, prospective trials are being performed to facilitate the employment of the novel designed treatment strategies, elucidating the need for specific treatments and detaching the one-size-fits-all treatment.[52] Isella C. and co-workers using CRC patient-derived xenografts (PDXs) assessed cancer-cell intrinsic transcriptional features of the different CMS subtypes evaluating the therapy response in those subtypes.[71] Moreover, Medema JP's team evaluated the therapy response using *in vitro* and *in vivo* models. Both of them observed a decrease in 5-FU therapy response in CMS1 and CMS4 subtypes.[72] The same approach was performed for CMS2 and CMS3 subtypes showing a better response with FOLFOX therapy in both cases.[71,72] Finally, in the CMS4 subtype no response for FOLFOX therapy was shown.[71,72] However, in that case FOLFIRI therapy was available with good rates of response.[71,72]

3.3. Targeted therapies and immunotherapy

Since 2004, targeted therapies have been developed and approved for CRC treatment.[43] Those therapies can directly inhibit cancer cell proliferation and migration or can indirectly act at the level of the TME, impairing the endothelial or immune cell function, hindering tumor growth, attacking or endorsing the immune surveillance.[43] Targeted agents can

Published on 04 March 2021. Downloaded by Universidade do Porto (UP) on 5/5/2024 9:05:19 PM.

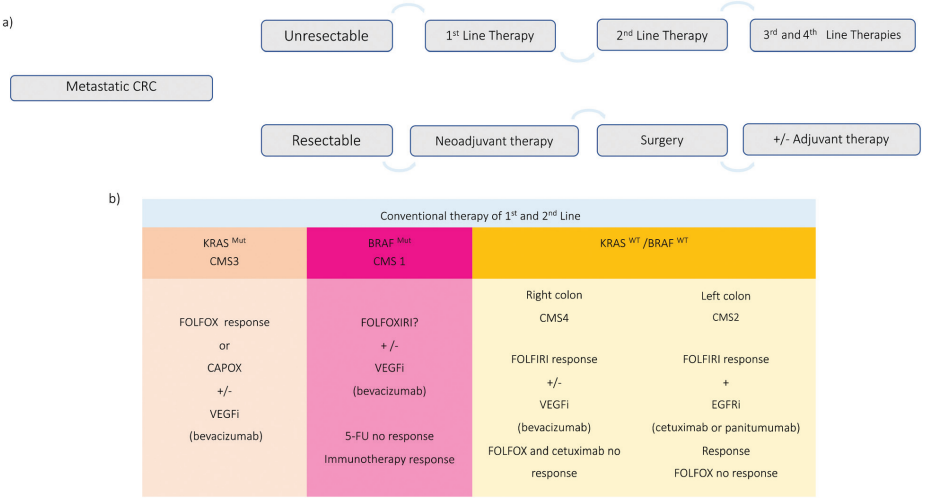


Fig. 3 Schematic illustration of the conventional treatment for mCRC: (a) summarized scheme of the therapeutic approaches, according to the resectability of the tumor; (b) summary of the response of the conventional options to treat mCRC according to the molecular stratification and CMS classification of CRC patients. Mutated (MT); wild-type (WT); with or without (±); vascular endothelial growth factor inhibitor (VEGFi); epidermal growth factor receptor inhibitor (EGFRi).

target specific receptors, inhibiting potential pathways involved in the promotion of cancer cell growth, migration, invasion and metastasis.[73] For instance, the anti-epidermal growth factor receptor (EGFR) inhibitor, Cetuximab, and the anti-angiogenesis inhibitor, Bevacizumab, were the first targeted therapies used to block pathways critical for CRC progression.[74] In fact, these targeted therapies led, when combined with chemotherapy, to an improvement of mCRC patient survival.[43] However, the success of those therapies often depends on KRAS and BRAF tumor status, revealing the crucial understanding of the molecular pathogenesis of the tumor, to appropriate treatment selection.[75]

To elucidate the impact of targeted therapies on CRC CMS subtypes, studies led by Medema JP's group and Isella C. correlated the use of different targeted therapies with the outcome in each CMS subtype.[71,72] Therefore, for the CMS1 group, bevacizumab treatment showed a favorable prognosis compared with cetuximab.[72] In contrast, in a clinical trial CALBG/SWOG80405, CMS2 patients with cetuximab treatment had favorable prognosis compared with those with bevacizumab treatment.[76] Both anti-EGFR antibody and anti-VEGF antibody treatments offered fewer benefits for CMS1/4 compared with CMS2/3.[76] Moreover, in the FIRE3 clinical trial, a prognostic difference between anti-EGFR or anti-VEGF agents was not found in accordance with the CMS subtype.[77] In other clinical trials, AGITG MAX trial, patients with CMS2/3 showed benefits from the combination chemotherapy with bevacizumab compared with CMS1/4 in the first line chemotherapy.[78]

Finally, in the CMS4 subtype cetuximab therapy was shown with no response as well as FOLFOX therapy.[71,72]

Furthermore, the discovery of immune checkpoints, like PD-1 and CTLA-4, that suppress the immune response against cancer, triggered the development and approval of blocking monoclonal antibodies with the purpose to impair their receptor binding and to enhance immune surveillance.[43]

CRC has an extensive and complex signature in terms of mutational and TME immune cell infiltration burden.[79] Therefore, the immunogenic microenvironment differs in subgroups of CRC limiting the applicability of the immunotherapy in that different subgroups.[50] Patients with CRC, who have mismatch repair-deficient (dMMR) and/or microsatellite instability-high (MSI-H) tumors, are treated with immune checkpoint inhibitor (ICI) therapy with durable responses.[80] Nivolumab and pembrolizumab, as well as nivolumab in combination with low-dose ipilimumab (all ICIs), are currently approved by the U.S. Food and Drug Administration (FDA) for patients with MSI-H/dMMR mCRC which progressed following treatment with fluoropyrimidine, oxaliplatin, and irinotecan.[81] With regard to CMS subtypes, studies led by Medema JP's group exhibited a good response in MSI CMS1 cell lines and MSI PDX treated with immunotherapy.[72]

Overman M. J. *et al.* examined the efficacy of nivolumab alone and in combination with ipilimumab in patients with dMMR-MSI-H CRC with high T cell infiltration burden, evidencing an increment of 73% and 85% twelve-month OS rate, respectively.[82] However, for tumors with reduced inflammation

 This journal is © The Royal Society of Chemistry 2021

Published on 04 March 2021. Downloaded by Universidade do Porto (UP) on 5/5/2024 9:05:19 PM.

and T cell infiltration, such as proficient MMR-MSI-low (pMMR-MSI-L) or microsatellite stable (MSS) colorectal tumors, immunotherapy was not effective. Thus, to develop a combinatory targeted therapy, Eng C. *et al.* combined a mitogen-activated protein kinase (MEK) inhibitor with an anti-PD-L1, demonstrating an increase of infiltrated $CD8^+$ T cells but without any improvement in the response or survival in mouse models.[83] Therefore, to apply the promising immunotherapy to tumors with a low mutational and immunogenic profile, unable to stimulate immune cell recruitment and activation, novel strategies, such vaccinations and adoptive T cell therapy (ATC), are currently being explored.[79]

Vaccines comprise a promising strategy which can induce an immune response through a direct stimulation of the immune system by delivering antigens to dendritic cells (DC) – antigen-presenting cells (APC), which prime and activate $CD4^+$ and $CD8^+$ T cells to initiate tumor destruction.[79] Cancer vaccines can deliver tumor-associated antigens (TAAs) or tumor-specific antigens (TSAs) allowing T cell binding to these antigens and promoting tumor cell recognition and elimination by the immune system.[84] Also, approaches like ATC, which are specific for a particular mutated antigen, may prove favorable options in combination with ICI.[79] Gros A. *et al.*, proved that circulating PD-1^+-expressing $CD4^+$ and $CD8^+$ lymphocytes can recognize human gastrointestinal cancer neoantigens, allowing the identification of circulating neoantigen-reactive lymphocytes or T cell receptors (TCRs) constituting an attractive strategy for the development of personalized immunotherapies targeting neoantigens.[85]

Furthermore, TGF-β signaling has been shown by Mariathasan S. *et al.* to cause resistance to ICI. They also proved that the inhibition of TGF-β signaling in combination with ICI led to a greater tumor regression, in preclinical studies using an EMT6 mouse mammary carcinoma model.[86]

Additionally, new combinations of treatments should be developed to produce an improvement in the response to ICI in dMMR-MSI-H CRC, and furthermore in the response that has not yet been achieved in pMMR-MSI-L CRC.

4. Immunomodulatory nanomedicine: can it improve CRC therapy?

Despite the success of the immunotherapy to target the cancer immune system, its applicability is still reduced and restricted to a small subset of patients, with low survival rates for the most solid cancers.[87] Furthermore, challenges associated with the limited efficacy and significant toxicity are also being faced.[88] Therefore, efforts to develop new immunotherapeutic agents, combined strategies or nanocarriers for their delivery are being made, in order to increase the number of patients who benefit from this therapy.[89]

In fact, nanomedicine can constitute a promising approach to improve the performance of the immunotherapy, decreasing the toxicity and refining its efficacy. In 1995, the commercial approval of Doxil, a liposomal nanomedicine, and afterwards of Abraxane, albumin nanoparticles, for cancer treatment led to the development of several nanoformulations.[26] Furthermore, those developed nanoformulations were achieved with higher tolerant dosages of chemotherapeutic drugs due to less accumulation at off-target organs and tissues, stimuli-sensitive behavior for safe trafficking and drug release, and prolonged half-lives of bioactive cargo molecules by avoiding degradation by enzymes during blood circulation.[90,91] Nowadays, preclinical and clinical data, including nanoformulations in clinical trials such mRNA nanovaccines (NCT03313778, NCT02410733) for the treatment of solid tumors and melanoma, have demonstrated that combining nanomedicine with immunotherapy can boost its therapeutic effect, due to improved ability to engage immune cells, immunomodulating the tumor, and accumulation at systemic compartments.[89]

Nano-immunotherapy has the potential to turn "cold" non-immunoresponsive tumors into "hot" immunoresponsive, due to its facility to target cancer cells or their TME and peripheral immune system, through the delivery of antigens, immunoregulatory agents and adjuvants.[88,92] Nanomedicines used to target cancer cells can induce immunogenic cell death (ICD), triggering the release of tumor antigens, proteins and adenosine triphosphate (ATP), which prime the activation of APC and consequently, promote T cell antitumoral activities.[93,94] Moreover, nanomedicines have the ability to target and inhibit immunosuppressive cells and molecules at the TME, reducing their expression.[95] They can also be employed to target the peripheral immune system to promote the activity of APC, cytotoxic T cell production and to increase the activity of peripheral effector immune cell populations, generating anti-cancer immunity (Fig. 4).[96]

Moreover, nanomedicines have also the ability to react with some up-regulated chemical species such as H^+, H_2O_2 and reactive oxygen species (ROS) within the TME leading to its modulation through its elimination, control and level reduction.[97]

Currently, nano-immunotherapy is included in the majority of the preclinical studies.[98] Considering the complexity of the CRC microenvironment, nano-immunotherapy can offer an opportunity to reverse immunosuppression, induce immune response and generate memory immune cells for long-term cancer control.[5] Although the majority of CRC patients have MSS or pMMR, new efforts to revert the immunosuppressive TME from non-responsive T cells into responsive ones have been made.[99]

The following sections and Table 1 focus and resume the relevance of nano-immunotherapy for CRC treatment.

4.1. Nanomedicine for antigen and adjuvant delivery in CRC

The use of safer and less immunogenic subunit antigens stimulates the development of efficient adjuvant delivery nanotechnologies.[111] Nanovaccines can be engineered to specifically interact with pattern recognition receptors, like toll-like

Published on 04 March 2021. Downloaded by Universidade do Porto (UP) on 5/5/2024 9:05:19 PM.

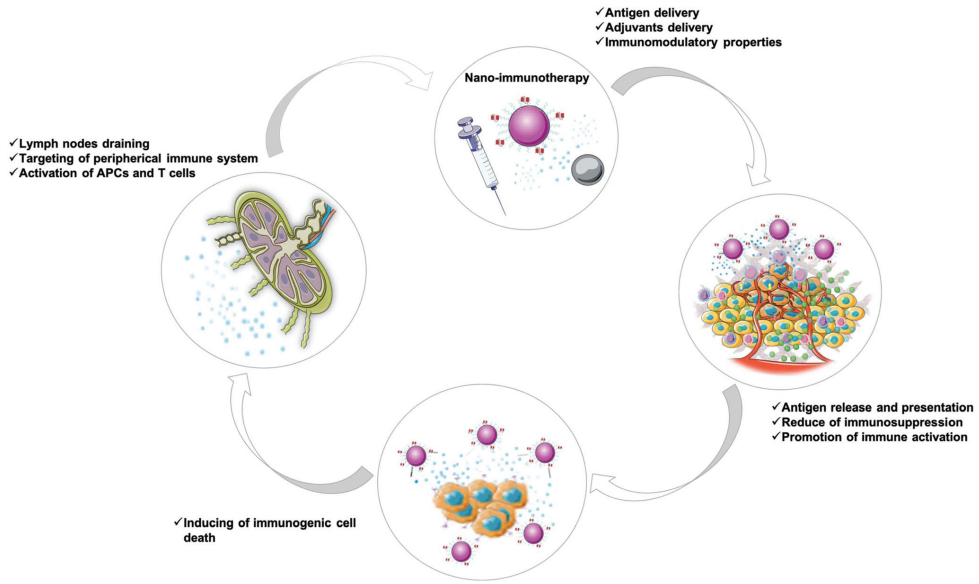


Fig. 4 Schematic illustration of the different targeting strategies in nano-immunotherapy.

receptors (TLRs) or mannose receptor (CD206), expressed on the APC surface, to trigger the innate immune response.[112] Alternatively, nanovaccines can passively target APCs, controlling antigen release or presentation and prolonging the exposure and duration of the immune response.[113] Moreover, nanocarriers can easily co-deliver TAAs and adjuvants to interact with TLRs on the DC surface, ensuring their effective activation and antigen presentation.[113] In CRC, Chen's group developed self-assembled intertwining DNA–RNA nanocapsules (iDR-NCs) to deliver synergistic DNA CpG and *Stat3*-silencing short hairpin RNA (shRNA) – microflowers (MFs).[100] CpG has the ability to trigger the toll like receptor 9 (TLR9) pathway to activate APCs, such as DCs and macrophages.[100] However, STAT3 suppresses CpG-activated immunostimulation being silenced by *Stat3*-silencing shRNA.[100] MFs were shrank into iDR-NCs using PEG-grafted cationic polypeptides to improve the delivery towards the lymph nodes. Moreover, to modulate the immune response in MC38 tumor syngeneic C57BL/6 mouse models, a specific CTL neoantigen (AdpgK) was incorporated into the NCs.[100] iDR-NC/AdpgK improved therapeutic efficacy and increased regression rates of the tumor. Furthermore iDR-NCs had the ability to deliver multiple tumor antigens to the lymph nodes for a broader spectrum of T cell response, leading to tumor cell killing and better therapeutic efficacy.[100]

Importantly, targeting lymph node tissues are being explored to generate effective immunotherapy responses.[114] APCs transporting antigen to tumor-draining lymph nodes (TdLNs) are able to prime naïve $CD8^+$ T cells.[115] Moreover, TdLNs are involved in mediating the effects of aCTLA-4 and aPD-1 therapy.[116,117] The presence of the stem-like $CD8^+$ T cell compartment has been observed in mouse and human LNs, in addition to the TME, suggesting these tissues as a potential source of tumor-infiltrating lymphocytes (TILs).[115] However, the TME and TdLNs are poorly accessed using systemic drug administration, the predominant route used in both preclinical tumor models and human patients, which may limit drug effects.[114] Nanomedicine can target specifically TdLNs improving the therapy as well demonstrated aforementioned in Chen's work.

Also, a nanovaccine based on mannose-targeted lipid calcium phosphate nanoparticles (NPs) co-encapsulating the colon cancer peptide antigen, p-AH1-A5 and each phosphorylated adjuvant, CpG, 2′3′cGAMP, or 5′pppdsRNA, was developed and the efficacy of the three adjuvants to incite similar pro-inflammatory responses was tested in an orthotopic CRC liver metastasis CT26 model.[101] To assess its pro-inflammatory effect *in vivo*, INF-γ was measured. The adjuvant 5′pppdsRNA was the only one, able to promote anti-cancer responses due to its ability to maintain low populations of immune suppressive T-reg and MDSCs in the TME.[101]

Neoantigen vaccines have been also investigated for personalized cancer immunotherapy. Ni *et al.*, developed a bi-adjuvant nanovaccine (banNV) which synergistically co-delivered

 This journal is © The Royal Society of Chemistry 2021

Published on 04 March 2021. Downloaded by Universidade do Porto (UP) on 5/5/2024 9:05:19 PM.

Table 1 Summary of the nano-immunotherapies being explored to improve CRC immunity and treatment

NP composition	NP cargo	Major advances	Immune phenotype advances	Ref.	Model
iDR-NCs PPT-*g*-PEG to assemble CPG and *Stat3*-silencing shRNA	Neoantigen (AdpgK)	Target delivery. Increase of APCs and activation of $CD8^+$ T cells. Increase of antitumor immunity	Higher expression of CD80, IL-6, IL-12p40 and TNFα in LNs	100	*In vitro* studies: RAW264.7 cell line; *in vivo* studies: C57BL/6 mice bearing MC38 syngeneic colon adenocarcinomas
LPC with DSPE-PEG-mannose	CpG, 2′3′cGAMP, or 5′pppdsRNA and p-AH1-A5	Efficient co-encapsulation of phosphorylated peptides/adjuvants Decrease of liver metastasis, Tregs and MDSC population	Higher expression of $CD8^+$. Lower expression of $CD4^+$, FOXP3+, CDllb+, and GR-1+ in primary CRC tumor	101	*In vivo* studies: BALB/c mice CRC liver metastasis using the CT-26 model
BanNV with PEG-PLA micelles and CpG-encoding template DNA, microparticles self-assembled with PEG-*g*-PPT	TLR7/8 agonist (R848); TLR9 agonist; CPG ODNs and a neoantigen (AdpgK)	Codelivery of adjuvants and neoantigens to LNs and LN-residing APCs Increase in antigen uptake and APCs, therapeutic efficacy and survival rates	Higher expression of $CD8^+$, IL-6, IL-12p40, TNFα. CD80, CD86 and CD11c in LNs	102	*In vivo* studies: C57BL/6 mice with MC38 cells injected
TCL@PDA NPs	—	Increase of the cellular uptake Delay of the tumor progression. Increase of activated $CD8^+$ and $CD4^+$ T cells Ability to modulate DC maturation	Higher expression of MHC I, MHC II, CD40, CD86, CD80, CD11c IL-6, IFN-γ and TNF-α, CCR7 in BMDCs and LNs. Higher percentage of CD44Hi CD62LHi cells in $CD4^+$ and $CD8^+$ T cell population in spleen and LNs.	103	*In vivo* studies: C57BL/6 mice with MC38 cells injected *In vitro* studies: MTT and cytotoxicity assay
PCN@FM	PDT	Increased safety Decreased cytotoxicity	Higher expression of CD86, CD80 and $CD3^+$ in the tumor tissues	104	*In vitro* studies: CT26 mouse colon cancer cells *In vivo* studies: BALB/c with injected 4T1cells
NP@FM PEG	—	Biocompatible Low cytotoxicity Achievement of LNs and APC Increase of T cell activation; $CD3^+$ and $CD8^+$ CTLs	Higher expression of CD86 and CD80 DC, IL-6, TNF-α, $CD3^+$, $CD8^+$ in BMDCs and higher expression of $CD3^+$, $CD8^+$ LNs	105	*In vitro* studies: 4T1 cells, 3T3 cells and CT26 cells *In vivo* studies: BALB/c with injected 4T1cells
AgNP	Anti-PD1	APC activation	Higher expression of CD86, CD80 and CD11c and CD86-positive M1-phenotype macrophages in BMDCs	106	*In vitro* studies: CT26 cells and 3T3 cells
M13@Ag	FOLFIRI	Increase of the survival	Higher expression of $CD8^+$ and IFN-γ in spleen and tumor tissues Decrease of Tregs and MDSC markers as well as IL-10 expression in spleen and tumor tissues		*In vivo* studies: BALB/c mice with injected CT26 cells
sHDL ApoA1	DOX	Stimulation of $CD8^+$ T cell responses Enhancement of the recognition of TAAs, neoantigens and tumor cells	Higher expression of IFN-γ + CD8α+ T cells at the basal level, CD11c + CD11b + Ly6c + DCs, and CD86+ in TDLNS	107	*In vivo* studies: BALB/c mice with CT26 and MC38 colon

Published on 04 March 2021. Downloaded by Universidade do Porto (UP) on 5/5/2024 9:05:19 PM.

Table 1 *(Contd.)*

NP composition	NP cargo	Major advances	Immune phenotype advances	Ref.	Model
PC7A NPs	Anti-PD1	Strong cytotoxic T cell response with low systemic cytokine expression Inhibition of tumor growth Generation of long-term anti-tumor memory	Higher expression of IFN-γ+ and $CD8^+$ T cells in BMDCs and spleen	108	*In vivo* studies: C57BL/6 mice with MC38
Ch/γ-PGA	—	T cell activation	Higher expression of CD86, CD40, HLA-DR, TNF-α, $CD4^+$ and $CD8^+$ IL-12p40 and IL-6 in co-cultures.	109	*In vitro* studies: RKO cell lines
		Decrease of the tumor invasion	Decrease of CD163 expression in co-cultures		
OCD	—	Excellent H_2O_2-eliminating capability Anti-inflammatory activity	Lower expression of MPO, TNF-α, IL-1β, and IL-6	110	*In vitro* studies: C26 mouse colon carcinoma cells and Caco-2 human intestinal epithelial cells; RAW264.7 cells

1,2-Distearoyl-*sn-glycero*-3-phosphoethanolamine-*N*-(polyethyleneglycol)-mannose (DSPE-PEG-mannose); apolipoprotein A1 (ApoA1); bi-adjuvant nanovaccine (banNV); bone marrow dendritic cells (BMDCs); chitosan and poly-γ-glutamic acid materials (Ch/γ-PGA NPs); cytomembranes (FM); DNA–RNA nanocapsules (iDR-NCs); doxorubicin (DOX); H_2O_2-eliminating β-CD material (OCD); lymph nodes (LNs); lipid calcium phosphate nanoparticles (LPC); myeloperoxidase (MPO); nanoparticles with cytomembrane (NP@FM); oligodeoxynucleotides (ODNs); photodynamic therapy (PDT); polydopamine nanoparticles with tumor cell lysate (TCL@PDA NPs); polyethylene glycol-grafted polypeptide (PPT-*g*-PEG); polyethylene glycol-polylactic acid (PEG-PLA); polymeric NPs and tumor antigens (PC7A NPs); porphyrin-based Zr-MOF and with FM (PCN@ FM); silver nanoparticles (AgNP); surface capsid protein (M13@Ag); synthetic high density lipoprotein (sHDL) nanodiscs; tumor associated antigens (TAAs); tumor-draining lymph nodes (TDLNs); lipid calcium phosphate nanoparticles (LPC); polyethylene glycol-polylactic acid (PEG-PLA).

the TLR7/8agonist (R848) and the TLR9 agonist CPG oligodeoxynucleotides (ODNs), as well as a neoantigen (Adpgk) peptide on PEG-PLA micelles to potentiate anti-PD-1 immunotherapy in CRC.[102] The codelivery of these neoantigens with the dual synergistic adjuvants led to a more than 3.65 fold tumor regression in treated mice when compared with the ones that have been treated with a single adjuvant plus the neoantigen.[102] Moreover, in a MC38 orthotopic C57BL/6 CRC model, BanNVs sensitized immune checkpoint PD-1 on T cells and, when combined with anti-PD-1 antibody, induced therapy response with an increased survival rate to 70% on day 48, compared with 40% of survival rate by BanNVs alone.[102]

Biomimetic nanotechnology, mainly cancer-derived membranes, has also been explored for the design of anticancer vaccines to improve the multi-antigenic immune response.[118]Therefore, it has been demonstrated that cancer-derived membrane nanoparticles, with an immunostimulatory adjuvant, could facilitate enhanced antigen presentation, leading to the activation of tumor-specific cellular responses.[118] In CRC, Wang *et al.*, developed polydopamine nanoparticles (PDA NPs) with tumor cell lysates (TCLs) covalently attached (TCL@PDA NPs).[103] This biomimetic nanosystem, TCL@PDA NPs, showed a safety improvement and decreased cytotoxicity when compared with TCL and PDA for 48 h.[103] TCL@PDA NPs could promote a 2.6 higher uptake of antigens, enhancing bone marrow dendritic cell (BMDC) maturation and the expression of surface co-stimulatory molecules and secretion of Th1-related cytokines.[103] The spleen and lymph nodes $CD4^+$ and $CD8^+$ of T cell subpopulations were also significantly enhanced, and the production of memory T cells increased, which sustained immune surveillance and provided long-term protection against the tumor.[103] Moreover, empty PDA NPs had the ability to modulate DC maturation by increasing their ability to express MHC II and secrete Th1-related cytokines.[103]

Inspired by the development of biomimetic nanotechnology, Liu *et al.*, explored the development of cytomembrane nanovaccines.[104] In this approach fused cytomembranes (FMs) acquired from the fusion of cancer and DCs contributed to APC activation.[104] This nanosystem was constructed using porphyrin-based Zr-MOF (PCN-224) and FM (PCN@FM) for the combination of photodynamic therapy (PDT) and immunotherapy (Fig. 5a). The targeting effectiveness of the nanosystem was evaluated in 4T1 cell lines and compared with mouse colon cancer cells CT26. The developed nanosystem exhibited high uptake for 4T1 cell lines due to the tumor antigen expression.[104] Next, in order to generate a cellular nanovaccine, with the ability to offer a powerful immune response towards multiple tumor types, the same team developed nanoparticles-supported stimulatory molecules on the cytomembrane (NP@FM).[105] Therefore, DCs and tumor cells were fused and NPs based on polyethylene glycol (PEG) were incorporated as a support of FMs.[105] The successful fusion of the DCs and 4T1 cells allowed the antigen peptide-major histo-

 This journal is © The Royal Society of Chemistry 2021

Published on 04 March 2021. Downloaded by Universidade do Porto (UP) on 5/5/2024 9:05:19 PM.

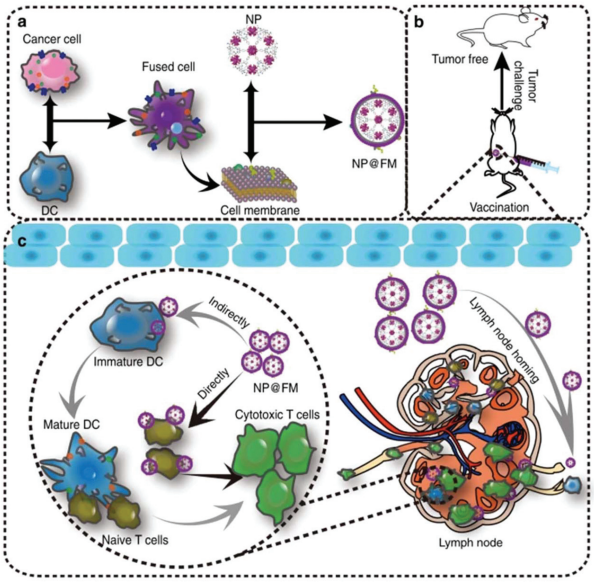


Fig. 5 Schematic illustration of NP@FM for tumor prevention: (a) schematization of the steps to develop NP@FM; (b) vaccination of mouse models with the developed NP@FM; (c) mechanisms of NP@FM to induce immune response.[105] Reproduced from Wen-Long Liu *et al.*[105] with permission from Springer Nature, copyright 2019.

compatibility complex (pMHC) expression on the cytomembrane.[105] Due to the similarity in outer membranes, NP@FM inherits and even amplifies the interfacial biofunctions of the two parent cell lines, such as the lymph node-homing capacity of DCs.[105] This nanosystem was also proved biocompatible and safe with low cytotoxicity *in vitro* using 4T1 cells, normal murine fibroblasts (3T3) and mouse colon cancer CT26 cells.[105] The transcriptome was also investigated in the cells treated with NP@FM and compared with those treated with phosphate buffer solution (PBS). An upregulation of the genes related to the immune system was verified demonstrating the ability of the system to induce the immune response.[105] *In vivo* assays using BALB/C mice with 4T1cells injected subcutaneously were performed in order to assess the properties of the nano-cytomembrane in the achievement of lymph nodes, favoring T cell antigen presentation (Fig. 5b).[105] That cytomembrane nanovaccine mimics APCs, and had the ability to directly act on T cell activation (Fig. 5c).[105]

In that study, mice were pretreated with cytomembrane-coated nanovaccines and compared with the nanosystem coated with the cancer membrane. Mice subjected to the treatment of cytomembrane-coated nanovaccines reached a tumor-free of 60% for at 36 days, compared with 20% of the mice treated with nanosystems coated with the cancer membrane.[105] Also, the secretion level of IL-6 and IFN-γ was determined by ELISA, being the levels of secretion of IFN-γ and IL-6 about 27 and 3 times more than the group treated with PBS.[105] Moreover, the vaccination with MOF@FM led also to a significant increment of $CD3^+$ $CD8^+$ CTLs.[105]

Protein-nanoparticles (PNPs) are other approach that are being studied as natural carriers for antigen delivery and can be obtained by the self-assembly of protein structures.[113] Particularly, PNPs derived from heat-shock proteins (HSPs) can exhibit strong receptor-specific interactions with APCs facilitating antigen presentation and, consequently, the immune stimulation.[113] Previous clinical studies led by Mazzaferro *et al.*, tested cancer vaccines, using antigenic peptides bound to HSP96, in patients with colorectal liver metastases.[119] This study demonstrated an increase in $CD8^+$ T cell response against colon cancer.[119] Notably, the OS was improved by two-years and the antitumor immune response revealed to be independent of clinical prognostic factors.[119] These results highlight the potential of HSP use to deliver antigens, which can be further improved when combined with PNPs.[119]

CRC development is associated with the gut microbiota. The enriched CRC tissue with bacteria such as *Fusobacterium nucleatum* (*Fn*) is associated with an immunosuppressive myeloid cell, at the TME to further diminish T cell responses. On the other hand, silver nanoparticles (AgNPs), an inorganic nanomaterial, are known to exhibit excellent antibacterial activity. Therefore, Dong *et al.* developed a phage-based bio-inorganic hybridization system to rebuild the tumor-immune

Published on 04 March 2021. Downloaded by Universidade do Porto (UP) on 5/5/2024 9:05:19 PM.

microenvironment *via* manipulation of gut microbiota for CRC suppression. In their study, AgNPs were assembled electrostatically on its surface capsid protein (M13@Ag) to achieve specific clearance of *Fn* and remodel the TME. Both *in vitro* and *in vivo* studies showed that M13@Ag treatment could scavenge *Fn* in the gut, and reduce MDSC amplification at the tumor site. In addition, antigen-presenting cells (APCs) were activated by M13 phages to further awaken the host immune system. M13@Ag combined with immune checkpoint inhibitors (α-PD1) or chemotherapeutics (FOLFIRI) significantly prolonged overall mouse survival in an orthotopic CRC model.[106]

Overall, nano-based formulations can potentiate the anticancer effects induced by vaccines, by protecting the antigens and adjuvants from degradation, and by increasing its delivery at the specific site as well as by activating immune cells through their inherent immunostimulatory properties.

4.2. Nanomedicine for immunomodulatory strategies in CRC

The physicochemical properties of the natural or synthetic materials used in the development of the immunomodulatory nanomedicines are extremely important once they can influence the interaction with immune cells and, consequently their biological response.[120] Particularly, molecular weight, and degree of acetylation, as well as properties of nano-based formulations such as size, hydrophobicity, surface charge and coating antigens determine their level of interaction with the TME.[121]

Nanomedicines when entering in circulation can adsorb molecules on their surface, causing their deformation, folding and immunogenic response, being recognized as foreign agents by the host immune system.[122] To overcome this, coating NPs with PEG (PEGylation) allow a reduction of protein adsorption avoiding clearance.[123] Moreover, depending on the material and formulation used, when NPs are administered they can interact with DCs, affecting antigen presentation to T cells and thereby, modulating the adaptive immune response.[124] For example, NPs can be engineered to engage and interact with APCs or T cells or act in a specific cell surface ligand.[98] Hence, smaller artificial APC (aAPC) NPs with about 50 nm are reported as less efficient to activate T cells than those with sizes around 300 nm.[125]

Regarding immunostimulatory strategies, Kuai *et al.* demonstrated the efficacy of synthetic high-density lipoprotein (sHDL) nanodiscs to improve, in CRC, DC antigen presentation.[107] Nanodiscs were synthesized with a synthetic high-density lipoprotein composed of apolipoprotein A1 (ApoA1) mimetic peptide and of phospholipids, for stimuli-responsive delivery of the chemotherapeutic agent. Afterwards nanodiscs were loaded with doxorubicin (DOX) to induce antitumor T cell responses.[107] Delivery of DOX *via* nanodiscs triggered immunogenic cancer cell death and exerted antitumor efficacy without any overt off-target side effects, eliciting $CD8^+$ T cell responses, and enhancing the recognition of TAAs, neoantigens and tumor cells.[107] The strategy was also combined with free anti-PD1 therapy in BALB/c mice, inducing a complete regression of established CT26 and MC38 colon carcinomas in 80 to 88% of the animals, and protecting survivors against tumor recurrence.[107] Therefore, engineered stimuli-responsive nanomaterials demonstrate to improve antitumor responses increasing the drug delivery effect.[126]

Luo M. *et al.*, developed a minimalist nanovaccine for colon cancer, comprising polymeric NPs (PC7A NPs) and tumor antigens, without incorporation of adjuvants. This vaccine efficiently delivered the antigen to the APCs in lymph nodes, inducing antigen surface presentation and type I interferon-stimulated genes, which was STING-dependent.[108] These PC7A NPs generated a strong cytotoxic T cell response with low systemic cytokine expression.[108] Additionally, the PC7A nanovaccine was combined with an anti-PD-1 inhibitor showing great synergy, with 100% survival over 60 days in MC38 colon cancer in the C57BL/6 mice model, and leading to a complete tumor growth inhibition, suggesting the generation of long-term antitumor memory.[108] Therefore, this nanovaccine not only enhances antigen delivery and cross-presentation, but also stimulates the STING pathway to boost antitumor immunity for colon cancer immunotherapy.[108]

Other studies showed the inherent immunostimulatory properties of chitosan and poly-γ-glutamic acid materials in CRC. Castro *et al.* demonstrated that empty Ch/γ-PGA NPs have also the ability to reprogram immunosuppressive human macrophages, as well as immature DCs, towards an immunostimulatory profile. This immune cell activation induced $CD4^+$ and $CD8^+$ T cell activation and decreased the invasion of CRC cells *in vitro*.[109] Furthermore, these Ch/γ-PGA NPs also potentiated radiotherapy effects, reinforcing their potential as immune adjuvants to anticancer therapy.[127]

In order to elucidate the impact of nanoparticles on macrophage physiology and cancer growth, Zanganeh *et al.* investigated the impact of iron oxide nanoparticle compound ferumoxytol *in vitro* and *in vivo* using MMTV-PyMT-derived cancer cells into the bilateral mammary fat pads of female FVB/N mice.[128] A similar therapeutic effect was also assessed using KP1-GFP-Luc cells intravenously injected into NOD.Cg-Prkdcscid Il2rgtm1Wjl/SzJ mice.[128] Iron oxide nanoparticles significantly suppressed tumor growth by inducing pro-inflammatory macrophage responses.[128] *In vitro* studies showed that superparamagnetic iron oxides induce a phenotypic shift in M2 macrophages towards a high $CD86^+$, TNFα positive M1 macrophage subtype 34.[128] This M1 polarization can induce a Fenton reaction which, in turn, can induce cancer cell apoptosis.[128] *In vivo* assays demonstrated the shift of macrophage polarization towards M1 phenotypes whereas tissue-resident macrophages lost their M2 polarization.[128] Moreover, pretreatment with ferumoxytol can inhibit tumor metastases.[128] Although these data were not validated or applied to CRC, ferumoxytol could be exploited to CRC TME in order to modulate the immunosuppressive TME.

A ROS-responsive and H_2O_2-eliminating material was synthesized by Zhang *et al.*, confirming the effectiveness of the developed NPs to attenuate oxidative stress and inflammatory response in CRC.[110]

 This journal is © The Royal Society of Chemistry 2021

Published on 04 March 2021. Downloaded by Universidade do Porto (UP) on 5/5/2024 9:05:19 PM.

4.3. Combinatory nanotherapies

Several approaches combining chemotherapy and immunotherapy are being investigated, to boost the immune response and to promote effective therapy. For example, in the CRC, Li *et al.* developed a bilayer system composed of paclitaxel (PTX)-loaded gelatin nanogels (GN) as the inner cores and HT-29 tumor cell membranes (TCM) as the outer shells (TCM/GN/PTX).[129] This TCM coated GN had the ability of tumor targeting and to effectively accumulate at the tumor site.[129] In that biomimetic cell membrane-coated nanosystem, NPs have the ability to possess the diversity of the surface antigen of the source cell. In particular TCM presents the natural ability to target homotypic tumor cells due to the presence of natural and multiple antigens on its surface such as homologous proteins and immune escape proteins.[129] The *in vivo* antitumor activity was towards HT-29 xenografts mouse models indicating that the TCM/GN/PTX strategy could suppress tumor cell growth through induction of tumor cell necrosis and apoptosis.[129] Moreover, He *et al.* designed a polymer core–shell NP carrying oxaliplatin and the photosensitizer pyropheophorbide-lipid (pyrolipid).[130] NPs were then combined with the ICIs anti-CTLA4 and anti-PDL-1 to improve its blocking, activating T cell signaling and reducing tumor immune escape.[131] The CT26 colorectal cancer model treated with those NPs and immune checkpoint inhibitors (anti-PD-L1) showed a significant reduction of primary and distant tumor cells when comparison to those treated with anti-PD-L1 alone.[130]

Yan S. *et al.* reported the preparation of microneedles (MN) with hyaluronic acid integrated in pH-sensitive dextran NPs encapsulating anti-PD-1 and glucose oxidase to impair CRC tumor progression.[131] Also, mannosylated chitosan (MC) was developed by Kim *et al.* to induce mannose receptor-mediated endocytosis of IL-12 directly into DCs which reside within the tumor. MC was proven to be suitable for IL-12 gene delivery to DCs leading to a clear suppression of CRC growth and angiogenesis.[132] Liu *et al.* developed a non-toxic hybrid nanosystem by the self-assembly method, DOTAP/MPEG-PLA-pIL12 (DMP-pIL12), able to inhibit colorectal tumor growth *in vivo* by increasing the secretion of the anti-proliferative and anti-angiogenic mediators IL-12, IFN-γ, and TNF-α, which promoted the increase of cytotoxic T cells.[133]

These studies highlighted the importance of the different approaches regarding NP design and material composition to modulate the TME and also to deliver immunomodulatory agents, proving immune cell reprograming and an efficient therapeutic response.[134]

5. Challenges and future perspectives

Far from patients with dMMR-MSI-H CRC, single immunotherapy has not evidenced a clinical benefit in patients with pMMR-MSI-L CRC, probably due to the lack of immune players at the tumor site. This feature remains a crucial obstacle to immunotherapy efficacy in these patients, being necessary for the development of new combinatory strategies. The combination of ICIs with other immunostimulatory agents, able to recruit immune cells to the TME, might be beneficial in patients with pMMR-MSI-L CRC, reviewed at ref. 18. Furthermore, colorectal tumors infiltrated with immunosuppressive cells (CSM2 and CSM3) can also be the target of immunotherapy, after reprogramming of their immune profile towards an immunostimulatory one. Several agents, like TLR ligands, MDSC inhibitors, and TGF-β inhibitors, might be employed to reeducate the immune cells at the tumor site. Besides the recruitment and reprograming of the tumor immune compartment, the therapeutic outcome of some immunotherapeutic strategies is still limited. While in cancer vaccines, the antigen and adjuvant delivery can face enzymatic degradation, the delivery of ICIs also has some drawbacks, like unspecificity for the TME, resulting in side-effects. To overcome these limitations, nanomedicine can contribute with formulations that specifically co-deliver antigens, adjuvants and immunotherapeutic drugs further potentiating immunotherapy efficacy. Despite promising, nanomedicine remains an expensive and time-consuming process. Important issues related to the clinical development of nano-based formulations, including biological challenges, biocompatibility, and biosafety as well as large-scale manufacturing and government regulations should be addressed.

6. Conclusion

Immunotherapy brought a breakthrough in the field of cancer treatment, changing after decades the disappointing results in the treatment of many cancers. Despite in CRC, only a few percentages of patients can take advantage of its benefits, several research studies continue to explore the role of this therapy not only for a selected group but for all patients, as monotherapy or in combination with other therapeutic approaches. However, the standard therapeutic regimens currently used to treat mCRC takes into account the potential of its benefit in comparison with chemotherapy. This approach of combined treatment produces enhanced anticancer effects, but due to its low bioavailability and toxicity new targeted therapies are emerging to reduce side effects and also increase the bioavailability of the drugs. Since nanosystems are able to improve the effect of conventional anticancer therapies, several researchers are exploring nanotechnology potential for immunotherapy modality. On their turn, NPs can affect immune cells and their responses within the TME. NPs can target and stimulate the immune system enhancing and activating immune cells, such as T cells. However, properties related to the design, size, material composition and surface modification are also important to explore and understand how engineered nanomaterials interact with the immune system. The advances in this field of nanotechnology remain with many challenges being extremely important to harness

Published on 04 March 2021. Downloaded by Universidade do Porto (UP) on 5/5/2024 9:05:19 PM.

immunomodulatory nanostrategies to improve the cancer patient's treatment and outcome.

Conflicts of interest

There are no conflicts to declare.

Acknowledgements

This paper was financed by Portuguese funds through FCT – Fundação para a Ciência e a Tecnologia/Ministério da Ciência, Tecnologia e Ensino Superior in the framework of the project "Institute for Research and Innovation in Health Sciences". UID/BIM/04293/2019. Maria José Silveira gratefully acknowledges FCT for the financial support through the BiotechHealth PhD Program grant and NORTE-01-0145-FEDER-000012 in the scope of the Project Structured Programme on Bioengineering Therapies for Infectious Diseases and Tissue Regeneration, funded by "FEDER – Fundo Europeu de Desenvolvimento Regional" and Norte Portugal Regional Operational Programme (NORTE 2020). Flávia Castro acknowledges Fundação para a Ciência e a Tecnologia (FCT), Portugal for the financial support in the framework of the project "p28Nano – Cell penetrating p28 peptide-mediated delivery of nanomedicines for cancer treatment" (POCI-01-0145-FEDER-030034).

References

1 L. R. Zarour, S. Anand, K. G. Billingsley, W. H. Bisson, A. Cercek, M. F. Clarke, L. M. Coussens, C. E. Gast, C. B. Geltzeiler, L. Hansen, K. A. Kelley, C. D. Lopez, S. R. Rana, R. Ruhl, V. L. Tsikitis, G. M. Vaccaro, M. H. Wong and S. C. Mayo, *Cell. Mol. Gastroenterol. Hepatol.*, 2017, **3**, 163–173.
2 W. H. Organization, A report about cancer, https://www.who.int/news-room/fact-sheets/detail/cancer.
3 I. Marmól, C. Sánchez-de-Diego, A. Pradilla Dieste, E. Cerrada and M. J. Rodriguez Yoldi, *Int. J. Mol. Sci.*, 2017, **18**, 197.
4 M. Kreidieh, D. Mukherji, S. Temraz and A. Shamseddine, *BioMed Res. Int.*, 2020, **2020**, 9037217.
5 R. Rampado, S. Crotti, P. Caliceti, S. Pucciarelli and M. Agostini, *J. Oncol.*, 2019, **2019**, 2740923.
6 M. P. Singh, S. Rai, A. Pandey, N. K. Singh and S. Srivastava, *Genes Dis.*, 2019, DOI: 10.1016/j.gendis.2019.10.013.
7 B. A. Cisterna, N. Kamaly, W. I. Choi, A. Tavakkoli, O. C. Farokhzad and C. Vilos, *Nanomedicine*, 2016, **11**, 2443–2456.
8 T. S. Hong, J. W. Clark and K. M. Haigis, *Cancer Discovery*, 2012, **2**, 117.
9 R. K. Yantiss, *Surg. Pathol. Clin.*, 2017, **10**, 961–976.
10 A. Jain and S. Jain, *Hawaii J. Med. Public Health*, 2019, **78**, 195–199.
11 J. Virostko, A. Capasso, T. E. Yankeelov and B. Goodgame, *Cancer*, 2019, 3706–3708.
12 R. L. Siegel, K. D. Miller and A. Jemal, *CA Cancer J. Clin.*, 2017, **67**, 7–30.
13 E. Dekker, P. J. Tanis, J. L. A. Vleugels, P. M. Kasi and M. B. Wallace, *Lancet*, 2019, **394**, 1467–1480.
14 I. S. Yu and W. Y. Cheung, *Can. J. Gastroenterol. Hepatol.*, 2018, **2018**, 9450754.
15 S.-y. Lee and S. C. Oh, *BioMed Res. Int.*, 2016, **2016**, 7590245.
16 G. Golshani and Y. Zhang, *Ther. Adv. Gastroenterol.*, 2020, **13**, 1756284820917527.
17 M.-J. Gorbet and A. Ranjan, *Pharmacol. Ther.*, 2020, **207**, 107456.
18 K. Ganesh, Z. K. Stadler, A. Cercek, R. B. Mendelsohn, J. Shia, N. H. Segal and L. A. Diaz Jr., *Nat. Rev. Gastroenterol. Hepatol.*, 2019, **16**, 361–375.
19 M. A. Morse, H. Hochster and A. Benson, *Oncologist*, 2020, **25**, 33–45.
20 J. Guinney, R. Dienstmann, X. Wang, A. de Reyniès, A. Schlicker, C. Soneson, L. Marisa, P. Roepman, G. Nyamundanda, P. Angelino, B. M. Bot, J. S. Morris, I. M. Simon, S. Gerster, E. Fessler, F. D. S. E. Melo, E. Missiaglia, H. Ramay, D. Barras, K. Homicsko, D. Maru, G. C. Manyam, B. Broom, V. Boige, B. Perez-Villamil, T. Laderas, R. Salazar, J. W. Gray, D. Hanahan, J. Tabernero, R. Bernards, S. H. Friend, P. Laurent-Puig, J. P. Medema, A. Sadanandam, L. Wessels, M. Delorenzi, S. Kopetz, L. Vermeulen and S. Tejpar, *Nat. Med.*, 2015, **21**, 1350–1356.
21 K. Thanki, M. E. Nicholls, A. Gajjar, A. J. Senagore, S. Qiu, C. Szabo, M. R. Hellmich and C. Chao, *Int. Biol. Biomed. J.*, 2017, **3**, 105–111.
22 A. Bittoni, V. Sotte, T. Meletani, L. Cantini, R. Giampieri and R. Berardi, *J. Cancer Metastasis Treat.*, 2018, **4**, 55.
23 M. S. Goldberg, *Nat. Rev. Cancer*, 2019, **19**, 587–602.
24 Y. Li, C. Ayala-Orozco, P. R. Rauta and S. Krishnan, *Nanoscale*, 2019, **11**, 17157–17178.
25 R. S. Riley, C. H. June, R. Langer and M. J. Mitchell, *Nat. Rev. Drug Discovery*, 2019, **18**, 175–196.
26 Q. Sun, X. Bai, A. M. Sofias, R. van der Meel, E. Ruiz-Hernandez, G. Storm, W. E. Hennink, B. De Geest, F. Kiessling, H.-j. Yu, T. Lammers and Y. Shi, *Acta Pharmacol. Sin.*, 2020, **41**, 954–958.
27 P. S. Erica, A. Golemis, T. N. Beck, E. M. Scolnick, D. J. Hunter, E. Hawk and N. Hopkins, *Genes Dev.*, 2018, **32**, 868–902.
28 A. Lasry, A. Zinger and Y. Ben-Neriah, *Nat. Immunol.*, 2016, **17**, 230–240.
29 C. Pottier, A. Wheatherspoon, P. Roncarati, R. Longuespee, M. Herfs, A. Duray, P. Delvenne and P. Quatresooz, *Expert Rev. Anticancer Ther.*, 2015, **15**, 943–954.
30 T. Colangelo, G. Polcaro, L. Muccillo, G. D'Agostino, V. Rosato, P. Ziccardi, A. Lupo, G. Mazzoccoli, L. Sabatino and V. Colantuoni, *Biochim. Biophys. Acta, Rev. Cancer*, 2017, **1867**, 1–18.

 This journal is © The Royal Society of Chemistry 2021

Published on 04 March 2021. Downloaded by Universidade do Porto (UP) on 5/5/2024 9:05:19 PM.

31 D. Hanahan and R. A. Weinberg, *Cell*, 2011, **144**, 646–674.
32 N. B. Janakiram and C. V. Rao, in *Inflammation and Cancer*, ed. B. B. Aggarwal, B. Sung and S. C. Gupta, Springer Basel, Basel, 2014, pp. 25–52, DOI: 10.1007/978-3-0348-0837-8_2.
33 L. M. Coussens and Z. Werb, *Nature*, 2002, **420**, 860–867.
34 A. G. Long, E. T. Lundsmith and K. E. Hamilton, *Curr. Colorectal Cancer Rep.*, 2017, **13**, 341–351.
35 R. Singh, G. Dumlupinar, S. Andersson-Engels and S. Melgar, *Int. J. Nanomed.*, 2019, **14**, 1027–1038.
36 M. Y. Tao, Z. H. Wang, M. H. Zhang, T. H. Ma, X. Z. Yang, S. N. Wu, X. F. Chen and H. G. Wang, *Medicine*, 2018, **97**, e13156.
37 J. N. Kather and N. Halama, *Br. J. Cancer*, 2019, **120**, 871–882.
38 G. Guo, Y. Wang, Y. Zhou, Q. Quan, Y. Zhang, H. Wang, B. Zhang and L. Xia, *J. Immunother. Cancer*, 2019, **7**, 179.
39 L. Fuhr, M. Abreu, A. Carbone, R. El-Athman, F. Bianchi, M. O. Laukkanen, G. Mazzoccoli and A. Relógio, *Cancers*, 2019, **11**, 988.
40 M. L. Pinto, E. Rios, C. Durães, R. Ribeiro, J. C. Machado, A. Mantovani, M. A. Barbosa, F. Carneiro and M. J. Oliveira, *Front. Immunol.*, 2019, **10**, 1875.
41 Y. Xiong, Y. Wang and K. Tiruthani, *Nanomedicine*, 2019, **21**, 102034.
42 J. M. Fritz and M. J. Lenardo, *J. Exp. Med.*, 2019, **216**, 1244–1254.
43 Y.-H. Xie, Y.-X. Chen and J.-Y. Fang, *Signal Transduction Targeted Ther.*, 2020, **5**, 22.
44 J. J. Havel, D. Chowell and T. A. Chan, *Nat. Rev. Cancer*, 2019, **19**, 133–150.
45 C.-C. Chang, B.-R. Lin, T.-S. Wu, Y.-M. Jeng and M.-L. Kuo, *World J. Gastroenterol.*, 2014, **20**, 6826–6831.
46 X. Zhang, S. Kelaria, J. Kerstetter and J. Wang, *J. Gastrointest. Oncol.*, 2015, **6**, 307.
47 J. S. O'Donnell, M. W. L. Teng and M. J. Smyth, *Nat. Rev. Clin. Oncol.*, 2019, **16**, 151–167.
48 D. S. Chen and I. Mellman, *Nature*, 2017, **541**, 321–330.
49 J. Galon and D. Bruni, *Nat. Rev. Drug Discovery*, 2019, **18**, 197–218.
50 E. Picard, C. P. Verschoor, G. W. Ma and G. Pawelec, *Front. Immunol.*, 2020, **11**, 369.
51 H. Sawayama, Y. Miyamoto, K. Ogawa, N. Yoshida and H. Baba, *Ann. Gastroenterol. Surg.*, 2020, **4**, 528–539.
52 J. Y. Buikhuisen, A. Torang and J. P. Medema, *Oncogenesis*, 2020, **9**, 66.
53 A. Spallanzani, F. Gelsomino, F. Caputo, C. Santini, K. Andrikou, G. Orsi, M. Rimini, S. Pipitone, L. Riggi, C. Bardasi, M. Salati and S. Cascinu, *J. Cancer Metastasis Treat.*, 2018, **4**, 28.
54 P. Bonaventura, T. Shekarian, V. Alcazer, J. Valladeau-Guilemond, S. Valsesia-Wittmann, S. Amigorena, C. Caux and S. Depil, *Front. Immunol.*, 2019, **10**, 168–168.
55 R. Dienstmann, G. Villacampa, A. Sveen, M. J. Mason, D. Niedzwiecki, A. Nesbakken, V. Moreno, R. S. Warren, R. A. Lothe and J. Guinney, *Ann. Oncol.*, 2019, **30**, 1622–1629.
56 D. Basile, S. K. Garattini, M. Bonotto, E. Ongaro, M. Casagrande, M. Cattaneo, V. Fanotto, E. De Carlo, F. Loupakis, F. Urbano, F. V. Negri, N. Pella, M. Russano, O. Brunetti, M. Scartozzi, D. Santini, N. Silvestris, A. C. Gardini, M. Puzzoni, L. Calvetti, N. Cardarelli and G. Aprile, *Expert Opin. Biol. Ther.*, 2017, **17**, 709–721.
57 R. M. McQuade, V. Stojanovska, J. C. Bornstein and K. Nurgali, *Curr. Med. Chem.*, 2017, **24**, 1537–1557.
58 R. Awasthi, A. Roseblade, P. M. Hansbro, M. J. Rathbone, K. Dua and M. Bebawy, *Curr. Drug Targets*, 2018, **19**, 1696–1709.
59 B. A. Cisterna, N. Kamaly, W. I. Choi, A. Tavakkoli, O. C. Farokhzad and C. Vilos, *Nanomedicine*, 2016, **11**, 2443–2456.
60 Y. Coyle, in *Shackelford's Surgery of the Alimentary Tract, 2 Volume Set*, ed. C. J. Yeo, Content Repository Only!, Philadelphia, 8th edn, 2019, pp. 2126–2136, DOI: 10.1016/B978-0-323-40232-3.00176-X.
61 E. Damilakis, D. Mavroudis, M. Sfakianaki and J. Souglakos, *Cancers*, 2020, **12**, 889.
62 F. Zhao, J. Wang, H. Yu, X. Cheng, X. Li, X. Zhu, X. Xu, J. Lin, X. Chen and S. Yan, *Radiat. Oncol.*, 2020, **15**, 49.
63 A. T. Hawkins, M. M. Ford, T. M. Geiger, M. B. Hopkins, L. A. Kachnic, R. L. Muldoon and S. C. Glasgow, *Surgery*, 2019, **165**, 469–475.
64 C. E. Atreya, R. Yaeger and E. Chu, *American Society of Clinical Oncology educational book. American Society of Clinical Oncology. Annual Meeting*, 2017, vol. 37, pp. 246–256.
65 L. Marcus, S. J. Lemery, S. Khasar, E. Wearne, W. S. Helms, W. Yuan, K. He, X. Cao, J. Yu, H. Zhao, Y. Wang, O. Stephens, E. Englund, R. Agarwal, P. Keegan and R. Pazdur, *Clin. Cancer Res.*, 2017, **23**, 2924–2927.
66 A. Falcone, T. André, J. Edeline, E. François, J. Taieb, J. Phelip, F. Portales, T. Price, M. Becquart, S. Moreno Vera, N. Mounedji, E. Van Cutsem and J. Seitz, *Ann. Oncol.*, 2018, **29**(5), 104–105.
67 A. Banerjee, S. Pathak, V. D. Subramanium, R. Murugesan and R. S. Verma, *Drug Discovery Today*, 2017, **22**, 1224–1232.
68 L. Kotelevets, E. Chastre, D. Desmaele and P. Couvreur, *Int. J. Pharm.*, 2016, **514**, 24–40.
69 J. Mishra, J. Drummond, S. H. Quazi, S. S. Karanki, J. J. Shaw, B. Chen and N. Kumar, *Crit. Rev. Oncol. Hematol.*, 2013, **86**, 232–250.
70 K. M. Augestad, M. A. Merok and D. Ignatovic, *Clin. Med. Insights: Oncol.*, 2017, **11**, 1179554917690766.
71 C. Isella, F. Brundu, S. E. Bellomo, F. Galimi, E. Zanella, R. Porporato, C. Petti, A. Fiori, F. Orzan, R. Senetta, C. Boccaccio, E. Ficarra, L. Marchionni, L. Trusolino, E. Medico and A. Bertotti, *Nat. Commun.*, 2017, **8**, 15107.
72 J. F. Linnekamp, S. R. v. Hooff, P. R. Prasetyanti, R. Kandimalla, J. Y. Buikhuisen, E. Fessler, P. Ramesh, K. Lee, G. G. W. Bochove, J. H. de Jong, K. Cameron, R. v. Leersum, H. M. Rodermond, M. Franitza,

Published on 04 March 2021. Downloaded by Universidade do Porto (UP) on 5/5/2024 9:05:19 PM.

P. Nürnberg, L. R. Mangiapane, X. Wang, H. Clevers, L. Vermeulen, G. Stassi and J. P. Medema, *Cell Death Differ.*, 2018, **25**, 616–633.
73 S. Piawah and A. P. Venook, *Cancer*, 2019, **125**, 4139–4147.
74 C. H. Lieu, R. B. Corcoran and M. J. Overman, *American Society of Clinical Oncology Educational Book*, 2019, pp. 207–215, DOI: 10.1200/edbk_240839.
75 P. Rawla, A. Barsouk, A. V. Hadjinicolaou and A. Barsouk, *Med. Sci.*, 2019, **7**, 83.
76 D. Aderka, S. Stintzing and V. Heinemann, *Lancet Oncol.*, 2019, **20**, 274–283.
77 S. Stintzing, P. Wirapati, H. J. Lenz, D. Neureiter, L. Fischer von Weikersthal, T. Decker, A. Kiani, F. Kaiser, S. Al-Batran, T. Heintges, C. Lerchenmüller, C. Kahl, G. Seipelt, F. Kullmann, M. Moehler, W. Scheithauer, S. Held, D. P. Modest, A. Jung, T. Kirchner, D. Aderka, S. Tejpar and V. Heinemann, *Ann. Oncol.*, 2019, **30**, 1796–1803.
78 J. K. Mooi, P. Wirapati, R. Asher, C. K. Lee, P. Savas, T. J. Price, A. Townsend, J. Hardingham, D. Buchanan, D. Williams, S. Tejpar, J. M. Mariadason and N. C. Tebbutt, *Ann. Oncol.*, 2018, **29**, 2240–2246.
79 C. R. Lichtenstern, R. K. Ngu, S. Shalapour and M. Karin, *Cells*, 2020, **9**, 618.
80 J. D. Fumet, N. Isambert, A. Hervieu, S. Zanetta, J. F. Guion, A. Hennequin, E. Rederstorff, A. Bertaut and F. Ghiringhelli, *ESMO Open*, 2018, **3**, e000375.
81 M. F. Tolba, *Int. J. Cancer*, 2020, 0020-7136.
82 M. J. Overman, R. McDermott, J. L. Leach, S. Lonardi, H.-J. Lenz, M. A. Morse, J. Desai, A. Hill, M. Axelson, R. A. Moss, M. V. Goldberg, Z. A. Cao, J.-M. Ledeine, G. A. Maglinte, S. Kopetz and T. André, *Lancet Oncol.*, 2017, **18**, 1182–1191.
83 C. Eng, T. W. Kim, J. Bendell, G. Argilés, N. C. Tebbutt, M. Di Bartolomeo, A. Falcone, M. Fakih, M. Kozloff, N. H. Segal, A. Sobrero, Y. Yan, I. Chang, A. Uyei, L. Roberts, F. Ciardiello, J. B. Ahn, J. Asselah, S. Badarinath, S. Baijal, S. Begbie, S. Berry, J. L. Canon, R. G. Carbone, A. Cervantes, Y. J. Cha, K. Chang, A. Chaudhry, E. Chmielowska, S. H. Cho, D. Chu, F. Couture, J. Cultrera, D. Cunningham, E. Van Cutsem, P. J. Cuyle, J. Davies, S. Dowden, M. Dvorkin, V. Ganju, R. V. Garcia, R. Kerr, T. Y. Kim, K. King, J. Kortmansky, M. Kozloff, K. O. Lam, J. Lee, A. S. Lee, B. Lesperance, G. Luppi, B. Ma, E. Maiello, R. Mandanas, J. Marshall, G. Marx, S. Mullamitha, M. Nechaeva, J. O. Park, N. Pavlakis, C. G. Ponce, P. Potemski, S. Raouf, J. Reeves, N. Segal, S. Siena, A. Smolin, J. O. Streb, A. Strickland, E. Szutowicz-Zielinska, J. M. Tabernero, B. Tan, J. S. Valera, M. Van den Eynde, P. Vergauwe, M. Vickers, M. Womack, M. Wroblewska and R. Young, *Lancet Oncol.*, 2019, **20**, 849–861.
84 R. E. Hollingsworth and K. Jansen, *npj Vaccines*, 2019, **4**, 7.
85 A. Gros, E. Tran, M. R. Parkhurst, S. Ilyas, A. Pasetto, E. M. Groh, P. F. Robbins, R. Yossef, A. Garcia-Garijo, C. A. Fajardo, T. D. Prickett, L. Jia, J. J. Gartner, S. Ray, L. Ngo, J. R. Wunderllich, J. C. Yang and S. A. Rosenberg, *J. Clin. Invest.*, 2019, **129**, 4992–5004.
86 S. Mariathasan, S. J. Turley, D. Nickles, A. Castiglioni, K. Yuen, Y. Wang, E. E. Kadel III, H. Koeppen, J. L. Astarita, R. Cubas, S. Jhunjhunwala, R. Banchereau, Y. Yang, Y. Guan, C. Chalouni, J. Ziai, Y. Şenbabaoğlu, S. Santoro, D. Sheinson, J. Hung, J. M. Giltnane, A. A. Pierce, K. Mesh, S. Lianoglou, J. Riegler, R. A. D. Carano, P. Eriksson, M. Höglund, L. Somarriba, D. L. Halligan, M. S. van der Heijden, Y. Loriot, J. E. Rosenberg, L. Fong, I. Mellman, D. S. Chen, M. Green, C. Derleth, G. D. Fine, P. S. Hegde, R. Bourgon and T. Powles, *Nature*, 2018, **554**, 544–548.
87 P. Zhang, Y. Zhai, Y. Cai, Y. Zhao and Y. Li, *Adv. Mater.*, 2019, **31**, 1904156.
88 H. Qiu, Y. Min, Z. Rodgers, L. Zhang and A. Z. Wang, *Wiley Interdiscip. Rev.: Nanomed. Nanobiotechnol.*, 2017, **9**, 5.
89 D. J. Irvine and E. L. Dane, *Nat. Rev. Immunol.*, 2020, **20**, 321–334.
90 I. Brigger, C. Dubernet and P. Couvreur, *Adv. Drug Delivery Rev.*, 2012, **64**, 24–36.
91 X. Feng, W. Xu, Z. Li, W. Song, J. Ding and X. Chen, *Adv. Sci.*, 2019, **6**, 1900101.
92 T. Matsu-ura, S. R. Moore and C. I. Hong, *J. Biol. Rhythms*, 2018, **33**, 5–14.
93 J. D. Martin, H. Cabral, T. Stylianopoulos and R. K. Jain, *Nat. Rev. Clin. Oncol.*, 2020, **17**, 251–266.
94 X. Duan, C. Chan and W. Lin, *Angew. Chem., Int. Ed.*, 2019, **58**, 670–680.
95 Y. Shi and T. Lammers, *Acc. Chem. Res.*, 2019, **52**, 1543–1554.
96 L. Ma, T. Dichwalkar, J. Y. H. Chang, B. Cossette, D. Garafola, A. Q. Zhang, M. Fichter, C. Wang, S. Liang, M. Silva, S. Kumari, N. K. Mehta, W. Abraham, N. Thai, N. Li, K. D. Wittrup and D. J. Irvine, *Science*, 2019, **365**, 162–168.
97 Y. Huai, M. N. Hossen, S. Wilhelm, R. Bhattacharya and P. Mukherjee, *Bioconjugate Chem.*, 2019, **30**, 2247–2263.
98 Z.-g. Liu, W. Jiang, J. Nam, J. Moon and B. Kim, *Nano Lett.*, 2018, **18**(11), 6655–6659.
99 J. Roelands, P. J. K. Kuppen, L. Vermeulen, C. Maccalli, J. Decock, E. Wang, F. M. Marincola, D. Bedognetti and W. Hendrickx, *Int. J. Mol. Sci.*, 2017, **18**, 2229.
100 G. Zhu, L. Mei, H. D. Vishwasrao, O. Jacobson, Z. Wang, Y. Liu, B. C. Yung, X. Fu, A. Jin, G. Niu, Q. Wang, F. Zhang, H. Shroff and X. Chen, *Nat. Commun.*, 2017, **8**, 1482–1482.
101 T. J. Goodwin and L. Huang, *Vaccine*, 2017, **35**, 2550–2557.
102 Q. Ni, F. Zhang, Y. Liu, Z. Wang, G. Yu, B. Liang, G. Niu, T. Su, G. Zhu, G. Lu, L. Zhang and X. Chen, *Sci. Adv.*, 2020, **6**, eaaw6071.
103 X. Wang, N. Wang, Y. Yang, X. Wang, J. Liang, X. Tian, H. Zhang and X. Leng, *Biomater. Sci.*, 2019, **7**, 3062–3075.
104 W.-L. Liu, M.-Z. Zou, T. Liu, J.-Y. Zeng, X. Li, W.-Y. Yu, C.-X. Li, J.-J. Ye, W. Song, J. Feng and X.-Z. Zhang, *Adv. Mater.*, 2019, **31**, 1900499.

 This journal is © The Royal Society of Chemistry 2021

Published on 04 March 2021. Downloaded by Universidade do Porto (UP) on 5/5/2024 9:05:19 PM.

105 W.-L. Liu, M.-Z. Zou, T. Liu, J.-Y. Zeng, X. Li, W.-Y. Yu, C.-X. Li, J.-J. Ye, W. Song, J. Feng and X.-Z. Zhang, *Nat. Commun.*, 2019, **10**, 3199.
106 X. Dong, P. Pan, D.-W. Zheng, P. Bao, X. Zeng and X.-Z. Zhang, *Sci. Adv.*, 2020, **6**, eaba1590.
107 R. Kuai, W. Yuan, S. Son, J. Nam, Y. Xu, Y. Fan, A. Schwendeman and J. J. Moon, *Sci. Adv.*, 2018, **4**, eaao1736–eaao1736.
108 M. Luo, H. Wang, Z. Wang, H. Cai, Z. Lu, Y. Li, M. Du, G. Huang, C. Wang, X. Chen, M. R. Porembka, J. Lea, A. E. Frankel, Y.-X. Fu, Z. J. Chen and J. Gao, *Nat. Nanotechnol.*, 2017, **12**, 648–654.
109 F. Castro, M. L. Pinto, A. M. Silva, C. L. Pereira, G. Q. Teixeira, M. Gomez-Lazaro, S. G. Santos, M. A. Barbosa, R. M. Gonçalves and M. J. Oliveira, *Acta Biomater.*, 2017, **63**, 96–109.
110 Q. Zhang, F. Zhang, S. Li, R. Liu, T. Jin, Y. Dou, Z. Zhou and J. Zhang, *Theranostics*, 2019, **9**, 3732–3753.
111 J. V. Gonzalez-Aramundiz, A. S. Cordeiro, N. Csaba, M. de la Fuente and M. J. Alonso, *Biol. Aujourd'hui*, 2012, **206**, 249–261.
112 J. Conniot, A. Scomparin, C. Peres, E. Yeini, S. Pozzi, A. I. Matos, R. Kleiner, L. I. F. Moura, E. Zupančič, A. S. Viana, H. Doron, P. M. P. Gois, N. Erez, S. Jung, R. Satchi-Fainaro and H. F. Florindo, *Nat. Nanotechnol.*, 2019, **14**, 891–901.
113 J. Zhuang, M. Holay, J. H. Park, R. H. Fang, J. Zhang and L. Zhang, *Theranostics*, 2019, **9**, 7826–7848.
114 D. M. Francis, M. P. Manspeaker, A. Schudel, L. F. Sestito, M. J. O'Melia, H. T. Kissick, B. P. Pollack, E. K. Waller and S. N. Thomas, *Sci. Transl. Med.*, 2020, **12**, eaay3575.
115 J. Rotman, B. D. Koster, E. S. Jordanova, A. M. Heeren and T. D. de Gruijl, *Cancer Immunol. Immunother.*, 2019, **68**, 1681–1688.
116 M. F. Fransen, M. Schoonderwoerd, P. Knopf, M. G. M. Camps, L. Hawinkels, M. Kneilling, T. van Hall and F. Ossendorp, *JCI Insight*, 2018, **3**(23), e124507.
117 Z. Zhou, J. Pang, X. Wu, W. Wu, X. Chen and M. Kong, *Nano Res.*, 2020, **13**, 1509–1518.
118 A. V. Kroll, R. H. Fang, Y. Jiang, J. Zhou, X. Wei, C. L. Yu, J. Gao, B. T. Luk, D. Dehaini, W. Gao and L. Zhang, *Adv. Mater.*, 2017, **29**, 47.
119 V. Mazzaferro, J. Coppa, M. G. Carrabba, L. Rivoltini, M. Schiavo, E. Regalia, L. Mariani, T. Camerini, A. Marchianò, S. Andreola, R. Camerini, M. Corsi, J. J. Lewis, P. K. Srivastava and G. Parmiani, *Clin. Cancer Res.*, 2003, **9**, 3235–3245.
120 L. Madkour, *Nucleic Acids as Gene Anticancer Drug Delivery Therapy*, 1st edn, 2019.
121 I. Mikelez-Alonso, A. Aires and A. L. Cortajarena, *Int. J. Mol. Sci.*, 2020, **21**(2), 519.
122 R. Rezaei, M. Safaei, H. R. Mozaffari, H. Moradpoor, S. Karami, A. Golshah, B. Salimi and H. Karami, *Open Access Maced. J. Med. Sci.*, 2019, **7**, 1884–1890.
123 B. Fadeel, *Front. Immunol.*, 2019, **10**, 133.
124 S. Sau, R. Alzhrani, K. Bhise, H. O. Alsaab, S. K. Kashaw and A. K. Iyer, *Nanomedicine*, 2019, **14**, 1515–1519.
125 J. W. Hickey, F. P. Vicente, G. P. Howard, H.-Q. Mao and J. P. Schneck, *Nano Lett.*, 2017, **17**, 7045–7054.
126 J. Calmeiro, M. Carrascal, C. Gomes, A. Falcão, M. T. Cruz and B. M. Neves, *J. Immunother. Cancer*, 2019, **7**, 238–238.
127 F. Castro, M. L. Pinto, R. Almeida, F. Pereira, A. M. Silva, C. L. Pereira, S. G. Santos, M. A. Barbosa, R. M. Gonçalves and M. J. Oliveira, *Biomater. Sci.*, 2019, **7**, 3386–3403.
128 S. Zanganeh, G. Hutter, R. Spitler, O. Lenkov, M. Mahmoudi, A. Shaw, J. S. Pajarinen, H. Nejadnik, S. Goodman, M. Moseley, L. M. Coussens and H. E. Daldrup-Link, *Nat. Nanotechnol.*, 2016, **11**, 986–994.
129 H. Li, J. Lu, C. Yan and L. Xu, *Int. J. Polym. Mater. Polym. Biomater.*, 2020, **69**, 1157–1166.
130 C. He, X. Duan, N. Guo, C. Chan, C. Poon, R. R. Weichselbaum and W. Lin, *Nat. Commun.*, 2016, **7**, 12499.
131 S. Yan, P. Zhao, T. Yu and N. Gu, *Cancer Biol. Med.*, 2019, **16**, 486–497.
132 T. H. Kim, H. Jin, H. W. Kim, M. H. Cho and C. S. Cho, *Mol. Cancer Ther.*, 2006, **5**, 1723–1732.
133 X. Liu, X. Gao, S. Zheng, B. Wang, Y. Li, C. Zhao, Y. Muftuoglu, S. Chen, Y. Li, H. Yao, H. Sun, Q. Mao, C. You, G. Guo and Y. Wei, *Nanomedicine*, 2017, **13**, 1993–2004.
134 M. A. Buabeid, E.-S. A. Arafa and G. Murtaza, *J. Immunol. Res.*, 2020, **2020**, 11.

Immunomodulatory nanomedicine for colorectal cancer treatment: a landscape to be explored?

M. J. Silveira, F. Castro, M. J. Oliveira and B. Sarmento, *Biomater. Sci.*, 2021, **9**, 3228 **DOI:** 10.1039/D1BM00137J

To request permission to reproduce material from this article, please go to the Copyright Clearance Center request page.

If you are **an author contributing to an RSC publication, you do not need to request permission** provided correct acknowledgement is given.

If you are **the author of this article, you do not need to request permission to reproduce figures and diagrams** provided correct acknowledgement is given. If you want to reproduce the whole article in a third-party publication (excluding your thesis/dissertation for which permission is not required) please go to the Copyright Clearance Center request page.

Read more about how to correctly acknowledge RSC content.

CCC RightsLink

SPRINGER NATURE

scFv biofunctionalized nanoparticles to effective and safe targeting of CEA-expressing colorectal cancer cells

Author: Maria José Silveira et al
Publication: Journal of Nanobiotechnology
Publisher: Springer Nature
Date: Oct 2, 2023

Copyright © 2023, The Author(s)

Creative Commons

This is an open access article distributed under the terms of the Creative Commons CC BY license, which permits unrestricted use, distribution, and reproduction in any medium, provided the original work is properly cited.

You are not required to obtain permission to reuse this article.

CC0 applies for supplementary material related to this article and attribution is not required.

© 2024 Copyright - All Rights Reserved | Copyright Clearance Center, Inc. | Privacy statement | Data Security and Privacy | For California Residents | Terms and ConditionsComments? We would like to hear from you. E-mail us at customercare@copyright.com